

UNIVERSITÉ DU QUÉBEC À MONTRÉAL

FACTEURS RÉGISSANT LA CROISSANCE DES PEUPLEMENTS BORÉAUX  
DU NORD DU QUÉBEC DANS UN CONTEXTE DE CHANGEMENTS  
CLIMATIQUES RÉCENTS

THÈSE  
PRÉSENTÉE  
COMME EXIGENCE PARTIELLE  
DU PROGRAMME DE DOCTORAT EN SCIENCES DE L'ENVIRONNEMENT

PAR  
WILLIAM MARCHAND

MARS 2021

UNIVERSITÉ DU QUÉBEC À MONTRÉAL  
Service des bibliothèques

Avertissement

La diffusion de cette thèse se fait dans le respect des droits de son auteur, qui a signé le formulaire *Autorisation de reproduire et de diffuser un travail de recherche de cycles supérieurs* (SDU-522 – Rév.04-2020). Cette autorisation stipule que «conformément à l'article 11 du Règlement no 8 des études de cycles supérieurs, [l'auteur] concède à l'Université du Québec à Montréal une licence non exclusive d'utilisation et de publication de la totalité ou d'une partie importante de [son] travail de recherche pour des fins pédagogiques et non commerciales. Plus précisément, [l'auteur] autorise l'Université du Québec à Montréal à reproduire, diffuser, prêter, distribuer ou vendre des copies de [son] travail de recherche à des fins non commerciales sur quelque support que ce soit, y compris l'Internet. Cette licence et cette autorisation n'entraînent pas une renonciation de [la] part [de l'auteur] à [ses] droits moraux ni à [ses] droits de propriété intellectuelle. Sauf entente contraire, [l'auteur] conserve la liberté de diffuser et de commercialiser ou non ce travail dont [il] possède un exemplaire.»

## REMERCIEMENTS

Ce doctorat n'aurait pu être et mené à son terme sans l'aide et le soutien de nombreuses personnes. En premier lieu, je tiens à remercier mon directeur, Martin Girardin, pour m'avoir formé à la recherche en dendroécologie ainsi que pour m'avoir transmis son enthousiasme et avoir partagé ses points de vue concernant le monde de la recherche. Merci également pour m'avoir soutenu et poussé à continuer lors de mes nombreux moments de doutes. En second lieu, je remercie Yves Bergeron pour m'avoir transmis ses connaissances concernant l'écologie forestière appliquée à la réalité des aménagistes forestiers. Je tiens à remercier chaleureusement Henrik Hartmann pour avoir accepté de faire partie de mon comité d'encadrement, pour m'avoir accueilli en stage à l'institut Max Planck pendant deux mois, et pour ses nombreux conseils et ses commentaires pertinents qui ont largement contribué à améliorer les trois chapitres composant cette thèse. Un grand merci, également, pour m'avoir aidé, lors de l'étape de rédaction et publication de ma synthèse, à améliorer mon style d'écriture. Merci également à Sylvie Gauthier, pour tes conseils en foresterie, tes commentaires sur mes manuscrits, et pour m'avoir, toi aussi, aidé à garder le cap et poussé à aller jusqu'au bout. Merci à Claire Depardieu, pour les conseils et l'aide dans la préparation du laboratoire, pour les relectures des manuscrits et surtout pour le soutien moral tout au long de ces quatre années de thèse. Merci à Daniel Houle, pour m'avoir accueilli en stage à Ouranos, et pour avoir partagé avec moi ses connaissances sur l'écophysiologie des espèces forestières boréales. Mes remerciements vont aussi à Flurin Babst, Olivier Bouriaud, Étienne Boucher et Nathalie Isabel pour avoir accepté de collaborer à mon manuscrit de synthèse (qui n'est pas inclus dans ce document mais que je considère cependant comme partie intégrante de ma thèse) et à mon troisième chapitre de thèse. Même s'ils ne font pas partie de mon comité ils m'ont, eux aussi, guidé et aidé dans la

rédaction et dans certains aspects plus théoriques de mes travaux. Un grand merci à Christine Simard et Marie Moulin pour l'aide, cruciale, dans la fastidieuse préparation des échantillons pour les analyses isotopiques. Un grand merci à Mathilde Pau, Benjamin Andrieux, Émeline Chaste, Marine Pacé, Dorian Gaboriau, Carole Bastianelli, et Ariane Mirabel pour m'avoir soutenu (et supporté) dans mes nombreux moments de doute, et aussi pour les bons moments passés en votre compagnie. Un remerciement tout particulier à Danielle Charron pour l'aide administrative. Enfin, merci à toutes les autres personnes que je ne cite pas personnellement ici mais qui ont également contribué, de près ou de loin, à ce doctorat, incluant les étudiants croisés au fil des cours et des congrès, les professeurs et le personnel de l'UQAM, du Centre de Foresterie des Laurentides, de l'Institut Max Planck, de l'Université Laval et de la Commission Géologique du Canada.

## AVANT-PROPOS

Ce doctorat s'insère dans un vaste projet de recherche intitulé *Capacité de régénération suite aux feux/coupes, de remise en production et de croissance des peuplements juvéniles/immatures en pessière dans un contexte de changement climatique*. L'objectif général de ce projet est de mieux cerner les facteurs, incluant le climat, l'environnement physique, les perturbations naturelles et la dynamique des peuplements, qui affectent la capacité de production des forêts boréales nordiques après feu ou après coupe. Le but de ce projet est notamment de pouvoir anticiper la capacité des peuplements à supporter un aménagement forestier durable dans le futur. Les données et échantillons analysés dans le cadre de ce doctorat avaient été récoltés entre 2005 et 2009 par les équipes du Ministère des Forêts, de la Faune et des Parcs du Québec (MFFPQ) dans le cadre du programme d'inventaire écoforestier nordique. Aucune campagne de terrain complémentaire n'a été réalisée au cours de ce doctorat.

Mon directeur, Martin Girardin, chercheur scientifique au Service Canadien des Forêts, m'a épaulé tout au long de ce doctorat avec ses conseils concernant les hypothèses de travail, la sélection des arbres et cernes pour les analyses isotopiques et les analyses statistiques. Il m'a également grandement aidé dans la structuration et la rédaction des articles. Il a contribué de façon majeure à l'ensemble des trois articles composant cette thèse et en est donc, logiquement, co-auteur.

Mon co-directeur, le professeur Yves Bergeron, titulaire de la Chaire industrielle CRSNG-UQAT-UQAM en Aménagement Forestier Durable, a contribué de façon majeure à la mise en place du projet, notamment concernant les objectifs et hypothèses

de travail initiaux. Il m'a également grandement aidé pour la rédaction des trois articles de cette thèse, notamment de par son expertise en écologie forestière. Il est donc co-auteur de ces trois articles.

Sylvie Gauthier, chercheure scientifique au Service Canadien des Forêts, membre de mon comité d'encadrement, est spécialiste des questions liées à la régénération forestière et à l'aménagement des forêts. De par son expertise et sa connaissance de la base de données du MFFPQ, elle a largement contribué à l'avancée de mon projet de doctorat, notamment à la construction des hypothèses de travail, l'interprétation des résultats et la rédaction des articles. Pour ces raisons, elle est co-auteure de l'ensemble des articles de cette thèse.

Le professeur Henrik Hartmann, chercheur à l'Institut Max Planck, est également membre de mon comité d'encadrement. Son expertise en écophysiologie végétale et dans l'analyse des isotopes stables a été précieuse pour mener ce doctorat à son terme. Il m'a épaulé à toutes les étapes du projet, et notamment lors des étapes de préparation des échantillons de bois pour les analyses isotopiques. Il a accepté de prendre en charge l'ensemble des analyses isotopiques qui constituent la base de mes second et troisième chapitres. Ses commentaires concernant chacun de mes trois chapitres ont été précieux et ont grandement contribué à en améliorer à la fois la forme et le contenu. Pour cela, il est co-auteur de chacun des trois articles de cette thèse.

Claire Depardieu, professionnelle de recherche à l'Université Laval, et Nathalie Isabel, chercheure scientifique au Service Canadien des Forêts, ont contribué de façon importante aux étapes de mise en place du protocole de laboratoire pour la préparation des échantillons de bois préalablement aux mesures isotopiques. Elles ont également contribué à faire évoluer le second chapitre de cette thèse de par leurs remarques et commentaires pertinents. À ce titre elles en sont co-auteures.

Étienne Boucher, professeur à l'UQAM, a lui aussi contribué à ce projet par ses conseils concernant la sélection des arbres et des cernes à échantillonner, et concernant les différentes étapes de préparation des échantillons. Il a également contribué de façon importante à faire évoluer le manuscrit du troisième chapitre de cette thèse, dont il est co-auteur.

Enfin, j'ai participé à l'ensemble des étapes de mon projet de doctorat, de l'élaboration des hypothèses à la rédaction du document final et notamment des trois manuscrits qui le composent, en passant par la mise en place du protocole de laboratoire pour la préparation des échantillons de bois, l'analyse statistique des données et l'interprétation des résultats.

## TABLE DES MATIÈRES

AVANT-PROPOS .....	iv
LISTE DES FIGURES.....	x
LISTE DES TABLEAUX.....	xiii
RÉSUMÉ .....	xiv
ABSTRACT .....	xvii
INTRODUCTION .....	1
CHAPITRE I TAXONOMY, TOGETHER WITH ONTOGENY AND GROWING CONDITIONS, DRIVES NEEDLELEAF SPECIES' SENSITIVITY TO CLIMATE IN BOREAL NORTH AMERICA .....	24
1.1 Introduction .....	29
1.2 Materials and methods .....	32
1.2.1 Sampling area.....	32
1.2.2 Tree-ring material.....	35
1.2.3 Climate data and explanatory variables .....	35
1.2.4 Statistical procedures .....	38
1.3 Results.....	44
1.3.1 Growth trends are spatially heterogeneous and species-specific .....	44
1.3.2 Sensitivity to climate is dissimilar across the landscape.....	47
1.3.3 Plot-level features had low but significant effects on growth-climate relationships .....	50
1.4 Discussion .....	54
1.5 Acknowledgements .....	59

CHAPITRE II HIGH STOMATAL LIMITATION ON PHOTOSYNTHESIS AS A DRIVER OF DROUGHT-INDUCED GROWTH DECLINE IN BOREAL CONIFERS .....	60
2.1 Introduction .....	64
2.2 Materials and Methods.....	69
2.2.1 Sampling area.....	69
2.2.2 Basal Area Increment data .....	70
2.2.3 Isotope measurements .....	71
2.2.4 Corrections for non-climatic variability in tree-ring isotope composition.....	73
2.2.5 Climate and environmental variables .....	74
2.2.6 Statistical procedure .....	75
2.3 Results.....	79
2.3.1 Spatial variability in growth, isotope discrimination and climate .....	79
2.3.2 Inter-annual differences in growth, carbon and oxygen isotope discrimination .....	80
2.3.3 Climate effects on tree growth and isotope discrimination.....	83
2.4 Discussion .....	86
2.4.1 A reduction in stomatal conductance during drought leads to growth declines .....	86
2.4.2 Black spruce responds stronger to low climatic water balance and high vapour pressure deficits in summer than jack pine.....	87
2.4.3 High inter-tree and inter-plot variability in physiological responses to drought .....	90
2.4.4 Conclusions .....	91
2.5 Acknowledgements .....	93
CHAPITRE III STRONG OVERESTIMATION OF WATER-USE EFFICIENCY RESPONSES TO RISING CO <sub>2</sub> IN TREE-RING STUDIES .....	94
3.1 Introduction .....	98
3.2 Materials and Methods.....	101
3.2.1 Study area.....	101
3.2.2 Tree sampling.....	105
3.2.3 Variables for tree and stand-level developmental changes, climate and growth conditions .....	106
3.2.4 Wood samples preparation for isotope measurements.....	108
3.2.5 Inference of iWUE from tree-ring carbon isotope ratios .....	109

3.2.6 Statistical analyses .....	111
3.3 Results.....	116
3.3.1 Temporal variability in $iWUE_{ring}$ , growth and leaf gas-exchange variables .....	116
3.3.2 Response of $iWUE_{ring}$ to rising $PCO_2$ .....	117
3.3.3 Diagnostics of collinear variables .....	124
3.4 Discussion .....	129
3.4.1 Tree size and stand age strongly contribute to long-term trends in $iWUE$ .....	129
3.4.2 Site fertility as a driver of heterogeneity in $CO_2$ effects .....	130
3.4.3 The apparent effect of $C_a$ on $iWUE$ is strongly lessened after removing effects of collinear variables .....	132
3.4.4 Species-specific sensitivity to $C_a$ .....	133
3.4.5 Methodological limitations .....	135
3.4.6 Conclusions .....	137
3.5 Acknowledgements .....	139
 CHAPITRE IV CONCLUSION GÉNÉRALE .....	140
4.1 Faits saillants et contributions à l'avancée des connaissances.....	140
4.2 Forte variabilité spatiale et temporelle des effets des changements climatiques sur la croissance et la physiologie des conifères boréaux .....	143
4.3 Un effet des variations interannuelles et des tendances climatiques dépendant de l'espèce .....	146
4.4 Préconisations et enjeux de recherche futurs .....	148
 ANNEXE A MATÉRIEL SUPPLÉMENTAIRE DU CHAPITRE I .....	157
 ANNEXE B MATÉRIEL SUPPLÉMENTAIRE DU CHAPITRE II .....	191
 ANNEXE C MATÉRIEL SUPPLÉMENTAIRE DU CHAPITRE III .....	203
 ANNEXE D MATÉRIEL SUPPLÉMENTAIRE DU CHAPITRE VI .....	219
 RÉFÉRENCES.....	222

## LISTE DES FIGURES

Figure	Page
0.1 Aire d'extension de la zone boréale Nord-Américaine et aires de distribution de l'épinette noire et du pin gris.....	3
0.2 Tendances climatiques dans la zone boréale québécoise .....	7
0.3 Principales étapes durant lesquelles une discrimination des isotopes lourds du carbone et de l'oxygène intervient.....	15
0.4 Trois scénarios de changements des conditions de croissance des arbres, et les modifications induites sur l'ouverture des stomates, les concentrations internes en vapeur d'eau et en CO <sub>2</sub> , les taux de photosynthèse et la conductance stomatique, et les rapports isotopiques du carbone ( $\delta^{13}\text{C}$ ) et de l'oxygène ( $\delta^{18}\text{O}$ ).....	16
0.5 Enveloppes climatiques des deux espèces .....	20
0.6 Différentes périodes temporelles étudiées selon les trois chapitres de la thèse, superposées sur l'évolution de la concentration en CO <sub>2</sub> atmosphérique depuis la période pré-industrielle (pré-1850).....	23
1.1 Forest inventory plot network and geographical units involved in statistical analyses.....	34
1.2 Growth trends for black spruce and jack pine, for the 1950-2005 and 1970-2005 periods, and distributions of growth trend slopes by species and bioclimatic domain .....	45
1.3 Median chronologies of black spruce and jack pine detrended BAI (growth change) per bioclimatic domain.....	46

1.4	Arithmetic means and bootstrapped 95 % confidence intervals of t-statistic values per bioclimatic domain for black spruce and jack pine, for each of the seasonal climatic variables.....	48
1.5	Kriging-interpolated growth response significance (based on t-statistics, 1970-2005) to seasonal climatic variable for black spruce and jack pine ...	49
1.6	The sets of independent variables used in variation partitioning, effect of each explanatory variable on tree sensitivity to climate, based on autocorrelation-corrected Pearson correlations, and proportion of variance explained by each set of independent variables, alone or in combination with other sets (Venn diagrams), by bioclimatic domain .....	52
1.7	Effect of topographic position on sensitivity to spring temperature, summer temperature, previous summer precipitation, and effect of the age of the stand on the sensitivity to previous summer temperature .....	53
2.1	Map of the study zone.....	77
2.2	Distribution of observed (i.e. raw) values of the growth index, $\Delta^{13}\text{C}_{\text{ring}}$ and $\Delta^{18}\text{O}_{\text{ring}}$ , by year and species.....	78
2.3	1985-1993 climate data.....	81
2.4	Z-scored growth index, $\Delta^{13}\text{C}$ and $\Delta^{18}\text{O}$ values, by year and species.....	82
3.1	Study area and sampling strategy for isotope analyses. ....	102
3.2	Workflow diagram summarizing the computation of intrinsic water use efficiency ( $i\text{WUE}_{\text{ring}}$ ) and the statistical procedure .....	115
3.3	Relationship between the partial pressure of $\text{CO}_2$ ( $\text{PCO}_2$ ) and $\delta^{13}\text{C}_{\text{ring}}$ - derived physiological parameters (ring-to-atmosphere carbon discrimination, $\Delta^{13}\text{C}_{\text{ring}}$ ; water use efficiency, $i\text{WUE}_{\text{ring}}$ ) or radial growth (basal area increments, BAI) .....	118
3.4	Temporal variation in three $\delta^{13}\text{C}_{\text{ring}}$ -derived physiological variables involved in the regulation of trees leaf gas-exchange .....	119

3.5	Median iWUE <sub>ring</sub> , $\Delta^{13}\text{C}_{\text{ring}}$ and basal area increments (BAI) for the period spanning 1 m height cambial ages 11-30 years and the period spanning calendar years 1985-1993, for trees recruited before and after 1950 .....	122
3.6	Partial effects of developmental processes, climate, total annual nitrogen deposition and site fertility index on iWUE <sub>ring</sub> .....	123
3.7	iWUE trends following each step of the statistical procedure.....	126
3.8	Assessment of the modulating effect of growth conditions on the iWUE <sub>ring</sub> response to C <sub>a</sub> .....	127

## LISTE DES TABLEAUX

Tableau	Page
1.1 Plot-level statistics for the studied explanatory variables, by bioclimatic domain .....	37
2.1 Outputs of linear mixed models of climate effects of on tree growth and isotope ratios.....	85
3.1 Climate and physiographic characteristics of the study area.....	104
3.2 Regression slopes ( $\beta$ ), standard deviations (Std.error), t-values and p-values from the linear mixed models assessing the effects of $\text{PCO}_2$ , SI and their interaction on $\text{RESiWUE}$ by species, according to the statistical procedure .....	120
3.3 Results from ‘Full’ and ‘Control’ Generalized Additive Mixed Models (GAMMs) .....	121

## RÉSUMÉ

Les changements intervenant dans l'environnement, et notamment les modifications dans les moyennes et extrêmes climatiques liées à l'augmentation de la concentration en CO<sub>2</sub> atmosphérique, ont d'ores et déjà des effets mesurables sur les écosystèmes. Les arbres, organismes sessiles et à relativement longue espérance de vie, y sont particulièrement sensibles et constituent par là même d'excellents modèles pour étudier les effets des changements climatiques. Les forêts boréales pourraient être particulièrement affectées par ces changements, qui, à ces latitudes, seront plus rapides et intenses que dans la plupart des autres biomes. Or, le biome boréal est l'un des acteurs majeurs dans le cycle global du carbone. De plus, la forêt boréale au Canada, est une source de nombreux services écologiques, tant en termes de loisirs que de biodiversité et de source de matière premières. Tout bouleversement dans ses capacités de production, et donc dans ses fonctions, pourrait avoir des répercussions sur la disponibilité de l'ensemble de ces services pour les populations humaines. Des prédictions réalistes de la capacité de résilience de cet écosystème forestier boréal aux conditions climatiques futures permettraient une meilleure estimation de sa capacité de production. Il est important d'étudier la manière dont les arbres ont d'ores et déjà répondu aux changements environnementaux intervenus au cours des dernières décennies.

Cette thèse a pour objectifs d'étudier les changements intervenus dans la croissance et la physiologie des arbres au cours des dernières décennies, et d'explorer les facteurs environnementaux responsables de ces modifications. L'étude s'est portée sur deux essences conifériennes largement distribuées en Amérique du Nord et d'intérêt commercial, l'épinette noire (*Picea mariana*) et le pin gris (*Pinus banksiana*). Nous nous sommes basés sur une base de données issue d'un inventaire forestier. Ces données couvrent un large gradient géographique d'est en ouest de la forêt boréale québécoise nordique et incluent plus de 2000 arbres. Les performances de croissance ont été approximées au moyen des largeurs de cernes annuels. Les paramètres physiologiques des arbres, incluant l'efficience d'utilisation de l'eau et la conductance stomatique, ont quant à eux été approximés en mesurant les rapports isotopiques du carbone et de l'oxygène dans le bois des cernes de croissance.

Le premier chapitre explore les relations entre les taux de croissance annuels, les variations inter-annuelles du climat et divers paramètres environnementaux. Ce chapitre a permis de montrer que les deux espèces présentaient une sensibilité différente au climat saisonnier. L'épinette, à l'inverse du pin, est apparue négativement impactée par des étés chauds ayant lieu la saison précédant la formation du cerne. Pour cette espèce, les arbres implantés plus en altitude étaient également négativement affectés par des printemps doux. Cela s'est traduit par des tendances de croissance généralement à la baisse chez l'épinette. Au contraire, la croissance du pin s'est maintenue, ou faiblement améliorée, au cours des trois dernières décennies. Le second chapitre étudie l'impact d'un épisode de sécheresse majeur, ayant eu lieu en 1989 dans notre territoire d'étude, sur la croissance et la physiologie des arbres. Ici, nous avons montré que les arbres réagissaient à des conditions plus sèches que la normale en augmentant leur efficience d'utilisation de l'eau, notamment à travers une diminution de leur conductance stomatique. Une perte de croissance intervenait de façon synchrone à ces modifications physiologiques et perdurait plus longtemps chez l'épinette. Enfin, le troisième chapitre s'est intéressé à l'effet de l'augmentation de la concentration en CO<sub>2</sub> atmosphérique sur l'efficience d'utilisation de l'eau des arbres. Il a été montré que cet effet était fortement amoindri après avoir retiré les tendances liées au développement des arbres et des peuplements. Cet effet était nettement plus important chez l'épinette que chez le pin. Par ailleurs, cet effet CO<sub>2</sub> était quasiment inexistant pour les épinettes sur les sites les plus pauvres.

L'ensemble de ces résultats laisse entrevoir un stress plus important pour l'épinette que pour le pin. De cela, nous pouvons poser l'hypothèse que l'épinette serait moins bien adaptée que le pin au réchauffement climatique à venir ; en raison notamment de ses particularités morpho-physiologiques. Nos résultats suggèrent également que certains environnements pourraient agir à titre de refuge climatique pour les espèces boréales. Certaines populations pourraient également être déjà mieux adaptées que d'autres à des conditions plus chaudes et sèches. Ces populations pourraient être de bonnes candidates pour des programmes de migration assistée et devraient faire l'objet d'études plus approfondies d'un point de vue génétique (expériences en jardin commun). Nos résultats tendent aussi à recommander un suivi régulier des peuplements d'épinette, incluant ceux sur les sites actuellement productifs sur lesquels les arbres pourraient être largement impactés par les stress climatiques à venir. Nous recommandons également une évaluation et une amélioration des méthodes d'analyse actuellement en vigueur. La vaste gamme d'analyses actuellement utilisées a, potentiellement, un impact sur les conclusions produites et limite la comparabilité des résultats entre études. Au regard de nos résultats, il serait attendu que la productivité des peuplements d'épinette décline au cours du siècle actuel. Les peuplements de pin, au contraire, pourraient demeurer productifs, s'ils maintiennent une bonne régénération sous un cycle de feu plus court (la réponse aux changements du cycle de feux n'a pas été étudiée ici).

Mots-clés : Changements climatiques, Québec, forêt boréale, *Picea mariana*, *Pinus banksiana*, dendroécologie, inventaires forestiers, isotopes stables, efficience d'utilisation de l'eau

## ABSTRACT

Changes in environmental conditions, and especially modifications in climate averages and extremes resulting from a rise in atmospheric CO<sub>2</sub> concentrations, have already measurable effects on natural ecosystems. Trees, which are sessile and long-lived organisms, are particularly sensitive to these changes, which makes these organisms of particular interest to study the effects of climate change. Since climate warming is stronger and faster at high latitudes, boreal forest ecosystems could be particularly at risk of significant impacts. The boreal biome plays a central role in global carbon cycling. Canadian boreal forests also provide numerous ecological services, e.g. providing jobs and raw materials for the forest industry sector and playing an important role in terms of biodiversity. An accurate prediction of the capacity of boreal forests to acclimate to a future warmer climate could help inferring its future production capacity. So, it is important to study the way boreal trees have already responded to environmental changes that have occurred in the past decades.

The main objectives of this thesis were to study changes that have occurred in the growth and physiology of trees during the last decades, and to identify which environmental factors were responsible for these changes. Our work focused on two boreal conifer species broadly distributed in North America and of high commercial value, black spruce (*Picea mariana*) and jack pine (*Pinus banksiana*). We used a dataset originating from a forest inventory network including more than 2000 trees and encompassing a broad gradient of growing conditions. This network covers the Quebec province from East to West north of 49°N. Annual ring widths were used as a proxy for growth performance of trees. Tree-ring carbon and oxygen isotopic signatures were measured to approximate intrinsic water use efficiency (iWUE) and stomatal conductance, respectively.

The first chapter examines the relationship between annual growth rates, inter-annual climate variability and environmental conditions. We observed that the climate sensitivity differed between the two species. Spruce, contrary to pine, was negatively impacted by hot summers occurring the year prior to ring formation. For this species, trees located at the high end of the elevation gradient (i.e. upslope trees) were also negatively impacted by warm springs. This translated to negative growth trends for black spruce. Jack pine experienced no change or a slight increase in growth rates

during the past three decades. The second chapter focused on the effect of a drought event that occurred in 1989 on growth and physiology of trees. Here, we showed that trees reacted to drier conditions by increasing iWUE, in particular via a decrease in stomatal conductance. We also observed that a growth decline occurred synchronously with these changes in physiological parameters. This low growth period was longer-lasting for black spruce than for jack pine. Finally, in the third chapter, we focused on the effect of rising atmospheric CO<sub>2</sub> concentrations on trees iWUE. We observed that the CO<sub>2</sub> effect was strongly lowered after removing the effects of tree and stand development. This effect was of higher magnitude for spruce than pine. Site fertility also modified the intensity of the CO<sub>2</sub> effect, which was almost non-existent within the least fertile areas.

Taken together, these results highlight a higher level of stress in black spruce compared to jack pine. From these observations, we can infer that black spruce would be less able to acclimate to warming than jack pine, notably because of its morpho-physiological traits. Our results also suggest that some areas could act as climatic refugia for boreal species. Some tree populations could already be more adapted than others to warmer and drier conditions. These populations would be interesting candidates for assisted migration programs, and additional studies should be conducted e.g. in terms of genetic adaptation (common garden experiments). Based on our results, we recommend a regular monitoring of black spruce stands included in the inventory network, especially the ones that are currently the most productive. Indeed, trees within these productive areas could be those which will experience the greatest impacts of climate change in the future. We also strongly encourage an assessment and an improvement of the analytical methods currently in use. There is a wide range of methods in use, which restrains the comparability of results between studies and could impact conclusions because of some limitations or falsified assumptions. In light of our results, the productivity of black spruce stands could decline over the current century. At the opposite, jack pine stands could maintain their productivity, if their regeneration remains unchanged with a shorter fire cycle (response to changes in fire cycle was not studied here).

Keywords : Climate change, Quebec, boreal forest, *Picea mariana*, *Pinus banksiana*, dendroecology, forest inventories, stable isotopes, water-use efficiency

## INTRODUCTION

### 0.1 Importance de la forêt boréale

Le biome forestier boréal, limité dans ses franges sud et nord par des isothermes de respectivement 18°C et 13°C en juillet, représente approximativement 29% de la superficie forestière mondiale, et 73% des forêts conifériennes. Au Canada, la zone boréale se situe entre ~ 45°N et 70°N (Larsen, 2013) et représente 552 millions d'hectares (Figure 0.1). De ceux-ci, 270 Millions d'hectares sont constitués de forêt boréale continue, soit 22% de la superficie mondiale (Brandt *et al.*, 2013). Le biome forestier boréal est caractérisé par un climat rigoureux, avec des étés courts et frais, des hivers longs et froids, d'importants contrastes de températures, et des précipitations estivales relativement faibles (Brandt *et al.*, 2013). En raison du climat froid et d'une faible proportion d'organismes décomposeurs, la matière organique morte se dégrade lentement et tend à s'accumuler, ce phénomène étant particulièrement accentué dans les zones de mauvais drainage et où l'humidité du sol est élevée (Hobbie *et al.*, 2000). Les écosystèmes forestiers boréaux forment donc un maillon clé du cycle global du carbone, permettant de stocker près de 32% du carbone mondial (Pan *et al.*, 2011). En particulier, 28 Pg de C sont stockés en forêt boréale aménagée au Canada (Kurz *et al.*, 2013), tout spécialement dans les sols organiques (Andrieux *et al.*, 2018 ; Kurz *et al.*, 2013 ; Tarnocai *et al.*, 2009).

Les basses températures, associées à une saison de croissance courte et à des sols pauvres en nutriments directement assimilables, sont autant de facteurs limitant la croissance et les capacités reproductives de la végétation (Black et Bliss, 1980 ; Jarvis

et Linder, 2000). Les forêts boréales sont ainsi relativement peu productives et composées d'un nombre restreint d'espèces ligneuses comparativement aux forêts tempérées et tropicales, ces espèces boréales étant par ailleurs adaptées au climat froid (Brandt, 2009 ; Sakai, 1983). En particulier, la strate arborescente est, au Canada, composée en majorité de conifères appartenant aux genres *Picea*, *Pinus*, *Larix* et *Abies* (Brandt, 2009). Parmi les feuillus, on retrouve principalement les genres *Populus* et *Betula*. Malgré sa faible productivité, la forêt boréale constitue une importante source d'emplois et de matière première pour les industries de pâte à papier et de bois d'œuvre et tient une place majeure dans l'économie du Canada. En effet, en 2017, le secteur forestier a contribué à 1,6% du PIB Canadien, soit 24,6 Milliards de dollars, et employé plus de 200 000 personnes (Ressources Naturelles Canada, 2018).

La majorité des espèces ligneuses boréales possède des traits morpho-physiologiques qui ont été sélectionnés au fil des générations pour assurer leur pérennité au sein d'un paysage façonné par les perturbations naturelles, et en particulier par le feu (Stocks *et al.*, 2002). Ces traits incluent le sérotinisme, c'est-à-dire la production de cônes protégés par une couche de cire qui ne s'ouvrent que sous une forte chaleur comme celle produite par un incendie, une écorce épaisse ou encore une régénération par drageons (Stocks *et al.*, 2002). Le degré d'adaptation des espèces est tel que certaines d'entre elles, comme le pin gris (*Pinus banksiana* Lamb.), sont dépendantes des incendies pour assurer leur régénération (Stralberg *et al.*, 2020). En consommant la matière organique accumulée, le feu rajeunit le sol et rend les conditions propices à la germination et à la croissance des semis (Payette, 1992). Les feux surviennent selon un schéma aléatoire et à différents degrés de sévérité selon le combustible disponible et les conditions climatiques (Whitman *et al.*, 2018). Ce caractère aléatoire contribue à la diversité d'âges et de composition des peuplements composant le paysage forestier boréal (Bergeron *et al.*, 2006; Whitman *et al.*, 2018). Des perturbations de moindre importance, comme les épidémies d'insectes ou les châblis, vont aussi participer, à plus fine échelle et dans une moindre mesure, à cette dynamique. Ces perturbations, dites

secondaires, ont des effets moins drastiques sur les peuplements forestiers et vont contribuer à faire évoluer leur structure et leur composition après le passage d'un feu (McCarthy, 2001). Cette diversité de structure et de composition permet à la forêt boréale d'offrir, outre le captage du carbone et la matière première des industries papetières, de nombreux autres services écologiques aux populations humaines, notamment comme source d'alimentation et de loisirs (Gauthier *et al.*, 2015a).

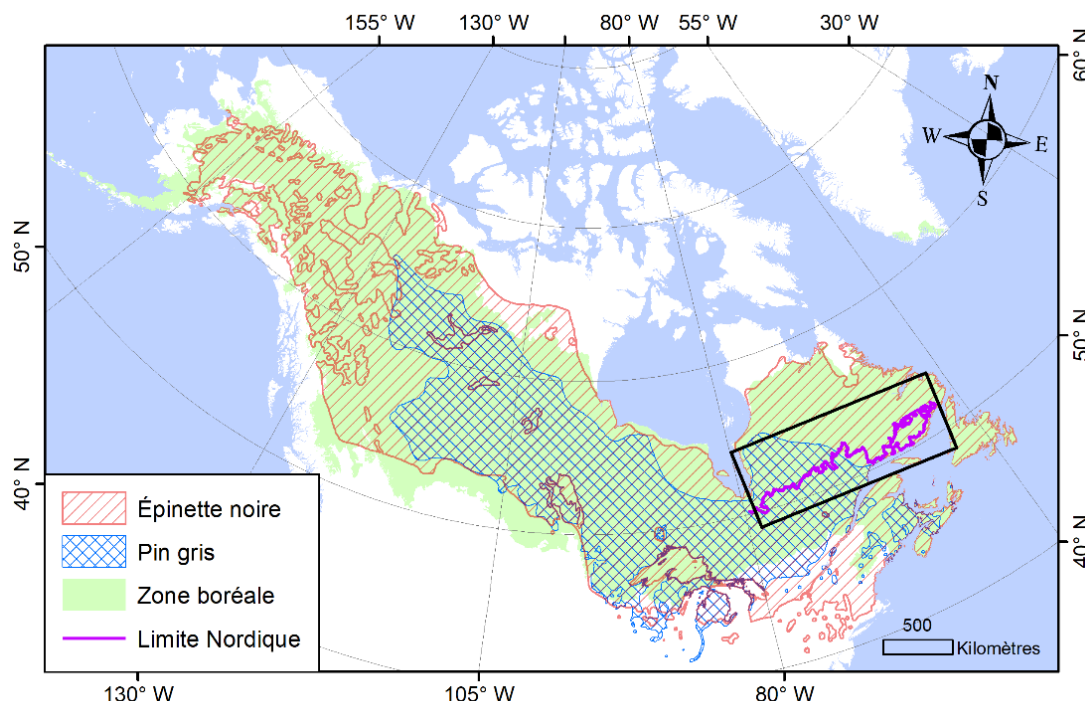


Figure 0.1. Aire d'extension de la zone boréale Nord-Américaine (vert clair; Brandt, 2009), et aires de distribution de l'épinette noire (*Picea mariana* (Mill.) B.S.P.; rayures rouges) et du pin gris (*Pinus banksiana* Lamb.; treillis bleu), deux des espèces conifériennes les plus largement distribuées dans cette zone (source des données: USDA Forest Service, 2002). À droite, le rectangle noir montre la zone d'étude, qui s'étend de part et d'autre de la province du Québec entre le 49<sup>ème</sup> et le 54<sup>ème</sup> degrés de latitude Nord. La ligne violette correspond au tracé de la limite d'attribution des forêts commerciales établie en 2018 au Québec.

## 0.2 Le contexte de la limite nordique des forêts attribuables Québécoises

De façon à assurer la pérennité de l'ensemble des services écologiques fournis aux populations, un aménagement écosystémique des forêts est mis en place au Québec. Celui-ci préconise des pratiques sylvicoles visant à rapprocher la forêt sous aménagement de la forêt naturelle (Gauthier et Vaillancourt, 2008). Ces préconisations suggèrent notamment d'adapter les pratiques sylvicoles dans le but de mimer au mieux l'effet des différentes perturbations naturelles intervenant au sein de la région. Les coupes totales, en particulier les coupes avec protection de la régénération et des sols (CPRS), devraient permettre l'obtention d'un paysage se rapprochant de celui laissé après le passage d'un feu (Belleau *et al.*, 2007 ; Bergeron *et al.*, 2002). Par ailleurs, les coupes partielles devraient aider à l'évolution des peuplements et à l'acquisition d'attributs de vieilles forêts reproduisant les effets des épidémies d'insectes et des châblis (Harvey *et al.*, 2002). Plus spécifiquement, les recommandations se focalisent sur le maintien d'une structure d'âges et de tailles et d'une composition en espèces proches de celles observées en forêt non aménagée (Gauthier et Vaillancourt, 2008). Une attention particulière est notamment portée à la répartition de ces attributs au sein du paysage (Belleau *et al.*, 2007). La conservation d'une proportion de vieilles forêts en adéquation avec le régime de feux historique régional y occupe une place majeure (Bélisle *et al.*, 2011 ; Bergeron *et al.*, 2002). L'objectif sous-jacent de cet aménagement écosystémique est de conserver et augmenter la diversité de structure et de composition des peuplements au sein du paysage forestier boréal, en vue d'améliorer sa résilience aux changements climatiques (Gauthier et Vaillancourt, 2008).

Les contraintes biophysiques des régions nordiques amènent des interrogations quant aux possibilités d'une exploitation des peuplements forestiers situés dans ces zones qui soit compatible avec les objectifs d'un aménagement forestier durable (Jobidon *et al.*, 2015). En particulier, un peuplement forestier, s'il est exploité, doit pouvoir se régénérer de telle façon que sa productivité soit au moins équivalente à celle observée

avant la coupe. Certains peuplements sont plus susceptibles de se régénérer, après feu ou après coupe, en un peuplement caractérisé par une faible densité de tiges et donc peu intéressant d'un point de vue économique. Les peuplements implantés dans les régions où les types de dépôts et le relief sont particulièrement contraignants pour la croissance de la végétation (Robitaille *et al.*, 2015), et dans les zones où le cycle de feux est particulièrement court (Gauthier *et al.*, 2015b) sont particulièrement à risque de se régénérer en un peuplement à faible densité de tiges. En 2002, une limite avait été établie par le Gouvernement du Québec, qui spécifiait jusqu'où il était possible d'exploiter la forêt boréale de façon durable. Or, le tracé de cette limite était basé sur un nombre restreint de données écoforestières. En 2005, un comité scientifique est formé afin d'évaluer cette limite, sur la base de quatre critères biophysiques, à savoir les contraintes liées à l'environnement physique comprenant le relief et le type de dépôt, la capacité du milieu à assurer une production forestière adéquate, cette dernière étant définie à la fois à l'échelle du peuplement et de la tige individuelle, le risque associé aux incendies forestiers et les enjeux en termes de maintien de la biodiversité notamment concernant le caribou forestier (Ministère des Ressources Naturelles du Québec, 2013). Pour ce faire, une étude à large échelle, incorporant des données d'inventaires forestiers, des photographies aériennes et des données satellitaires, est réalisée dans un but d'acquisition de connaissances et de cartographie des attributs biophysiques des forêts nordiques (Ministère des Ressources Naturelles du Québec, 2013). Le facteur de risque associé à chacun des quatre critères biophysiques est déterminé à l'échelle du district écologique, une unité géographique à l'intérieur de laquelle les caractéristiques biophysiques sont homogènes. Des seuils ont été définis qui caractérisent chaque district écologique en fonction de sa sensibilité à l'aménagement forestier pour chacun des quatre indicateurs biophysiques. Basée sur ces seuils, une nouvelle limite d'attribution des forêts commerciales a été délimitée et mise en place à partir de 2018 (voir Figure 0.1). Cependant, les analyses réalisées n'incluaient pas, jusqu'à maintenant, d'information sur la sensibilité des arbres au climat et sur leur réponse aux changements climatiques observés récemment. L'une

des recommandations du rapport du comité scientifique était donc de réévaluer la limite établie lorsque des informations seraient disponibles quant à l'effet des changements climatiques sur la capacité de production des forêts (Ministère des Ressources Naturelles du Québec, 2013).

### 0.3 Effets des changements climatiques sur la forêt boréale

Les activités humaines, et en particulier l'utilisation de combustibles fossiles à des fins énergétiques depuis la seconde moitié du 19<sup>ème</sup> siècle, ont d'ores et déjà induit des changements significatifs dans les conditions environnementales, en modifiant notamment le climat (Allen *et al.*, 2014). Une augmentation des températures de surface consécutive à un accroissement des concentrations en CO<sub>2</sub> atmosphérique de plus de 35% depuis la période d'industrialisation aux alentours de 1850 a été observée à l'échelle mondiale. L'intensité et la rapidité de ces changements sont telles qu'ils ont renversé une tendance au refroidissement enregistrée au cours du dernier millénaire (Kaufman *et al.*, 2009, 2020). Ce réchauffement est d'autant plus intense et rapide aux hautes latitudes, en particulier dans la zone boréale, où une augmentation de 0.5 à 3°C des températures de surface a été enregistrée au cours du 20<sup>ème</sup> siècle, et où une hausse de 4 à 5°C y est attendue d'ici la fin du siècle (IPCC, 2013). Par exemple, dans la zone boréale québécoise, il a été observé une hausse de près de 1°C depuis le début du 20<sup>ème</sup> siècle, et cette tendance est plus forte sur la période 1970-2018 (Figure 0.2). Pour cette même période récente, les précipitations annuelles tendent au contraire à diminuer (Figure 0.2). Il est également prévu des extrêmes climatiques, incluant les épisodes de sécheresse et les vagues de chaleur extrême, plus fréquents, plus intenses, et se produisant plus tôt dans l'année comparativement à ce qui était observé durant la période pré-industrielle (Christidis *et al.*, 2015 ; Vicente-Serrano *et al.*, 2014).

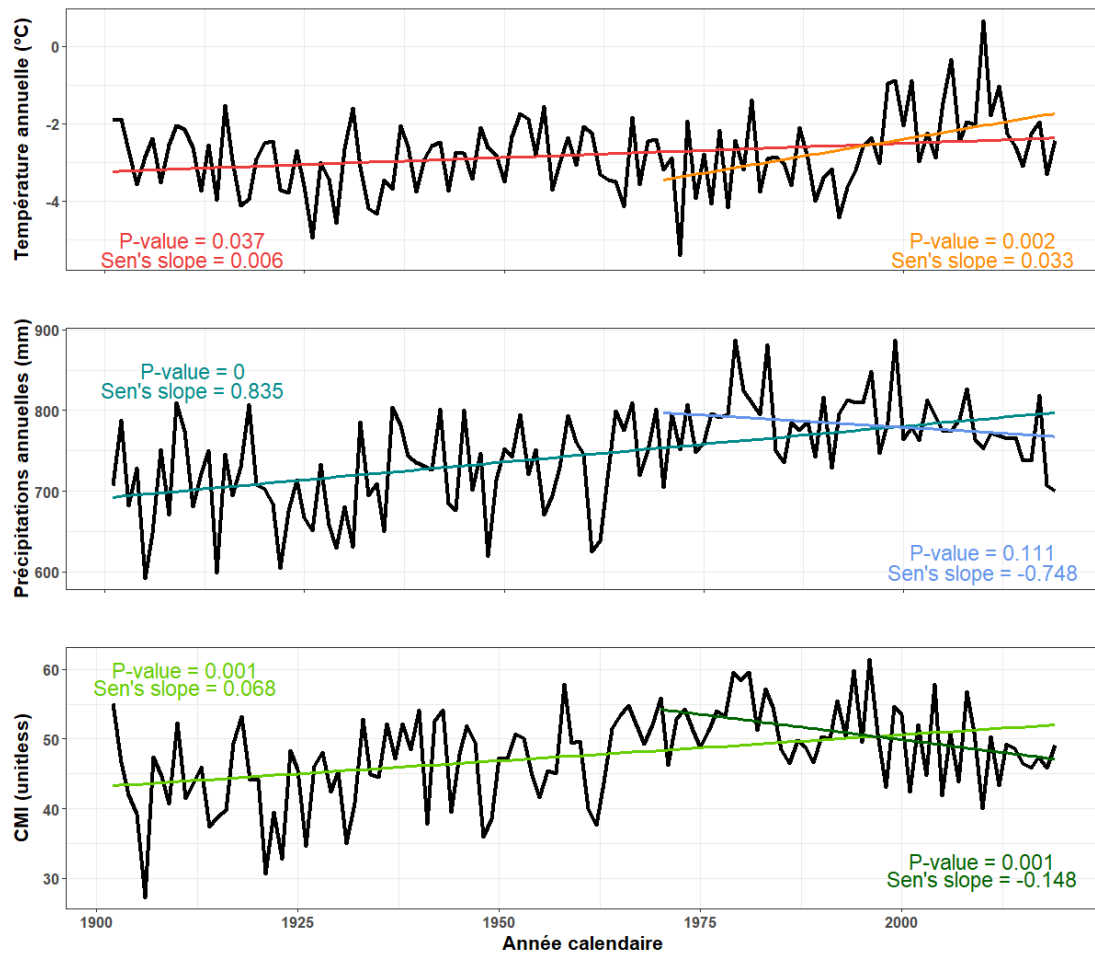


Figure 0.2. Tendances climatiques dans la zone boréale québécoise. Les lignes noires présentent les valeurs médianes de températures annuelles moyennes (panneau du haut), de précipitations annuelles totales (panneau du milieu), et d'un indice de sécheresse, le Climate Moisture Index (CMI, panneau du bas) pour 840 points répartis aléatoirement dans la zone boréale québécoise. Le climat journalier a été extrait sur la période 1901-2019 à partir de BioSIM 11. Les tendances (i.e. régressions des variables climatiques (médianes) au cours du temps; droites colorées) sont présentées pour deux périodes temporelles : 1901-2019 et 1970-2019. La pente (Sen's slope) est également reportée pour chacune des périodes, ainsi que sa p-value (corrigée pour tenir compte de l'autocorrélation temporelle, d'après Yue et Wang (2004)).

Les répercussions de ces modifications dans les moyennes et extrêmes climatiques sur les écosystèmes naturels et sur les organismes vivants qui les composent sont déjà visibles et mesurables. Les arbres, en tant qu'organismes sessiles, sont particulièrement exposés à ces changements, dont les effets sont retracés notamment dans les taux de croissance annuels. Les tendances à l'augmentation des températures et les changements dans la fréquence, l'intensité et la saisonnalité des extrêmes climatiques vont affecter la croissance de l'arbre, *via* des effets sur ses processus physiologiques et sa phénologie. Il était communément admis que des conditions plus chaudes étaient bénéfiques à la croissance des espèces ligneuses boréales en allongeant la période d'activité photosynthétique et en améliorant les taux d'assimilation via une efficacité accrue des enzymes (Charru *et al.*, 2014 ; Kauppi *et al.*, 2014 ; Norby *et al.*, 2003 ; Ols *et al.*, 2020). Un climat plus chaud pourrait aussi accroître les taux de minéralisation de l'azote organique dans les sols boréaux (Guntiñas *et al.*, 2012 ; Lükewille et Wright, 1997). Cette minéralisation plus importante pourrait alors augmenter la capacité d'assimilation des arbres et, par conséquent, leur croissance annuelle (Bonan et Cleve, 1992 ; Melillo *et al.*, 2011 ; Strömgren et Linder, 2002). Une atmosphère plus riche en CO<sub>2</sub> devrait également contribuer à améliorer les taux d'assimilation photosynthétique puisque les arbres seraient à même de capter plus de carbone pour une même quantité d'eau transpirée (Norby et Luo, 2004). Cependant, cette relation n'est pas linéaire, puisqu'il a été observé que l'effet bénéfique de concentrations plus importantes en CO<sub>2</sub> s'amoindrit lorsque ces concentrations deviennent de plus en plus élevées (Dusenge *et al.*, 2020 ; Gill *et al.*, 2002). De plus, les conclusions des études divergent. Certaines études rapportent effectivement une hausse des taux de croissance et de la productivité forestière dans les dernières décennies (Bond-Lamberty *et al.*, 2014 ; Hember *et al.*, 2017). D'autres auteurs n'observent aucun changement significatif (Giguère-Croteau *et al.*, 2019). Enfin, certaines études rapportent, au contraire, une diminution des taux de croissance pour plusieurs espèces et régions (Dietrich *et al.*, 2016 ; Girardin *et al.*,

2014, 2016a, 2016b). Les auteurs attribuent ces affaiblissements de croissance à des stress hydriques et thermiques consécutifs à l'augmentation de la fréquence et de l'intensité des périodes de sécheresse et des vagues de chaleur extrêmes. En effet, des fortes températures peuvent provoquer l'inactivation des enzymes photosynthétiques et freiner le transport d'électrons, réduisant ainsi les taux d'assimilation (Kumarathunge *et al.*, 2020 ; Reich *et al.*, 2018). Les arbres implantés en climat plus froid, qui présentent une moins grande acclimatation aux hautes températures, y sont particulièrement sensibles (Isaac-Renton *et al.*, 2018 ; Way et Sage, 2008b). À ces stress thermiques s'ajoutent les effets du déficit hydrique. L'entrée d'eau dans la vacuole de la cellule juvénile permet son élongation par la pression de turgescence exercée sur la paroi cellulaire (Rossi *et al.*, 2009). De plus, l'eau transportée du sol vers les feuilles véhicule les nutriments et apporte les protons nécessaires aux réactions photochimiques du cycle de la photosynthèse (Körner, 2015 ; Peel, 2013). Ainsi, en cas de déficit hydrique important, le CO<sub>2</sub> capté ne sera pas, ou seulement partiellement, assimilé.

Ces effets négatifs pourraient venir supplanter les effets bénéfiques des changements globaux sur les taux d'assimilation photosynthétiques et donc avoir un impact important sur la productivité de la forêt boréale. En effet, à l'échelle plus large du peuplement forestier, les impacts des stress climatiques se traduisent par des taux de mortalité en augmentation au cours des dernières décennies (Allen *et al.*, 2010 ; Michaelian *et al.*, 2011). Cette plus forte mortalité est le résultat combiné de l'effet direct de la hausse des températures et d'un déficit hydrique plus prononcé sur le métabolisme des arbres et de leurs effets indirects par l'intermédiaire de modifications du cycle des perturbations naturelles. En effet, des conditions plus sèches et plus chaudes peuvent augmenter la fréquence, l'intensité et la sévérité des incendies forestiers et allonger la saison de feux (Terrier *et al.*, 2015). Une augmentation des années de feux extrêmes, c'est-à-dire les années durant lesquelles une proportion exceptionnellement importante du territoire a brûlé, a été observée au Canada (Hanes

*et al.*, 2018). L'année 1989 est notamment caractérisée par la surface brûlée la plus importante enregistrée sur la période 1950-2019 (près de 8 millions d'hectares; Hanes *et al.*, 2018 ; Soja *et al.*, 2007). La hausse des températures peut aussi modifier la phénologie des insectes et autres pathogènes (Pureswaran *et al.*, 2015). Un cycle de vie plus court pourrait favoriser l'occurrence d'épidémies, ainsi que leur remontée plus au nord (Jamieson *et al.*, 2012 ; Logan *et al.*, 2003 ; Parmesan et Yohe, 2003 ; Powell et Bentz, 2009 ; Pureswaran *et al.*, 2015). Des températures plus élevées ont ainsi été associées à une perte de croissance plus marquée et à des dégâts plus importants occasionnés par les pathogènes (Brodde *et al.*, 2019 ; Cortini et Comeau, 2020). Les stress climatiques pourraient alors entraîner une plus forte susceptibilité pour les arbres de succomber aux attaques d'insectes (Jamieson *et al.*, 2012), puisque moins de ressources carbonées sont disponibles pour alimenter les mécanismes de défense et de réparation (De Grandpré *et al.*, 2019). Une diminution de la capacité de régénération des espèces a également été observée ces dernières décennies, résultant potentiellement là-aussi d'effets directs et rétroactifs des changements climatiques (Boucher *et al.*, 2020).

#### 0.4 De l'arbre à la cellule: les stratégies d'adaptation

Les arbres peuvent ajuster certains de leurs paramètres physiologiques de façon à limiter les effets négatifs des stress hydriques et thermiques sur leur croissance. Par exemple, en période de fortes chaleurs et si la ressource en eau est suffisante, les stomates, lieux des échanges gazeux entre la feuille et l'atmosphère, s'ouvrent plus largement pour augmenter la quantité d'eau transpirée et abaisser la température à la surface de la feuille (Urban *et al.*, 2017). En conditions de forte chaleur mais de faible humidité, la tendance sera, inversement, à une fermeture plus prononcée des stomates. La fermeture des stomates permet, en diminuant la quantité d'eau transpirée, de maintenir le potentiel hydrique du xylème et ainsi limiter le nombre de canaux conducteurs rendus inopérants à la suite d'embolies (Brodrribb *et al.*, 2014). La capacité

des arbres à maintenir leurs taux de croissance, à limiter les dégâts au sein de leur réseau hydraulique et donc à survivre aux épisodes climatiques extrêmes dépend de leur stratégie de gestion des échanges gazeux, c'est-à-dire la rapidité et l'intensité avec laquelle ils vont fermer leurs stomates lorsque les conditions deviennent préjudiciables.

Différentes stratégies de gestion des échanges gazeux sont adoptées selon les espèces et les populations. Ces stratégies, dont il est fait référence dans la littérature sous le terme « isohydrie », peuvent être classées le long d'un gradient (Hochberg *et al.*, 2018). Certaines espèces et populations, classées comme « plus isohydriques », vont adopter une stratégie consistant à fermer leurs stomates rapidement lorsque les conditions deviennent chaudes et sèches. Cela limitera les dégâts au xylème mais rendra les arbres plus à risque de mourir d'un manque de ressources pour assurer leur métabolisme de base (« carbon starvation hypothesis »; McDowell et Sevanto, 2010 ; Sala *et al.*, 2010). D'autres espèces et populations, classées comme « plus anisohydriques », vont maintenir leurs stomates ouverts plus longtemps après le début de la période de sécheresse, leur permettant de conserver un apport de carbone élevé, mais les mettant à risque de mourir des suites d'un pourcentage de vaisseaux embolisés trop important (« hydraulic failure hypothesis »; Anderegg *et al.*, 2015a). L'utilisation d'une stratégie plus ou moins proche de l'une ou l'autre des extrémités du gradient d'isohydrie va dépendre, entre autres, des traits d'histoire de vie des espèces et en particulier ceux touchant à l'anatomie du xylème. Ces différences sont conditionnées par l'environnement. Par exemple, la disponibilité en eau et les conditions édaphiques agissent comme facteurs de forçage sur la sélection génétique de traits de résistance à la cavitation (Cochard *et al.*, 2008 ; Maherali *et al.*, 2004). Ainsi, les conifères, étant souvent implantés dans des milieux plus contraignants que les feuillus, présentent des tissus conducteurs plus résistants à la cavitation (Larter *et al.*, 2015 ; Maherali *et al.*, 2004). Plus généralement, les espèces et populations exposées à des conditions plus arides seront moins vulnérables à la sécheresse que celles se retrouvant en milieux où l'humidité n'est habituellement pas limitante (Maherali *et al.*, 2004).

## 0.5 Les cernes de croissances : des indicateurs environnementaux

Une grande majorité des changements dans les conditions environnementales qui influencent la physiologie et la croissance d'un arbre sont retracés dans les cernes que cet arbre forme chaque année. Ainsi, la variabilité inter-annuelle dans les dimensions, la composition chimique et la structure de ces cernes nous renseigne sur les modifications de l'environnement de croissance de l'arbre et dans leur adéquation avec les optimums écologiques de l'espèce (Babst *et al.*, 2018). Par exemple, plus les conditions environnementales sont éloignées des conditions de croissance optimales de l'espèce, plus le cerne produit par l'arbre sera mince. Par ailleurs, les changements dans les processus physiologiques de l'arbre en réponse aux variations de son environnement modifient la composition relative en isotopes stables du carbone et de l'oxygène du bois produit annuellement (Gessler *et al.*, 2014). Il y est fait référence sous le terme de « discrimination » de l'isotope lourd comparativement à l'isotope léger. La discrimination de l'isotope lourd du carbone intervient majoritairement à deux étapes clés des échanges gazeux entre l'arbre et l'atmosphère (Figure 0.3). Premièrement, lors de la diffusion du CO<sub>2</sub> à travers les stomates, les molécules formées d'un atome de carbone plus léger, i.e. <sup>12</sup>CO<sub>2</sub>, diffusent préférentiellement comparativement aux molécules plus lourdes <sup>13</sup>CO<sub>2</sub> selon un rapport de 4,4‰. Le dioxyde de carbone de la chambre sous-stomatiq[ue]ue est ainsi appauvri en <sup>13</sup>C comparativement à la composition chimique de l'atmosphère. Dans un second temps, lors de l'assimilation du carbone sous forme de sucres, les molécules plus légères sont préférentiellement utilisées selon un rapport de 27‰. Les sucres formés sont donc encore appauvris en <sup>13</sup>C comparativement à l'air de la chambre sous-stomatiq[ue]ue. Selon l'intensité avec laquelle l'arbre aura fermé ses stomates, et selon l'efficacité des enzymes contrôlant l'assimilation photosynthétique, le bois produit annuellement pourra donc être plus ou moins appauvri en <sup>13</sup>C (Figure 0.4; Farquhar *et al.*, 1982a). La composition en isotopes stables du carbone du cerne, outre les processus

physiologiques internes à l'arbre, dépend de la composition chimique de l'atmosphère. Le rapport  $^{13}\text{C}/^{12}\text{C}$  de l'atmosphère était relativement constant jusqu'au début de l'industrialisation (~ -6,4%; McC Carroll et Loader, 2004). Or, la consommation d'énergies fossiles et le rejet de CO<sub>2</sub> appauvri en  $^{13}\text{C}$  ont, depuis 1850, conduit à une raréfaction de l'isotope lourd du carbone dans l'atmosphère (Keeling, 1979 ; Tans *et al.*, 1979). Ce phénomène, dont il est fait référence sous le terme « Suess effect » dans la littérature scientifique, est relativement bien connu et documenté (Keeling, 1979). Il est alors possible de corriger la composition isotopique du carbone des cernes de croissance pour la rendre relativement indépendante de toute influence environnementale directe (Keeling, 1979 ; McC Carroll et Loader, 2004). Elle est donc uniquement sous l'influence directe des deux mécanismes physiologiques majeurs gouvernant la croissance des arbres, à savoir la conductance stomatique et l'assimilation photosynthétique. Cette relation permet alors d'approximer l'efficience d'utilisation de l'eau d'un arbre, correspondant au rapport entre le carbone assimilé et l'eau transpirée, à partir du ratio  $^{13}\text{C}/^{12}\text{C}$  des cernes annuels de croissance (Farquhar *et al.*, 1982a ; Gessler *et al.*, 2014 ; Medrano *et al.*, 2015).

D'autre part, les molécules d'eau formées de l'isotope léger de l'oxygène, i.e. H<sub>2</sub><sup>16</sup>O, sont préférentiellement transpirées au détriment des molécules plus lourdes H<sub>2</sub><sup>18</sup>O (Figure 0.3). Ainsi, plus l'arbre aura fermé ses stomates avec intensité, par exemple en réponse à un épisode de sécheresse long et intense, plus l'eau restant disponible pour la formation de la cellulose sera riche en <sup>18</sup>O (Figure 0.4). Le signal isotopique du bois retranscrit donc celui de l'eau dans la feuille avec un enrichissement de ~27‰ et un bruit additionnel lié à l'effet Péclet, c'est à dire la diffusion inverse d'eau enrichie en <sup>18</sup>O vers le xylème, et aux échanges d'atomes d'oxygène avec l'eau véhiculée par le xylème (Sternberg *et al.*, 1986). Cette relation permet alors d'utiliser le ratio  $^{18}\text{O}/^{16}\text{O}$  comme approximation des changements intervenus dans la conductance stomatique des arbres au cours du temps (Gessler *et al.*, 2014 ; McC Carroll et Loader, 2004). Néanmoins, la composition en isotopes de l'oxygène d'un cerne retranscrit aussi, en partie, la

signature isotopique de facteurs externes. Ceux-ci incluent la composition isotopique des précipitations qui elle-même dépend de la température (et varie ainsi spatialement et temporellement), et la discrimination ayant lieu lors de l'évaporation de l'eau au niveau du sol, les couches profondes du sol présentant une eau moins enrichie en  $^{18}\text{O}$  que les couches superficielles (Brienen *et al.*, 2012 ; Xu *et al.*, 2020). Ces facteurs sont difficilement mesurables directement et doivent être estimés, ou encore leurs effets doivent être supposés constants entre les arbres et les années. Malgré ces incertitudes, le ratio en isotopes stables de l'oxygène des cernes de croissance est souvent mesuré en parallèle du ratio isotopique du carbone afin de mieux cerner les changements intervenus dans la conductance stomatique indépendamment de ceux ayant eu lieu dans les taux d'assimilation photosynthétique des arbres (Gessler *et al.*, 2014 ; McCarroll et Loader, 2004 ; Scheidegger *et al.*, 2000).

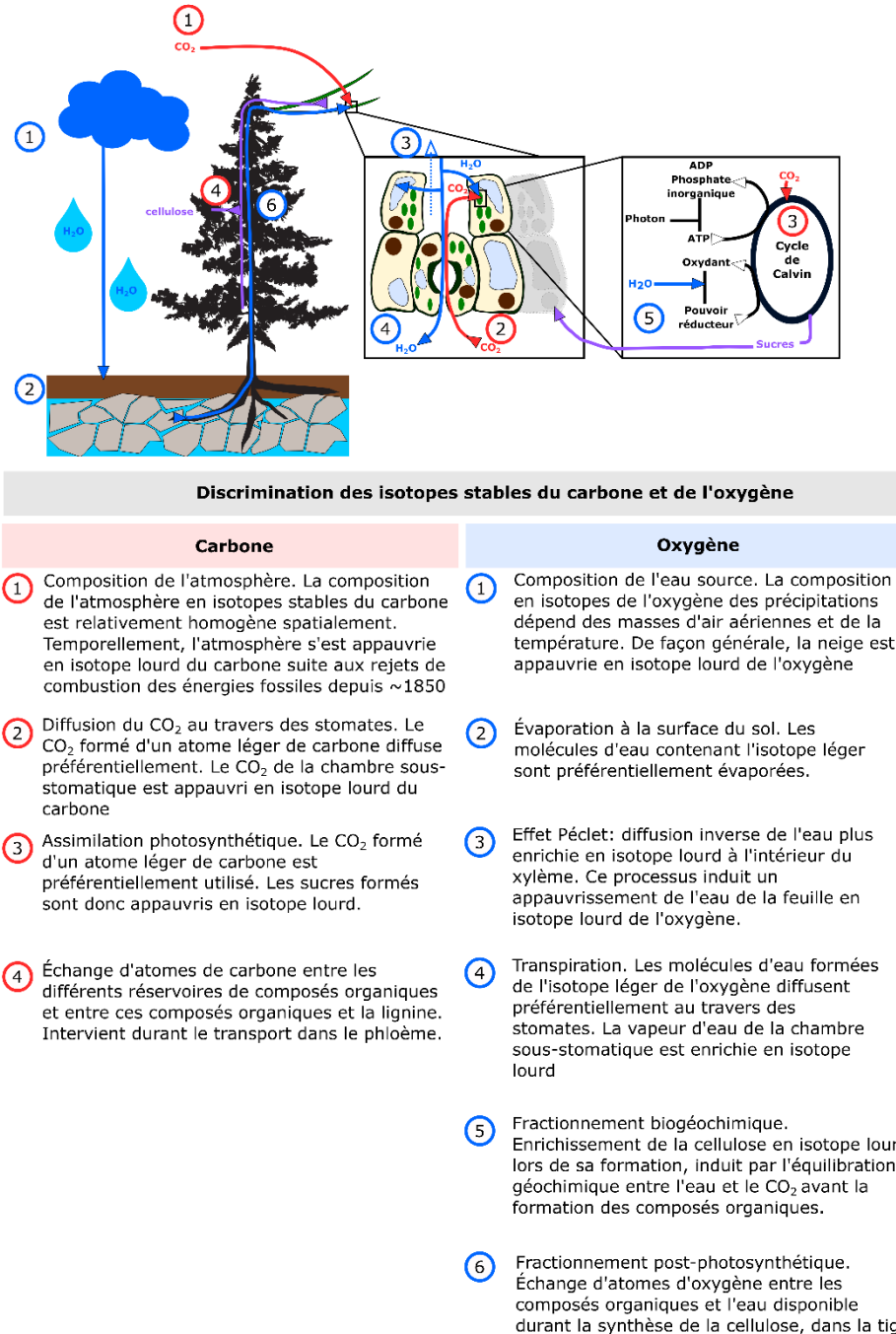


Figure 0.3. Principales étapes durant lesquelles une discrimination des isotopes lourds du carbone et de l'oxygène intervient. Modifié de McC Carroll & Loader (2004).

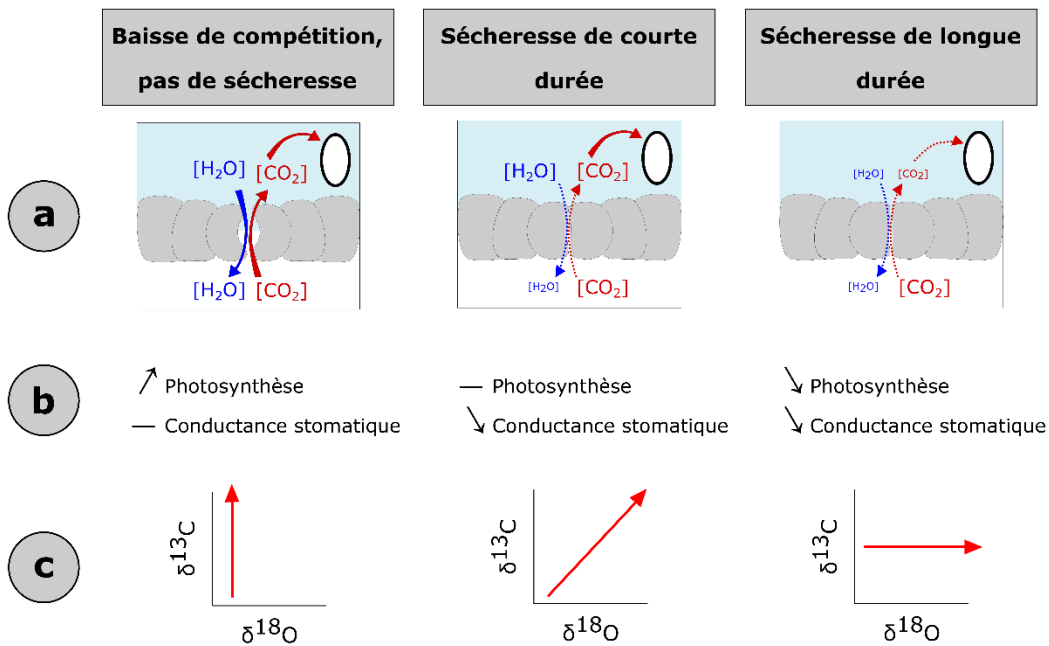


Figure 0.4. Trois scénarios de changements des conditions de croissance des arbres, et les modifications induites sur (a) l'ouverture des stomates, les concentrations internes en eau et en CO<sub>2</sub>, (b) les taux de photosynthèse et la conductance stomatique, et (c) les rapports isotopiques du carbone ( $\delta^{13}\text{C}$ ) et de l'oxygène ( $\delta^{18}\text{O}$ ). Adapté de Scheidegger et al. (2000).

## 0.6 Territoire d'étude, base de données utilisée, et espèces étudiées

Cette thèse repose sur un ensemble de données compilé par le Ministère des Forêts, de la Faune et des Parcs du Québec (MFFPQ) dans le cadre du Programme d'Inventaire Écoforestier Nordique (PIEN). Au cours de cet inventaire, 875 placettes-échantillon temporaires ont été délimitées, couvrant le Québec d'est en ouest entre le 49<sup>ème</sup> et le 54<sup>ème</sup> parallèles de latitude nord (Létourneau *et al.*, 2008). Le territoire couvert est représenté par des peuplements non aménagés régénérés après feu, en majorité composés de conifères. Ce territoire intersecte trois grands domaines bioclimatiques : la pessière à mousses de l'est, la pessière à mousses de l'ouest et la pessière à lichens. Le réseau de placettes couvre un large gradient longitudinal, englobant des conditions environnementales relativement contrastées. Le climat est, en général, plus chaud et plus sec à l'ouest, induisant un cycle de feu plus court. Les conditions édaphiques et physiographiques diffèrent également le long du gradient. À l'ouest, le paysage est quasiment dépourvu de relief et caractérisé par des sols mal drainés riches en matière organique. Au centre du gradient, le relief est le plus prononcé et le territoire caractérisé par des dépôts de till. La zone la plus à l'est se distingue par un paysage vallonné et des dépôts rocheux ou de moraines (Robitaille *et al.*, 2015). Diverses données écologiques et dendrométriques ont été recueillies au sein des placettes-échantillon, dont des données édaphiques, le diamètre à hauteur de poitrine (DHP) et la taxonomie des arbres de plus de 9 cm de DHP. Entre un et trois arbres dominants ou co-dominants ont été échantillonnés par placette et essence en vue d'analyser la dynamique temporelle de croissance des différentes espèces. Il est à noter que, bien que très étendu à l'échelle de la province québécoise, le réseau de placettes ne couvre qu'une petite partie du gradient climatique inclus dans l'aire de répartition des deux espèces (Figure 0.5).

Les données et échantillons de cet inventaire ont été initialement amassés dans un but de production de cartes descriptives des attributs biophysiques de la région boréale

nordique dans le cadre de l'évaluation de la limite nordique des forêts attribuables (Jobidon *et al.*, 2015). L'inventaire écoforestier nordique a permis de compléter le réseau de placettes-échantillon permanentes de l'inventaire provincial, dont la couverture était limitée au sud de l'ancienne limite nordique d'aménagement des forêts. Ces données constituent également une base idéale pour étudier les effets des changements climatiques récents sur la croissance et la physiologie des arbres en milieu naturel. De telles analyses constituaient l'une des recommandations du comité scientifique chargé de l'évaluation de la limite nordique des forêts, afin d'obtenir une image plus précise de la sensibilité du territoire à l'aménagement forestier dans les conditions environnementales futures.

La thèse est focalisée sur les deux essences majoritaires dans cette zone à savoir l'épinette noire et le pin gris, représentant respectivement 78% et 15% du total des arbres échantillonnés. Ces deux espèces, d'importance commerciale majeure, présentent des différences morpho-physiologiques marquées qui pourraient influencer leur sensibilité au climat et leur réponse aux changements globaux. Le système racinaire de l'épinette noire est en effet restreint aux premiers centimètres de sol, essentiellement dans la couche organique. Ce système racinaire est composé en majorité de racines adventives, des racines formées au-dessus du collet racinaire de l'arbre, qui sont une adaptation de l'espèce à des sols généralement mal drainés et gorgés d'eau (Burns et Honkala, 1990). Chez le pin, même si la majorité des racines se situe également dans les couches supérieures du sol, une racine pivot permet aux arbres un meilleur ancrage et un accès aux ressources en eau et en nutriments situées plus en profondeur dans le sol minéral (Burns et Honkala, 1990). Le pin se retrouve par ailleurs sur des sites plus drainants et à composante sableuse, contrairement à l'épinette qui est une espèce plutôt généraliste au regard des conditions édaphiques des sites qu'elle occupe. Les deux espèces présentent également différents modes de reproduction. Chez l'épinette, les cônes semi-sérotineux et une reproduction végétative par marcottage permettent à l'espèce de se maintenir même dans les régions où le cycle de feux est

relativement long. Le pin, au contraire, produit des cônes dont l'extrême majorité sont sérotineux et ne possède aucun mode de reproduction végétative, ce qui le rend dépendant de l'occurrence des feux pour sa régénération. Au Québec, cette espèce est restreinte à la portion ouest de la province, où le cycle de feux est plus court, tandis que l'épinette est présente sur toute la largeur de la zone boréale nord-américaine (Figure 0.1 et 0.5).

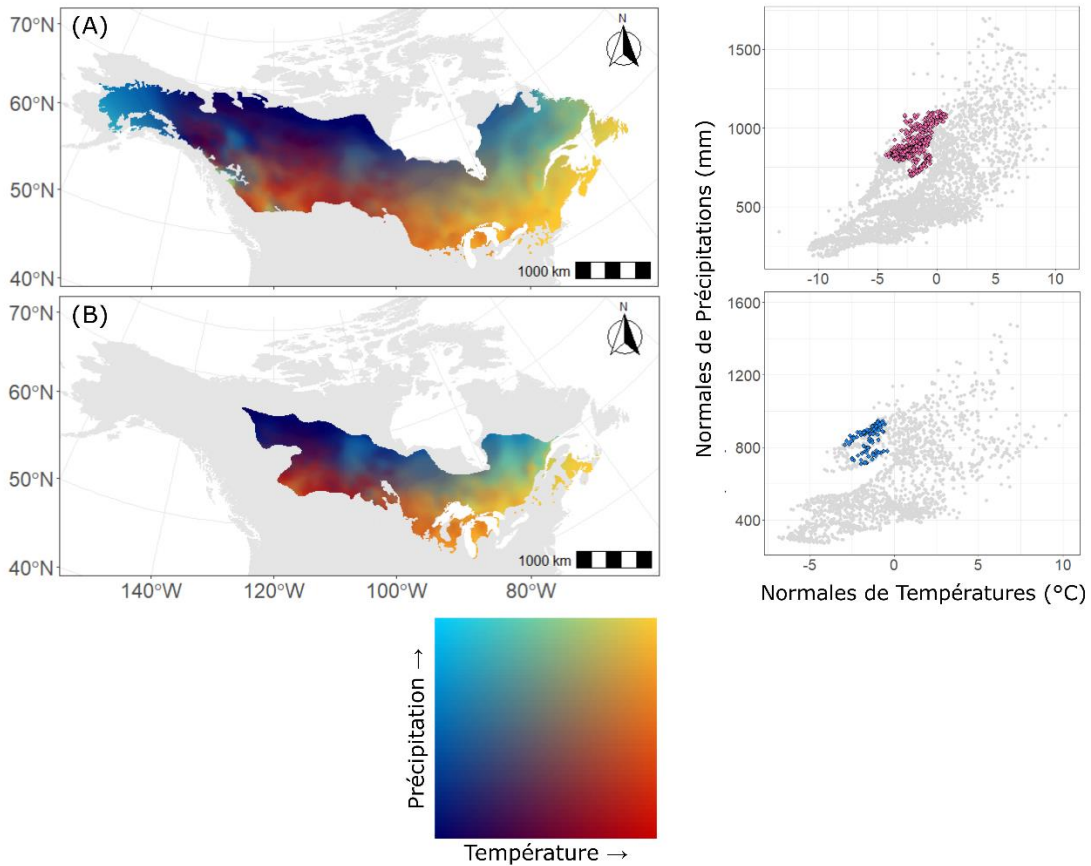


Figure 0.5. Enveloppes climatiques des deux espèces. À gauche : cartes bivariées présentant la variabilité des normales 1981-2010 de températures et de précipitation à l'intérieur de l'aire de répartition de l'épinette noire (A) et du pin gris (B). L'échelle est en percentiles : les régions les plus chaudes et sèches sont représentées en rouge; celles les plus froides et humides en bleu clair ; et celles caractérisées par des conditions plus chaudes et plus humides sont représentées en jaune. À droite : biplots des normales de température et de précipitation. Les points gris représentent des localisations réparties tous les 0.5 degrés à travers l'aire de répartition des espèces. Les points colorés représentent les normales climatiques (température et précipitations, sur la période 1981-2010) des placettes-échantillon. Le climat a été extrait à partir de BioSIM 11.

## 0.7 Objectifs généraux et structure de la thèse

L'objectif de cette thèse est d'étudier les effets des changements climatiques intervenus depuis la période d'industrialisation sur la physiologie et la croissance de l'épinette noire et du pin gris en forêt boréale québécoise. Pour ce faire, nous avons estimé les changements intervenus dans les taux de croissance et la physiologie des arbres que nous avons approximés par des mesures des dimensions et de la composition chimique des cernes de croissance. Plus spécifiquement, la largeur des cernes a été utilisée pour évaluer l'accroissement annuel radial des arbres. Par ailleurs, le ratio isotopique du carbone a été employé pour estimer l'efficience d'utilisation de l'eau, à savoir le rapport entre la quantité de carbone assimilée et la quantité d'eau transpirée par un arbre. Enfin, le ratio isotopique de l'oxygène a été mesuré en complément de celui du carbone pour évaluer les changements intervenus dans la conductance stomatique des arbres indépendamment de ceux ayant eu lieu dans leur taux d'assimilation photosynthétique. Selon les hypothèses et objectifs, nous avons étudié la croissance, l'efficience d'utilisation de l'eau et la conductance stomatique sur différentes périodes temporelles (Figure 0.6). Le but global de ce travail de thèse est d'avoir une vision à large échelle spatiale de la capacité des deux espèces à s'adapter à un environnement plus chaud et plus sec, comme celui prévu dans les prochaines décennies par les modèles climatiques.

La présente thèse est subdivisée en trois chapitres. Dans le premier chapitre, intitulé "Taxonomy, together with ontogeny and growing conditions, drives needleleaf species' sensitivity to climate in boreal North America", l'objectif est de vérifier quelles ont été les trajectoires de croissance des arbres au sein de notre zone d'étude entre 1970 et 2005, et quels facteurs environnementaux les ont influencées. Pour répondre à cet objectif, les trajectoires de croissance sont calculées, à l'échelle de la placette-échantillon et pour chaque espèce, à partir des largeurs de cernes annuels. La sensibilité des arbres au climat est ensuite déterminée par placette et espèce. Enfin, l'effet de

divers paramètres environnementaux, incluant des paramètres liés à l'ontogénie, à la compétition, à la physiographie, aux conditions édaphiques et au climat régional, sur la sensibilité des arbres au climat est déterminé au sein de chacun des trois domaines bioclimatiques recouvrant notre zone d'étude.

L'objectif du second chapitre, intitulé “High stomatal limitation on photosynthesis as a driver of drought-induced growth decline in boreal conifers”, est de déterminer si une perte de croissance observée entre 1989 et 1992 pour les deux espèces sur notre zone d'étude est couplée à une réponse physiologique des arbres à un épisode de sécheresse extrême ou à une vague de chaleur. Pour ce faire, le ratio en isotopes stables du carbone et de l'oxygène est mesuré pour chaque cerne de la période 1985-1993 sur un sous-échantillon de 144 arbres (81 arbres pour l'oxygène). Les ratios isotopiques sont comparés entre les années, et mis en relation avec le climat de la saison de croissance correspondante.

Enfin, le dernier chapitre, intitulé “Strong overestimation of water-use efficiency responses to rising CO<sub>2</sub> in tree-ring studies” a pour objectif principal de tester l'effet de l'augmentation de la concentration en CO<sub>2</sub> atmosphérique sur l'efficience d'utilisation de l'eau des arbres. L'efficience d'utilisation de l'eau est estimée sur un sous-échantillon de 148 arbres à partir du ratio en isotopes stables du carbone des cernes de croissance, sur la période 1783-2004. Dans ce chapitre, l'aspect méthodologique est particulièrement important, puisque l'effet CO<sub>2</sub> est estimé avant et après avoir tenu compte de plusieurs variables pouvant intervenir en parallèle du CO<sub>2</sub> sur l'efficience d'utilisation de l'eau, comme la taille de l'arbre, l'âge du peuplement, le climat estival, les dépositions azotées et la fertilité du site. Les résultats de trois modèles statistiques différents sont comparés et discutés.

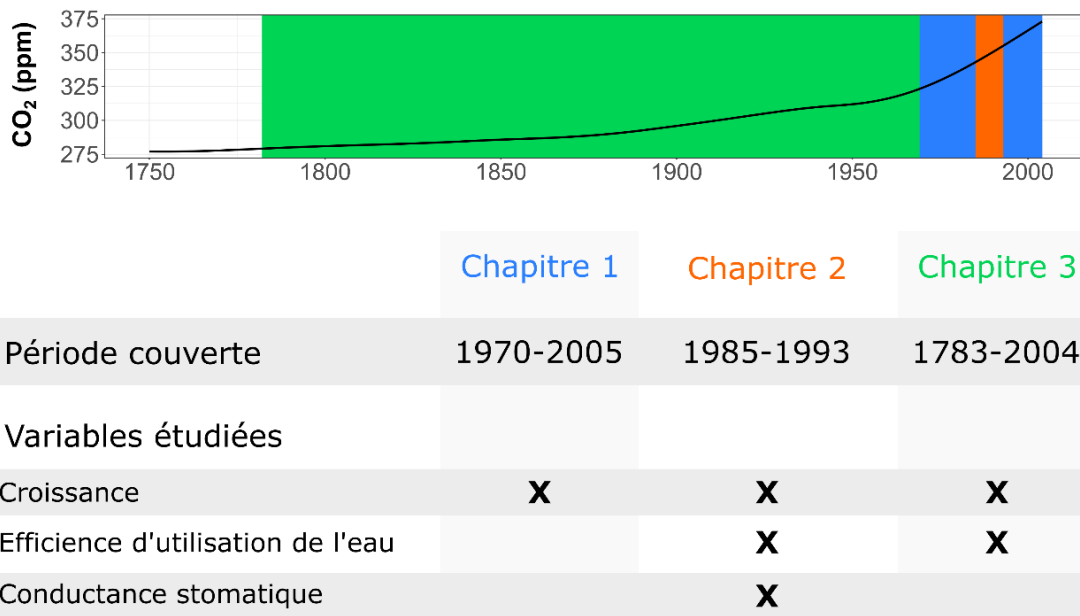


Figure 0.6. Différentes périodes temporelles étudiées selon les trois chapitres de la thèse, superposées sur l'évolution de la concentration en CO<sub>2</sub> atmosphérique depuis la période pré-industrielle (pré-1850). Les différentes variables réponses étudiées pour chaque chapitre sont aussi résumées.

## CHAPITRE I

# TAXONOMY, TOGETHER WITH ONTOGENY AND GROWING CONDITIONS, DRIVES NEEDLELEAF SPECIES' SENSITIVITY TO CLIMATE IN BOREAL NORTH AMERICA

William Marchand<sup>1, 2</sup>, Martin P. Girardin<sup>1, 2</sup>, Henrik Hartmann<sup>3</sup>, Sylvie Gauthier<sup>1, 2</sup>,  
Yves Bergeron<sup>2</sup>

<sup>1</sup>Natural Resources Canada, Canadian Forest Service, Laurentian Forestry Centre,  
1055 du P.E.P.S, P.O. Box 10380, Stn. Sainte-Foy, Québec, QC, Canada; <sup>2</sup>Centre  
d'étude de la forêt, Université du Québec à Montréal, C.P. 8888, succ. Centre-ville,  
Montréal, QC, H3C 3P8, Canada; and Forest Research Institute, Université du Québec  
en Abitibi-Témiscamingue, 445 boul. de l'Université, Rouyn Noranda , QC, Canada;

<sup>3</sup>Max-Planck Institute for Biogeochemistry, Department of Biogeochemical Processes,  
Hans-Knöll Str. 10, 07745 Jena, Germany

\*Auteur correspondant: William Marchand. Email: [william.marchand@uqat.ca](mailto:william.marchand@uqat.ca)

Publié dans Global Change Biology (2019) 25: 2793– 2809

<https://doi.org/10.1111/gcb.14665>

## Résumé

Il n'y a, actuellement, aucun consensus quant à la manière dont les changements dans les conditions climatiques vont affecter la croissance de la forêt boréale, où le réchauffement est plus rapide que dans les autres biomes. Certaines études suggèrent des effets négatifs dus aux stress climatiques, alors que d'autres apportent des preuves de taux de croissance en hausse induits par une saison de croissance plus longue. Les études s'intéressant aux effets des conditions environnementales sur les relations croissance-climat sont, en général, limitées à des aires d'étude de dimensions restreintes qui n'incluent pas l'ensemble de la gamme de variabilité des conditions environnementales. Ces études fournissent donc une compréhension limitée des processus en jeu. Nous avons étudié comment les variations environnementales et l'ontogénie ont modulé les tendances de croissance et les relations croissance-climat de l'épinette noire (*Picea mariana*) et du pin gris (*Pinus banksiana*) en utilisant un jeu de données fortement répliqué spatialement provenant d'un réseau de placettes d'inventaire forestier. Nous avons quantifié les tendances de croissance à long terme à l'échelle de la placette-échantillon en nous basant sur l'analyse de mesures de largeurs de cernes de 2266 arbres. Nous avons évalué la relation entre les taux de croissance annuels et les variables climatiques saisonnières. Nous avons évalué les effets de plusieurs variables explicatives sur les tendances de croissance à long terme et sur les relations croissance-climat. Ces dernières étaient toutes deux spécifiques à l'espèce et spatiallement hétérogènes. Alors que la croissance du pin gris a à peine augmenté au cours de la période d'étude, nous avons observé une diminution de la croissance de l'épinette. Cette baisse de croissance était plus prononcée pour les peuplements les plus vieux. Ce déclin était potentiellement du à un rapport négatif entre les gains de croissance directs induits par une meilleure photosynthèse durant les conditions estivales plus chaudes que la moyenne et la perte de croissance intervenant l'année suivante en raison de l'effet indirect des vagues de chaleurs à la fin de l'été sur l'accumulation des réserves carbonnées. Pour les peuplements les plus en élévation, les

dégâts provoqués par les gels tardifs durant les printemps plus doux que la moyenne pourraient constituer un facteur de stress additionnel pour les arbres. La compétition et les facteurs édaphiques ont aussi modifié la sensibilité au climat, ce qui suggère que les effets des changements climatiques seront fortement hétérogènes à travers le biome boréal.

Mots-clés : Forêt boréale, Canada, changements climatiques, stress climatiques, dendroécologie, Québec

## Abstract

Currently, there is no consensus regarding the way that changes in climate will affect boreal forest growth, where warming is occurring faster than in other biomes. Some studies suggest negative effects due to drought-induced stresses, while others provide evidence of increased growth rates due to a longer growing season. Studies focusing on the effects of environmental conditions on growth-climate relationships are usually limited to small sampling areas that do not encompass the full range of environmental conditions; therefore, they only provide a limited understanding of the processes at play. Here, we studied how environmental conditions and ontogeny modulated growth trends and growth–climate relationships of black spruce (*Picea mariana*) and jack pine (*Pinus banksiana*) using an extensive dataset from a forest inventory network. We quantified the long-term growth trends at the stand scale, based on analysis of the absolutely dated ring-width measurements of 2,266 trees. We assessed the relationship between annual growth rates and seasonal climate variables and evaluated the effects of various explanatory variables on long-term growth trends and growth-climate relationships. Both growth trends and growth-climate relationships were species-specific and spatially heterogeneous. While the growth of jack pine barely increased during the study period, we observed a growth decline for black spruce which was more pronounced for older stands. This decline was likely due to a negative balance between direct growth gains induced by improved photosynthesis during hotter-than-average growing conditions in early summers and the loss of growth occurring the following year due to the indirect effects of late-summer heat waves on accumulation of carbon reserves. For stands at the high end of our elevational gradient, frost damage during milder-than-average springs could act as an additional growth stressor. Competition and soil conditions also modified climate sensitivity, which suggests that effects of climate change will be highly heterogeneous across the boreal biome.

Keywords: Boreal forest, Canada, climate change, climate-induced stress, dendroecology, Quebec

## 1.1 Introduction

The boreal biome is warming faster than other regions of the world (IPCC, 2013). As a result of a 35 % increase in atmospheric CO<sub>2</sub> concentrations relative to pre-industrial conditions, mean annual air temperature has risen by 0.5 to 3 °C in boreal North America and an additional increase of 4-5 °C is expected by 2100 (Price *et al.*, 2013). Climate change threatens the ecological, social and economic services that boreal forests provide (Gauthier *et al.*, 2015a). It is also unclear whether boreal forests will continue to act as a carbon sink or will shift to become a carbon source (Kurz *et al.*, 2013), thereby renewing the scientific focus on boreal forest ecosystems and on their ability to cope with, and to mitigate, global warming. As a proxy for tree vigour, secondary growth can be used to study the response of trees to a changing climate and, thus, to assess current and future trajectories of the boreal forest.

In the Northern Hemisphere, evidence of increased mortality rates and decreases in tree growth and forest productivity is accumulating, not only for the interior of the boreal forest (Cahoon *et al.*, 2018 ; Girardin *et al.*, 2016a ; Hember *et al.*, 2016 ; Zhu *et al.*, 2016), but also at its northern edge (D'Arrigo *et al.*, 2004). These 'negative' trends were linked, amongst other factors, to heat and hydric stresses resulting from rising temperatures and more frequent, longer-lasting, and harsher drought episodes (Barber *et al.*, 2000 ; Girardin *et al.*, 2016a ; Juday et Alix, 2012 ; Nicklen *et al.*, 2018 ; Trugman *et al.*, 2018 ; Zhang *et al.*, 2008). In contrast, other studies provided strong evidence for increased growth rates and higher stand productivity (Beck *et al.*, 2011 ; Girardin *et al.*, 2011 ; Hember *et al.*, 2017). These 'positive' trends, which were observed mainly for the northernmost forested area, namely, the taiga, were likely due to higher rates of carbon assimilation and a longer growing season (Gennaretti *et al.*, 2014 ; Ju et Masek, 2016). These contrasting observations demonstrate uncertainties regarding the persistence of the existing structure, composition and function of the boreal biome under future warmer and dryer climatic conditions.

Tree sensitivity to climate is highly variable across the globe and is modulated by environmental drivers that vary at local to global scales (Babst *et al.*, 2012b ; Girardin *et al.*, 2016a). Amongst these drivers, topography creates spatially heterogeneous macroclimatic conditions and can modify the way that trees respond to changes in regional climate (Hasler *et al.*, 2015 ; Matías *et al.*, 2017). For example, in Central Europe, water-limited lowland forests are more sensitive to drought, whereas forests in the upland portion of the elevational gradient are primarily temperature-limited (Altman *et al.*, 2017) and can benefit from stronger and faster warming, which is expected for mountainous areas (Pepin *et al.*, 2015). More specifically, higher mean summer temperatures could improve the growth of trees at the high end of the elevational gradient by increasing the number of wood cells that are produced annually through improved xylogenetic processes and hydraulic performance (Castagneri *et al.*, 2015 ; Dulamsuren *et al.*, 2017). In contrast, some studies have observed decreased growth rates, even for trees growing in mountainous sites in both central Europe and North America (Dittmar *et al.*, 2003 ; McLaughlin *et al.*, 1987 ; Piovesan *et al.*, 2008), which questions the capacity of high-elevation forested ecosystems to better cope with climate change (Austin et Niel, 2011).

The annual growth performance of a tree is linked to its ability to access optimal amounts of water, light and nutrients (Fritts, 1971), the availability of which is primarily controlled by site-specific abiotic factors, such as soil conditions (e.g., Hember *et al.*, 2017). Soil structure, drainage and thickness of the organic layer determine soil water-holding capacity (Minasny et McBratney, 2017) and drive nutrient cycling (e.g., Cavard *et al.*, 2018). In addition to its direct effects on tree growth, soil moisture content alters microclimate and, thus, evapotranspiration rates, which may modulate growth-climate relationships (Manrique-Alba *et al.*, 2017). By modifying resource availability, inter-individual competition can exacerbate tree sensitivity to harsh climatic conditions (e.g. Buechling *et al.*, 2017 ; Ford *et al.*, 2016 ; Gleason *et al.*, 2017 ; Jiang *et al.*, 2018 ; Nicklen *et al.*, 2018), or buffer growth gains

from favourable periods (Cortini *et al.*, 2012). Ultimately, the capacity of a tree to efficiently use resources will also dictate its response to climate (e.g., Carrer et Urbinati, 2004). Apart from genotype-driven differences, ontogeny-related changes in a tree's physiological needs and in the efficiency of its hydraulic network (Ryan *et al.*, 2006) can modify its sensitivity to climate (e.g., Altman *et al.*, 2017).

The high spatial variability in growing conditions that is encountered in boreal forests, together with the multiplicity of interacting effects and feedbacks of environmental variables that are present, hinder our understanding of the response of boreal forest trees to climate. In regions with geographically limited and sparsely replicated sample networks (Gewehr *et al.*, 2014), assessing climate effects on tree growth is very difficult (but see Girardin *et al.*, 2016a), given that field-based measurements do not cover the full range of variation in growing conditions. Some studies in western boreal North America and boreal Europe have examined variations in growth-climate relationships along latitudinal and longitudinal gradients (Lloyd *et al.*, 2011) or between sites with different slope directions (i.e. north vs south facing sites; Johnstone *et al.*, 2010 ; Walker et Johnstone, 2014) and moisture conditions (Walker et Johnstone, 2014 ; Wilmking et Myers-Smith, 2008). However, studies testing the effect of elevation gradient on the trees sensitivity to climate are lacking, particularly in the eastern boreal North America. Furthermore, most past studies have focused upon the direct effects of abiotic or biotic factors on tree growth, while the feedback effects of environmental conditions on growth-climate relationships are still rarely described (But see Nicklen *et al.*, 2016, 2018 for the Pacific Coast of North America).

Here, we used an extensive and well-replicated provincial inventory network that provides absolutely dated and annually resolved tree-growth data, as well as site-specific environmental information for unmanaged forests in eastern boreal North America. This network is located at the boundary between the interior boreal forest and the taiga, and includes sample plots characterized by highly contrasting growing

conditions. Our overall objective was to examine whether the potential impacts of recent changes in climate varied as functions of explanatory variables with respect to the growth of two needleleaf species that are broadly distributed across North America, black spruce (*Picea mariana* (Miller) B.S.P.) and jack pine (*Pinus banksiana* Lambert). We first quantified the recent growth trends for the two species which, given the high variability in growing conditions, were expected to be heterogeneous across the study zone. Then, we determined the climate sensitivity of the two species, i.e., the relationship between inter-annual variation of secondary growth rates and fluctuations in seasonal values of mean temperature and total precipitation over the period 1970-2005. We hypothesized that the growth of both species would be negatively impacted by higher-than-average temperature during summer and positively affected by higher-than-average temperature during spring and by higher-than-average precipitation during summer. Finally, we assessed how explanatory variables (e.g. climate, competition and soil conditions) affected spatial variability in growth-climate relationships. We hypothesized that the negative effect of hotter- and dryer-than-average summers, as well as the positive effect of high spring temperature on tree growth, would be exacerbated in stands in the upper portion of the elevational gradient because of soil conditions (e.g. higher slope and rocky substrate) prone to a faster drainage. We also hypothesised that old stands, as well as trees growing in a highly competitive environment and in well-drained sites, would respond more negatively to summer heatwaves.

## 1.2 Materials and methods

### 1.2.1 Sampling area

Our sampling network covered three degrees of latitude ( $50.25\text{-}53.25^{\circ}\text{N}$ ) and nearly extended across the entire Province of Quebec (Canada) from east to west ( $57.5\text{-}78.25^{\circ}\text{W}$ ). It was located in the boreal biome, which is characterised by needleleaf-

dominated forests (Robitaille *et al.*, 2015). Some regional patterns of climatic conditions, dominant vegetation and natural disturbance regimes make it possible to divide this wide biome into bioclimatic domains (Ansseau *et al.*, 1997). In the north portion of the region, the spruce-lichen bioclimatic domain is characterised by a harsh, cold and dry climate, resulting in an open black spruce-dominated forest with a lichen mat, i.e., the taiga vegetation subzone. South of the 52<sup>nd</sup> parallel, continuous boreal forest that is composed mostly of pure black spruce stands covers the spruce-moss bioclimatic domain. The later is subdivided into western and eastern zones based on precipitation patterns and fire cycles. The western part is drier and, consequently, more prone to wildfire than the eastern zone (Gouvernement du Québec, 2003). Within these three main bioclimatic domains, hereafter referred to as “Boreal West,” “Boreal East” and “Taiga” (Figure 1.1), lower-level landscape units are defined based upon the recurrent arrangements of the main permanent ecological and vegetation features (48 landscape units are present in our sampling area), which in turn are divided into ecological districts (284 ecological districts within our sampling area) that are based upon their geological and physiographic features (Ansseau *et al.*, 1997). Please refer to the Figure 1.1B for examples of geographical units mentioned throughout the paper.

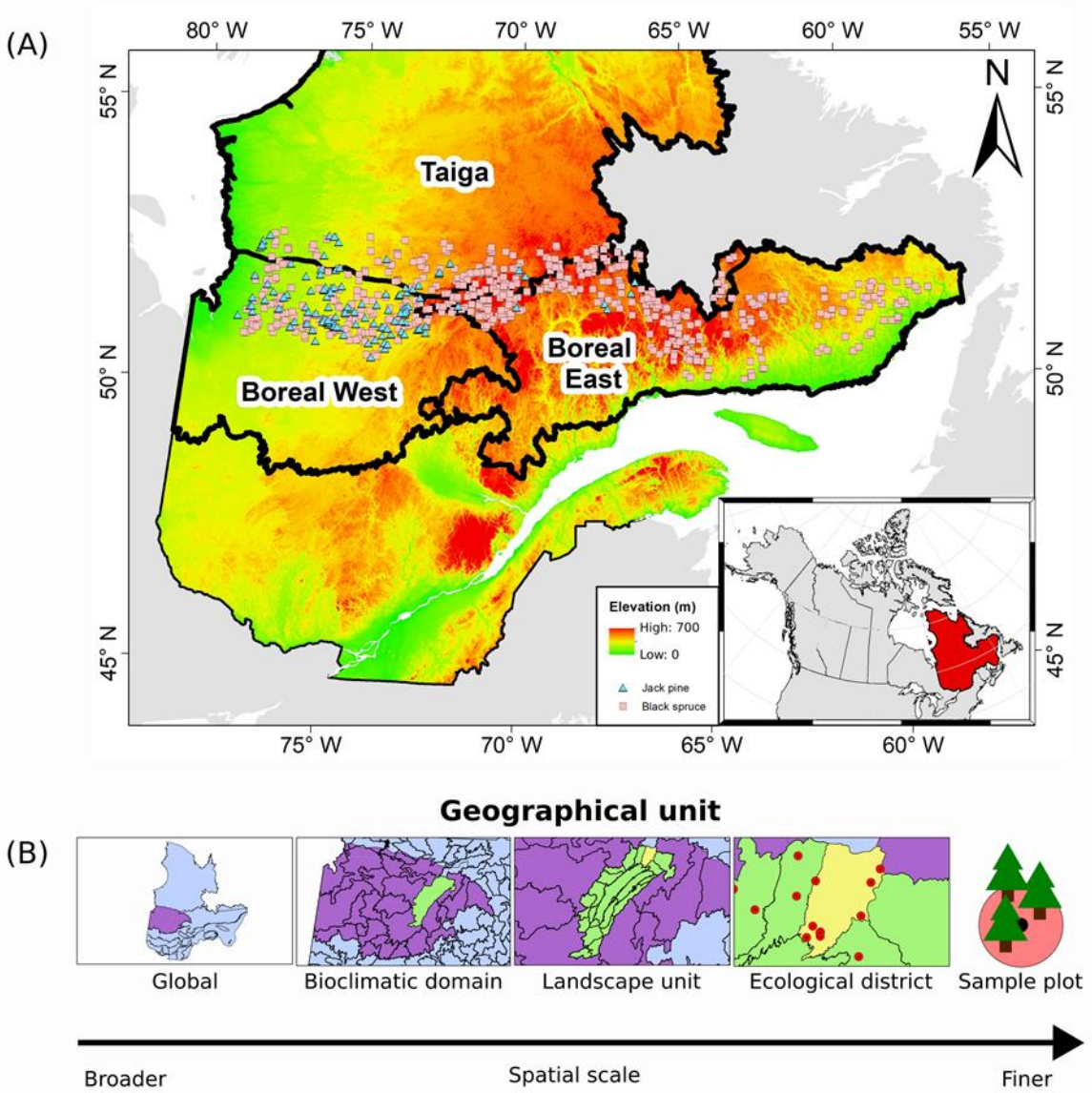


Figure 1.1. (A) Forest inventory plot network. The pink squares and blue triangles represent black spruce and jack pine temporary sample plots, respectively. The three main bioclimatic domains encompassing the sample network are also delineated. The background colour gradient represents the elevation gradient. (B) Geographical units involved in statistical analyses, from the broader global scale of the province of Quebec to the finer scale of the sample plot.

### 1.2.2 Tree-ring material

The data that we used for this study were acquired from a sampling program of 400-m<sup>2</sup> randomly distributed temporary circular sample plots ( $n = 875$  plots), which was established by the Ministère des Ressources naturelles et de la Faune du Québec (MRNFQ) from 2005 to 2009 (Programme d'inventaire écoforestier nordique; Létourneau *et al.*, 2008). In each sample plot, the diameter at breast height (DBH, 1.3 m) of all living and dead stems (DBH > 9 cm) was measured and environmental and stand-level conditions were recorded. Disks were collected for stem analysis from one to three dominant or co-dominant trees per species according to the provincial normative sampling protocol (Ministère des Ressources Naturelles du Québec, 2008). We used only black spruce and jack pine data since these species represented most (76 % and 15 %, respectively) of the sampled trees. We selected 1-m-height stem-disks as a trade-off between basal ring distortion and the number of visible rings (DesRochers et Gagnon, 1997). A total of 1914 black spruce and 352 jack pine disks with each having a minimum of 20 visible rings, representing 812 sample plots, were retained for subsequent analyses. Sample disks were processed using standard dendrochronological procedures for acquisition of ring-width measurement series across four radii per disk (Ministère des Ressources Naturelles du Québec, 2008). For each ring-width series, cross-dating and measurements were statistically verified using the program COFECHA (Holmes, 1983). No major anomaly in these tree-ring measurements was observed, and therefore all were retained for subsequent analyses.

### 1.2.3 Climate data and explanatory variables

For each plot, daily maximum and minimum temperatures (°C) and total precipitation (mm) were obtained for the period of 1970-2005 using thin plate spline smoothing algorithms (ANUSPLIN), which interpolate site-specific estimates at a 0.08° x 0.08° spatial resolution from historical weather observations, as described in Price *et al.*

(2011). Mean temperatures, which were computed as the average of monthly maximum and minimum temperature values, were averaged and precipitation was summed at a seasonal scale (meteorological seasons according to Trenberth, 1983: spring = March-May, summer = June-August, autumn = September-November, winter = December-February). Readers should refer to Figure S1.1 in Annexe A for an overview of the trends in seasonal climate in the study area.

Stand and environmental conditions were acquired from the plot survey conducted by the Ministère de la Faune, des Forêts et des Parcs du Québec (Table 1.1, MFFPQ; Robitaille *et al.*, 2015). We considered the proportion of clay, sand and silt in the mineral soil, organic layer thickness (OLT) and hydrological conditions of the sample plot assessed as drainage classes. Elevation and slope were extracted for our sample plots from the SRTM 90m Digital Elevation Database v4.1 (Jarvis *et al.*, 2008). For stand-level demographic features, minimum stand age was defined as the age of the oldest sampled tree in the plot. Stand basal area (BA) was computed as the sum of basal areas of all trees with DBH > 9 cm within the plot, on a per-hectare basis. A tree-level competition index (CI) was computed as the number of trees that were taller than the focal tree, divided by the total number of trees within the plot, to assess asymmetric competition (Ford *et al.*, 2016), following Weber *et al.* (2008). To do so, the height of all trees within a plot was estimated from DBH using the allometric equations of Fortin *et al.* (2009). Individual CI values were averaged at the plot level to ensure consistency with the working scale of the growth-climate analyses. Temperature and precipitation normals were computed for the 1970-2005 period to account for the west-to-east (continental-to-oceanic) climate gradient. For brevity's sake, these plot-level characteristics will be referred hereafter to as “explanatory variables”.

Table 1.1 Plot-level statistics for the studied explanatory variables, by bioclimatic domain

	Boreal West			Boreal East			Taiga		
	mean	sd	range (min   max)	mean	sd	range (min   max)	mean	sd	range (min   max)
<b>Clay (%)</b>	6.69	13.32	0   79	4.76	2.86	0   18	4.96	6.34	0   47.9
<b>Sand (%)</b>	63.51	30.71	0   99.5	66.77	24.13	0   99.5	68.55	23.94	0   96.5
<b>Silt (%)</b>	12.11	11.95	0   52	18.75	11.31	0   53.9	17.93	12.29	0   72
<b>OLT (cm)</b>	21.23	25.45	1   > 100	18.49	17.35	0   > 100	15.93	19.66	0   > 100
<b>Drainage (unitless)</b>	3 (median class)	-	1   6	3 (median class)	-	1   6	3 (median class)	-	1   6
<b>Elevation (m a.s.l.)</b>	320.22	89.84	96   637	549.55	167.39	100   860	522.59	171.4	113   912
<b>Slope (degree)</b>	2.28	1.97	0.13   13.15	3.55	3.33	0.13   19.58	2.32	2.29	0.13   12.36
<b>Age (years)</b>	105.23	55.82	28   294	163.69	65.81	28   331	145.59	63.68	30   309
<b>BA (m<sup>2</sup> ha<sup>-1</sup>)</b>	15.89	10.59	0.78   49.88	17.27	10.21	0.90   55.39	10.57	6.60	0.59   35.44
<b>CI (unitless)</b>	0.77	0.19	0.07   1.00	0.79	0.16	0.02   0.98	0.69	0.21	0.07   1
<b>Prec. (mm)</b>	807.11	59.07	685.56   927.26	956.09	106.87	775.83   1174.67	803.74	75.3	668.60   955.34
<b>Temp. (°C)</b>	-1.71	0.61	-3.07   -0.31	-2.21	1.28	-4.02   0.49	-2.28	1.03	-4.35   -0.93

Note: Clay = percentage of clay within the soil; Sand = percentage of sand within the soil; Silt = percentage of silt within the soil; OLT = organic layer thickness; Drainage = drainage classes: from 1: rapid drainage to 6: poor drainage ; Elevation = altitudinal gradient; Slope = terrain's slope, in degrees; Age = stand age (age of the oldest tree in a plot, computed as the number of years between the calendar year of the oldest ring and the calendar year of the most recent ring recorded for a tree); BA = basal area; CI = competition index; Prec. = average annual precipitation over the 1970-2005 period; Temp. = average mean annual temperature over the 1970-2005 period.

### 1.2.4 Statistical procedures

To test our working hypotheses, we applied a 3-step statistical procedure involving different spatio-temporal scales (see workflow diagram Figure S1.2 in Annexe A).

#### Step 1 : Trend analysis

Ring-width measurements of the four radii were averaged (arithmetic mean statistics, see Annexe A, Table S1.3.1 for descriptive statistics of the raw series), and the mean ring-width series were converted into basal area increments ( $BAI_t = \pi R_t^2 - \pi R_{t-1}^2$ ) using the function *bai.out* in the R-package *dplr* (Bunn, 2008). We assumed the cross-sections were perfectly circular in shape, and used these as a proxy for secondary growth to provide an accurate quantification of wood production with ever-increasing tree diameter (Biondi et Qeadan, 2008). Rings that were formed during the first 10 years were then eliminated, given that they usually exhibit an atypical response to environmental drivers compared with more mature rings (Loader *et al.*, 2007). Next, BAI were detrended using Generalised Additive Mixed Models (GAMM) to remove the remaining ontogeny-induced (i.e., tree age and size) trends. One model was constructed for each species and ecological district (See Annexe A, Supplement S1.4 for information about the BAI chronologies and diagnostic plots of the GAMM models). Organic layer thickness was added as a fixed term to account for the spatially-heterogeneous and mostly time-independent effect of site quality on tree growth (Lavoie *et al.*, 2007). BAI values were log-transformed to improve the normality of their distributions. The structure of the GAMM model is as follows:

$$\log(BAI_{ijkl}) = \log(BA_{ijkl}) + OLT_{kl} + s(AgeC_{ijkt}) + (TreeID_{ijkl}) + corAR1_{ijkl}$$

where i represents the individual tree, j represents the species, k represents the plot, l represents the ecological district, and t represents the year. BAI is the basal area

increment of tree  $i$  at specific year  $t$ ,  $BA$  is the basal area of tree  $i$  at specific year  $t$  (computed as the sum of  $BAI$  of previous years),  $OLT$  is the organic layer thickness of plot  $k$ , and  $AgeC$  is the cambial age (1-m height ring count) of tree  $i$  at year  $t$ . An autoregressive term,  $AR1$  (autoregressive order  $p = 1$ , moving average order  $q = 0$ ), was added to account for temporal autocorrelation. We tested the significance of a nested random effect (tree nested in plot) by conducting ANOVAs and likelihood ratio tests. Because it did not improve the model's fit and led to the same results (data not shown), we discarded the random term of the plot from the final model and kept only the random effect of the tree (TreeID).

Annual Growth Changes (GC), which were expressed as the percent deviation from predicted values of the GAMM model, were then computed following Girardin *et al.* (2016a). GC values were aggregated by year, plot and species using the median statistics for computation of GCmedian chronologies (robust statistics; Huber, 2005). Because, for several trees, the 2005 growth-ring was the last whole growth-ring, the upper temporal limit of the analyses was fixed to 2005 to ensure consistency between chronologies. From the GCmedian chronologies, growth trends were examined over two time periods: 1950-2005 and 1970-2005. These periods were marked by significant increases in mean annual temperatures of the area (Price *et al.*, 2013) and characterized by the highest number of tree rings per calendar year (i.e. the highest sample depth, see Annexe A Figure S1.3.2). Linear regressions were applied (GCmedian ~ year), and the estimated regression slope was used as a proxy for the long-term growth trend. Trend significance was assessed following the statistical procedure described by Yue *et al.* (2004). This method corrects the p-value of the non-parametric Mann-Kendall trend test with the effective sample size of the time series to reduce the influence of serial correlation (function *mkTrend* in the R-package *fume*; Santander Meteorology Group, 2012). Even if there were trend reversals for a few plots (Figure 1.2), the 1970-2005 and 1950-2005 trends were globally highly correlated (see Annexe A, Figure S1.5.1). For the purposes of comparison, 1970-2005 GAMM-based trends were compared with

trends that were estimated from the application of two other commonly used detrending methods, namely modified negative exponential models and regional curve standardisation (See Annexe A, Figure S1.5.2).

### Step 2 : Growth-climate relationships

Since weather station data availability and, therefore, climate data accuracy, is better for the most recent time periods (Ols *et al.*, 2017), we decided to retain data from the shorter and most recent period, i.e., 1970-2005, for climate-growth analyses. Linear mixed models were fitted by plot and species, which included residuals of GAMM-detrended BAI as response variables, together with the set of seasonally aggregated climatic variables as fixed terms, and tree identity as a random term. Mean seasonal temperature and total precipitation of the year of ring formation were considered as explanatory variables. Since trees can allocate carbohydrates that were acquired in the growing season to the biomass production of the following year (Granda et Camarero, 2017), climate data from summer and autumn of the previous year were also considered as fixed terms, leading to a total of ten climatic variables (please refer to Annexe A, Figure S1.6.1 for the list of climate variables used in linear mixed models). The structure of the global model is as follows:

$$Res_{ijkt} = \sum_{n=1}^{10} Clim_{kt} + (TreeID)_{ijk} + corAR1_{ijk}$$

where i represents the tree, j represents the species, k represents the plot and t represents the year. (TreeID) is a random term that accounts for the variability between individual trees. An error term with an AR1 ( $p = 1, q = 0$ ) correlation structure was added to the model which accounts for the serial correlation. Collinearity amongst climatic variables was low, with the mean of pairwise Pearson correlations between variables below a stringent threshold value of 0.4 (Annexe A, Figure S1.6.1; maximum value of  $|0.37|$ ;

Dormann *et al.*, 2013). Multi-model selection based upon the Akaike information criterion corrected for small sample size (AICc), was performed for this global model using the package *MuMIn* (Bartoń, 2018). A 95% confidence set of models was selected for multi-model inference as models whose cumulative Akaike weight is below 0.95 (Burnham et Anderson, 2002). Readers can consult Annexe A Figure S1.6.3 for AICc values of all of the 1024 evaluated models, along with Akaike weights of the best model and the number of models used for multi-model inferences. Weighted averages of parameter estimates were derived from this set of best approximating models, and Student's t-statistics were computed as the ratio between the average model estimate and its corresponding standard error. These statistics provide both the general direction of the growth-climate relationship (i.e., negative or positive slope), and the strength of this relationship (the farther from zero the t-value is, the stronger is the effect), weighted by the model's predictive capacity and based upon the selected climatic variables. The 95 % adjusted confidence intervals of the t-statistics were also computed, together with Pearson correlations between residuals from the GAMM models and predicted values from the climate models (Annexe A, Figure S1.6.2) as an additional means of assessing the model's predictive capacity. Results of growth-climate analyses that were based upon residuals from the two additional detrending methods are provided in Annexe A, Figure S1.7.

Slopes from the linear regressions and t-statistics from the climate-growth mixed models were interpolated across the whole area using the Empirical Bayesian Kriging algorithm of the Geostatistical Analyst tool in ArcGIS v.10.4 (input options: empirical transformation of the data, semi-variogram model = exponential-type, search radius = 1°, smoothing factor = 0.2). The output raster maps permitted visual examination of geographical patterns in long-term growth trends and climate sensitivity.

### Step 3 : Link with explanatory variables

The relationships between explanatory variables (listed in Table 1.1) and tree sensitivity to climate were assessed by conducting redundancy analyses (RDA) using Canoco software v.4.5 (ter Braak et Smilauer, 2009). Because tree sensitivity to climate and environmental conditions are highly variable from east to west (see Figure 1.4 and Table 1.1), site conditions might affect growth-climate relationships depending upon the location of the plot (Wu *et al.*, 2018). If averaged over the whole gradient, the effect of these conditions could cancel each other out. Consequently, one RDA was conducted per bioclimatic domain as a trade-off between data aggregation and ecological relevance, as recommended by Ols *et al.* (2018b). The t-statistics from the climate mixed models were considered as response variables (i.e., the “species” data matrix) and explanatory variables were considered as independant variables (i.e., the “environment” matrix). Climate normals were also included as independent variables, together with a dummy variable accounting for the species identity of the sampled tree, i.e., the difference in sensitivity to climate between jack pine (the reference level) and black spruce. Please refer to Annexe A, Table S1.8.1 for the list of independant variables considered in RDA analyses. Latitude, longitude and the average distance to the four nearest weather stations (ranging from 3.8 km to 153.1 km, see Annexe A, Figure S1.8.1) were added as conditioning variables to remove the effects of spatial non-independence of the plots and the potential lack of accuracy in the climate data set prior to analysis. Independant variables were transformed to improve the normality of their distributions, and then standardised prior to analysis (R package *rcompanion*; Mangiafico, 2017; Tukey’s ladder of powers; Tukey, 1977). Forward selection of independant variables was done using Monte-Carlo permutation tests ( $n = 9999$  permutations under the reduced model;  $\alpha = 0.05$ ). Growth trends were included passively in the RDA in order to examine these in context with climate-environmental

relationships (such supplementary ‘passive’ variables do not influence the ordination). To summarise the information that was displayed by the ordination plots (Annexe A, Figure S1.8.2), modified t-tests accounting for spatial autocorrelation were conducted between each of the RDA-selected independant variables and response variables (i.e., tree sensitivity to climate). The function *modified.ttest* of the R package *SpatialPack* was used (Osorio *et al.*, 2018;  $\alpha = 0.05$ ).

Significant variables were grouped into six sets according to the ecological process they represent: stand maturity, competition, altitudinal gradient, soil conditions, regional climate, and species identity (also see Annexe A, Table S1.8.1). Variation partitioning was then conducted to identify common and unique contributions to the total percentage of variation in the matrix of response variables (adjusted  $R^2$ ) explained by the model and better address the question of relative influences of the six sets of independant variables that were considered in the model (Peres-Neto *et al.*, 2006). The forward selection procedure used in the RDA led to up to five sets of independant variables by bioclimatic domain. The variation partitioning algorithm (*varpart*) in the R-package *vegan* was used (9999 permutations, partitions computed from adjusted  $R^2$ ; Oksanen *et al.*, 2018), which only allows a maximum of four sets of independant variables to be considered in a same analysis. To overcome this limitation, we determined the unique and common contributions of stand maturity, competition, altitudinal gradient, soil conditions and regional climate. Next, we determined the contribution of the taxonomic identity of the tree (selected in each of the three bioclimatic domains) by comparing it to the contribution of all other independant variables grouped together. The dummy species variable in RDAs allowed the quantification of the variability in growth-climate relationships resulting from the difference between the two species without splitting the data by species, which would have lowered the number of sample plot by analysis and consequently the statistical power, i.e. the likelihood to correctly reject the null hypothesis. Analyses by species

were also tested and results of these analyses are provided as Figure S1.8.3 in Annexe A.

### 1.3 Results

#### 1.3.1 Growth trends are spatially heterogeneous and species-specific

When averaged over the sample plots, dissimilar long-term growth trends appeared between species (Annexe A, Table S1.9). Growth rates of black spruce decreased, with a trend estimated at  $-0.35\% \text{ y}^{-1} \pm (\text{std}) 1.61\% \text{ y}^{-1}$  from 1950 to 2005. For the 1970-2005 period, the trend in the annual growth rate was  $-0.14\% \text{ y}^{-1} \pm 2.44\% \text{ y}^{-1}$ . For jack pine, both the 1950-2005 and 1970-2005 periods were characterised by an annual increase in growth of  $0.21\% \text{ y}^{-1} \pm 3.31\% \text{ y}^{-1}$  and  $0.21\% \text{ y}^{-1} \pm 3.37\% \text{ y}^{-1}$ , respectively. However, species-specific growth trajectories were not homogeneous across the study region (Figures 1.2 and 1.3; Annexe A, Table S1.9). Growth of black spruce increased in the western part of the Boreal West and in the central part of the Boreal East between 1970 and 2005, but decreased elsewhere (Figure 1.2). Growth of jack pine increased regardless of bioclimatic domain between 1950 and 2005, but decreased in the western parts of Boreal West and Taiga between 1970 and 2005 (Figures 1.2 and 1.3).

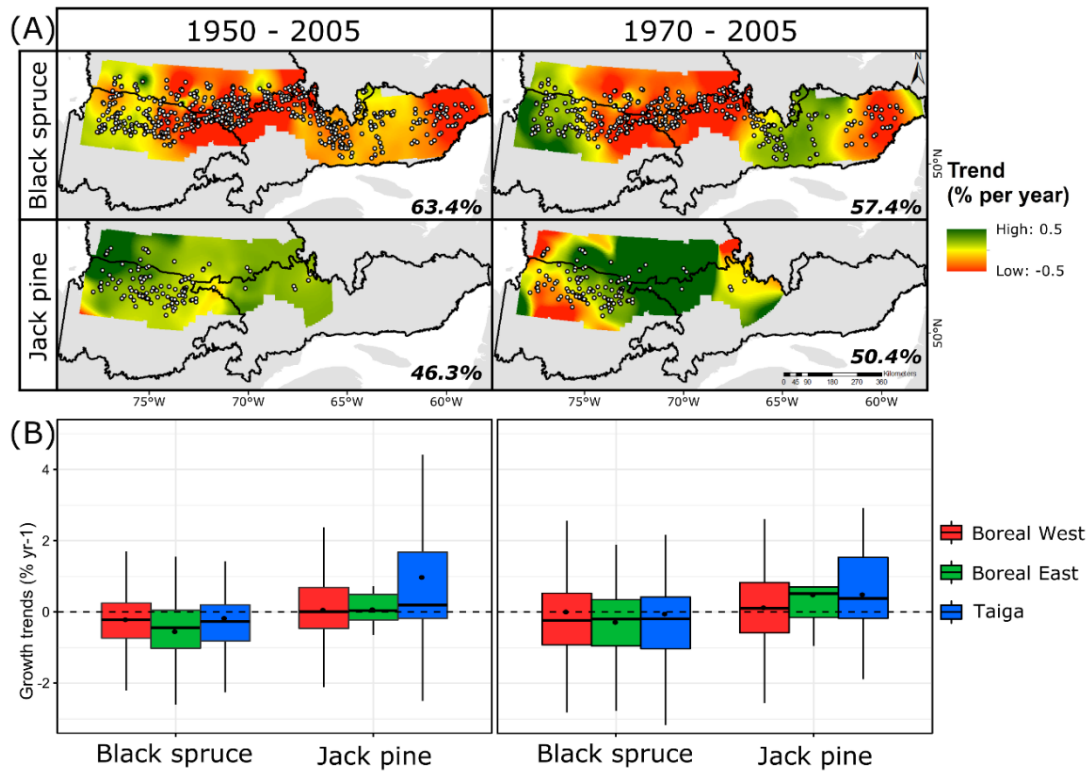


Figure 1.2. (A) Growth trends for black spruce and jack pine, for the 1950-2005 and 1970-2005 periods, shown as slope coefficients of the plot-scaled regression models of detrended BAI values against calendar years. Empirical Bayesian kriging was applied to interpolate plot-based trends across the entire area. Dots highlight significant trends ( $\alpha = 0.1$ ). The proportion of significant trends is shown at the bottom of each map. (B) Distributions of growth trend slopes by species and bioclimatic domain (boxplots). Black dots represent the mean value for the specific species and bioclimatic domain. Black lines inside the boxplots are median values, and error bars represent the lower and upper whiskers (representing the variability outside the upper and lower quartiles). The dotted line represents a value of zero, i.e., no trend in long-term growth.

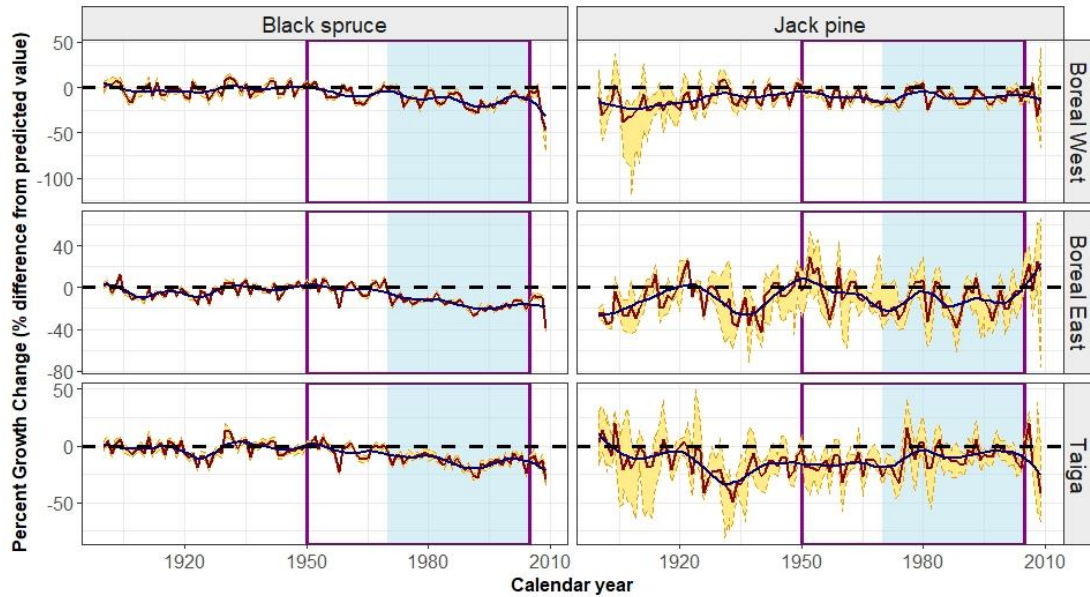


Figure 1.3. Median chronologies (red curves) of black spruce (left panels) and jack pine (right panels) detrended BAI (growth change) per bioclimatic domain (upper row: Boreal West; middle row: Boreal East; lower row: Taiga). Yellow shading and dotted lines delimit the bootstrapped 95 % confidence intervals, with LOESS smoothing shown by the blue lines (span = 0.2). Violet box and blue shading highlight the two time intervals (1950-2005 and 1970-2005, respectively). Black dashed lines denote a zero effect, i.e., no deviation compared to the value predicted by the GAMM model.

### 1.3.2 Sensitivity to climate is dissimilar across the landscape

Growth-climate response patterns were estimated for the two tree species to identify the key climate factors that were driving observed variability in growth (Figure 1.4). Summer temperature of the year preceding growth and spring precipitation in the year of growth had significant negative relationships with black spruce growth, while winter precipitation and winter temperature had a positive influence. The importance of these variables was not limited to particular regions but extended across vast areas (Figure 1.5). Black spruce tree sensitivity to other climate variables was more spatially heterogeneous (Figures 1.4 and 1.5). A high level of precipitation during previous-year summers had a significant positive effect upon the growth of black spruce within the Boreal East and Boreal West; this effect was not statistically significant in the Taiga (Figure 1.4). Excess-heat and high precipitation during previous-year autumns negatively affected spruce growth in the Boreal West and Taiga but had no significant effect in the Boreal East. Within the Boreal East and Taiga, the growth of black spruce was increased by hotter-than-average summers occurring during the year of ring formation and was decreased by milder-than-average springs. These relationships were mostly the opposite of what was observed within the Boreal West.

The response of jack pine to climate was less statistically significant and often opposite to that of black spruce. Regardless of bioclimatic domain, jack pine growth was increased by previous-year warm autumns and current-year summer warmth, but it was decreased by high winter precipitation (Figures 1.4 and 1.5). Current- and previous-year wet summers significantly increased the growth of jack pine within the Boreal East and Boreal West (Figure 1.4). Jack pine growth was positively correlated with mild and wet springs within the Taiga and with mild winters within the Boreal West, but was negatively impacted by wet springs within the Boreal East (Figure 1.4).

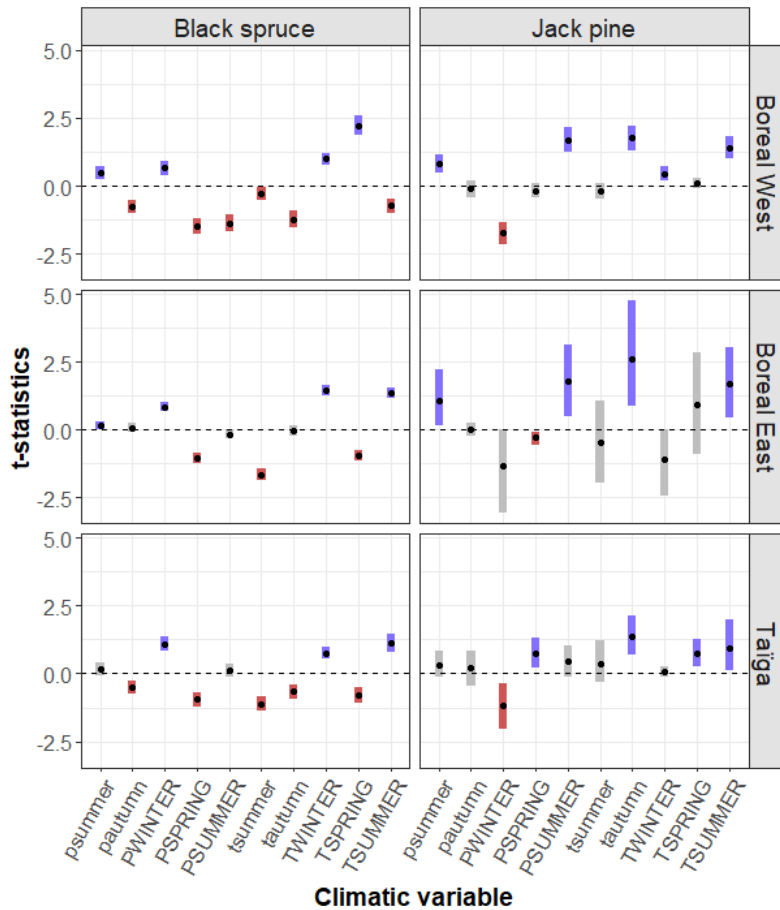


Figure 1.4. Arithmetic means (black dots) and bootstrapped 95 % confidence intervals (rectangles,  $R=10000$  replications) of t-statistic values per bioclimatic domain for black spruce and jack pine, for each of the seasonal climatic variables. “T” and “P” at the beginning of a variable’s name denote temperature and precipitation, respectively. Uppercase letters denote climatic variables for the current growing season (winter, spring, summer), and lowercase letters denote climatic variables of the previous growing season (previous summer, previous autumn). Blue and red rectangles indicate a significant (95 % confidence interval excluding zeroes) positive and negative effect, respectively, of the climatic variable at the scale of the bioclimatic domain, and grey rectangles are for non-significant values.

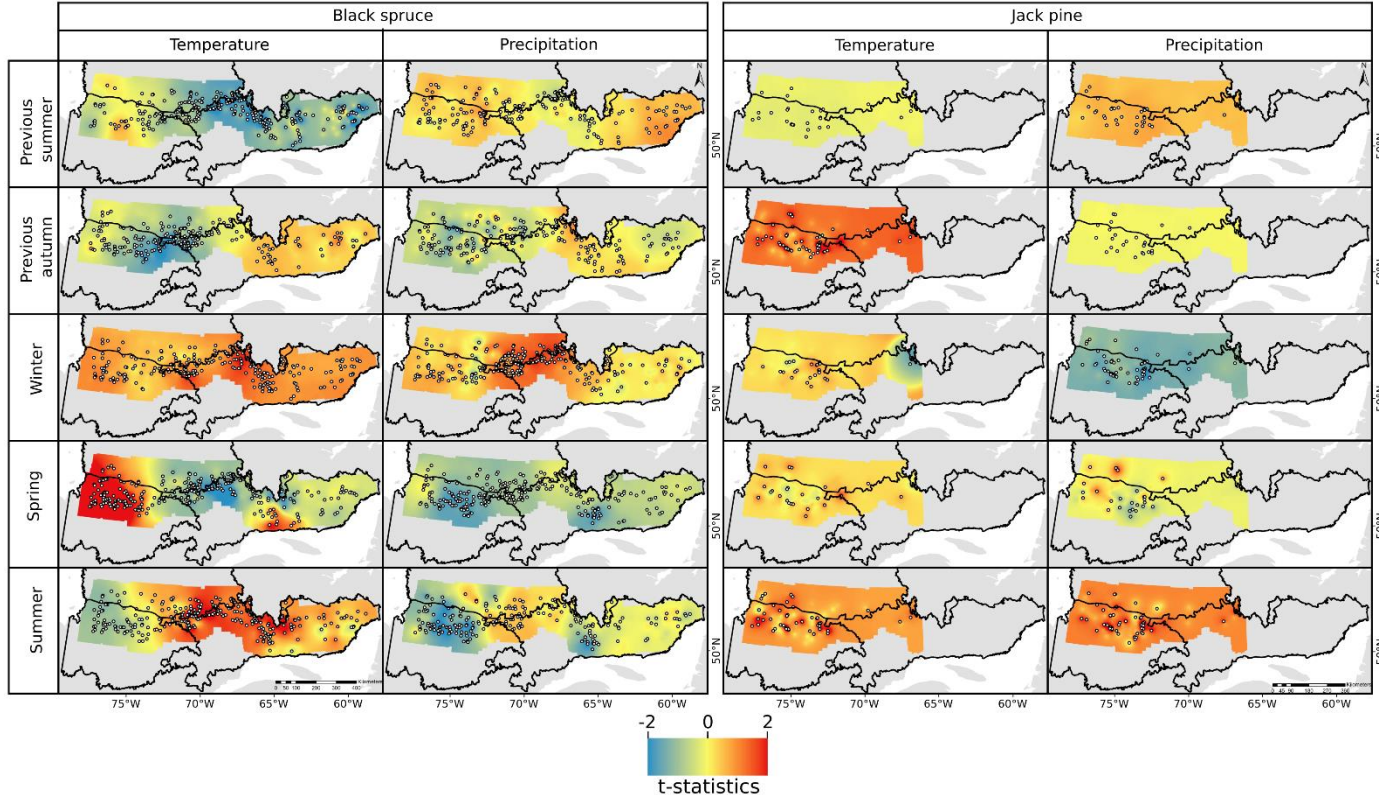


Figure 1.5. Kriging-interpolated growth response significance (based on t-statistics, 1970-2005) to seasonal climatic variable (left: temperature, right: precipitation) for black spruce (left panel) and jack pine (right panel). Green-to-blue colours denote a negative effect of the climate variable on tree growth, yellow colour means no impact of the climate variable on tree growth, and orange-to-red colours denote a positive effect. Dots display significant values, i.e., plots for which the 95 % confidence interval of the t-statistics excludes zero.

### 1.3.3 Plot-level features had low but significant effects on growth-climate relationships

Sensitivity to climate differed between the two species, especially within the Boreal West, where species identity of the sampled trees alone accounted for 15 % of variation in growth-climate relationships (Figure 1.6). Such taxonomic variability in growth sensitivity to climate can be readily noted in Figures 1.4 and 1.5. Contributions of the sets of explanatory variables stand maturity, competition, altitudinal gradient, soil conditions, and regional climate to the climate sensitivity variance were much lower. The elevational gradient explained the highest proportion of variation in tree response to climate within the Boreal East and Taiga (5 % and 9 %, respectively; Figure 1.6). Stand maturity, alone or in combination with other explanatory variables, accounted for 7 %, 1 % and 5 % of the variation in growth-climate relationships within the Boreal West, Boreal East and Taiga, respectively. For competition, these values were respectively 3 %, 2 % and 2 %.

Stands that were composed mainly of old black spruce trees exhibited growth that was more negatively correlated with previous-year summer and autumn temperatures, but more positively correlated with winter precipitation compared to recently regenerated stands (Figures 1.6 and 1.7, and Annexe A, Figure S1.10.1). These old-growth black spruce stands also exhibited the steepest declines in growth rates during 1970-2005 (Annexe A, Figure S1.11.1). The positive effect of warmer-than-average autumns, winter and springs on the growth of jack pine was lower for stands that were composed of old trees in comparison with more recently regenerated stands (Annexe A, Figure S1.8.3). Snowy and mild winters increased the growth of black spruce more than that of jack pine, but black spruce growth was more negatively correlated with wet and warm springs and with excess-heat during autumns of the previous years than that of jack pine. Previous-year wet summers and current-year mild springs decreased the growth of stands in the upper portion of the elevational gradient (i.e., above 500 m a.s.l.), while excessively high temperatures during current-year summers increased

their growth more strongly than for stands at lower elevations (Figures 1.6 and 1.7, and Annexe A, Figures S1.10.1 and S1.10.2). Similarly, growth in stands that were composed of taller trees (higher CI) was more negatively affected by excess-heat during previous-year summers than those stands that were composed of smaller-sized trees. Tree growth in more densely populated stands (higher BA) was also more positively correlated with winter temperature, but less positively correlated (within Boreal East and Taiga) or more negatively correlated (within Boreal West) with current-year summer precipitation than stands of lower densities (Figures 1.6 and 1.7 and Annexe A, Figure S1.8.3).

The effect of other explanatory variables on tree sensitivity to climate was restricted to a specific region, such as soil conditions within the Boreal West and the continental-to-oceanic climate gradient within the Boreal East, which accounted for 3 % and 5 % of the variation in growth-climate relationships, respectively (Figure 1.6).

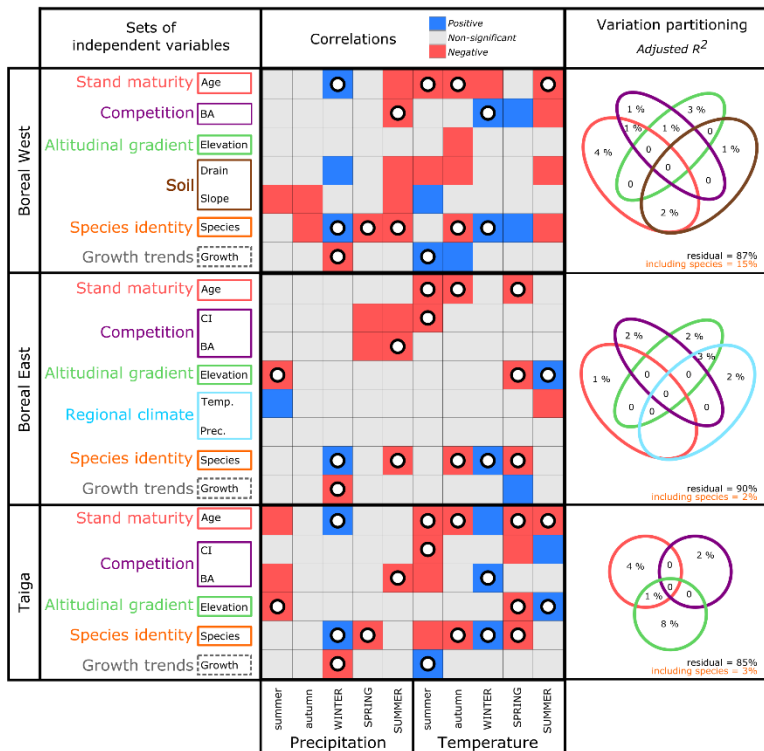


Figure 1.6. Left: The sets of independent variables used in variation partitioning (Please refer to Table 1.1 for variable ranges). Middle: Effect of each explanatory variable on tree sensitivity to climate, based on autocorrelation-corrected Pearson correlations. The relationship between long-term growth trends and climatic variables is also shown (uppercase letters: current year; lowercase letters: previous year). Red and blue shadings are for negative and positive relationships, respectively, that are significant at  $\alpha = 0.05$ . Gray shadings denote non-significant relationships. Significant relationships common to at least two bioclimatic domains are emphasised with a dot. Right: Proportion of variance explained by each set of independent variables, alone or in combination with other sets (Venn diagrams), by bioclimatic domain. The proportion of variance explained only by the species (pine or spruce) and the proportion of variance unexplained by the selected variables are shown below the diagrams.

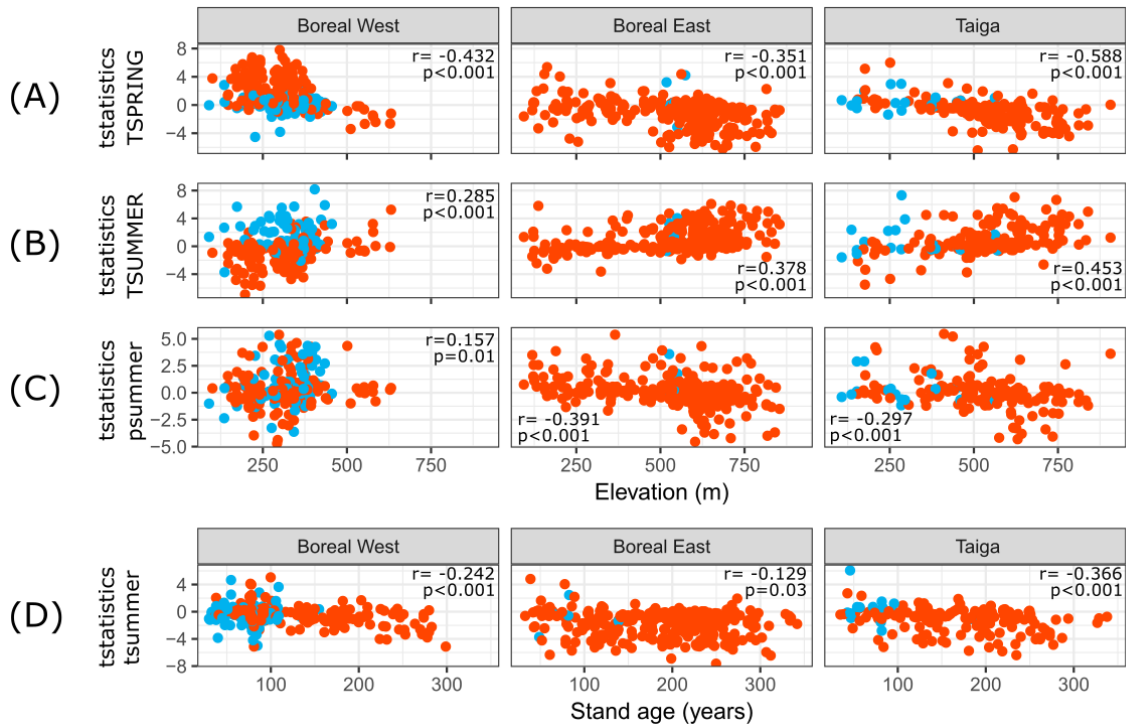


Figure 1.7. Effect of topographic position on sensitivity to (A) spring temperature, (B) summer temperature, (C) previous summer precipitation, and (D) effect of the age of the stand on the sensitivity to previous summer temperature. Blue and orange dots are observed values for jack pine and black spruce, respectively. Also shown are the Spearman's rho coefficient ( $r$ ) and p-value of the modified t-test corrected for the effect of spatial correlation.

## 1.4 Discussion

Using a dendroecological dataset from a randomly distributed forest inventory network that consisted of 812 plots and 2266 trees, we provided an overview of the response of two major boreal needleleaf species to recent climate change, across explanatory variables that include stand maturity, competition, elevational gradient, soil conditions, and regional climate within eastern boreal North America. Our results highlighted spatial heterogeneity in long-term growth trends across the studied forest: in some areas growth rates decreased, while in others growth increased over the last few decades. Tree sensitivity to climate was also highly spatially heterogeneous. Our study underscores the utility of employing broadly distributed datasets for assessing the complexity of climate change effects on a forest ecosystem (Klesse *et al.*, 2018 ; Nicklen *et al.*, 2018).

The species identity of the tree explained a greater proportion of variation in growth-climate relationships than did all other explanatory variables in the Boreal West. Further, we observed contrasting growth trends between the two species. Our analyses suggest that sensitivity to climate is determined primarily by a species-specific set of functional traits. Black spruce and jack pine usually occupy sites with different soil structures (Balland *et al.*, 2006) and have very different root system architectures and physiological efficiencies (Blake et Li, 2003 ; Strong et La Roi, 1983), which could explain differences in climate sensitivity.

We identified previous-year summer temperature and, to a lesser extent, previous-autumn temperature as two of the climatic factors with the greatest negative effects on annual growth rates of black spruce trees. Excess-heat during late summer and autumn may lead to declines in carbohydrate reserve accumulation at the end of the growing season, thereby negatively affecting spring growth, as was previously observed in both boreal North America and northern Europe (Girardin *et al.*, 2016a ; Ols *et al.*, 2018b).

Decreased reserve formation of heat-stressed trees can result from accelerated respiration, which leads to higher and more rapid use of photosynthates that otherwise would be available for storage (Anderegg et Anderegg, 2013 ; Granda et Camarero, 2017 ; Sala *et al.*, 2012). The steepest declines in observed growth for individuals that were the most greatly affected by above-average temperature during summer of the year prior to ring formation suggest that hot extremes are one of the primary determinants of growth trajectories for boreal black spruce forests, as has been observed for white spruce seedlings in plantations by Benomar *et al.* (2018). The deeper root system of jack pine trees could have allowed them to access additional water resource in deeper soil layers, and their greater resource use efficiency could have prevented them from an overuse of carbon reserves during heatwaves, potentially leading to an uninterrupted carbohydrates storage during hotter-than-average late growing seasons. The resulting higher amount of photosynthates available the following spring could explain the positive correlation between jack pine growth and previous autumn temperature. Our results also suggest that in addition to the effect of species-specific traits, some variation originated from spatially varying site features like stand maturity, position along the elevational gradient, regional climate and soil conditions. Yet, these site-level features explained a lower proportion of the variance in patterns of growth-climate relationships within bioclimatic domains.

As predicted from our main working hypothesis, position along the elevational gradient explained a low but significant proportion of the variation in tree response to spring and summer temperature and to previous summer precipitation. This finding illustrates diverging climatic constraints, from water-limited trees at low elevation to trees constrained by cold temperatures during the growing season at the high end of the elevational gradient. Contrary to our expectations, growth of black spruce was more negatively affected by mild springs when located in the upper portion of our elevational gradient. This counter-intuitive effect of mild springs was recently observed elsewhere (Babst *et al.*, 2012a ; Ols *et al.*, 2017) and could result from earlier onset of

physiological activity and growth in response to warming (Gu *et al.*, 2008 ; Richardson *et al.*, 2018 ; Vitasse *et al.*, 2017). Late-frost events generally occur more frequently at higher elevations and in cold regions such as the Boreal East and Taiga than at lower elevation or in relatively warmer regions such as the Boreal West. These events can damage early formed shoots and roots, thereby reducing total seasonal growth (Kidd *et al.*, 2014 ; Marquis *et al.*, 2020b, 2020a, 2021).

Summer warmth had a contrasting effect on tree growth, depending upon its occurrence. While previous-year high temperatures had negative effects on growth during the following growing season, hotter-than-average summers had an immediate and positive effect on growth rates during the year of occurrence. The later relationship, which had been observed in the Boreal East and Taiga, was more pronounced for stands at upper elevation sites than at lower elevations and could be linked to a decrease in the risk of late-frost damage and faster snowmelt in early summer (Vitasse *et al.*, 2017). Hot summers are also correlated with high solar radiation and, consequently, with higher rates of photosynthesis, especially in sites where water is not a factor limiting to tree growth, such as stands at the high end of our elevational gradient in the Boreal East and Taiga. Temperature generally decreases with elevation, so an increase in summer temperature can lead to a greater net beneficial effect on tree growth at higher elevations (see Annexe A, Figure S1.12). However, the resulting growth gain would have been outweighed by the growth decline due to late frost damage, which could explain that growth trends in stands within the central hilly area were more negative than in the westernmost stands.

Effects of other variables on climate sensitivity, such as stand maturity and competition, were generally consistent across regions. Excess-heat during previous-year summers and autumns had a significantly greater negative impact on black spruce growth in older stands compared to more recently regenerated stands. The increase in climate sensitivity with age has been extensively documented (e.g. Altman *et al.*, 2017 ;

Schuster et Oberhuber, 2013), and was linked to ontogeny-related morphophysiological changes (Ryan *et al.*, 2006) leading to a decrease in hydraulic conductance (Magnani *et al.*, 2000). During drought, hydraulic conductance may decrease more strongly in old and tall trees because of greater path resistance (Ryan et Yoder, 1997); the resulting decreases in stomatal conductance and photosynthesis may entail, along with greater metabolic demand in tall trees (Hartmann, 2011), depletion of carbohydrate reserves in older stands. This response is a potential explanation for the negative relationship between 1970-2005 growth trends and stand age (Annexe A, Figure S1.11.1; see also Chen *et al.*, 2016 ; Girardin *et al.*, 2014).

Competition pressure also significantly modulated the growth-climate relationships. Growth of trees in densely vegetated (high BA) stands that were composed of taller individuals (high CI) was more negatively correlated with excess-heat during previous-year summers and less positively correlated to current-year wet summers than in a less competitive environment. These relationships could have originated from lower carbon assimilation and carbohydrate reserve formation originating from reduced water availability (Gleason *et al.*, 2017). In contrast, black spruce trees responded more positively to mild winters in densely vegetated compared to more sparsely populated stands. This may be due to the stabilizing effect of a dense canopy on local-scale hydrothermal properties (Gu *et al.*, 2008 ; Vaganov *et al.*, 1999), similar to the effect of high structural diversity (Aussenac *et al.*, 2017).

Soil conditions accounted for a significant proportion of the variation in growth-climate relationships, but this was true only for black spruce in the Boreal West. This region is characterised by a contrasting physiography spanning comparatively flat landscapes with a high proportion of peatlands in the west to hilly terrain with sandy-loam soils in the east (Robitaille *et al.*, 2015; also see Figure 1.1 and Table 1.1), together with resulting differences in soil hydrology. During hot summers, the water table of soils with a high proportion of organic material is lowered, and in combination with the high

degree of dessication of the peat substrate (Gewehr *et al.*, 2014 ; Voortman *et al.*, 2013), may have reduced water availability and exacerbated summer heat stress, particularly for trees with shallow rooting systems such as black spruce. Paradoxically, an excess of water during consecutive wet springs and summers also reduced growth of black spruce in Boreal West (Figure 1.5), most likely because of hypoxic stresses resulting from elevation of the water table in poorly drained sites (Zobel, 1990). A positive correlation between growth of western black spruce trees and the annual area burned, which is a proxy for litter and deep organic layer dryness (Molinari *et al.*, 2018), adds credibility to the assumption that tree sensitivity to precipitation was strongly modulated by soil hydrology in the Boreal West (Annexe A, Figure S1.13).

Overall, we identified mostly negative growth trends for black spruce and only barely positive trends for jack pine during the 1970-2005 period, which confirms the absence of climatically-induced stimulation of tree vigour that was previously observed for the boreal forest (Girardin *et al.*, 2016a ; Hember *et al.*, 2016 ; Ju et Masek, 2016 ; Zhu *et al.*, 2016). However, forest growth trends were spatially heterogeneous, and the productivity of some areas increased over the last few decades. Variability in growth-climate relationships that was explained by the set of variables considered in our analysis remained low (< 25 %), as is the case in many studies focusing on ecological processes. Our random sampling strategy implies that many factors, which are potentially involved in growth-climate relationships, were not considered and could not be controlled for, such as the effect of non-tree vegetation, insect epidemics, or nutrient cycling. In addition, the genetic diversity of the species under study surely induced different responses to climate between populations (Avanzi *et al.*, 2019 ; Housset *et al.*, 2016). Based upon our results, we suggest that the warming threshold beyond which the productivity of the boreal forest will shift from positive to negative (~ +2 °C; D'Orangeville *et al.*, 2018) is likely very heterogeneous across the boreal biome, but may already have been reached in many of our black spruce stands.

### 1.5 Acknowledgements

This research was conducted as part of the International Research Group on Cold Forests. This study was made possible thanks to the financial support that was provided by the Strategic and Discovery programs of NSERC (Natural Sciences and Engineering Research Council of Canada), and a MITACS scholarship co-funded by NSERC and Ouranos. Additional financial support was provided by the Canadian Forest Service and the UQAM Foundation (De Sève Foundation fellowship and TEMBEC forest ecology fellowship). We thank Dan McKenney and Pia Papadopol (Canadian Forest Service) for providing the ANUSPLIN climate data. Many thanks to XiaoJing Guo (Canadian Forest Service) for the initial version of the R-scripts and helpful advice during statistical analyses, to Claire Depardieu for relevant comments on the manuscript, and to Isabelle Lamarre and W. F. J. Parsons for language editing.

## CHAPITRE II

HIGH STOMATAL LIMITATION ON PHOTOSYNTHESIS AS A DRIVER OF  
DROUGHT-INDUCED GROWTH DECLINE IN BOREAL CONIFERS

William Marchand<sup>1, 2, \*</sup>, Martin P. Girardin<sup>1, 2</sup>, Henrik Hartmann<sup>3</sup>, Sylvie Gauthier<sup>1, 2</sup>,  
Yves Bergeron<sup>1, 4</sup>

<sup>1</sup>Centre d'étude de la forêt, Université du Québec à Montréal, C.P. 8888, succ. Centre-ville, Montréal, QC, Canada, and Forest Research Institute, Université du Québec en Abitibi-Témiscamingue, 445 boul. de l'Université, Rouyn Noranda, QC, Canada;

<sup>2</sup>Natural Resources Canada, Canadian Forest Service, Laurentian Forestry Centre, 1055 du P.E.P.S, P.O. Box 10380, Stn. Sainte-Foy, Québec, QC, Canada; <sup>3</sup>Max-Planck Institute for Biogeochemistry, Department of Biogeochemical Processes, Hans-Knöll Str. 10, 07745 Jena, Germany; <sup>4</sup>Institut de recherche sur les forêts, Université du Québec en Abitibi-Témiscamingue, 445 boul. de l'Université, Rouyn-Noranda, QC, Canada

\*Auteur correspondant : william.marchand@uqat.ca

Manuscrit en préparation en date du dépôt.

## Résumé

Les écosystèmes forestiers sont affectés par une augmentation de la fréquence, de l'intensité et de la durée des sécheresses. Les arbres réagissent à ces changements en ajustant leur conductance stomatique pour maximiser le compromis entre les apports de carbone et les pertes d'eau. Une meilleure compréhension des conséquences de ces ajustements physiologiques qui interviennent en réponse à la sécheresse sur la croissance des arbres pourrait aider à prédire le potentiel de productivité futur des forêts boréales. Ici, nous avons utilisé des échantillons provenant d'un réseau d'inventaire forestier englobant une vaste aire d'étude où un déclin dans les taux de croissance de l'épinette noire et du pin gris a eu lieu entre 1988 et 1992, période exceptionnellement sèche. Notre objectif était de vérifier si ce déclin de croissance résultait d'ajustements physiologiques des arbres à la sécheresse. Nous avons mesuré les rapports isotopiques du carbone et de l'oxygène dans les cernes de croissance de 95 épinettes et 49 pins sur la période 1985-1993. Nous avons utilisé la discrimination isotopique du carbone ( $\Delta^{13}\text{C}$ ) et de l'oxygène ( $\Delta^{18}\text{O}$ ) pour approximer respectivement l'efficience d'utilisation de l'eau et la conductance stomatique des arbres. Nous avons étudié la manière dont la variabilité inter-annuelle dans la discrimination isotopique était liée à un indice de sécheresse (Climate Moisture Index, CMI), au déficit de pression de vapeur et aux chutes de neige annuelles. Nous avons observé des valeurs significativement plus faibles de  $\Delta^{13}\text{C}$  sur la période 1988-1990 et des valeurs significativement plus élevées de  $\Delta^{18}\text{O}$  en 1988-1989 et 1991 comparativement à la moyenne de la période 1985-1993. Nous avons aussi observé qu'un déclin dans la disponibilité en eau du sol et une hausse dans le déficit de pression de vapeur étaient liés à des valeurs significativement plus faible de  $\Delta^{13}\text{C}$  et des valeurs significativement plus élevées de  $\Delta^{18}\text{O}$ , en parallèle d'une croissance significativement plus faible. Cette croissance plus faible persistait durant l'année suivante chez l'épinette mais pas chez le pin. Ces résultats soulignent qu'une réduction de la conductance stomatique résultant de conditions plus sèches se traduit pas des taux de croissance annuels plus faibles, peut-être à cause d'une diminution des

apports de carbone et d'une modification des stratégies d'allocation des ressources. L'impact plus fort et plus long sur l'épinette comparativement au pin suggère, pour cette espèce, une utilisation du carbone moins efficace et un potentiel d'acclimatation plus faible aux conditions climatiques plus chaudes et plus sèches dans le futur.

Mots-clés : forêt boréale; épinette noire; pin gris; composition isotopiques des cernes de croissance; stress hydrique

## Abstract

An increase in frequency, intensity and duration of drought events affects forested ecosystems. Trees react to these changes by adjusting stomatal conductance to maximize the trade-off between carbon gains and water losses. A better understanding of the consequences of these drought-induced physiological adjustments for tree growth could help inferring future productivity potentials of boreal forests. Here, we used samples from a forest inventory network in Canada encompassing a large study area where a decline in growth rates of black spruce and jack pine occurred in 1988-1992, an exceptionally dry period, to verify if this growth decline resulted from physiological adjustments of trees to drought. We measured carbon and oxygen isotope ratios in growth rings of 95 spruces and 49 pines spanning the years 1985-1993. We used  $\Delta^{13}\text{C}$  discrimination ( $\Delta^{13}\text{C}$ ) and  $\Delta^{18}\text{O}$  enrichment ( $\Delta^{18}\text{O}$ ) as proxies for water use efficiency and stomatal conductance, respectively. We studied how inter-annual variability in isotopic ratios was linked to climate moisture index, vapour pressure deficit and annual snowfall amount. We found significantly lower  $\Delta^{13}\text{C}$  over 1988-1990, and significantly higher  $\Delta^{18}\text{O}$  in 1988-1989 and 1991 compared to the 1985-1993 averages. We also observed that a low climatic water balance and a high vapor pressure deficit were linked with low  $\Delta^{13}\text{C}$  and high  $\Delta^{18}\text{O}$  in the two study species, in parallel with low growth rates. The later effect persisted into the year following drought for black spruce, but not for jack pine. These findings highlight that a reduction in stomatal conductance resulting from drier conditions translates into lower annual growth rates, maybe because of reduced carbon gains and changes in carbon allocation strategies. The stronger and longer lasting impact on black spruce compared to jack pine suggests a less efficient carbon use and a lower acclimation potential to future warmer and drier climate conditions.

Key words: boreal forest; black spruce; jack pine; tree ring isotopes; drought stress

## 2.1 Introduction

Earth's surface temperature has increased by an average of 1°C since the industrial revolution (i.e. ~ 1850; IPCC, 2013). This is largely the result of a rise in atmospheric CO<sub>2</sub> concentrations caused by the burning of fossil fuels as an anthropogenic energy source (Keeling *et al.*, 2015 ; Willeit *et al.*, 2019). Global climate models predict an additional warming up to 3°C by the end of the 21<sup>st</sup> century (IPCC, 2013) that will increase evaporative demand over large parts of the terrestrial surface, without being compensated by higher precipitation inputs (Dai, 2013). An increase in the frequency, duration and intensity of climate extremes, such as droughts and heatwaves, is also highly likely (Christidis *et al.*, 2015 ; Vicente-Serrano *et al.*, 2014). These changes in climate averages, variability and seasonality are already affecting the integrity of natural ecosystems worldwide. Forest ecosystems, for example, can be impacted both directly through water and heat stresses affecting plant physiology (e.g. Grossiord *et al.*, 2020), and indirectly, e.g. via an alteration of disturbance regimes which feed back on mortality rates and regeneration capacity of trees (Adams *et al.*, 2010 ; Allen *et al.*, 2010 ; Boucher *et al.*, 2020 ; Mantgem *et al.*, 2009 ; Peng *et al.*, 2011). Such hot and dry extremes could severely decrease the productivity of forest biomes over an extended time-period (Restaino *et al.*, 2016 ; Williams *et al.*, 2013 ; Yuan *et al.*, 2019). Knowledge on mechanisms governing the physiological response of trees to extreme drought events is thus of crucial importance for estimating the future C storage capacity of forests.

Inter-annual and long-term changes in tree growth rates are driven in large parts by carbon and water inputs which, in turn, are controlled by two major physiological processes: photosynthesis and transpiration. Water inputs, mainly driven by soil moisture availability, directly influence plant growth by creating turgor pressure which is necessary for wood cells enlargement (Rossi *et al.*, 2009). Water is the main component of xylem sap which conveys nutrients from roots to leaves (Peel, 2013).

These nutrient inputs cover biochemical requirements of plants, including the intake of electron donors needed to convert sunlight energy to adenosine triphosphate (ATP) and nicotinamide adenine dinucleotide phosphate (NADPH), the chemical energy and reducing power necessary for sugar building (Körner, 2015). In other words, without sufficient water inputs, trees will not use the carbon acquired because of reduced photosynthesis rates and decreased needs for organs elongation (“sink limitation”; Körner, 2015). Furthermore, photosynthetic enzyme kinetics are temperature-dependent and when temperature increases above a certain threshold, carbon assimilation rates decrease as a function of soil moisture availability (Kumarathunge *et al.*, 2020 ; Reich *et al.*, 2018). Trees can buffer these heat stresses by increasing transpiration rates to cool leaf surface, but this is conditional to a sufficient soil moisture availability to cover evaporative demand (Urban *et al.*, 2017). Therefore, the growth performance of a tree is partly governed by a trade-off between maintaining hydraulic integrity (and sufficient water inputs) via stomatal closure and keeping high carbon inputs via stomatal opening (i.e. the “safety-efficiency trade-off”; see Manzoni *et al.*, 2013). The intensity by which a tree will need to regulate stomatal aperture is largely dependent on the capacity of xylem conduits to resist embolism (Eisenach et Meinzer, 2020 ; Hacke *et al.*, 2001 ; Lens *et al.*, 2011 ; Li *et al.*, 2018). Stomatal regulation is thus the key, short-term physiological mechanism by which trees are able to avoid xylem cavitation to survive low atmospheric and soil moisture conditions (Brodribb *et al.*, 2014).

Tree species can be located on a continuous gradient of stomatal regulation on the basis of the strategy used to control plant water potential during a drought, through the notion of isohydricity (Hochberg *et al.*, 2018 ; Tardieu et Simonneau, 1998). Historically, isohydricity has been viewed as strictly dichotomic, separating plant species between “drought tolerant” and “drought avoider” depending on their propensity to maintain a high hydraulic conductance under dry conditions (Tardieu et Simonneau, 1998). However, results are now accumulating that demonstrate that different species could

use different stomatal regulation strategies distributed along a isohydricity continuum (Hartmann *et al.*, 2021 ; Hochberg *et al.*, 2018 ; Klein, 2014 ; Martínez-Vilalta *et al.*, 2014 ; McDowell *et al.*, 2008). More specifically, some tree species are differentiating from others by closing stomata early when dry conditions occur in order to maintain their hydraulic function. However, when dry conditions last over an extended time period, this high stomatal sensitivity implies a prolonged period without carbon input, which leads to a reduction of non-structural carbohydrate supply. Ultimately, trees from these more isohydric species are at a higher risk of being impacted by biotic agents such as insects, fungus or diseases as a side effect of the lower amount of carbon available for defense mechanisms (McDowell et Sevanto, 2010 ; Sala *et al.*, 2010). On the other hand, more anisohydric tree species are able to maintain a high stomatal conductance and very low water potentials under dry conditions, operating closer to their hydraulic limits. These species keep high carbon assimilation rates at the expense of a high risk of hydraulic failure, i.e. a too high percentage of faulty conductive vessels, which could ultimately kill them (Anderegg *et al.*, 2015a). The stomatal sensitivity of plants, and thus their position along the isohydricity gradient, is varying both in space and time. First, the selection pressure of environmental factors, especially moisture availability, on life-history traits such as the characteristics of conductive vessels and rooting system, drive differences in isohydricity between species (Bhaskar *et al.*, 2007 ; Feng *et al.*, 2019 ; Isaac-Renton *et al.*, 2018 ; McDowell *et al.*, 2019 ; Wu *et al.*, 2020). Secondly, the stomatal sensitivity of a species can change depending on inter-annual variations in moisture availability and in drought intensity (Wu *et al.*, 2020). Thus, species more prevalent on mesic sites or xeric sites with cold climates usually exhibit a high stomatal sensitivity in response to low-magnitude changes in their environment. However, these species typically possess more cavitation-resistant xylem vessels (Brodrribb *et al.*, 2014) allowing them to maintain only a weak stomatal control under exceptionally dry conditions (Bréda *et al.*, 2006 ; Li *et al.*, 2018 ; Wu *et al.*, 2020). By contrast, species growing in more humid environments generally exhibit a more isohydric behaviour but possess xylem vessels more vulnerable to cavitation which

force them to apply a very strict stomatal control during extreme droughts (Bréda *et al.*, 2006 ; Tissier *et al.*, 2004 ; Wu *et al.*, 2020). These differences in isohydricity between species drive their resistance to and recovery from droughts (Li *et al.*, 2020).

Tree rings are archiving inter-annual changes in physiological processes through variations in the number of annual wood cells, their properties (e.g. cell wall thickness) and chemical composition (e.g. stable isotopes; see e.g. Babst *et al.*, 2018). In particular, leaf gas exchange drives the ratio of stable carbon and oxygen isotopes that are imprinted in tree-ring biomass (Farquhar *et al.*, 1982b ; Gessler *et al.*, 2014). Tree-ring carbon isotope ratio,  $\delta^{13}\text{C}$ , depends on atmosphere-to-tree-ring carbon isotopic discrimination, which is modulated by the ratio of CO<sub>2</sub> concentration within the leaf to that within the atmosphere. Thus,  $\delta^{13}\text{C}$  is driven both by stomatal conductance and by photosynthesis rates (Farquhar *et al.*, 1982b). This relationship makes  $\delta^{13}\text{C}$  a good proxy for the quantity of carbon a tree assimilates per unit of water transpired, i.e. the intrinsic water use efficiency (iWUE; see Farquhar *et al.*, 1989). Indeed, tree-ring oxygen isotope ratio,  $\delta^{18}\text{O}$ , partly depends on external influences such as the oxygen isotopic composition of the source water and the enrichment in <sup>18</sup>O occurring before water enters the tree hydraulic pathway (Brienen *et al.*, 2012 ; Tang et Feng, 2001 ; Xu *et al.*, 2020). The main tree physiological process directly influencing  $\delta^{18}\text{O}$  is the control of stomatal aperture, which regulates oxygen isotopic discrimination occurring when water is transpired (Gessler *et al.*, 2014). Other internal processes, such as the “Péclet effect” and the exchange of oxygen atoms between carbohydrates and stem water prior to cellulose formation also act to modify the final  $\delta^{18}\text{O}$  signal in tree rings (Gessler *et al.*, 2014 ; Sternberg, 2009), but these processes are not influenced by changes in environmental conditions.  $\delta^{18}\text{O}$  is often measured in combination with  $\delta^{13}\text{C}$  to gain better understanding of past changes in stomatal control that have occurred independently of changes in assimilation rates (i.e. the “dual isotope approach”; Scheidegger *et al.*, 2000). Thus, tree rings offer an annually-resolved proxy to study past modifications in trees’ physiological processes resulting from environmental

changes. For example, during conditions causing stomatal closure but under which trees can maintain high photosynthesis rates, such as short-term droughts and heatwaves, transpiration is reduced while carbon assimilation is still fuelled by the remaining leaf internal CO<sub>2</sub>. This lowers the discrimination against the heavier isotopic species (i.e. <sup>13</sup>C and <sup>18</sup>O), leading to less negative  $\delta^{13}\text{C}$  and  $\delta^{18}\text{O}$  isotope ratios in growth rings (Cernusak *et al.*, 2013). However, during a long-lasting drought, internal CO<sub>2</sub> concentrations fall below the level required to efficiently fuel photosynthesis, leading to growth rings less depleted in <sup>13</sup>C but more enriched in <sup>18</sup>O compared with a growth ring formed under average climate conditions (Sternberg, 2009). By contrast, changes in environment can improve photosynthesis and keep non-limiting moisture availability, e.g. after release from overstory competition. Under these conditions,  $\delta^{13}\text{C}$  will increase as a result of higher photosynthesis rates. By contrast, tree-ring  $\delta^{18}\text{O}$  will show no change compared with growth rings formed under a highly competitive environment.

Here, we used carbon and oxygen isotope composition of these natural archives to approximate iWUE and stomatal conductance of jack pine and black spruce growing in non-managed forests of northeastern North America. These two conifer species are broadly distributed and of high commercial value. They occupy contrasting ecological niches and possess highly different life-history traits. Black spruce is a mostly generalist species, growing on a large gradient of soil conditions. This species is particularly well adapted to waterlogged, poorly-drained and organic-rich soils, with a superficial rooting system mostly composed of adventitious structures (Burns et Honkala, 1990). Jack pine is specific to well-drained and sand-rich soils. Its rooting habits include a taproot, allowing access to deep soil water reserves (Burns et Honkala, 1990). These differences lead to contrasting climate sensitivities, black spruce being more negatively affected by exceptionally hot conditions during spring and previous summer compared to jack pine (Marchand *et al.*, 2019). We previously observed a punctual but marked drop in growth rates for these two species within the period 1988-

1992 (Girardin *et al.*, 2014 ; Marchand *et al.*, 2019), and wanted to understand whether carbon and water limitations may have been driving these declines. Here, our main objective was to determine if this growth decline was synchronous with a physiological response of trees to dry and hot extremes that occurred within the area. We were particularly interested in determining the extent to which the contrasting life-history traits of black spruce and jack pine influenced their physiological response to drought and the magnitude of the subsequent impacts on growth rates. More specifically, we made the following hypotheses:

- (1) iWUE would have increased at the same time or close to the date upon which trees started to experience a slowdown in growth, so we expect 1988-1989 growth rings to be more enriched in  $^{13}\text{C}$  compared to adjacent rings.
- (2) This increase in iWUE would be mainly the result of a decrease in stomatal conductance, so we also expect 1988-1989 growth rings to be more enriched in  $^{18}\text{O}$  than adjacent rings.
- (3) Both carbon and oxygen isotope composition in tree rings would be dependent on moisture availability, i.e. drier the conditions, more  $^{13}\text{C}$  and  $^{18}\text{O}$ -enriched the growth-rings.
- (4) Because jack pine is more abundant on well drained, sandy areas and can access deep water reserves, this species should exhibit a more anisohydric behavior than black spruce, i.e. we expect a lower inter-annual variability in tree-ring isotope composition of jack pine compared to black spruce.

## 2.2 Materials and Methods

### 2.2.1 Sampling area

In this study, we took advantage of a provincial forest inventory network covering three degrees of latitude and nearly 20 degrees of longitude north of the Quebec limit of

commercial forests, i.e. north of 49°N (Létourneau *et al.*, 2008). The territory had recorded in 1989 its highest forest area burned (Canadian Forest Service, 2010; two million ha; Soja *et al.*, 2007) within the 1959–2019 period, which is an indication of a severe seasonal drought occurrence during that particular period (Girardin *et al.*, 2014). As part of the forest inventory, 400m<sup>2</sup> circular, randomly distributed, temporary sample plots (TSP;  $n = 875$  plots) were established from 2005 to 2009 within needleleaf-dominated, fire-originating unmanaged forests. These plots encompass a broad gradient of climate conditions, from warm and dry climate at the westernmost locations (mean 1981-2010 temperature and precipitation normals of -1.40°C and 849mm, respectively) to cold and moist climate in the eastern portion of the area (mean 1981-2010 temperature and precipitation normals of -2.17°C and 909mm, respectively). As a result, the average climatic water balance during the growing season (May-September) is more than two times higher in the eastern than in the western part of the study area (Figure 2.1). Together with this climate gradient are changes in physiography and soil conditions, from flat terrains composed of organic-rich soils in the west to hillsides composed of tills in the central portion of the territory, to rocky hilltops further east (Robitaille *et al.*, 2015). As a consequence of these differences in regional climate, topography and surficial deposits, climatic water balance during the growing season (May-September) is more than two times higher in the east than in the west (Figure 2.1).

### 2.2.2 Basal Area Increment data

Within each TSP, stem disks were collected for stem analyses from one to three upper canopy trees per species. Disks were prepared and processed for ring-width measurement following standard dendrochronological procedures across four radii per disk (Ministère des Ressources Naturelles du Québec, 2008). Cross-dating and measurements were validated using the program COFECHA (Holmes, 1983). For each stem disk, ring widths of the four radii were averaged and converted to basal area

increments ( $BAI_t = \pi R^2_t - \pi R^2_{t-1}$ ; function *bai.out* of the R package *dplR*; Bunn, 2008). As a means of removing biological trends (i.e. those trends arising from increase in tree age and size and from changes in competition pressure with stand development), BAIs were detrended applying generalized additive mixed models (GAMMs). Readers are referred to Marchand *et al.* (2019) for the detailed statistical procedure (also see Annexe B, Supplement S2.1). A growth index (hereafter GI, unit-centered, i.e. a value below 1 means an observed BAI lower than the BAI expected for a tree of a specific age and size and growing under specific environmental conditions) was then computed as the ratio between observed BAIs and values predicted by the GAMMs, for the whole trees life-period.

### 2.2.3 Isotope measurements

A subsample of 144 trees (95 spruces and 49 pines) more than 30 years old and exempt of missing rings were selected for carbon isotope analysis. The sampled trees were randomly selected among a pool of candidate trees growing on relatively similar conditions, with elevation ranging between 250 m and 550 m a.s.l., organic layer thickness lower than 30 cm, and located on well-drained, sandy or loamy soils. Note that the two species never co-occurred within a TSP among the randomly selected trees. Trees from stands with highly diverse age and diameter structures were avoided to exclude spruce individuals that have had regenerated vegetatively by layering and those that have experienced a prolonged period of suppressed growth. The stable oxygen isotope ratio, i.e.  $\delta^{18}\text{O}_{\text{ring}}$ , was measured for a subset of 53 spruces and 28 pines randomly chosen among the 144 individuals sampled for carbon isotope analysis.

From each stem disk, a 0.8cm x 0.8cm wood strip, from bark to bark and including the pith was cut using a bandsaw. We focused on the year 1989 as an exceptionally dry year. We chose to analyse growth rings formed during the four years directly preceding and following this focal year, in order to be able to compare isotopic signatures between

years with average climate conditions and extremely dry and hot years, including the year 1989. This choice also allows to capture any lag (legacy effect) in the physiological response of trees to drought. So, rings covering the period 1985-1993 were individually separated using a scalpel under a binocular microscope. The thinnest rings (ring widths < ~0.1 mm) were separated using a sledge microtome coupled with digital cameras. Rings were ground to fine particles using a Retsch MM400 ball mill. To limit the risk of contamination by plastic particles (Isaac-Renton *et al.*, 2016), we used stainless steel balls and vials during the milling step; coupled with racks allowing to process up to 20 samples per batch. Knowing that isotopic signals of wholewood and  $\alpha$ -cellulose of studied species are highly correlated (Bégin *et al.*, 2015 ; Harlow *et al.*, 2006 ; Walker *et al.*, 2015), we did not proceed with resin, lignin and hemi-cellulose extractions. We are aware that wholewood leads to additional noise (Gessler *et al.*, 2014), which we can account for when studying the link between isotopic signals and environmental gradients. About 0.3-1.0 mg of the milled wood material was loaded into tin foil capsules and combusted for  $\delta^{13}\text{C}_{\text{ring}}$  analysis in an elemental analyser (EA 1100, CE Instruments, Milan, Italy) coupled to an IRMS (Delta+, Thermo Finnigan, Bremen, Germany), with an analytical precision better than  $\pm 0.07 \text{ ‰}$  (standard deviation). About 0.5 mg of wood particles was weighted into silver capsules and pyrolyzed for  $\delta^{18}\text{O}_{\text{ring}}$  analysis in an elemental analyser (Hekatech-HTO, Wegberg, Germany) coupled to an IRMS (Delta+ XL, Thermo Finnigan, Bremen, Germany), with an analytical precision better than  $\pm 0.14 \text{ ‰}$  (standard deviation). Values are reported in parts per thousand (per mill, ‰), relative to the Vienna Pee Dee Belemnite (VPDB) for carbon ratios and to the Vienna Standard Mean Ocean Water (VSMOW) for oxygen ratios. All isotope measurements were conducted at the Stable Isotope Laboratory (BGC-IsoLab, Max Plank Institute for Biogeochemistry, Jena, Germany). The total number of samples analysed was 1292 for carbon isotope ratio, and 726 for oxygen isotope ratio.

## 2.2.4 Corrections for non-climatic variability in tree-ring isotope composition

The  $\delta^{13}\text{C}_{\text{ring}}$  values were converted to ring-to-atmosphere carbon isotope discrimination ( $\Delta^{13}\text{C}_{\text{ring}}$ ) using Eq.1 in order to account for the decline in  $\delta^{13}\text{C}$  of atmospheric CO<sub>2</sub> resulting from the combustion of fossil fuels by human populations since the industrial revolution (Suess effect; Keeling, 1979):

$$\underline{\text{Eq.1}} \quad \Delta^{13}\text{C}_{\text{ring}} = \frac{(\delta^{13}\text{C}_a - \delta^{13}\text{C}_{\text{ring}})}{1 + \left( \frac{\delta^{13}\text{C}_{\text{ring}}}{1000} \right)},$$

where  $\delta^{13}\text{C}_a$  represents the atmospheric stable carbon isotope ratio, obtained from Graven *et al.* (2017).

Contrary to  $\delta^{13}\text{C}_{\text{ring}}$  that is primarily driven by plant stomatal regulation and carbon assimilation, inter-annual variations in tree-ring  $\delta^{18}\text{O}$  ( $\delta^{18}\text{O}_{\text{ring}}$ ) could strongly depend on the oxygen isotope composition of source water (i.e. mainly precipitation), which is in turn related to temperature and atmospheric circulation patterns. As we were interested in inter-annual variability in  $\delta^{18}\text{O}_{\text{ring}}$  as a proxy for changes in tree stomatal regulation, it was important to make it free of other time-varying influences. To do so, we estimated the stable oxygen isotope content of precipitation ( $\delta^{18}\text{O}_{\text{prec}}$ ) at a monthly scale using Eq.2 following Guerrieri *et al.* (2019):

$$\underline{\text{Eq.2}} \quad \delta^{18}\text{O}_{\text{prec}} = 0.52 * T_{\text{mean}} - 0.006 * (T_{\text{mean}})^2 + 2.42 * P - 1.43 * (P)^2 - 0.46 * \sqrt{Elev.} - 13.00,$$

where  $T_{\text{mean}}$  is the monthly average temperature (°C),  $P$  is the monthly total precipitation (in m) obtained from BioSIM 11 (described below), and  $Elev.$  is the elevation (m a.s.l.), extracted for our sample plots from the SRTM 90m Digital Elevation Database v4.1 (Jarvis *et al.*, 2008).

Then, we averaged  $\delta^{18}\text{O}_{\text{Prec}}$  at an annual scale, and calculated the  $^{18}\text{O}$  enrichment in tree rings relative to the oxygen isotopic composition of precipitations using Eq.3. By doing so, we assumed that no discrimination occurred before water entered the hydraulic pathway:

$$\text{Eq.3} \quad \Delta^{18}\text{O}_{\text{ring}} = \frac{(\delta^{18}\text{O}_{\text{ring}} - \delta^{18}\text{O}_{\text{prec}})}{1 + \left( \frac{\delta^{18}\text{O}_{\text{prec}}}{1000} \right)}$$

## 2.2.5 Climate and environmental variables

BioSIM 11 was used to obtain climate data for our study plots over the period 1985-1993. The BioSIM software provides, for a specific location, elevation-adjusted daily weather estimates interpolated based on historical observations from the four nearest weather stations (Régnière et Bolstad, 1994). Monthly averages of vapour pressure deficit (VPD, in hPa) were derived from this daily data. Summer (June-August) VPD was used as a proxy for atmospheric water demand. Climate moisture index (CMI, in mm) was computed as the difference between monthly precipitation and monthly potential evapotranspiration. Growing season (May-September) CMI was used as a proxy for climatic water balance during the period of the year when trees are physiologically active in our territory. We also extracted the total annual (January-December) snowfall (converted to water equivalent, in mm). This variable incorporates information about inter-annual variability in the length of the growing season as well as in the water input as snow (Gaboriau *et al.*, s. d. manuscript submitted).

An approximation of the time-since-fire (TSF) was computed for each plot from the ground-level cambial age of the oldest sampled tree within the plot (obtained from the stem analysis). This variable was used in models to control for changes in growth and physiology related to modifications occurring in stand's demography (e.g. competition pressure) and in soil parameters (e.g. nutrient availability) through time.

Between-plot differences in environmental conditions were accounted for in analyses by computing a site index (SI). This index is defined as the average height reached by a dominant undamaged tree at age 50 (measured at breast height, 1.3m); used as a measure of how a tree would, theoretically, perform in regard of a specific set of environmental conditions. It was extrapolated to the entire area based on similarities with the sampled stands in terms of environmental conditions, which include climate, soil surficial deposits, elevation, slope and exposition (Gauthier *et al.*, 2015b; also see Supplementary Figure S2.2.1). SI values were available for black spruce only but were also a good indicator for jack pine productivity potential for comparable site conditions (See Supplementary Figure S3.1).

## 2.2.6 Statistical procedure

To test for inter-annual differences in GI,  $\Delta^{13}\text{C}_{\text{ring}}$  and  $\Delta^{18}\text{O}_{\text{ring}}$ , linear mixed models (LMMs) were fitted, which included z-scores of these variables as response variables, the year of ring formation, the species identity and their interaction as explanatory factorial variables, and the random effect of the tree nested within the plot. z-score standardization (i.e. mean-centering and dividing each value by the standard deviation of the corresponding individual 9 years time-series) was especially relevant in our case because of the high geographical coverage and the high variability that could be the result of differences in site conditions and individual performances. Post-hoc comparisons between years were performed using the function *lsmeans* of the R-package *emmeans*, with a Tukey adjustment for multiple comparisons.

To verify if inter-annual variability in growth rates and tree-ring carbon and oxygen enrichment was linked with climate variability, LMMs were fitted by species using the function *lme* of the R-package *nlme*. These models included raw (i.e. non z-scored) GI,  $\Delta^{13}\text{C}_{\text{ring}}$  or  $\Delta^{18}\text{O}_{\text{ring}}$  as response variables, summer VPD, May-September CMI, and annual snowfall as explanatory variables, the random effect of the tree nested within

the plot and an error term with a first-order autocorrelation structure. Since climate can affect tree growth of the next growing season, we also included summer VPD and May–September CMI of the year prior to ring formation as explanatory variables. To control for the differences in tree and stand developmental stages and in site conditions, we included the inner-bark basal area of the tree, the minimum time-since fire and the site fertility index as fixed-effect variables in our models. The inner-bark basal area (BA, in mm<sup>2</sup>) is defined here as the sum of BAIs of previous years. This variable was incorporated in models to account for changes in physiology (e.g. drought sensitivity; see Girardin *et al.*, 2012) occurring as a result of the increase in tree size. In order to obtain comparable estimated regression slopes, explanatory variables were standardized (centered using the average value of all plots and divided by the corresponding standard deviation) prior to analyses. This standardization also helped to keep a low collinearity (VIFs below 3) among explanatory variables:

$$\text{Eq.4} \quad X_{ijt} \sim VPD_{jt} + VPD_{prev_{jt}} + CMI_{jt} + CMI_{prev_{jt}} + Snow_{jt} + SI_j + BA_{ijt} + TSF_{jt} + \left( \frac{\text{Tree}_{ij}}{\text{Plot}_j} \right) + corCAR1_{ij} + \varepsilon_{ijt},$$

where  $X_{ijt}$  is the response variable (either GI of the year of ring formation (t),  $\Delta^{13}\text{C}_{\text{ring}}$  or  $\Delta^{18}\text{O}_{\text{ring}}$ ) of a tree i in a plot j at a year t;  $VPD_{jt}$  is the summer vapor pressure deficit in a plot j at year t;  $VPD_{prev_{jt}}$  is the summer VPD of the year prior to ring formation in a plot j at year t;  $CMI_{jt}$  is the climate moisture index in a plot j at a year t;  $CMI_{prev_{jt}}$  is the CMI of the year prior to ring formation in a plot j at year t;  $Snow_{jt}$  is the total annual snowfall at a plot j at a year t;  $SI_j$  is the site fertility index of the plot j at the time of sampling (a time-invariant term);  $BA_{ijt}$  is the basal area of a tree i at a year t;  $TSF_{jt}$  is the time elapsed from the last fire for a plot j at a year t (computed as the ground-level cambial age of the oldest tree of the plot at year t);  $\text{Tree}_{ij}$  and  $\text{Plot}_j$  denote the tree and plot identities;  $corCAR1$  is the error term with a first-order autocorrelation structure; and  $\varepsilon$  denotes the residuals of the model.

Normality and homoskedasticity of residuals were visually assessed, with no deviations from statistical assumptions for linear models. All statistical analyses were performed using the R statistical software version 3.6.0.

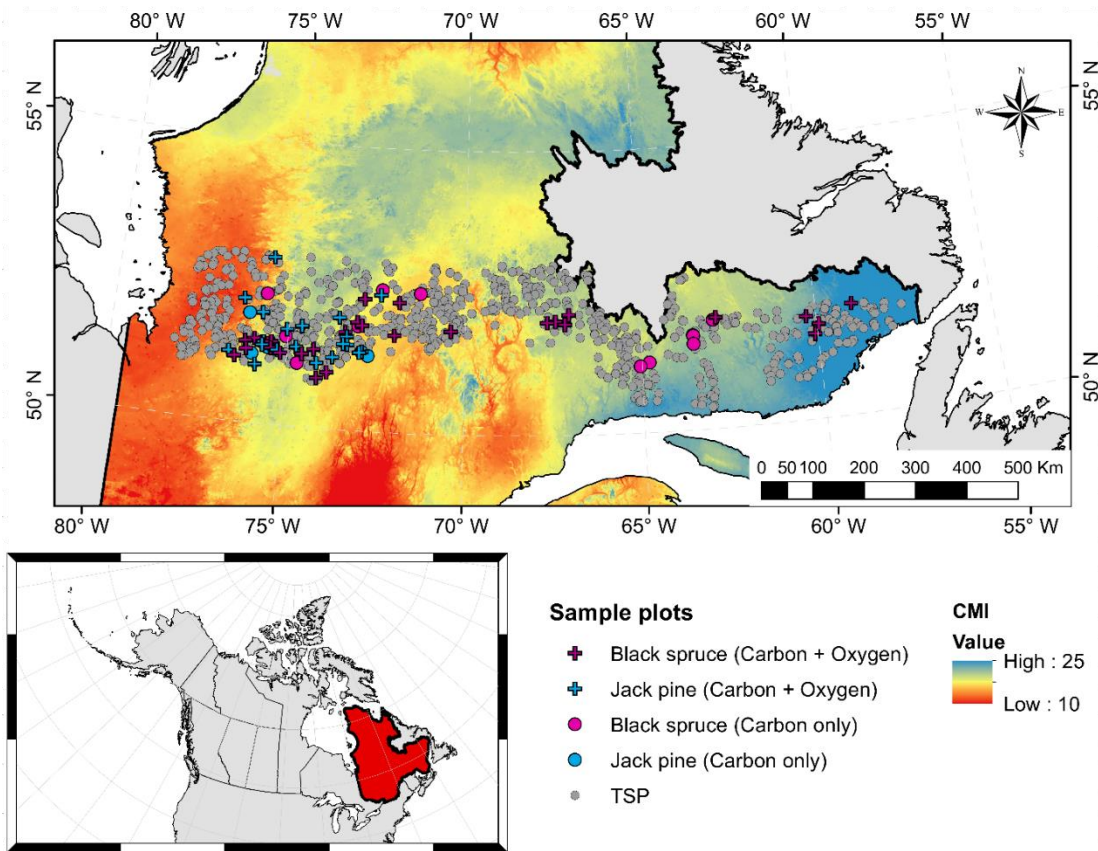


Figure 2.1. Map of the study zone. Color gradient represents 1981-2010 normals of the average May-September Climate Moisture Index (CMI, a proxy for the climatic water balance). Symbols represent locations where at least one tree was sampled for isotope analyses. Coloured circles are for plots where trees were sampled for carbon isotope analysis only, while coloured crosses are for plots where oxygen isotope measurements were also conducted. Pink and blue symbols denote black spruce and jack pine trees, respectively. Grey circles show locations of the 875 temporary sample plots (TSP) established as part of the Northern Ecoforest Inventory program.

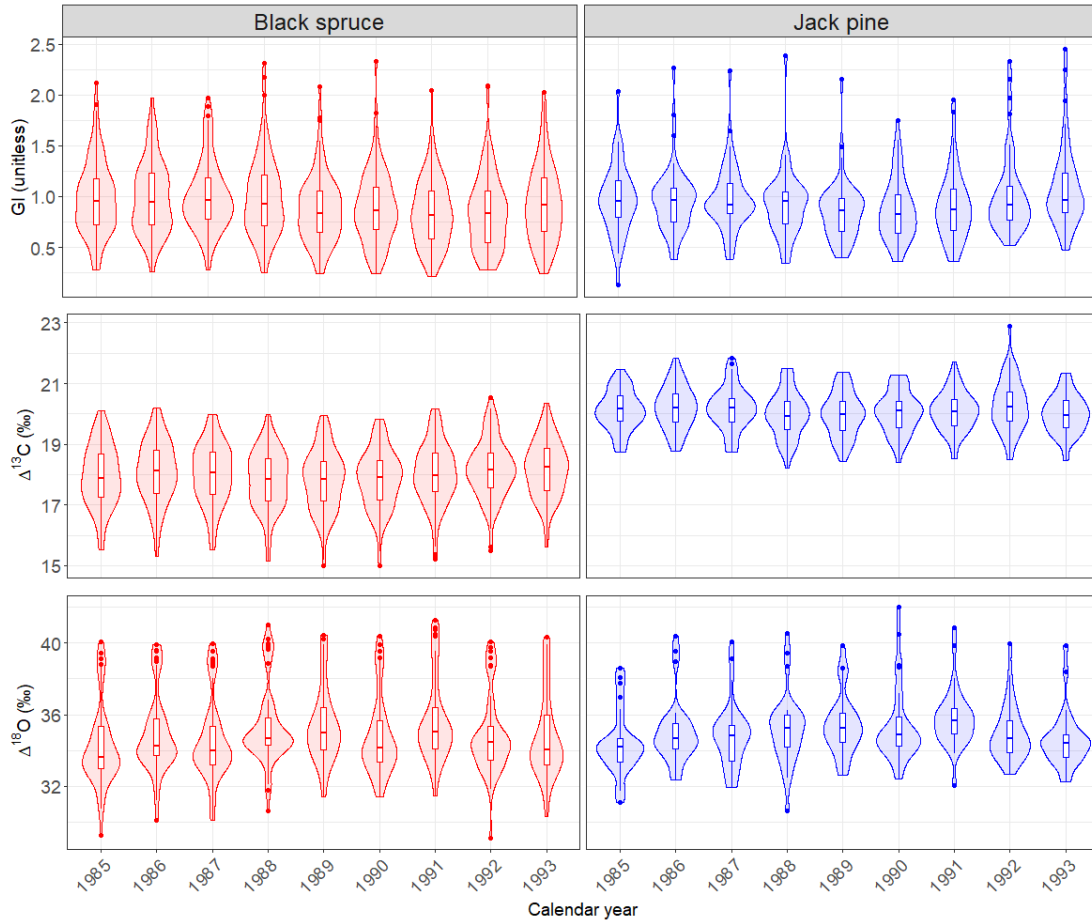


Figure 2.2. Distribution of observed (i.e. raw) values of the growth index (GI, as the ratio between observed BAI and BAI predicted by the Generalized Additive Mixed Models, see methods),  $\Delta^{13}\text{C}_{\text{ring}}$  and  $\Delta^{18}\text{O}_{\text{ring}}$ , by year and species. The lower and upper hinges of boxplots inside each violin plot show the 25th and 75th percentiles and the horizontal line denotes median value.

## 2.3 Results

### 2.3.1 Spatial variability in growth, isotope discrimination and climate

Average 1985-1993 BAI was 240.54 mm<sup>2</sup> for black spruce and 306.23 mm<sup>2</sup> for jack pine. However, these average growth rates were highly variable between trees and plots, as standard deviations (S.D.) reached  $\pm 201.02$  mm<sup>2</sup> for black spruce and  $\pm 191.29$  mm<sup>2</sup> for jack pine. Once variability from biological processes such as tree ageing and demographic processes, and from differences in soil parameters such as thickness of the organic layer, was removed (i.e., after detrending), average growth indices became highly similar between species (Figure 2.2). However, standard deviation was still high (0.34 and 0.29 for black spruce and jack pine respectively). Approximately two third of the trees experienced an average 1985-1993 GI below 1, i.e. an average growth rate lower than the value expected for a tree of similar age and size.

A high variability was also observed in tree-ring isotope data. For  $\Delta^{13}\text{C}_{\text{ring}}$ , the two species exhibited different 1985-1993 carbon discrimination levels, with an average  $\Delta^{13}\text{C}_{\text{ring}}$  of 17.99 ‰ ( $\pm 1$  ‰) and 20.09 ‰ ( $\pm 0.72$  ‰) for black spruce and jack pine, respectively.  $^{18}\text{O}$  enrichment above source water was of similar magnitude between the two species, with 1985-1993 averages of 34.92 ‰ and 35.09 ‰ for black spruce and jack pine respectively. However, these values were also highly variable between trees and stands, with S.D. of 2.17 ‰ and 1.69 ‰ for black spruce and jack pine, respectively.

Climate conditions prevailing during 1985-1993 were highly variable depending on the geographic location. Figure 2.3 shows that summer atmospheric water demand ( $\text{VPD}_{\text{jja}}$ ) was higher in the west than in the east (average summer VPD of 6.10 hPa and 3.25 hPa in the western and eastern locations, respectively), but that, on average, climatic water balance levels did not differ (average May-September CMI of 21.54 and 21.81 mm, in the west and east, respectively). Dates of occurrences of dry extremes also differed

between east and west. In the west, trees experienced dryer-than-average soil moisture conditions in 1989 and 1991 while, in the east, CMI was lower than average in 1988 only. For atmospheric dryness, both east and west locations experienced dry atmospheric conditions in 1989 and 1991.

### 2.3.2 Inter-annual differences in growth, carbon and oxygen isotope discrimination

When disparities resulting from individual and site-specific differences were removed (i.e. using z-scored values), inter-annual differences in terms of growth rates and isotopic discrimination were emphasized (Figure 2.4). In particular, jack pine trees exhibited significantly lower-than-average growth rates during the 1989-1991 period, with least-square means of growth indices being 0.44-0.60 standard deviations (S.D.) below the 1985-1993 average. For black spruce, this slow growth period persisted during the 4-years period 1989-1992, with least-square means of GI 0.32-0.65 S.D. below the 1985-1993 average.

Significant inter-annual differences were also detected in the species-averaged z-scored isotope chronologies (Figure 2.4). For black spruce, least-square means of carbon isotopic discrimination were 0.51-0.67 S.D. lower in 1988-1990 compared to the 1985-1993 average, and significantly different from values of adjacent rings. For jack pine the decline in  $\Delta^{13}\text{C}_{\text{ring}}$  was less severe, but the 1988-1990 least-square means were statistically different from 1986-1987 and 1992 values. This pattern was inverted when looking at 1985-1993 least-square means of z-scored iWUE (i.e. higher-than-average iWUE during 1988-1990; Supplementary Figure S2.3.1). Least-square mean of  $^{18}\text{O}$  enrichment was the highest in 1991 for both species (0.98 and 1.16 S.D. above the 1985-1993 averages for black spruce and jack pine respectively). Mean of  $\Delta^{18}\text{O}_{\text{ring}}$  was also 0.55-0.60 S.D. higher-than-average in 1988-1989 for black spruce and 0.42 S.D. above the 1985-1993 average in 1989 for jack pine. Interestingly, when looking at the least-square means of  $\delta^{18}\text{O}$  (non-corrected for precipitation  $\delta^{18}\text{O}$ ), 1991 values were

still higher than the average value for both species, but 1989 values were not significantly different from or slightly lower than 1985-1993 averages (Figure S2.4.1).

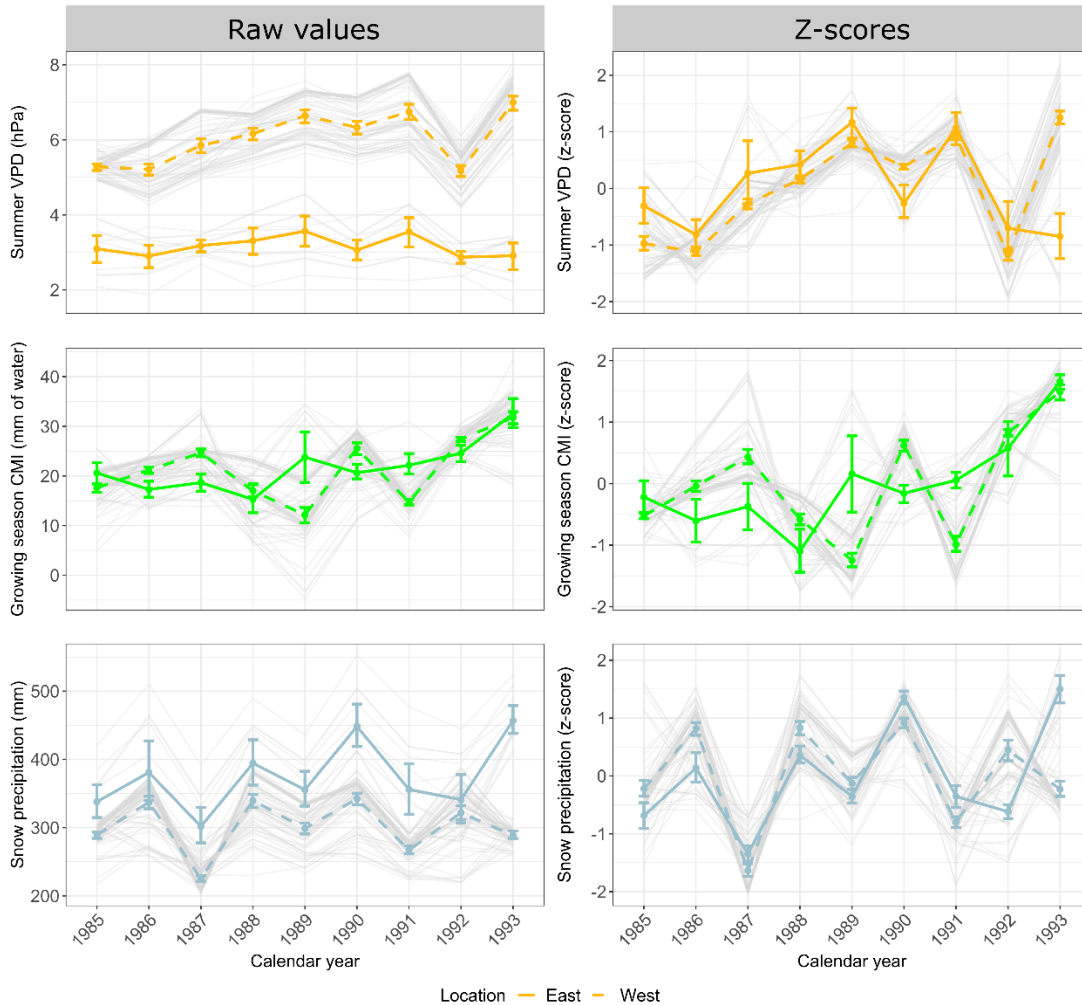


Figure 2.3. 1985-1993 climate data. Upper panels show summer (June-August) vapor pressure deficit, middle panels show growing season (May-September) climate moisture index, lower panels show annual total snowfall. Both raw (left panels) and z-scored (right panels) values are displayed. Solid lines (“West”) display average climate (computed as 50<sup>th</sup> percentiles of bootstrapped values; 5000 replications) for plots 78-65 W; dashed lines (“East”) are for plots 65-58 W. Error bars are 95% confidence intervals (2.5<sup>th</sup> and 97.5<sup>th</sup> percentiles of bootstrapped values). Gray lines display time-series for each plot location.

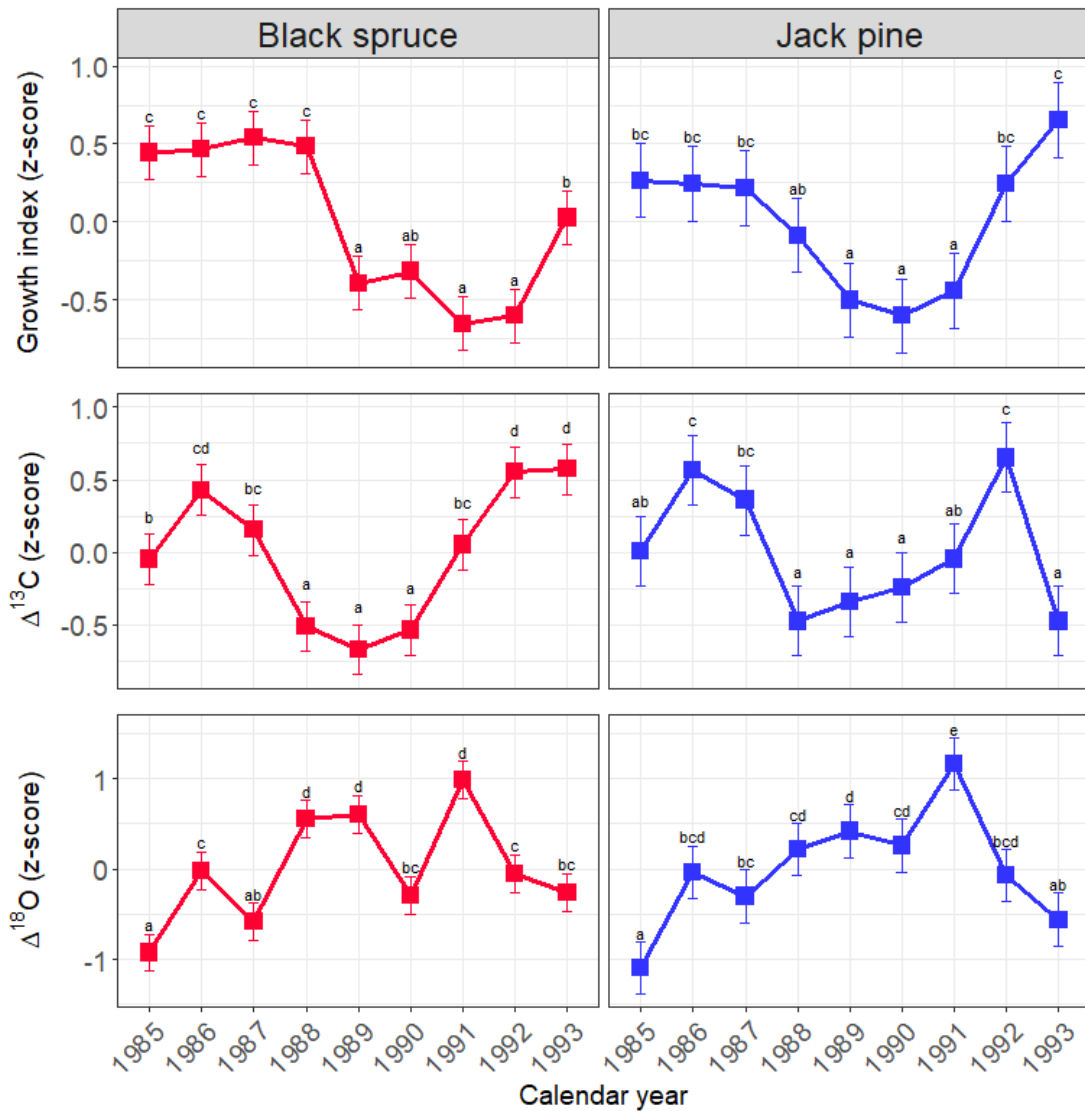


Figure 2.4. Z-scored (i.e. the difference between each value and the average value of the individual 1985–1993 series was divided by the standard deviation of the series) growth index,  $\Delta^{13}\text{C}$  and  $\Delta^{18}\text{O}$  values, by year and species. Squares are least square means. Error bars are 95% confidence intervals. For a given variable and species, different letters indicate significantly different values between years for a given species ( $\alpha = 0.05$ ).

### 2.3.3 Climate effects on tree growth and isotope discrimination

High CMI occurring the year of ring formation was linked with significantly higher growth indices (GIs) in both black spruce and jack pine, and a high CMI during the previous growing season was associated with significantly higher GIs in black spruce only (Table 2.1). Lower black spruce and jack pine GIs were observed when summer VPD occurring the year of ring formation was high, but only black spruce GIs were significantly lower when summer VPD of the year prior to ring formation was high. High snowfall was associated with significantly lower jack pine GIs but with significantly higher black spruce GIs.

The significance of the relationships between climate and isotope discrimination was also species-specific. High summer VPD the year of ring formation was associated with significantly lower carbon isotope discrimination and significantly higher oxygen isotope enrichment in both species compared to years of low summer VPD (Table 2.1). The relationship between isotopic values and VPD of the previous summer was similar, but non-significant in the case of jack pine  $\Delta^{13}\text{C}_{\text{ring}}$ . A high growing season CMI was linked with significantly higher  $\Delta^{13}\text{C}_{\text{ring}}$  in black spruce only, but significantly lower  $\Delta^{18}\text{O}_{\text{ring}}$  in both species when it occurred the year of ring formation. The significant effect of growing season CMI disappeared when looking at the raw  $\delta^{18}\text{O}$  of pine (Table S2.4.2), and at the iWUE of spruce (Table S2.3.2). When it occurred the year prior to ring formation, it was linked with higher  $\Delta^{18}\text{O}_{\text{ring}}$  in black spruce, but was not associated with any significant change in jack pine  $\Delta^{18}\text{O}_{\text{ring}}$ . A high annual snowfall was linked with significantly lower  $\Delta^{13}\text{C}_{\text{ring}}$  and significantly higher  $\Delta^{18}\text{O}_{\text{ring}}$  in black spruce only, with no significant relationships in the case of jack pine. The effect of snowfall was no longer significant when using black spruce  $\delta^{18}\text{O}$ , while this effect switched to significantly positive in the case of jack pine (Table S2.4.2). Outputs from models also confirmed the high between-tree and between-plot variability both in terms of growth rates and isotope discrimination, with a very low amount of variance

explained by the fixed-effect variables alone (very low marginal r-squared values but high conditional r-squared values, see Table 2.1).

Table 2.1. (next page). Outputs of linear mixed models of climate effects on tree growth and isotope ratios. One model was fitted by species and response variable, for a total of 6 models. Significant effects are highlighted with gray shadings, with significance levels as follows: “ \*\*\* ” means  $p\text{-value} \leq 0.001$ ; “ \*\* ” means  $p\text{-values} \leq 0.01$ ; “ \* ” means  $p\text{-value} \leq 0.05$ ; “ . ” means  $p\text{-value} \leq 0.1$  (i.e. marginally-significant) and “ NS ” indicates non-significant values. Also shown the marginal and conditional r-squared, i.e. the percentage of variance explained by the fixed part and the fixed plus random part of the model, respectively. Explanatory variables were mean centered and divided by the corresponding standard-deviation prior to analyses, leading to regression coefficients that are directly comparables between each others. Readers are referred to Supporting Information S2.5 for a biplot from a principal component analysis (PCA) summarizing results displayed in Table 2.1.

		Variables	Growth Index				$\Delta^{13}\text{C}$				$\Delta^{18}\text{O}$			
			Estimate	Std.Error	t-value	Signif.	Estimate	Std.Error	t-value	Signif.	Estimate	Std.Error	t-value	Signif.
Black Spruce	Fixed effects	Intercept	0.918	0.051	18.004	***	17.914	0.127	140.871	***	35.156	0.486	72.299	***
		CMI	0.017	0.005	3.804	***	0.024	0.012	2.024	*	-0.306	0.037	-8.166	***
		$\text{CMI}_{\text{prev}}$	0.023	0.005	4.830	***	-0.008	0.013	-0.639	NS	0.081	0.041	2.003	*
		Snow	0.008	0.004	1.966	*	-0.034	0.011	-3.190	**	0.164	0.039	4.221	***
		VPD	-0.024	0.01	-2.343	*	-0.119	0.027	-4.495	***	0.211	0.081	2.607	**
		$\text{VPD}_{\text{prev}}$	-0.039	0.012	-3.276	**	-0.126	0.030	-4.167	***	0.212	0.089	2.385	*
		BA	-0.156	0.042	-3.709	***	0.114	0.117	0.984	NS	0.351	0.296	1.185	NS
		TSF	0.003	0.044	0.070	NS	0.040	0.114	0.355	NS	0.207	0.391	0.530	NS
		SI	0.102	0.047	2.173	*	-0.074	0.120	-0.624	NS	-0.385	0.458	-0.839	NS
	Random effects (SD)	Plot	0.261				0.558				2.439			
		Tree in Plot	0.209				0.734				1.030			
		$R^2$ (Marginal/Conditional)				0.153 / 0.819				0.068 / 0.828				0.053 / 0.922
Jack Pine	Fixed effects	Intercept	1.078	0.060	18.082	***	20.167	0.138	145.943	***	35.068	0.435	80.644	***
		CMI	0.029	0.008	3.590	***	0.021	0.015	1.338	NS	-0.127	0.059	-2.166	*
		$\text{CMI}_{\text{prev}}$	0.015	0.009	1.581	NS	-0.013	0.020	-0.675	NS	0.021	0.072	0.295	NS
		Snow	-0.018	0.007	-2.437	*	-0.019	0.018	-1.062	NS	0.040	0.070	0.574	NS
		VPD	-0.046	0.018	-2.499	*	-0.145	0.032	-4.562	***	0.291	0.127	2.297	*
		$\text{VPD}_{\text{prev}}$	-0.012	0.022	-0.538	NS	0.002	0.036	0.050	NS	0.369	0.149	2.471	*
		BA	-0.010	0.043	-0.235	NS	-0.018	0.093	-0.194	NS	-0.433	0.317	-1.366	NS
		TSF	0.168	0.081	2.082	*	-0.004	0.180	-0.023	NS	0.289	0.540	0.534	NS
		SI	0.007	0.053	0.124	NS	-0.165	0.126	-1.310	NS	-0.390	0.447	-0.872	NS
	Random effects (SD)	Plot	< 0.001				0.254				< 0.001			
		Tree in Plot	0.127				0.604				1.701			
		$R^2$ (Marginal/Conditional)				0.089 / 0.204				0.073 / 0.847				0.089 / 0.795

## 2.4 Discussion

### 2.4.1 A reduction in stomatal conductance during drought leads to growth declines

We observed that 1988-1989 black spruce  $\Delta^{13}\text{C}_{\text{ring}}$  values were lower and  $\Delta^{18}\text{O}_{\text{ring}}$  values were higher compared to the 1985-1993 averages (Figure 2.4). According to the conceptual model of Scheidegger *et al.* (2000), this suggests that trees have closed stomata more stringently than before and after the drought period, which could have decreased stomatal conductance without inducing changes in photosynthesis rates that can be detected using isotopic signatures in tree rings. This decrease in  $\Delta^{13}\text{C}_{\text{ring}}$  and increase in  $\Delta^{18}\text{O}_{\text{ring}}$  was coupled with lower growth rates for both species ( $\text{GI} < 1$ ; z-scored  $\text{GI} < 0$ ). To our knowledge, no insect epidemics occurred within our sampling area over the study period (also see Figure 6 in Ols *et al.*, 2018a). A plausible explanation for this counter-intuitive relationship (i.e. a reduced growth coupled with – the hypothesis of – a reduced stomatal conductance and unchanged or slightly reduced assimilation rates) could be a modification in carbon allocation strategy of black spruce trees to reduce secondary stem and root growth (Way et Sage, 2008a) and preferentially save and invest in non-structural carbohydrate (NSC) reserves (Hartmann *et al.*, 2015). Indeed, Way and Sage (2008a) found that black spruce seedlings grown at elevated temperature experienced up to 60% lower growth rates compared to seedlings at ambient temperature because of a heat- and drought-induced reduction in cell expansion and division. This decreases the need of carbon for structural building and instead allows trees to store carbon in the form of starch and sugars (Balducci *et al.*, 2013 ; Muller *et al.*, 2011 ; Way et Sage, 2008a). For jack pine, the isotopic signatures of these two years were close to the 1985-1993 averages, maybe meaning that this species maintained physiological processes relatively unchanged during the drought. However, in 1991, tree ring  $\Delta^{18}\text{O}_{\text{ring}}$  significantly increased for both species and this was not mirrored by any change in  $\Delta^{13}\text{C}_{\text{ring}}$ . This pattern can be

explained by a decrease in assimilation rates that paralleled the decrease in stomatal conductance (Scheidegger *et al.*, 2000), maybe the result of a more stringent regulation of stomatal aperture which significantly lowered carbon uptake.

Oxygen isotopic signal in tree rings is strongly dependent on the composition of source water. Even if we tried to estimate and remove oxygen isotopic composition of precipitation (Eq.2), additional non-physiological mechanisms could have been involved in the inter-annual differences in  $\Delta^{18}\text{O}_{\text{ring}}$ . First, the taproot of jack pine (Burns et Honkala, 1990) makes this species more responsive than black spruce to deep groundwater inputs, especially when comparing jack pine with lowland black spruce (Girardin *et al.*, 2008). During years characterized by a fast depletion of surficial water, jack pine trees could have relied more into deep-water reserves which are usually characterized by a lower  $^{18}\text{O}$  enrichment compared with water from soil layers closer to the surface (Tang et Feng, 2001). Then, we analysed isotopic signature of the whole ring which is integrated over the entire growing season. So, we were unable to distinguish changes in  $\Delta^{18}\text{O}_{\text{ring}}$  occurring as a result of a modification in the seasonality of precipitation inputs (Xu *et al.*, 2020). Finally, black spruce and jack pine individuals selected in this study were located in different sample plots. So, we cannot exclude that between-species differences originate from an effect of environmental conditions on the sensitivity of trees to drought.

#### 2.4.2 Black spruce responds stronger to low climatic water balance and high vapour pressure deficits in summer than jack pine

As hypothesized, results from linear mixed models show that an increase in summer vapour pressure deficit significantly decreased carbon isotope discrimination and increased oxygen enrichment of black spruce and jack pine. On the other hand, growing season CMI had only a marginally significant positive effect on black spruce carbon discrimination but a highly significant negative effect on oxygen discrimination of both species. This later effect was especially high in the case of black spruce. Because of a

shallow, adventitious rooting system, black spruce trees have limited access to deep groundwater reserves and are almost exclusively rooted in the soil organic layer. These findings suggest that spruce trees close stomata more stringently when atmosphere and soil conditions become increasingly dry, as a means to save water and maintain their hydraulic integrity. This is not surprising since tree species inhabiting wetter environments, such as black spruce, generally show a lower resistance to embolism and likely have narrower safety margins than species specific to dry environments such as jack pine\_(Choat *et al.*, 2012 ; Wu *et al.*, 2020). Thus, carbon assimilation rates of spruce could have declined early during drought and this species could be less efficient than pine at refilling embolized vessels and storing carbohydrates within the stem (Adams *et al.*, 2017). This could make black spruce particularly prone to a so-called “legacy” or “lag” effect in which a dry event induces low growth rates not only the year it occurs but also several years later (Anderegg *et al.*, 2015b ; Huang *et al.*, 2018). This was observed here through the significant negative effect of summer VDP and positive effect of growing season CMI of the year prior to ring formation on black spruce growth (Table 2.1 and Annexe B, Supplement S2.5). Interestingly, we did not observe any statistically significant lag effect for jack pine. In addition, average carbon discrimination was higher for jack pine than black spruce, but there was no difference in average oxygen discrimination between the two species.

Taken together, these results suggest that, instead of different hydraulic behaviours which would have led to different  $\Delta^{18}\text{O}_{\text{ring}}$ , the difference between the two species in terms of  $\Delta^{13}\text{C}_{\text{ring}}$  could originate from different carbon use efficiencies. Lavigne and Ryan (1997) and Ryan *et al.* (1997) previously observed a lower carbon use efficiency for black spruce compared to jack pine in the boreal forest of Saskatchewan. Additionally, black spruce reduces the root to shoot ratio as a response to an increase in temperature, which exacerbates the negative impacts of droughts by lowering the capacity of trees to access water (Way et Sage, 2008a). Together with other morphophysiological adaptations to a stressful, waterlogged and cold environment (Burns et

Honkala, 1990), this species exhibits a low acclimation potential to warmer temperatures (Way et Sage, 2008a). These findings suggest that spruces will be more negatively impacted by droughts and heatwaves than pines; with a slower and less complete recovery and a more marked lag effect, as observed here.

We observed a significant effect of total annual snowfall on black spruce growth, carbon and oxygen isotope discrimination. Black spruce growth indices were generally higher in regions and years characterized by high annual snowfall, which means that trees had either higher growth rates than, or growth rates closer to those (in case of GI below 1), expected under average climate conditions. The corresponding growth rings were more depleted in  $^{13}\text{C}$  and enriched in  $^{18}\text{O}$  than rings from years and regions with low annual snowfall. In jack pine, annual snowfall had a significant, negative effect on growth indices only. In years and regions characterized by a more abundant annual snowfall, snowmelt and soil thawing can occur late in the season; which can delay the start of growth (Vaganov *et al.*, 1999 ; Verbyla, 2015). This is a likely explanation for the lower growth indices observed for jack pine trees in years and sites with higher snow accumulation. For black spruce, an additional snowpack can have helped to protect the shallow root system of trees (Frey, 1983), as well as the newly formed buds (Marquis *et al.*, 2020a), which would have outbalanced the negative effect of a delayed soil thaw and growth onset. For this species, the significant effect of annual snowfall observed on  $\Delta^{13}\text{C}_{\text{ring}}$  and  $\Delta^{18}\text{O}_{\text{ring}}$  was opposite in direction to the effect of soil moisture availability and vapor pressure deficit (i.e.  $\Delta^{13}\text{C}$  decreased and  $\Delta^{18}\text{O}$  increased with high snowfall, with high VPD and low CMI during summer, Table 2.1, Annexe B, Supplement S2.5). This is likely an indication of hydric stress, as already stated by Walker *et al.* (2015) in Alaska for the same species. This could also be the result of a higher proportion of wood cells formed during the summer season. More summer-formed cells would lead to a stronger summer drought signal compared to growth rings whose initiation started early in spring. It is interesting to note that, for spruce, the effect of snow was no longer present when looking at  $\delta^{18}\text{O}$  values (Supplementary

Table S.4.2). This could be an indication that the  $\delta^{18}\text{O}$  signature in tree rings is likely a mixing between the signal from source water (snow water and water from deeper soil layers is usually more depleted in  $^{18}\text{O}$  compared with rain water and water from soil layers closer to the surface) and the enrichment occurring after water entered the trees hydraulic pathway.

#### 2.4.3 High inter-tree and inter-plot variability in physiological responses to drought

Besides the effects of climate variables on  $\Delta^{13}\text{C}_{\text{ring}}$  and  $\Delta^{18}\text{O}_{\text{ring}}$ , we observed a high inter-tree and inter-plot variability on isotopic signatures. This becomes particularly apparent through the strong variability associated with random factors in LMMs, coupled with far higher conditional r-squared than marginal r-squared values. We hypothesize that such variability results from the high spatial heterogeneity in growth conditions. First, climate averages differed within the study zone. Easternmost locations were, on average, more humid than westernmost plots (Figures 2.1 and 2.3); and this could have influenced the impact of a below-average summer aridity on trees physiology. Additionally, the intensity of 1988-1989 and 1991 droughts differed between the study plots. Some plots did not experience drier-than-average conditions during these years (Figure 2.3). Second, some types of substrates, such as poorly weathered (i.e. relatively young, mainly rocky substrate with no or thin organic horizon) and dry soils (Levanič *et al.*, 2011 ; Raney *et al.*, 2016), could exert a long-term impact on tree physiology, as hypothesized by Levanič *et al.* (2011) to explain the difference in  $\Delta^{13}\text{C}$  between healthy and dying oaks in Slovenia. In our case, there is a possibility that this effect occurred at the scale of the micro-environment (i.e. variations in topography and soil conditions within the plot), even if we constrained the selection of trees to similar soil conditions. Competition for water, light and nutrients also decreases the capacity of trees to physiologically react and adapt to fast and episodic changes in their environment (Sohn *et al.*, 2012, 2014, 2016). Those tree populations subjected to such a prolonged stress, including a drier regional climate, can thus be more sensitive

to short-term stressors such as droughts (Levanić *et al.*, 2011 ; Raney *et al.*, 2016). By contrast, some microenvironments, referred to as “hydrological [micro]refugia”, buffer the impacts of droughts on trees because of an enhanced capacity to maintain soil water availability under dry conditions (McLaughlin *et al.*, 2017 ; Stralberg *et al.*, 2020). Our climate dataset, and more generally gridded and interpolated climate datasets, often do not accurately estimate differences in microenvironmental conditions and in groundwater depth, another factor influencing tree-ring isotope discrimination (Sun *et al.*, 2018). This high inter-tree variability was previously observed in *Pinus uncinata* trees in the Spanish Pyrenees by Konter *et al.* (2014) and was attributed both to variations in microclimate conditions, to differences in rooting depth of trees and to genetically-driven differences in trees’ physiological status (Konter *et al.*, 2014). Such differently performing genotypes are linked with diverging forcing factors on the selection of life-history traits. Indeed, environmental gradients, such as differences in regional climate and photoperiod, can influence the genetic structure of trees (McKown *et al.*, 2014) and more specifically their hydraulic traits (Depardieu *et al.*, 2020 ; Isaac-Renton *et al.*, 2018 ; Li *et al.*, 2018).

#### 2.4.4 Conclusions

We identified that decreases in tree growth from drought in our study area can be linked to differential physiological responses of the studied species. Inferring physiological variables from tree-ring isotopic composition, which are measures integrated over the whole growing season and the whole tree canopy, likely induced some uncertainties in the estimated effects of climate. More specifically, we observed a high inter-individual variability in these isotopic signatures, which could be related to contrasting microsite conditions instead of to differences in physiological response to climate. However, this high heterogeneity may also suggest that some tree populations are better adapted and can better acclimate to warmer and dryer conditions than others, and that some areas could buffer the impact of climate warming on forest productivity. We identified

differences between the two study species, with a longer lasting and stronger impact of drought on black spruce growth compared to jack pine. This suggests that the productivity of black spruce stands could decline in the future as more frequent and more severe drought episodes are likely to occur.

To better target areas most severely impacted by climate change, additional data from trees growing on contrasting environments are needed. More specifically, there is currently a lack of knowledge about the response of trees growing on the least accessible and least economically attractive forested areas, i.e. organic-rich, paludified stands, which represent a high proportion of the boreal biome (Boisvenue *et al.*, 2016 ; Drobyshev *et al.*, 2010). We also used bulk wood material, which could contain carbon from non-structural carbohydrates formed during the previous growing seasons. To address these issues, a network of monitored trees could be established in a subset of forest inventory plots, where direct measurements of foliar gas-exchanges would provide high temporal resolution measures of photosynthesis and respiration. This would allow to pinpoint causal relationships between physiological processes and environmental variables directly instead of inferring them from tree-ring data.

## 2.5 Acknowledgements

This study was made possible thanks to the financial support that was provided by the Strategic and Discovery Grant programs of NSERC (Natural Sciences and Engineering Research Council of Canada), doctoral and travel scholarships funded by FRQNT (B2X and international internship programs), and a MITACS scholarship cofunded by Ouranos. Additional financial support was provided by the Centre for Forest Research (Centre d'Étude de la Forêt, CEF), the Canadian Forest Service, the UQAM Foundation (De Sève Foundation fellowship and TEMBEC forest ecology fellowship) and the Quebec Ministère de l'économie, de la Science et de l'innovation (programme PSR-SIIRI). We thank Rémi Saint-Amant (Canadian Forest Service) for providing helpful advices on the use of BioSIM software. We are very grateful to Marie Moulin, David Gervais and Christine Simard for the huge help with the processing of wood samples. Many thanks to Xiao Jing Guo (Canadian Forest Service) for helpful advice during statistical analyses, to Savoyane Lambert, Heike Geilmann and Iris Kuhlmann (Max Planck Institute for Biogeochemistry) for isotope measurements, and to Martine Savard, Joëlle Marion, Lauriane Dinis, Joëlle Berthier, Claude Durocher, Marie-Claude Gros-Louis, Philippe Labrie, Alexis Achim, Étienne Boucher, Nathalie Isabel, Claire Depardieu, and Mathilde Pau for help and advice with the processing of wood samples.

## CHAPITRE III

### STRONG OVERESTIMATION OF WATER-USE EFFICIENCY RESPONSES TO RISING CO<sub>2</sub> IN TREE-RING STUDIES

William Marchand<sup>1, 2, \*</sup>, Martin P. Girardin<sup>1, 2</sup>, Henrik Hartmann<sup>3</sup>, Claire Depardieu<sup>2, 4</sup>, Nathalie Isabel<sup>2, 4</sup>, Sylvie Gauthier<sup>1, 2</sup>, Étienne Boucher<sup>5, 6, 7</sup>, Yves Bergeron<sup>1, 8</sup>

<sup>1</sup>Centre d'étude de la forêt, Université du Québec à Montréal, C.P. 8888, succ. Centre-ville, Montréal, QC, Canada, and Forest Research Institute, Université du Québec en Abitibi-Témiscamingue, 445 boul. de l'Université, Rouyn Noranda, QC, Canada;

<sup>2</sup>Natural Resources Canada, Canadian Forest Service, Laurentian Forestry Centre, 1055 du P.E.P.S, P.O. Box 10380, Stn. Sainte-Foy, Québec, QC, Canada; <sup>3</sup>Max-Planck Institute for Biogeochemistry, Department of Biogeochemical Processes, Hans-Knöll Str. 10, 07745 Jena, Germany; <sup>4</sup>Chaire de recherche du Canada en génomique forestière, Université Laval, Sainte-Foy, QC, Canada; <sup>5</sup>GEOTOP, Université du Québec à Montréal, Montréal, QC, Canada; <sup>6</sup>Department of Geography, Université du Québec à Montréal, Montréal, QC, Canada; <sup>7</sup>Centre d'Études Nordiques, Université Laval, Québec, QC, Canada; <sup>8</sup>Institut de recherche sur les forêts, Université du Québec en Abitibi-Témiscamingue, 445 boul. de l'Université, Rouyn-Noranda, QC, Canada

\*Auteur correspondant: [william.marchand@uqat.ca](mailto:william.marchand@uqat.ca)

Publié dans Global Change Biology (2020) 26 : 4538-4558.  
<https://doi.org/10.1111/gcb.15166>

## Résumé

Le rapport en isotopes stables du carbone ( $\delta^{13}\text{C}$ ) des cernes de croissance est communément utilisé pour estimer le rapport entre les taux d'assimilation et la conductance stomatique des arbres, c'est-à-dire l'efficience d'utilisation de l'eau intrinsèque (iEUE). Des études récentes ont observé une augmentation de l'iEUE en réponse à l'accroissement de la concentration en CO<sub>2</sub> atmosphérique (C<sub>a</sub>), pour un grand nombre d'espèces, de genres et de biomes. Cependant, les taux d'accroissement de l'iEUE varient beaucoup d'une étude à l'autre, probablement à cause des nombreux facteurs covariants impliqués. Ici, nous avons quantifié les changements dans l'iEUE de deux espèces majeures de conifères boréaux en utilisant des échantillons d'arbres provenant d'un réseau d'inventaire forestier. Les arbres ont été échantillonnés le long d'un gradient important de conditions de croissance (estimées en utilisant l'indice de qualité de station, IQS), de stades de développement et d'histoire du peuplement. En analysant le signal isotopique des cernes de croissance, nous avons évalué l'ampleur de l'augmentation de l'iEUE après avoir tenu compte des effets reliés à la taille de l'arbre, à l'âge du peuplement, au climat et à l'IQS. Nous avons aussi estimé la manière dont les conditions de croissance avaient modulé la réponse physiologique des arbres à l'accroissement en CO<sub>2</sub>. Nous avons observé que l'accroissement en taille des arbres et le développement du peuplement avaient grandement influencé l'iEUE. L'effet CO<sub>2</sub> sur l'iEUE était fortement amoindri après avoir tenu compte de ces deux variables. L'iEUE a augmenté en réponse à l'accroissement en CO<sub>2</sub>, surtout chez les arbres implantés dans les peuplements fertiles. Au contraire, l'iEUE est restée quasiment inchangée dans les sites les plus pauvres. Nos résultats suggèrent que les études antérieures ont pu surestimer l'effet CO<sub>2</sub> sur l'iEUE, ce qui a potentiellement induit des conclusions biaisées quant à la balance carbonnée future de la forêt boréale. Nous avons également observé que cet effet CO<sub>2</sub> s'affaiblissait, ce qui pourrait affecter la

capacité future des arbres à résister et à recouvrer leur croissance suite à des épisodes de sécheresse.

Mots-clés : Forêt boréale, Canada, pin gris, épinette noire, rapport en isotopes stables du carbone

## Abstract

The carbon isotope ratio ( $\delta^{13}\text{C}$ ) in tree rings is commonly used to derive estimates of the assimilation-to-stomatal conductance rate of trees, i.e. intrinsic water use efficiency (iWUE). Recent studies have observed increased iWUE in response to rising atmospheric CO<sub>2</sub> concentrations (C<sub>a</sub>), in many different species, genera and biomes. However, increasing rates of iWUE vary widely from one study to another, likely because numerous covarying factors are involved. Here, we quantified changes in iWUE of two widely distributed boreal conifers using tree samples from a forest inventory network that were collected across a wide range of growing conditions (assessed using the site index, SI), developmental stages and stand histories. Using tree-ring isotopes analysis, we assessed the magnitude of increase in iWUE after accounting for the effects of tree size, stand age, nitrogen deposition, climate and SI. We also estimated how growth conditions have modulated tree physiological responses to rising C<sub>a</sub>. We found that increases in tree size and stand age greatly influenced iWUE. The effect of C<sub>a</sub> on iWUE was strongly reduced after accounting for these two variables. iWUE increased in response to C<sub>a</sub>, mostly in trees growing on fertile stands, whereas iWUE remained almost unchanged on poor sites. Our results suggest that past studies could have overestimated the CO<sub>2</sub> effect on iWUE, potentially leading to biased inferences about the future net carbon balance of the boreal forest. We also observed that this CO<sub>2</sub> effect is weakening, which could affect the future capacity of trees to resist and recover from drought episodes.

**Keywords:** Boreal forest, Canada, jack pine, black spruce, carbon isotope ratios

### 3.1 Introduction

The burning of fossil fuels by human populations has led to an unprecedented increase in the atmospheric carbon dioxide concentration ( $C_a$ ) since 1850 (Keeling *et al.*, 2015 ; Willeit *et al.*, 2019). As a consequence, average air temperature has risen by 0.5-3°C since the last century (Johns *et al.*, 2003), increasing the vapor pressure deficit (Ficklin et Novick, 2017). Trees are sessile and long-lived organisms that may acclimate to these abrupt changes through various mechanisms. Among these, phenotypic plasticity allows the current generation of trees to alter their morphological traits (e.g. stomatal density; Hetherington et Woodward, 2003) or to regulate physiological processes (e.g. transpiration rates; Gunderson *et al.*, 2010) in response to prevailing environmental conditions. Consequently, the amount of carbon assimilated each year would vary. Given the central role of trees and forests in the terrestrial carbon cycle (Bonan, 2008), there is an urgent need to assess to what extent do current global vegetation models perform: are they able to provide accurate predictions of forest response to future warmer growing conditions (Babst *et al.*, 2014)?

Under rising  $C_a$ , assimilation rate (A) of trees is expected to increase and stomatal conductance ( $g_s$ ) to decrease (Franks *et al.*, 2013). Thus, trees may regulate their stomatal aperture to either maximise carbon gain (i.e. higher A) or minimise transpiration loss (i.e. lower  $g_s$ ). Three theoretical strategies for stomatal regulation of leaf gas-exchanges have been extensively described in the literature, that link the leaf intercellular space CO<sub>2</sub> concentration ( $C_i$ ) to  $C_a$ : either a constant  $C_i$ , a constant  $C_a - C_i$  or a constant  $C_i/C_a$  could be maintained (Frank *et al.*, 2015 ; Saurer *et al.*, 2004 ; Voelker *et al.*, 2016). Until recently, most studies have reported results that are consistent with a constant  $C_i/C_a$  strategy (Bonal *et al.*, 2011 ; Franks *et al.*, 2013 ; Saurer *et al.*, 2004 ; Ward *et al.*, 2005). This strategy supposes changes in A and/or  $g_s$  of moderate intensity compared with the strong changes required to keep a constant  $C_i$ ; and with the relatively small changes needed to follow a constant  $C_a - C_i$  in response

to rising  $C_a$ . Voelker *et al.* (2016) proposed that instead of maintaining a single homeostatic gas-exchange strategy through time, trees can maximize carbon gain while minimizing the amount of water transpired by dynamically adjusting anatomical and physiological parameters to changing environmental conditions. However, this dynamic strategy is still under debate, and the leaf gas-exchange strategies followed by plants under a  $\text{CO}_2$ -enriched atmosphere remain uncertain (Lavergne *et al.*, 2019). These annual and long-term modifications in leaf gas-exchange variables are imprinted in growth rings, resulting in density and chemical composition variations of the wood that is produced annually (Gessler *et al.*, 2014). More specifically, during periods of high iWUE, with high  $A/g_s$ , a greater proportion of the heavier  $^{13}\text{CO}_2$  carbon isotope is assimilated and incorporated into biomass (Cernusak *et al.*, 2013 ; Scheidegger *et al.*, 2000), thereby increasing the  $^{13}\text{C}/^{12}\text{C}$  ratio within the produced wood cells.

A long-term increase in iWUE since 1850 was consistently reported for numerous tree species and geographic locations, and has been attributed to the rise in  $C_a$  (Battipaglia *et al.*, 2013 ; Frank *et al.*, 2015 ; Giguère-Croteau *et al.*, 2019 ; Lavergne *et al.*, 2019 ; Rezaie *et al.*, 2018 ; Saurer *et al.*, 2004 ; Savard *et al.*, 2020). Yet, the magnitude of this increase was highly variable between studies, ranging from 10 to 60% (Peñuelas *et al.*, 2011 ; Silva et Madhur, 2013). Such variability was also observed when comparing predictions from terrestrial ecosystem models (Masri *et al.*, 2019). This is likely because different taxa have different morphological traits, physiological strategies and evolutionary histories which could influence their response to rising  $C_a$ . A common observed pattern is a stronger sensitivity to  $C_a$  in angiosperms than gymnosperms (Klein et Ramon, 2019). Another explanation for the high range of variability between studies could be the existence of developmental and environmental factors that affect tree physiological processes. For instance, iWUE levels are higher in older and taller trees than in younger and smaller trees (Arco Molina *et al.*, 2019 ; Helama *et al.*, 2015 ; McDowell *et al.*, 2011 ; Monserud et Marshall, 2001). In this regard, Brienen *et al.* (2017) suggested that a large component of the positive trends in

iWUE could be the result of an increase in size with tree ageing, thereby confounding the influence of  $C_a$  on iWUE.

Another source of uncertainty comes from spatial heterogeneity in growth conditions, and their potential effects on tree iWUE (Saurer *et al.*, 2014 ; Shestakova *et al.*, 2019). For example, high elevation trees generally exhibit lower iWUE levels and weaker increasing trends than trees growing in lowlands (Liu *et al.*, 2007 ; Wu *et al.*, 2015). Gradients of moisture availability also influence iWUE levels and trends, but there is currently no consensus regarding the direction of this relationship (Arco Molina *et al.*, 2019 ; Waterhouse *et al.*, 2004). Yet, studies accounting for developmental trends and effects of environmental conditions when studying the effects of a CO<sub>2</sub>-enriched atmosphere on tree-ring derived iWUE are still scarce. Improved estimation of iWUE in light of the many processes that are involved could help testing vegetation models (Frank *et al.*, 2015), together with constraining these with more comprehensive parameter estimates (e.g. Girardin *et al.*, 2016a), thereby improving predictions of forest response to future global changes (Lavergne *et al.*, 2019).

Here, we present unpublished annually resolved iWUE data for two widely-distributed conifer species of boreal North America, black spruce (*Picea mariana* (Mill.) B.S.P.) and jack pine (*Pinus banksiana* Lamb.), for which historical iWUE data are still scarce. The two study species occupy different ecological niches and, therefore, have developed different life-history traits. Black spruce is characterized by a shallow rooting system and is mostly generalist in terms of soil hydrological conditions, from relatively well-drained stands to organic substrata to bog-like areas. Jack pine has deeper roots, and is more specific to well-drained, sandy substrata. We analyzed temporal variability in  $\delta^{13}\text{C}$ -derived iWUE of 3,929 tree-ring samples from 98 black spruce and 50 jack pine trees extending back to the pre-industrial period, spread across the Eastern Canadian boreal forest and growing under highly diverse conditions (Figure 3.1a; Table 3.1). We assessed the extent to which this variability is related to the rise

in C<sub>a</sub>, before and after removing confounding effects of ecological variables, such as tree size, stand age, climate, nitrogen deposition, and site fertility.

## 3.2 Materials and Methods

### 3.2.1 Study area

The study area covers the territory of the Quebec Northern Ecoforest Inventory program (NEI; Létourneau *et al.*, 2008; Figure 3.1a). Within the NEI, 875 plots were sampled from 2005 to 2009 and distributed over a 20 degree-wide longitudinal gradient north of Quebec's limit of commercial forests, i.e. north of 49°N. Plots were established within naturally regenerated and unmanaged conifer-dominated forests. The plot network encompasses a broad climate gradient. Westernmost trees are growing in a warmer and drier climate than trees that are located further east (Table 3.1). The relief and surficial deposits are also highly variable across the study area, from relatively flat landscapes and organic-rich soils in the west, to hillsides and thick till deposits in the central area, to high hills and rocky substrates further east (Robitaille *et al.*, 2015). As a result of these environmental gradients, fire return intervals are longer in the east, making it difficult for jack pine to regenerate naturally (Le Goff et Sirois, 2004). Consequently, this species is mostly located in the western part of the study area (i.e. 72-80°W).

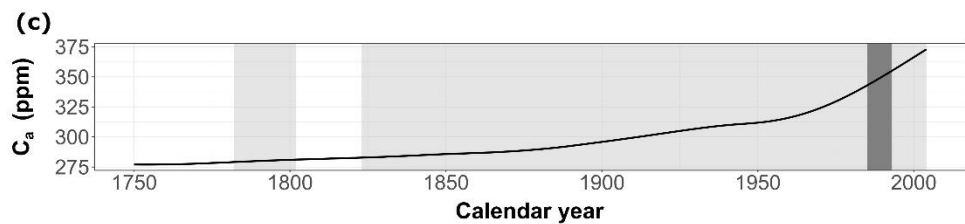
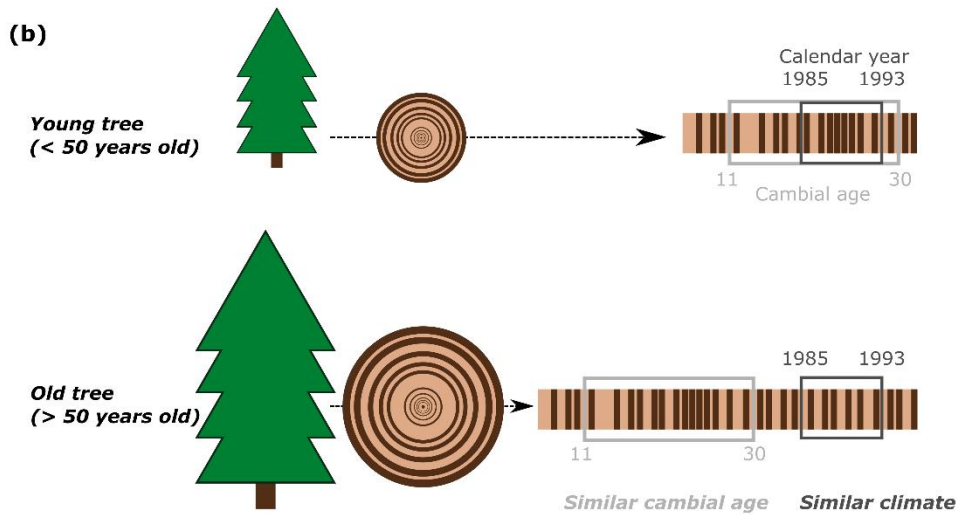
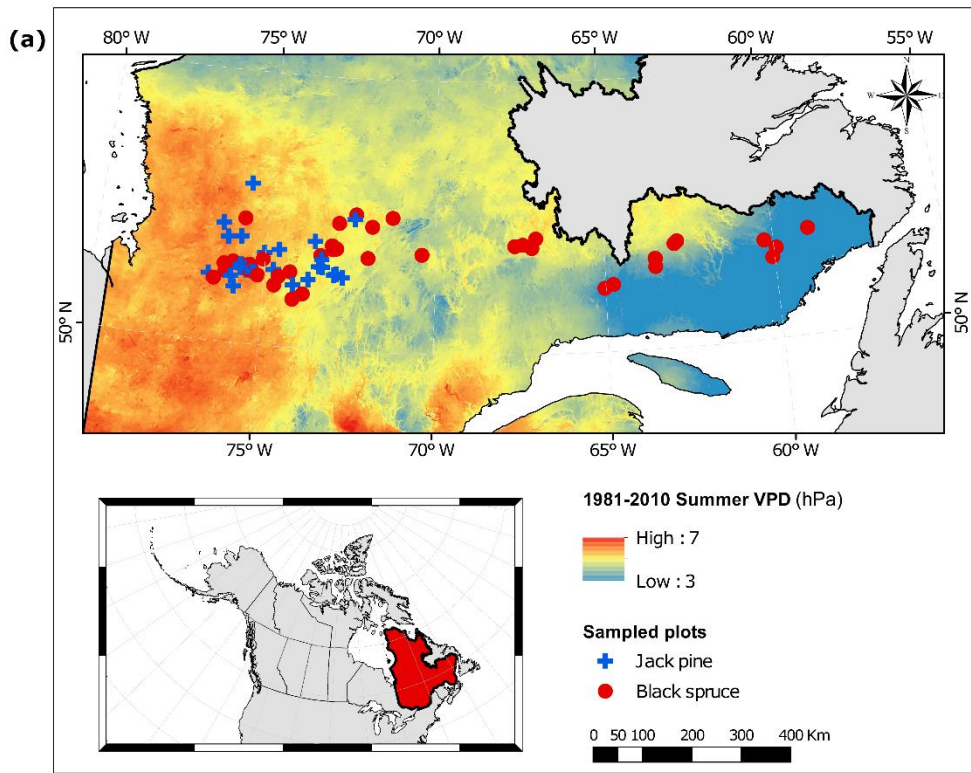


Figure 3.1. Study area and sampling strategy for isotope analyses. (a) Study area and distribution of the sample plots; (b) sampling strategy of growth rings for isotope analyses. Color gradient in (a) shows the 1981-2010 averages of summer (June-August) vapor pressure deficits. Note that jack pine is absent from the central and eastern portions of the study area. This corresponds to the spatial extent of the species (only present in the west) and is likely the result of different fire cycles (low fire cycles in the central and eastern portions, which prevent jack pine regeneration, since this species produces mostly serotinous cones). In (b), the two targeted periods are indicated by gray tones: a period corresponding to calendar years 1985-1993 (dark gray), and a period corresponding to 1 m-height cambial ages 11-30 years (light gray). Two cases are illustrated, depending on tree age: in the case of young trees, the period of calendar years 1985-1993 is included within the period of cambial ages 11-30 years; in the case of old trees, the two periods are distinct from one another. (c) Atmospheric CO<sub>2</sub> concentration (C<sub>a</sub>) for the period 1750-2005. Shading denotes time-periods covered by isotope analyses: light gray shading is for the period of 1 m height ring ages 11-30 years; dark gray shading is for the 1985-1993 time-period. Note that the rise in C<sub>a</sub> is faster after 1950.

Table 3.1. Climate and physiographic characteristics of the study area. Also shown are the number of trees and stands that were selected, averages, minimum and maximum values of BAI, iWUE<sub>ring</sub> and tree age (number of rings at ground level) by geographic location and species.

Statistics	Tree species	West (78-72°W)	Center (72-65°W)	East (65-57°W)
<b>Annual temperature (°C)</b>		-0.98	-1.33	-0.65
<b>Total annual precipitation (mm)</b>		868	892	1002
<b>Snow precipitation (mm)</b>		281	335	395
<b>Precipitation as rain (mm)</b>		587	557	607
<b>Elevation (m asl)</b>		352	532	352
<b>Tree number</b>	<b>Black spruce</b>	60	15	23
	<b>Jack pine</b>	50	0	0
<b>Stand number</b>	<b>Black spruce</b>	24	9	11
	<b>Jack pine</b>	29	0	0
<b>BAI (in mm<sup>2</sup>; mean; min-max)</b>	<b>Black spruce</b>	263.2 (2.5-1276.7)	146.2 (4.3-594.2)	295.3 (10.9-1547.4)
	<b>Jack pine</b>	389.5 (20.4-1830.6)	NA	NA
<b>iWUE (in µmol.mol<sup>-1</sup>; mean; min-max)</b>	<b>Black spruce</b>	64.2 (35.4-105.7)	69.7 (49.3-94.7)	69.4 (45.3-106.3)
	<b>Jack pine</b>	51.6 (29.4-73.9)	NA	NA
<b>Tree age (mean; min-max)</b>	<b>Black spruce</b>	92.1 (33-194)	104.9 (37-185)	82 (35-237)
	<b>Jack pine</b>	64.0 (32-129)	NA	NA

### 3.2.2 Tree sampling

As part of the inventory program, stem disks were collected at multiple heights on the stem from 1-3 upper-canopy trees per plot and species for dendrochronological analysis (see Girardin *et al.*, 2014 ; Marchand *et al.*, 2019 ; Ols *et al.*, 2018b). Disks were prepared and processed for ring-width measurement following standard dendrochronological procedures across four radii per disk (Ministère des Ressources Naturelles du Québec, 2008). Cross-dating and measurements were validated using the program COFECHA (Holmes, 1983). For the purpose of isotope analyses, we focused on the 1m-height stem disks as a trade-off between the number of available rings and the regularity of ring boundaries.

The total number of tree samples that was made available for this study was 1914 black spruce and 352 jack pine (Marchand *et al.*, 2019). From those trees, 98 black spruce and 50 jack pine trees were randomly selected from a pool of candidate trees that satisfied the following conditions: (1) tree age at 1 m height was greater than 30 years in 2005; (2) samples did not contain missing rings; (3) plots were located between 250 m and 550 m a.s.l.; (4) plots were located on moderate to well-drained sites with an organic layer < 0.3 m thick; and (5) soil texture was either sand or loam. This sampling strategy allowed to control for the altitudinal effect on iWUE (Wu *et al.*, 2015), and to compare trees that experienced relatively similar soil moisture conditions (i.e. only stands on well-drained soils were selected, not on clayey soils or bogs where standing water could be found). Plots that were composed of trees with highly diverse age and diameter structures were excluded to avoid individuals that have regenerated by layering. This selection led to a low-replicated tree-by-plot network (an average of two trees were processed per plot for isotope analyses). Such strategy, used in some dendroecological studies (e.g. Bert *et al.*, 1997 ; Ponton *et al.*, 2001 ; Sullivan *et al.*, 2017) allowed to optimize the trade-off between covering the gradient of growth conditions and stand-disturbance histories and obtaining results more representative of

the response of the average boreal forest. However, this is at the expense of the representativeness of each of the individual plot populations (Daux *et al.*, 2018).

### 3.2.3 Variables for tree and stand-level developmental changes, climate and growth conditions

As a variable accounting for tree-level developmental changes, the basal area (BA) that a tree reached at a specific year was computed from ring-width measurements for all trees sampled during the forest inventory campaign. For each disk, ring widths of the four radii were averaged and converted to basal area increments (BAI; function *bai.out* of the R package *dplR*; Bunn, 2008). Inner-bark BA was then computed as the sum of BAIs of the previous years. We assume that basal area incorporates changes occurring in physiological processes and architecture as the tree grows larger. In our analysis, changes in stand development were accounted for through an estimate of the minimum time-since-fire (TSF). This is a time-dependent variable, computed as the ground-level ring count (i.e. ground-level cambial age) of the oldest of the sampled trees within a plot. TSF incorporates changes in stand structure and composition (species succession), as well as in edaphic parameters (accumulation of organic material) since last fire.

A fertility index (Site Index, SI) was used as a variable summarizing the aforementioned differences in physiographic and climatic conditions within the longitudinal gradient. This index is defined as the maximum height that an unrepreserved, undamaged upper-canopy tree attains at age 50 (measured at breast height, 1.3 m). It is a measure of how trees perform in view of the site's biophysical specificities and is a proxy for the suitability of environmental conditions for growth. SI values, which were available only for black spruce (Létourneau *et al.*, 2008), were extrapolated to the entire area using measures of similarity of a given location with the sampled stands in terms of several biophysical variables including climate conditions, soil surficial deposits, elevation, slope and exposition (Gauthier *et al.*, 2015b). Jack pine is known for growing more rapidly than black spruce during its juvenile stage, yet the black spruce site

fertility index is nonetheless a good indicator of jack pine's productivity potential for comparable site conditions (see Annexe C, Figure S3.1).

To examine the effect of inter-annual variation in climate on iWUE<sub>ring</sub>, monthly averages of maximum and minimum temperature and monthly total precipitation were obtained at a 0.08° x 0.08° spatial resolution for the period 1866-2004, using thin-plate spline smoothing algorithms which interpolate monthly climate data from Canada's weather stations (ANUSPLIN; McKenney *et al.*, 2006 ; Price *et al.*, 2011). Since dewpoint temperature or relative humidity data were not available in our study area for a time-period extending back to 1866, monthly vapor pressure deficits (VPD) were then estimated following Landsberg and Sands (2010):

$$\text{Eq.1} \quad VPD_{month} = 0.5 \times (\varepsilon_{Tmax} - \varepsilon_{Tmin})$$

where  $\varepsilon_{Tmax}$  and  $\varepsilon_{Tmin}$  are the saturated vapor pressures at maximum and minimum temperatures, respectively, which were assumed to be equal to saturation pressure and air vapor pressure. Vapor pressure is given, for a specific temperature T, by:

$$\text{Eq.2} \quad \varepsilon_T = 0.61078 \times e^{17.269 \times T / (273.3 + T)}$$

VPD values derived from Eq.1 are highly correlated to values obtained using a more conventional equation including actual vapor pressure (Allen *et al.*, 1998; see Annexe C, Figure S3.2). Monthly VPD were averaged and monthly precipitation was summed at a seasonal scale. Data from the summer season (June to August) were used for statistical analyses since the growing season is generally restricted to this short time interval within the study area.

We also obtained total annual nitrogen deposition (Ndeposit, in kg N ha<sup>-1</sup> yr<sup>-1</sup>) for the period 1866-2004, extracted for our plots from the Mendeley – NACID-NDEP1 database that provides annual estimates of nitrogen depositions at a 1-km spatial

resolution, which were interpolated based on in-situ measurements, satellite data and modelled values (Hember, 2018).

### 3.2.4 Wood samples preparation for isotope measurements

A sampling experiment was designed to optimize time and resources while allowing to account for temporal changes in both developmental processes and climate. From the 148 trees that were selected, two different sets of growth-rings were analyzed (Figure 3.1b). First, the 11<sup>th</sup> to 30<sup>th</sup> rings from the pith (i.e. 1 m-height cambial ages of 11-30 years) were targeted to focus on a life-period where trees were in their maturation phase. In addition, growth rings formed during calendar years 1985-1993 were also targeted (Figure 3.1b) to focus on a time-period during which trees had reached different developmental stages (cambial ages ranging from 11 to 221 years). The 1985-1993 period was characterized by a high climatic variability, and comprised three consecutive hot and dry summers (1989-1991) as well as one extremely wet summer in 1992 (Annexe C, Figure S3.3). Together, these two sampling periods allowed us to disentangle the effect of rising C<sub>a</sub> on iWUE from those of changes that were incurred in developmental stages (Figure 3.1b,c).

From each stem disk, a 0.8cm x 0.8cm wood strip, from bark to bark and including the pith was excised using a bandsaw. Annual rings were individually separated using a razor blade under a binocular microscope. For the thinnest rings (207 samples, ring widths < ~0.1 mm), a sledge microtome that was coupled with digital cameras was used. Wood samples were milled to fine particles using a Retsch MM400 (Retsch, Haan, Germany) ball mill with stainless steel balls and stainless steel vials to avoid any potential contamination that would be incurred when using standard plastic vials (Isaac-Renton *et al.*, 2016). The whole wood samples were used for isotope measurements since several studies have already demonstrated strong correlations between isotopic signatures of whole wood and  $\alpha$ -cellulose in black spruce (Bégin *et*

*al.*, 2015 ; Walker *et al.*, 2015) and in many other tree species (Harlow *et al.*, 2006). The relative proportion of resins, lignin and hemi-cellulose in whole wood of conifers can vary from one year to another, which could generate additional variability in the isotopic signal, not related to changes in environmental conditions (Gessler *et al.*, 2014). However, this additional noise in the isotopic data does not affect correlations between isotopic signals and environmental gradients (e.g. Fernández-de-Uña *et al.*, 2016 ; Fu *et al.*, 2020 ; Isaac-Renton *et al.*, 2018 ; Walker *et al.*, 2015). About 0.3-1.0 mg of the milled wood material was weighed into tin capsules.  $\delta^{13}\text{C}_{\text{ring}}$  (per mill, ‰) was measured using a Finnigan Delta+ IRMS coupled to an EA 1100 (CE, Milan, Italy) at the Stable Isotope Laboratory (BGC-IsoLab, Max Planck Institute for Biogeochemistry, Jena, Germany), with an average analytical precision better than  $\pm 0.07\text{ ‰}$  standard deviation (monitored both by repeated measurements of QC caffeine standard and duplicated samples, see Annexe C, Figure S3.4). One should note that rings that were too thin to be individually separated were not processed, resulting in a total of 3,929  $\delta^{13}\text{C}_{\text{ring}}$  samples spanning the period 1783-2004.

### 3.2.5 Inference of iWUE from tree-ring carbon isotope ratios

Assuming that no additional discrimination occurred between CO<sub>2</sub> assimilation and growth ring formation,  $\delta^{13}\text{C}_{\text{ring}}$  values were converted to atmosphere-to-tree-ring isotope discrimination (Farquhar et Richards, 1984) using the following equation:

$$\text{Eq. 3} \quad \Delta^{13}\text{C}_{\text{ring}} = \frac{(\delta^{13}\text{C}_a - \delta^{13}\text{C}_{\text{ring}})}{1 + \frac{\delta^{13}\text{C}_{\text{ring}}}{1000}}$$

where  $\delta^{13}\text{C}_a$  is the atmospheric stable carbon isotope ratio. From 1850 to 2004,  $\delta^{13}\text{C}_a$  values were obtained from Graven *et al.* (2017). 1783-1849  $\delta^{13}\text{C}_a$  values were linearly regressed based on the Francey *et al.* (1999) dataset.

According to Farquhar *et al.* (1982b), the relationship between atmosphere-to-plant isotope discrimination and the ratio of intercellular-to-atmospheric CO<sub>2</sub> concentration (C<sub>i</sub>/C<sub>a</sub>) is as follows:

$$\text{Eq.4} \quad \Delta^{13}C_{ring} = a + (b - a) \times \frac{C_i}{C_a} - f \frac{\Gamma^*}{C_a}$$

where a is the fractionation rate of <sup>13</sup>CO<sub>2</sub> relative to <sup>12</sup>CO<sub>2</sub> during stomatal diffusion ( $\approx 4.4\text{‰}$ ), and b the fractionation rate during assimilation ( $\approx 27\text{‰}$ ). f is the fractionation associated with photorespiration ( $\approx 12\text{‰}$ ) and  $\Gamma^*$  is the CO<sub>2</sub> compensation point in the absence of mitochondrial respiration (Bernacchi *et al.*, 2001).  $\Gamma^*$  was computed using the *rpmmodel* R package (Stocker *et al.*, 2019) using the average summer maximum temperature, which is representative of the temperature of the photosynthetically-active period. Since no climate data were available before 1866 in our study area, 1783-1865  $\Gamma^*$  values were estimated using the average summer maximum temperature of the 1866-1900 period. The fractionation term for photorespiration ( $-f \frac{\Gamma^*}{C_a}$ ) was added as recommended by several previous studies (Keeling *et al.*, 2017 ; Lavergne *et al.*, 2019, 2020 ; Schubert et Jahren, 2018).

Intrinsic water use efficiency (iWUE<sub>ring</sub>) is defined as the ratio of assimilation rate (A) to stomatal conductance (g<sub>s</sub>). A can be calculated from C<sub>i</sub> / C<sub>a</sub> using Fick's law:

$$\text{Eq.5} \quad A = \frac{g_s \times (C_a - C_i)}{1.6}$$

where 1.6 is the ratio of diffusivity of water vapor and CO<sub>2</sub> in the atmosphere.

Using Eq.4-5, iWUE<sub>ring</sub> can be derived as:

$$\text{Eq.6} \quad iWUE_{ring} = \frac{A}{g_s} = \frac{(C_a - C_i)}{1.6} = \frac{C_a \left( b - \left[ \frac{(\delta^{13}C_a - \delta^{13}C_{ring})}{1 + \frac{\delta^{13}C_{ring}}{1000}} \right] - f \frac{\Gamma^*}{C_a} \right)}{1.6 \times (b - a)}$$

with  $C_a$  the atmospheric CO<sub>2</sub> concentration, obtained from Frank *et al.* (2010).

### 3.2.6 Statistical analyses

The relationship between BAI and iWUE<sub>ring</sub> was assessed by computing Spearman rank correlation coefficients using the *stats* R package, by species. To account for spatial autocorrelation, the p-values associated with these tests were adjusted to an effective sample size by performing a Dutilleul's modified t-test (Legendre *et al.*, 2002).

The main statistical procedure consisted of three distinct steps, which are summarized in the workflow diagram (Figure 3.2). The first step, previously described, was the estimation of iWUE<sub>ring</sub> based on tree-ring δ<sup>13</sup>C. During the second step, the effects of environmental and developmental variables on iWUE<sub>ring</sub> were estimated and removed. The final step (Step III in Figure 3.2) consisted of the assessment of the relationship between iWUE<sub>ring</sub> and  $C_a$ , converted to partial pressure of CO<sub>2</sub> (P<sub>CO<sub>2</sub></sub>, Pascal), depending on SI. The P<sub>CO<sub>2</sub></sub>, which corrects for the elevation effect on  $C_a$ , was calculated using Eq.7:

$$\text{Eq.7} \quad P_{CO_2} = 10^{-6} \times C_a \times P_{atm}$$

where  $P_{atm}$  (in Pascal) is the atmospheric pressure, computed using site elevation following Allen *et al.* (1998).

Generalized Additive Mixed Models (GAMM) were used to examine the relationship between iWUE<sub>ring</sub> and  $C_a$  (*gamm* function of the R package *mgcv*; Wood, 2017). The effect of the statistical procedure on the removal of developmental trends and, ultimately, the estimation of the effect of  $C_a$  on iWUE<sub>ring</sub>, was assessed using three different GAMM models by species (see Figure 3.2).

A first set of GAMMs (the ‘null’ models) including the intercept only was run, assuming that the variables had no effect on  $iWUE_{ring}$ . The null models took the following form:

$$\text{Eq.8} \quad iWUE_{ring} \sim 1 + \left( \frac{\text{Plot}}{\text{Tree}} \right) + \text{corCAR1} \left( \text{year} | \left( \frac{\text{Plot}}{\text{Tree}} \right) \right)$$

where  $\left( \frac{\text{Plot}}{\text{Tree}} \right)$  represents the random effect of the tree nested within the plot and  $\text{corCAR1}$  is an autocorrelation structure allowing for unequally-spaced observations (Singer et Willett, 2003).

In the second set of GAMMs (the ‘full’ models), tree size, TSF, summer VPD and precipitation, annual nitrogen deposition, and SI were added as covariates. The full models took the following form:

$$\text{Eq.9} \quad iWUE_{ring} \sim 1 + s(\text{Size}) + s(\text{TSF}) + s(\text{VPD}) + s(\text{Prec.}) + s(\text{N}_{\text{deposits}}) + s(\text{SI}) + \left( \frac{\text{Plot}}{\text{Tree}} \right) + \text{corCAR1} \left( \text{year} | \left( \frac{\text{Plot}}{\text{Tree}} \right) \right)$$

were  $\text{Size}$  is the basal area of a tree at a specific year ( $\text{mm}^2$ ),  $\text{TSF}$  is the (time-varying) minimum time-since-fire (number of years),  $\text{VPD}$  is the summer vapor pressure deficit (kPa),  $\text{Prec.}$  is the summer precipitation (mm of water),  $\text{N}_{\text{deposits}}$  is the total annual nitrogen deposition ( $\text{kg N ha}^{-1} \text{ yr}^{-1}$ ) and  $\text{SI}$  is the site index (unitless). Smooth terms in the GAMMs are indicated by  $s()$  in the equation.

In our dataset, tree BA, TSF and total annual nitrogen deposition were highly correlated with  $\text{PCO}_2$ . Because of this, it is plausible that the ‘full’ models will (partly or fully) remove the part of variability in  $iWUE_{ring}$  that is attributable both to  $\text{PCO}_2$  and to these factors. Therefore, we tested for a third situation (the ‘control’ models) where three new variables,  $\text{RES TSF}$ ,  $\text{RES Size}$  and  $\text{RES N}_{\text{deposits}}$ , were obtained using a partial regression

procedure (Dormann *et al.*, 2013 ; Fernández-de-Uña *et al.*, 2016). These variables represent the raw variables from which the part of variability that is common with  $P_{CO_2}$  was removed. ‘Control’ GAMMs thus included these three new variables, together with summer VPD, summer precipitation and SI as covariates:

$$\text{Eq.10} \quad iWUE_{ring} \sim 1 + s(resSize) + s(resTSF) + s(VPD) + s(Prec.) + s(resN_{deposits}) + \\ s(SI) + \left( \frac{Plot}{Tree} \right) + corCAR1 \left( year | \left( \frac{Plot}{Tree} \right) \right)$$

Estimated degrees-of-freedom (EDF) were checked and, if equal or close to 1, the corresponding covariate was set as a linear term. Otherwise, covariates were set as smooth terms. Normality and homoskedasticity of residuals were visually assessed. Concurvity (nonparametric analog of multicollinearity) between fixed terms remained low ((“estimate” concurvity index below 0.4, *concurvity* function of the R package *MuMIn*; Barton, 2018)).

Having eliminated these collinear effects from the  $iWUE_{ring}$  estimates, residuals of the GAMMs (i.e.  $\text{RESiWUE}_{ring}$ ) were used to assess the relationship between  $iWUE_{ring}$  and  $P_{CO_2}$ . Although residuals from the ‘full’ and ‘control’ models were free of the variability in average  $iWUE_{ring}$  originating from different SI levels, we suspected that SI could modulate the rate at which  $\text{RESiWUE}_{ring}$  would vary with  $P_{CO_2}$ . Therefore, the interaction between the two variables (See step III in Figure 3.2) was included in our models. GAMMs are efficient at describing non-linear relationships such as those between iWUE and climate. This could increase the accuracy of model predictions compared to linear mixed models (LMMs). However, this is at the expense of interpretation ease, since GAMMs do not provide an estimated regression slope for such non-linear relationships. LMMs were used instead of GAMMs in order to obtain a range of estimates for the effect of  $P_{CO_2}$  on  $iWUE_{ring}$  (i.e. the regression slope between  $\text{RESiWUE}_{ring}$  and  $P_{CO_2}$ , one slope per model). They were fitted, for each species, using the R package *nlme* (Pinheiro *et al.*, 2019). These LMMs included  $\text{RESiWUE}_{ring}$  as the

response variable,  $P_{CO_2}$ , SI and their interaction as fixed terms, the effect of the tree nested within the plot as a random term, and a first order autocorrelation error:

$$\text{Eq.11} \quad \text{resi}WUE_{ring} \sim P_{CO_2} + SI + P_{CO_2} \times SI + \left( \frac{\text{Plot}}{\text{Tree}} \right) + \text{corCAR1} \left( \text{year} \mid \left( \frac{\text{Plot}}{\text{Tree}} \right) \right)$$

Normality and homoskedasticity of residuals were visually assessed. Collinearity was assessed through variance inflation factors (VIF, *vif* function of the R package *car*; Fox et Weisberg, 2019). Given that the variables involved in the interaction term were highly collinear (VIFs higher than 10) explanatory variables were mean-centered prior to analyses. All statistical analyses were performed using the R statistical software version 3.6.0.

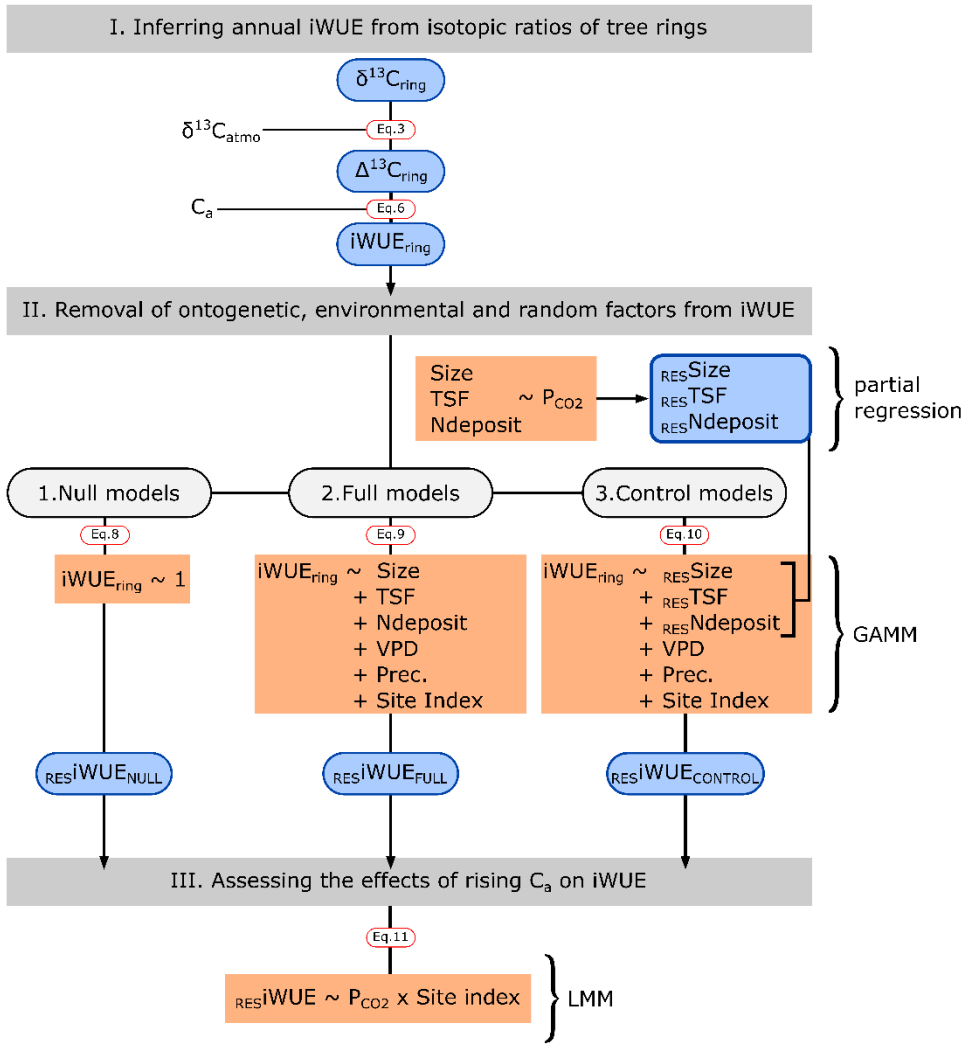


Figure 3.2. Workflow diagram summarizing the computation of intrinsic water use efficiency ( $i\text{WUE}_{\text{ring}}$ ) and the statistical procedure. In a first step,  $i\text{WUE}_{\text{ring}}$  was inferred from tree-ring-derived  $\delta^{13}\text{C}_{\text{ring}}$ . Next, species-specific generalized additive mixed models (GAMMs) were fitted to remove effects of developmental, environmental and site factors on  $i\text{WUE}_{\text{ring}}$ . Finally, the magnitude of the signal resulting from  $C_a$ , (converted to partial pressure of  $\text{CO}_2$ ,  $P_{\text{CO}_2}$ ) and the modulating effect of site index (SI) were assessed using linear mixed models (LMMs). Equation numbers within red frames refer to those in the Methods section.

### 3.3 Results

#### 3.3.1 Temporal variability in iWUE<sub>ring</sub>, growth and leaf gas-exchange variables

On average, iWUE<sub>ring</sub> was lower and  $\Delta^{13}\text{C}_{\text{ring}}$  higher for jack pine (mean  $\pm$  std. dev.  $51.64 \pm 7.50 \mu\text{mol mol}^{-1}$  for iWUE<sub>ring</sub>,  $18.51 \pm 1.14 \text{‰}$  for  $\Delta^{13}\text{C}_{\text{ring}}$ ) than for black spruce ( $66.19 \pm 13.17 \mu\text{mol mol}^{-1}$  for iWUE<sub>ring</sub>,  $20.23 \pm 0.69 \text{‰}$  for  $\Delta^{13}\text{C}_{\text{ring}}$ ; Figure 3.3a,b). Even if there was an apparent positive relationship between iWUE<sub>ring</sub> and BAI (Figure 3.3b,c), this relationship was no longer significant when accounting for the spatial correlation between samples (Spearman rho for all black spruce samples = 0.15, with an adjusted p-value = 0.75; rho for all jack pine samples = 0.016, adjusted p-value = 0.93). iWUE<sub>ring</sub> increased steeply after 1950, at a higher rate for black spruce ( $0.46 \mu\text{mol.mol}^{-1.\text{year}^{-1}}$ ) than for jack pine ( $0.25 \mu\text{mol.mol}^{-1.\text{year}^{-1}}$ ; Annex C, Figure S3.5). For both species, the intercellular CO<sub>2</sub> concentration (C<sub>i</sub>), and the difference between C<sub>a</sub> and C<sub>i</sub> (C<sub>a</sub> - C<sub>i</sub>) also increased, especially after 1975 (Figure 3.4a,b). This parameter reached a value of 253 ppm and 288 ppm at the end of the study period for black spruce and jack pine, respectively. C<sub>i</sub>/C<sub>a</sub> was temporally unstable for black spruce, especially since 1900. For jack pine, this ratio was quite stable since 1900, with a value around 0.75 (Figure 3.4c). In fact, black spruce trees that were recruited directly after the start of the exponential increase in C<sub>a</sub>, i.e. after 1950 (Figure 3.5a), exhibited iWUE<sub>ring</sub> about 35% higher than pre-1950 trees when considering the life-period 11-30 years, while BAI of the two cohorts were not statistically different (Figure 3.5a). These differences were of smaller amplitude in the  $\Delta^{13}\text{C}_{\text{ring}}$  data, with values not statistically different between the two cohorts for some cambial ages (Figure 3.5a). For jack pine, the ratio post- to pre-1950 iWUE<sub>ring</sub> was about +20% during the same life-period. For the time-period spanning 1985-1993, differences in iWUE<sub>ring</sub> were no longer observed between

older and younger trees (Figure 3.5b). However, post-1950 jack pines exhibited higher BAIs (Figure 3.5b).

### 3.3.2 Response of $i\text{WUE}_{ring}$ to rising $\text{PCO}_2$

As expected,  $i\text{WUE}_{ring}$  increased with the rise in  $C_a$  for both species (Figure 3.3b). Assuming that collinear variables did not influence  $i\text{WUE}_{ring}$  (i.e. ‘null’ models), we found that black spruce  $i\text{WUE}_{ring}$  linearly increased in response to rising  $C_a$ ; and this increase was about  $3.64 \mu\text{mol mol}^{-1}$  ( $\pm 0.15 \mu\text{mol mol}^{-1}$ ) per +1 Pa of  $\text{PCO}_2$ . For jack pine,  $i\text{WUE}_{ring}$  increased by  $2.64 \mu\text{mol mol}^{-1}$  ( $\pm 0.13 \mu\text{mol mol}^{-1}$ ) per +1 Pa of  $\text{PCO}_2$  (Table 3.2). However, results from the ‘full’ and ‘control’ models showed that  $i\text{WUE}_{ring}$  included confounding effects from both tree and stand developmental changes, climate and site fertility (Figure 3.6; see diagnostic below). After accounting for these, the linear response of black spruce  $i\text{WUE}_{ring}$  to +1 Pa of  $\text{PCO}_2$  was an increase of  $0.14 \mu\text{mol mol}^{-1}$  ( $\pm 0.13 \mu\text{mol mol}^{-1}$ , non-significant at  $\alpha=0.05$ ), and  $2.56 \mu\text{mol mol}^{-1}$  ( $\pm 0.15 \mu\text{mol mol}^{-1}$ ) for the ‘full’ and the ‘control’ models, respectively (Table 3.2). For jack pine, the estimated regression slopes were  $0.11 \mu\text{mol mol}^{-1}$  ( $\pm 0.12 \mu\text{mol mol}^{-1}$ , non-significant at  $\alpha=0.05$ ) and  $0.94 \mu\text{mol mol}^{-1}$  ( $\pm 0.14 \mu\text{mol mol}^{-1}$ ) using the ‘full’ and ‘control’ models, respectively (Table 3.2).

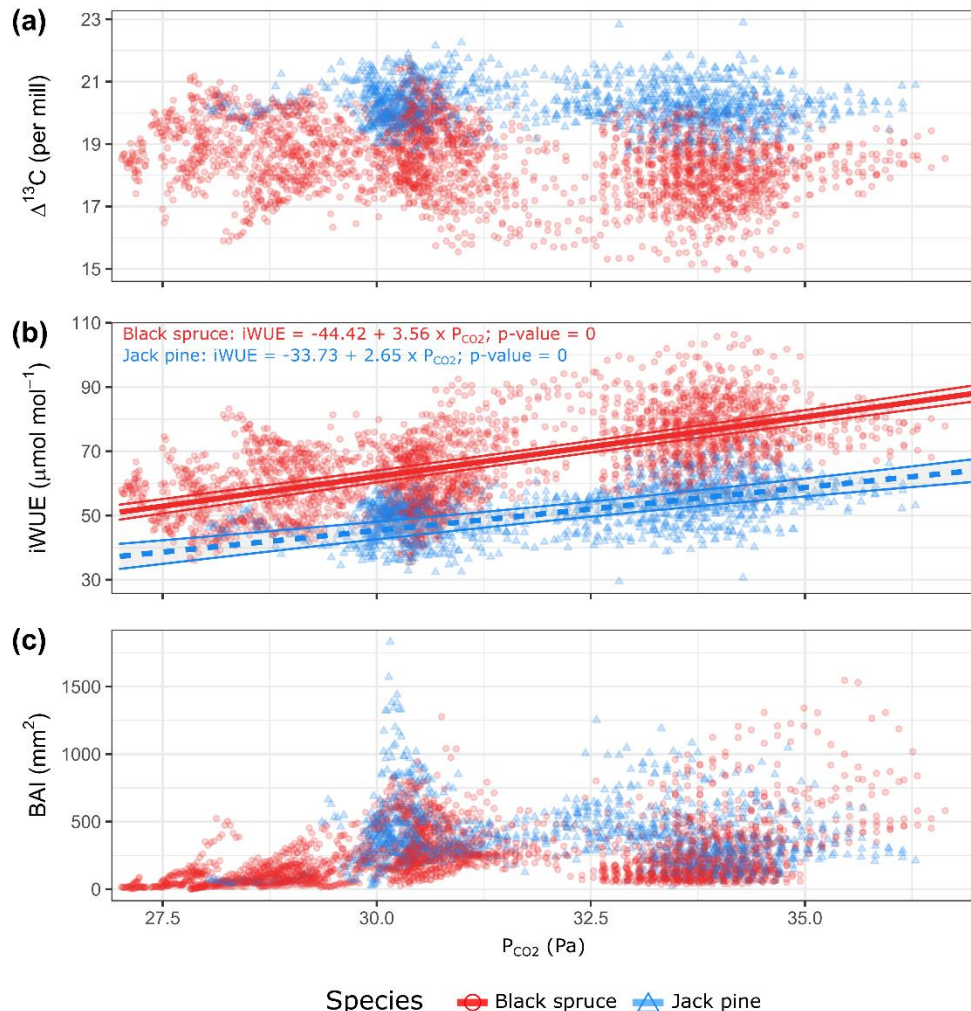


Figure 3.3. Relationship between the partial pressure of  $\text{CO}_2$  ( $P_{\text{CO}_2}$ ) and  $\delta^{13}\text{C}_{\text{ring}}$ -derived physiological parameters (ring-to-atmosphere carbon discrimination,  $\Delta^{13}\text{C}_{\text{ring}}$ ; water use efficiency,  $i\text{WUE}_{\text{ring}}$ ) or radial growth (basal area increments, BAI). (a):  $\Delta^{13}\text{C}_{\text{ring}}$  expressed as a function of  $P_{\text{CO}_2}$ , by species. (b):  $i\text{WUE}_{\text{ring}}$  expressed as a function of  $P_{\text{CO}_2}$ , by species. Regression formulas and p-values are shown for linear mixed models that are derived from the ‘null’ models, indicating an increase of  $i\text{WUE}$  of  $3.56 \mu\text{mol mol}^{-1}$  per  $+1 \text{ Pa}$  of  $P_{\text{CO}_2}$  for black spruce, and of  $2.65 \mu\text{mol mol}^{-1}$  for jack pine. (c): BAI expressed as a function of  $P_{\text{CO}_2}$ , by species.

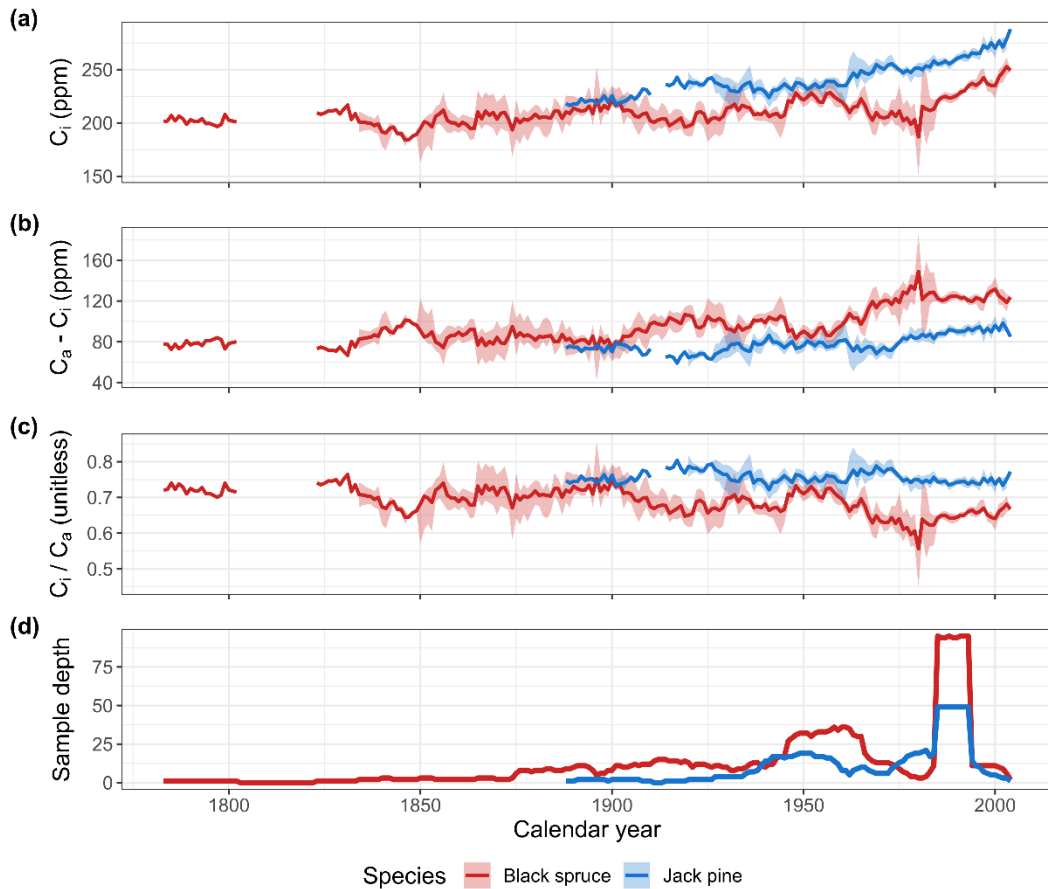


Figure 3.4. Temporal variation in three  $\delta^{13}\text{C}_{\text{ring}}$ -derived physiological variables involved in the regulation of trees leaf gas-exchange. The intercellular CO<sub>2</sub> concentration ( $C_i$ , panel a), the difference between the atmospheric CO<sub>2</sub> concentration and  $C_i$  ( $C_a - C_i$ , panel b), and the ratio  $C_i/C_a$  (panel c) are presented for the period 1783–2004. Lines represent median values, by year and species. Shadings denote bootstrapped 95% confidence intervals around the median ( $N=10\,000$  replications), which were computed for years represented by at least 2 trees ( $N \geq 2$ , see panel d for the sample depth, i.e. the number of samples by year and species).

Table 3.2. Regression slopes ( $\beta$ ), standard deviations (Std.error), t-values and p-values from the linear mixed models assessing the effects of  $P_{CO_2}$ , SI and their interaction on resiWUE by species, according to the statistical procedure. Significant effects at  $\alpha = 0.05$  are indicated in bold.

			Black spruce				Jack pine			
			$\beta$	Std. error	t-value	p-value	$\beta$	Std. error	t-value	p-value
<b>Null</b>	$P_{CO_2}$		<b>3.642</b>	<b>0.148</b>	<b>24.551</b>	<b>&lt;0.001</b>	<b>2.644</b>	<b>0.131</b>	<b>20.140</b>	<b>&lt;0.001</b>
	SI		<b>-3.081</b>	<b>0.822</b>	<b>-3.746</b>	<b>&lt;0.001</b>	1.086	0.935	1.161	0.256
	$P_{CO_2} \times SI$		<b>1.430</b>	<b>0.124</b>	<b>11.537</b>	<b>&lt;0.001</b>	0.171	0.130	1.323	0.186
<b>Full</b>	$P_{CO_2}$		0.140	0.129	1.087	0.278	0.106	0.117	0.905	0.365
	SI		0.066	1.018	0.064	0.949	0.067	1.008	0.067	0.947
	$P_{CO_2} \times SI$		<b>1.098</b>	<b>0.107</b>	<b>10.234</b>	<b>&lt;0.001</b>	<b>0.250</b>	<b>0.115</b>	<b>2.180</b>	<b>0.030</b>
<b>Control</b>	$P_{CO_2}$		<b>2.555</b>	<b>0.152</b>	<b>16.765</b>	<b>&lt;0.001</b>	<b>0.941</b>	<b>0.143</b>	<b>6.603</b>	<b>&lt;0.001</b>
	SI		-0.329	0.891	-0.369	0.714	-0.024	1.231	-0.020	0.984
	$P_{CO_2} \times SI$		<b>1.165</b>	<b>0.127</b>	<b>9.148</b>	<b>&lt;0.001</b>	0.008	0.140	0.056	0.956

Table 3.3. Results from ‘Full’ and ‘Control’ Generalized Additive Mixed Models (GAMMs). Estimated degree of freedom (EDF), F-value (indicative of the relative contribution of each explanatory variable to the variance of the response variable) and p-value are provided for each explanatory variable, as well as the adjusted r-squared values (total amount of variance explained by the model) and number of observations processed, by species.

		Black spruce			Jack pine		
Variable		EDF	F-value	p-value	EDF	F-value	p-value
Full models	Size	2.55	28.05	< 0.001	4.04	5.64	< 0.001
	TSF	3.83	6.52	< 0.001	2.69	5.12	< 0.01
	VPD	4.86	6.78	< 0.001	4.49	10.12	< 0.001
	Prec.	6.39	6.79	< 0.001	6.20	2.57	0.010
	SI	2.28	8.61	< 0.001	1.38	0.76	0.300
	Ndeposits	2.37	8.20	< 0.001	1	9.46	< 0.01
	Adjusted R-squared	0.439			0.285		
Control models	RESSize	1	33.95	< 0.001	1	5.71	0.020
	RES TSF	3.70	12.39	< 0.001	5.48	29.48	< 0.001
	VPD	4.91	8.04	< 0.001	4.77	11.89	< 0.001
	Prec.	6.36	6.94	< 0.001	6.12	2.39	0.020
	SI	1	10.76	< 0.010	1	0.80	0.370
	RES Ndeposits	1	6.46	< 0.010	3.10	3.36	0.020
	Adjusted R-squared	0.237			0.0476		
Sample number		2560			1266		

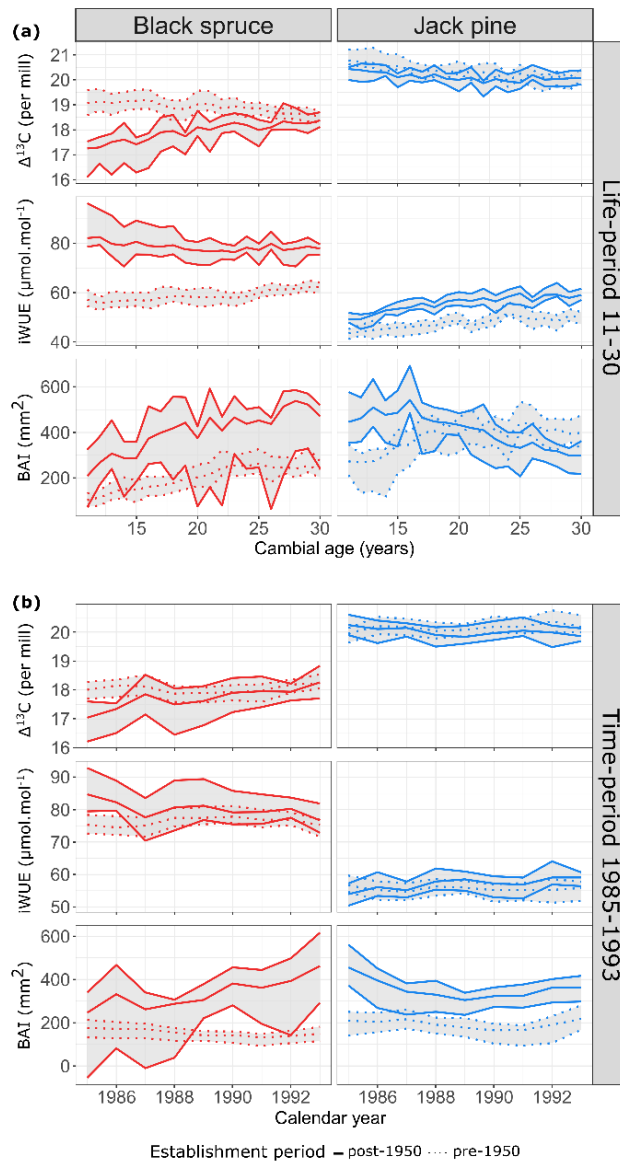


Figure 3.5. Median  $i\text{WUE}_{\text{ring}}$ ,  $\Delta^{13}\text{C}_{\text{ring}}$  and basal area increments (BAI) for (a) the period spanning 1 m height cambial ages 11-30 years and (b) the period spanning calendar years 1985-1993, for trees recruited before (dotted lines) and after (solid lines) 1950. 1950 corresponds to the start of exponential increase in  $C_a$ . Gray shadings are for bootstrapped 95% confidence intervals ( $N=10\,000$  replications). The establishment date of the trees was determined based on the first (i.e. minimum) calendar year that was registered in ground-level stem radial-sections.

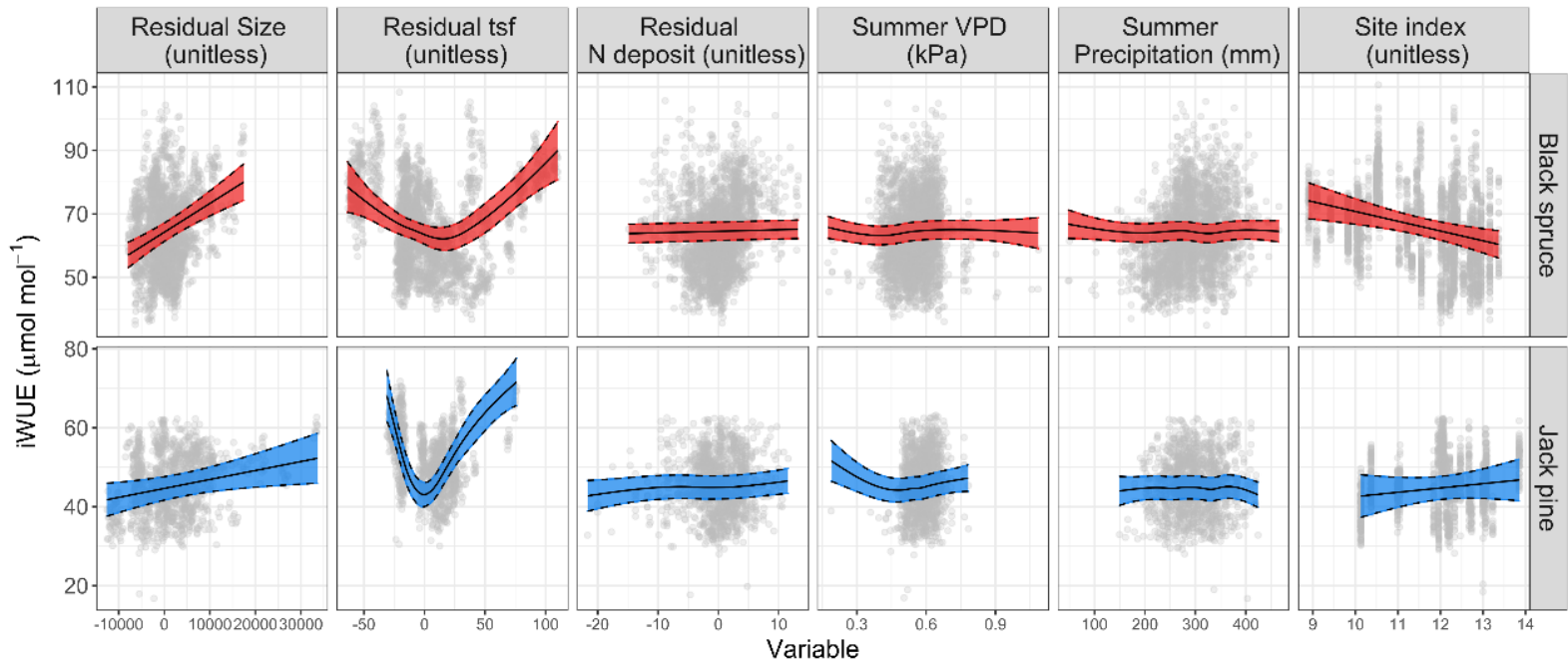


Figure 3.6. Partial effects of developmental processes (Residual Size, Residual tsf), climate (Summer VPD, Summer Precipitation), total annual nitrogen deposition (Residual N deposit) and site fertility index (Site index) on  $i\text{WUE}_{\text{ring}}$ . Gray dots represent partial residuals from the “Control” Generalized Additive Mixed Models (GAMMs), i.e. the estimates for the variable plus the residuals. Black lines and red and blue shadings are respectively for the predicted values and 95% confidence intervals from the GAMMs.

### 3.3.3 Diagnostics of collinear variables

Among all collinear variables that were tested, we found that TSF and tree size significantly influenced  $i\text{WUE}_{\text{ring}}$ , even after removing the variation common to these variables and  $\text{PCO}_2$  (Figure 3.6). For both species,  $i\text{WUE}_{\text{ring}}$  varied non-linearly with  $\text{RES}_{\text{TSF}}$ : the period spanning  $\text{RES}_{\text{TSF}} = -60$  to 5 (i.e. during the first 66 years after a fire, see Annexe C, Figure S3.6) was characterized by a  $20 \mu\text{mol mol}^{-1}$  decrease in black spruce  $i\text{WUE}_{\text{ring}}$ . After that, black spruce trees recovered their initial  $i\text{WUE}_{\text{ring}}$  level. For jack pine,  $i\text{WUE}_{\text{ring}}$  decreased from 70 to  $45 \mu\text{mol mol}^{-1}$  during the period corresponding to  $-30 < \text{RES}_{\text{TSF}} < -4$  (i.e. during the first 46 years after a fire, see Annexe C, Figure S3.6), then returned to its initial level.  $i\text{WUE}_{\text{ring}}$  increased linearly with the size of black spruce trees, i.e. an increase of  $0.92 \mu\text{mol mol}^{-1}$  in  $i\text{WUE}_{\text{ring}}$  for each  $+1000$  increment in  $\text{RES}_{\text{Size}}$  (i.e. approx. for each  $+10 \text{ cm}^2$ , see Annexe C, Figure S3.6). For jack pine, the effect of tree size on  $i\text{WUE}_{\text{ring}}$  was far lower than for black spruce ( $+0.22 \mu\text{mol mol}^{-1}$  for each  $+1000$  increment in  $\text{RES}_{\text{Size}}$ ).

Interannual variability in vapor pressure deficit during summer months, together with its long-term trend, influenced  $i\text{WUE}_{\text{ring}}$ . For each  $+1 \text{ kPa}$  in summer VPD, the  $i\text{WUE}_{\text{ring}}$  of black spruce increased by  $4.25 \mu\text{mol mol}^{-1}$ . For jack pine, this increase was about twice the value that was observed for black spruce ( $8.95 \mu\text{mol mol}^{-1}$  increase in  $i\text{WUE}_{\text{ring}}$  for each  $+1 \text{ kPa}$ ). The effect of summer precipitation on  $i\text{WUE}_{\text{ring}}$  was negative, but barely significant for the two species (Figure 3.6). Residualized nitrogen deposition ( $\text{RES}_{\text{Ndeposit}}$ ) slightly but significantly increased the  $i\text{WUE}_{\text{ring}}$  of both species, with a  $0.05 \mu\text{mol mol}^{-1}$  increase in  $i\text{WUE}_{\text{ring}}$  of the two species for each 1 unit increase in  $\text{RES}_{\text{Ndeposit}}$ , i.e. approximately for each  $1 \text{ kgN ha}^{-1} \text{ yr}^{-1}$  increase (Table 3.3,

Figure 3.6). These variables largely contributed to the positive trend in  $i\text{WUE}_{ring}$  since, after removing these effects, trends were greatly lowered (Figure 3.7).

Temporal variability in BAI depended on the fertility level of the site, especially for black spruce after 1970s. For this species, trees on the most fertile stands experienced better and increasing growth rates (median 1970-2005 BAI = 288.27 mm<sup>2</sup> for trees on stands with SI above 13.5, red colour in Figure 3.8a) while, on the poorer stands, black spruce growth rates were lower and declined (median 1970-2005 BAI = 112.00 mm<sup>2</sup> for trees on stands with SI below 10.5, blue colour in Figure 3.8a). For jack pine, BAI declined since 1950 whatever the fertility level, but the decline was steeper on the poorer stands (median 1970-2005 BAI on poor stands = 185.13 mm<sup>2</sup>; median BAI on fertile stands = 276.53 mm<sup>2</sup> Figure 3.8a). This pattern persisted when removing trends from developmental processes and considering a higher range of growth conditions (Annexe C, Figure S3.7 and Table S3.1). Site fertility index also significantly modulated the response of black spruce  $i\text{WUE}_{ring}$  to  $C_a$ . For this species, trees that have grown on fertile stands (i.e. stands where trees were expected to reach at least 12 m at 50 years) had lower average  $i\text{WUE}_{ring}$ , while they also experienced the highest increases in  $i\text{WUE}_{ring}$ , with a 3.64  $\mu\text{mol mol}^{-1}$  increase for each 1 Pa increase in  $\text{PCO}_2$  (Figure 3.6 and Annexe C, Figure S3.8). In poor stands (i.e. sites where the expected height of a 50-year-old tree is about 9 m),  $i\text{WUE}_{ring}$  did not increase significantly with rising  $\text{PCO}_2$  (Table 3.2 and Figure 3.8), partly because  $i\text{WUE}_{ring}$  levels were already high in these stands at low  $\text{PCO}_2$  (Annexe C, Figure S3.8). At higher  $\text{PCO}_2$ ,  $i\text{WUE}_{ring}$  levels seem similar for different site fertility indices (Annexe C, Figure S3.8). In contrast, the increase in  $i\text{WUE}_{ring}$  was of similar magnitude regardless of the site index for jack pine (Table 3.2 and Figure 3.8). After accounting for the  $\text{CO}_2$  effect, the remaining long-term trends in  $\text{RESI}\text{WUE}_{ring}$  were almost null (Figure 3.7c).

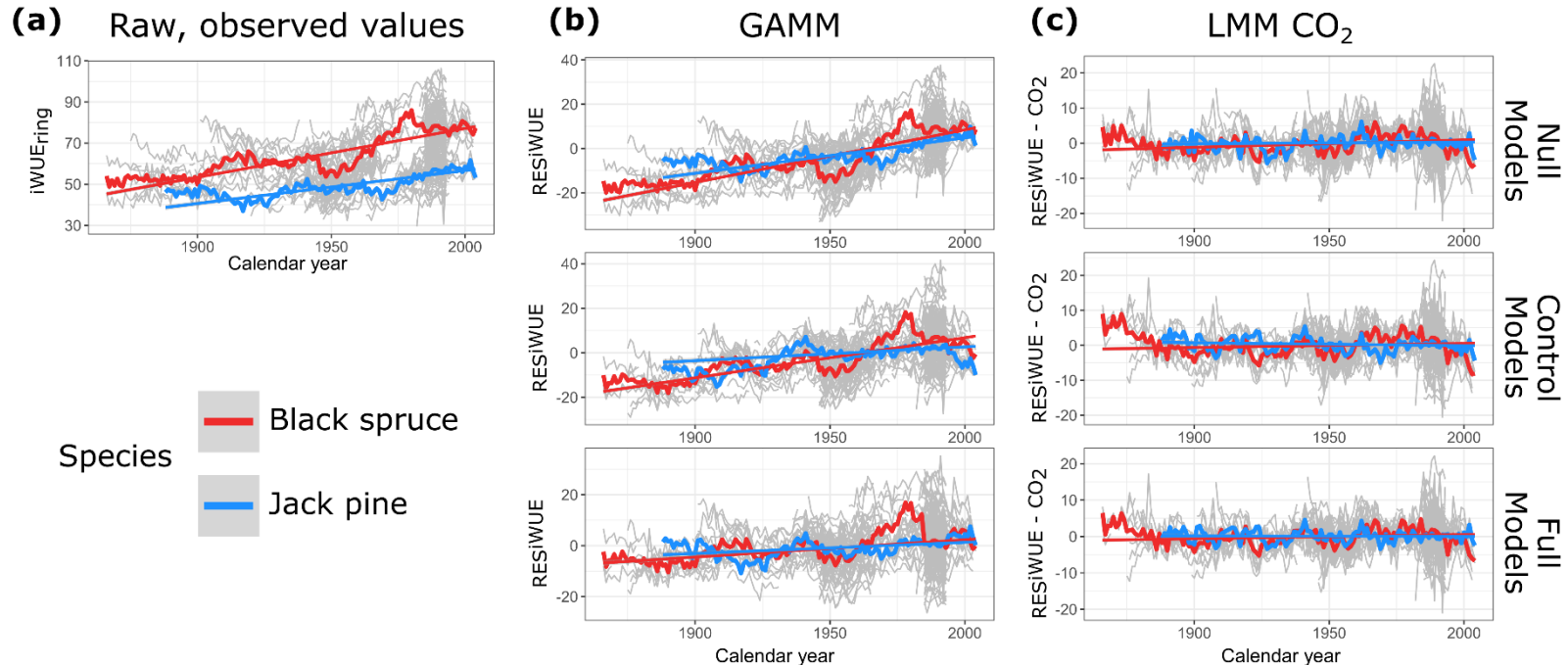


Figure 3.7. iWUE trends following each step of the statistical procedure. (a) Raw (observed)  $\delta^{13}\text{C}$ -derived iWUE. (b) Residuals from the Generalized Additive Mixed Models (RESiWUE), from which the variability due to tree and stand development (increase in size, time-since-fire), climate (summer VPD, summer Precipitation), nitrogen deposition and site fertility index were removed, depending on the three statistical procedures. (c) Residuals from linear mixed models that were used to assess the effect of  $\text{P}_{\text{CO}_2}$  interacting with site index (RESiWUE -  $\text{CO}_2$ ). Red and blue thick lines are for average values, by species. Regression lines for black spruce and jack pine are also shown.

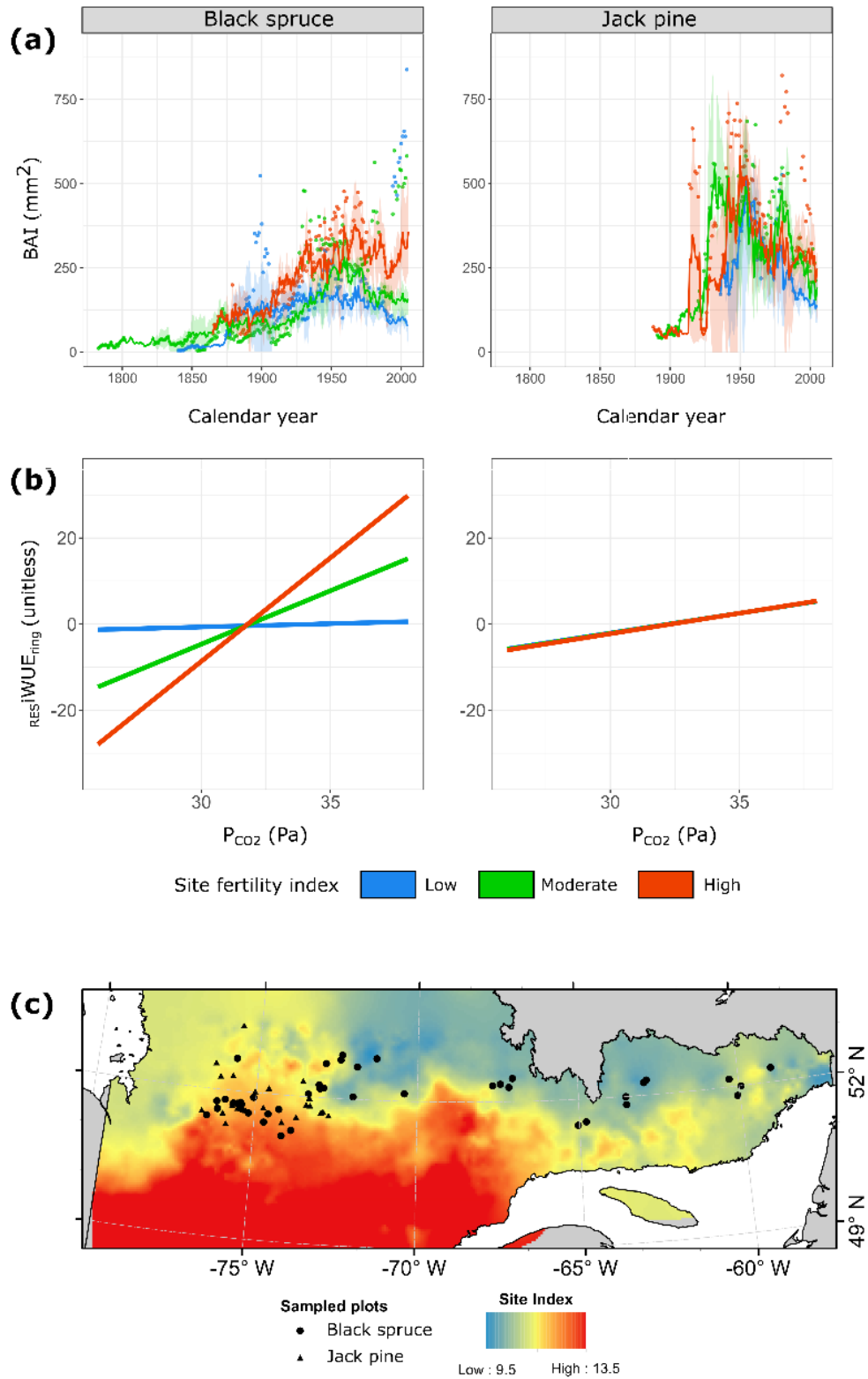


Figure 3.8. Assessment of the modulating effect of growth conditions on the  $iWUE_{ring}$  response to  $C_a$ . (a) Median basal area increment (BAI), by species and stratified according to the site fertility. Lines are for median values of observed BAI, by year, range of site fertility and species. Shadings are bootstrapped 90% confidence intervals ( $N = 10\,000$  replications). Dots represent median BAI of growth rings that were sampled for isotope analysis. The blue curve (“Low” site index) encompasses sample plots with SI below 10.5; the green curve (“Moderate” site index) encompasses plots with SI between 10.5 and 12.5; and the red curve (“High” site index) includes plots with SI above 12.5. A low site fertility index is an indication of poor growing conditions. (b) Residual  $iWUE$  ( $resiWUE$ ) depending on the Partial pressure of  $CO_2$  ( $P_{CO_2}$ ) and the species, predicted for three specific values of site fertility index (SI, “Low” = 9.5; “Moderate” = 11.5; “High” = 13.5). Predictions are based on a linear mixed model fitted using  $resiWUE$  from the ‘control’ Generalized Additive Mixed models. Differences in average  $iWUE_{ring}$  due to different site fertility levels were previously accounted for and removed (see Figure 3.2 and 3.6). In an ecological point of view,  $resiWUE$  represents the variability in  $iWUE$  that is not the direct result of climate (VPD and precipitation), tree and stand development (tree size, TSF), site fertility level or nitrogen deposition. This residual variability could thus be attributed to changes in atmospheric  $CO_2$  concentrations. Here, the figure displays only the changes in  $resiWUE_{ring}$  with  $P_{CO_2}$  at different site fertility levels, i.e. the way SI modify the effect of  $P_{CO_2}$  on  $resiWUE_{ring}$  (different regression slopes for different SI levels). (c) Position of our sampled plots (black dots and triangles) along the longitudinal gradient, together with the SI of the area (color gradient: blue = low SI to red = high SI).

### 3.4 Discussion

In this study, we identified large uncertainties about the proportion of positive trends in  $i\text{WUE}_{\text{ring}}$  effectively attributable to  $C_a$ , and the proportion that is merely the result of changes in tree and stand developmental stages and site attributes. We have shown that, especially for black spruce, the magnitude of the  $\text{CO}_2$  effect varies across the landscape because of differences in site fertility. We identified that estimates of the  $\text{CO}_2$  effect are sensitive to the statistical procedure. We also observed different  $i\text{WUE}_{\text{ring}}$  levels and trends between the two species. Below we discuss further in details these aspects in addition to pointing out some methodological limitations of our approach.

#### 3.4.1 Tree size and stand age strongly contribute to long-term trends in $i\text{WUE}$

Marshall and Monserud (1996) used tree-ring  $\delta^{13}\text{C}$  measurements from three conifer species as a means of demonstrating, for the first time, that  $C_a$  and tree ageing act together to modify leaf gas-exchange variables in woody plants. Twenty years later, Brienen *et al.* (2017) extended these findings to four other woody species, including three broadleaved species. The later study highlighted the strong bias in the estimation of the  $\text{CO}_2$  effect on  $i\text{WUE}$  that could arise from not removing or accounting for tree and stand developmental trends. Voelker *et al.* (2006) also observed an age effect on the relationship between tree growth rates and  $C_a$ .

Here, we show that the combined effect of tree size and stand age on black spruce and jack pine  $i\text{WUE}_{\text{ring}}$  is far higher in magnitude when compared to the effect of climate. We observed that these developmental effects persist much longer than the earliest phase of stand regeneration (the “juvenile phase,” usually set as the first 50 years of growth; see e.g. Gagen *et al.*, 2008) and probably last over the entire tree lifespan. Such developmental effects on  $i\text{WUE}_{\text{ring}}$  were previously reported for other tree species (Esper *et al.*, 2010 ; Gagen *et al.*, 2008 ; Hietz *et al.*, 2005). For example, the magnitude of increase in  $i\text{WUE}$  with tree size varies, depending upon the species studied (Brienen

*et al.*, 2017). Indeed, we show that the increase in  $i\text{WUE}_{\text{ring}}$  with tree basal area was far lower for jack pine than for black spruce. This, together with a stronger partial effect of soil moisture availability (Hogg *et al.*, 2013) on  $i\text{WUE}_{\text{ring}}$  of black spruce compared to jack pine over the period 1901-2004 (Annexe C, Figure S3.9, Table S3.2), suggests that for the former, size-related hydraulic limitations and changes in water needs (Koch *et al.*, 2004) have a strong effect on tree physiology. Moreover, stand age induced significant trends in  $i\text{WUE}_{\text{ring}}$  of both species. The U-shaped relationship between TSF and  $i\text{WUE}_{\text{ring}}$  suggests the existence of a threshold for the balance between water needs and supply, perhaps linked with stand-level developmental changes such as canopy closure occurring about 45-70 years after a fire. Inter-individual competition for water could have increased with the increase in tree biomass and foliage area, which would have forced trees to use water resources more efficiently. An increase in assimilation rates with canopy expansion could also explain the increase in  $i\text{WUE}_{\text{ring}}$  with tree and stand development.

### 3.4.2 Site fertility as a driver of heterogeneity in CO<sub>2</sub> effects

We determined that site fertility had a strong effect on  $i\text{WUE}_{\text{ring}}$  of black spruce, both directly and indirectly through a modulating effect on the response to C<sub>a</sub>. For this species,  $i\text{WUE}_{\text{ring}}$  was lower, on average, for trees growing on areas that were characterized by a higher site index than trees in low SI areas, especially for early formed growth-rings (i.e. life-period 11-30 years; Figure 3.6 and Annexe C, Figure S3.9). Moreover, these trees that were located on fertile stands also exhibited the strongest  $i\text{WUE}_{\text{ring}}$  response to C<sub>a</sub> (Figure 3.8 and Annexe C, Figure S3.8). This highlights a far higher increase in  $i\text{WUE}_{\text{ring}}$  for these trees compared to those growing on poor soils, for which  $i\text{WUE}_{\text{ring}}$  level remains high and relatively stable over the whole study period. This pattern, already reported in Alaska (Sullivan *et al.*, 2017) and similar to the pattern observed along an altitudinal gradient (Maxwell *et al.*, 2018 ; Wu *et al.*, 2015), could result from lower nutrient and moisture constraints on

photosynthetic processes (de Oliveira *et al.*, 2012 ; Leonardi *et al.*, 2012) on fertile sites compared to poorer ones. The later were characterized by shallower, less weathered soils (Annexe C, Figure S3.10). Maybe trees on these poor stands kept a constantly high  $iWUE_{ring}$  level in response to chronic environmental stresses; while trees on fertile stands were not stressed under pre-industrial conditions but progressively increased their  $iWUE_{ring}$  as a response to global warming. Black spruce trees on poor stands experienced lower growth rates and a steeper decline in their growth than trees on more fertile stands since the 1970s (Figure 3.8a), which adds credibility to the hypothesis of nutrient-limited photosynthesis processes. Note that these fertility-dependent differences in black spruce BAI levels and trends persist even after removing trends arising from developmental and demographic processes in addition to considering a wider range of growth conditions (Annexe C, Figure S3.7 and Table S3.1). This hypothesis could also explain the absence of growth stimulation concurrent with the increase in  $iWUE_{ring}$  that was observed here (Figure 3.3b,c) and which has been previously reported in many studies (Giguère-Croteau *et al.*, 2019 ; Peñuelas *et al.*, 2011 ; Savard *et al.*, 2020 ; Silva *et al.*, 2015 ; Zhang *et al.*, 2019). The significant increase in  $iWUE_{ring}$  with nitrogen deposition we observed was already stated in previous studies (Leonardi *et al.*, 2012 ; Savard *et al.*, 2020). This is likely the result of an interception of a large portion of atmospheric nitrogen inputs by tree crowns (Gaige *et al.*, 2007), that increases leaf nitrogen concentrations, boosts photosynthesis capacity and, consequently, increases carbon assimilation rates (Evans, 1989 ; Zhou *et al.*, 2018). Thus, this is an additional indication of a nutrient limitation on photosynthesis rates. These findings indicate that highly positive  $iWUE$  trends that have been previously reported in tree-ring studies could be mostly representative of tree populations growing in the most fertile areas and in areas where plant growth is strongly limited by climate (Klesse *et al.*, 2018).

### 3.4.3 The apparent effect of $C_a$ on iWUE is strongly lessened after removing effects of collinear variables

The integration of site fertility and developmental changes in models would enable more accurate estimation of  $i\text{WUE}_{ring}$  responses to rising  $C_a$  and may decrease discrepancies between modeled and observed values (Lavergne *et al.*, 2020 ; Masri *et al.*, 2019). These developmental trends, until now, were rarely taken into account when assessing the effects of a CO<sub>2</sub>-enriched atmosphere on tree  $i\text{WUE}_{ring}$  (but see Marshall et Monserud, 1996). A high degree of uncertainty remains regarding the way in which the effect of  $C_a$  can be disentangled from trends that are induced by developmental changes. When accounting for such variables in the ‘full’ models, one could conclude - erroneously - that rising  $C_a$  had absolutely no effect on tree physiology (Table 3.2). When using residualized variables (i.e.  $\text{RESSize}$ ,  $\text{RESTSF}$  and  $\text{RESNdeposit}$  through ‘control’ models),  $C_a$  effect was significant but considerably lessened compared to the situation where developmental changes were not accounted for (‘null’ models; Table 3.2). Thus, the ‘true’ effect of  $C_a$  on  $i\text{WUE}_{ring}$  should lie somewhere between values that have been reported through the ‘control’ and ‘full’ models.

We found that long-term  $i\text{WUE}_{ring}$  variability that is attributable to  $C_a$  could be overestimated, at least, by 43-181 % if developmental changes, climate and differences in site conditions are not accounted for. Previously reported iWUE trends for the study species (Dietrich *et al.*, 2016 ; Sullivan *et al.*, 2017) and many other tree species (Peñuelas *et al.*, 2011 ; Silva et Madhur, 2013) could thus contain a strong signal attributable to developmental changes and should not be viewed as the result of global change alone. Here, we assumed the ‘control’ statistical approach to be the most accurate in removing unwanted signals (Figure 3.7). Such an approach, or an improved version, should be used as a standard procedure in future studies.

An overestimated  $i\text{WUE}_{ring}$  response to  $C_a$  would lead to overestimates of the efficiency gain of a tree, which, under a CO<sub>2</sub>-enriched atmosphere, results in less water being

transpired per unit carbon assimilated. For example, if we make the assumptions of a starting iWUE value of 70  $\mu\text{mol.mol}^{-1}$  and a VPD of 0.55 kPa (which corresponds to the average 1981-2010 summer VPD normal at our plot locations), with an increase of 1 Pa in  $\text{PCO}_2$  at a given site, the ‘null’ models predict that the iWUE of a black spruce tree will increase by 3.64  $\mu\text{mol.mol}^{-1}$ . In other words, assuming a fixed annual assimilation rate of 1 mole of carbon (i.e. 12 grams of pure  $^{12}\text{C}$ ) the estimated decrease in stomatal conductance by 706.12 moles of water translates into a decrease of 3.83 moles of water being transpired, and to a seasonal saving of 69 mL of water from increased  $\text{C}_a$ . However, after accounting for developmental changes, nitrogen deposition, climate and site fertility (i.e. using slopes from ‘control’ models), the expected water saving under a +1 Pa atmosphere is only of 52 mL of water per mole of carbon assimilated. For jack pine, the saving would be about 51 mL of water per mole of carbon if estimated using ‘null’ models, and only of 21 mL of water per mole of carbon if estimated using the ‘control’ models. The high spatial heterogeneity in the  $\text{iWUE}_{\text{ring}}$  response to  $\text{C}_a$  that is induced by stand fertility suggests the existence of huge uncertainties in vegetation model predictions of carbon sequestration at large spatial scales, such as the whole forest biome (Lavergne *et al.*, 2020), and could amplify overestimates resulting from not considering collinear factors.

#### 3.4.4 Species-specific sensitivity to $\text{C}_a$

We observed that the magnitude of the  $\text{iWUE}_{\text{ring}}$  response to  $\text{PCO}_2$  differed strongly between the two species. The effect of  $\text{PCO}_2$  on  $\text{iWUE}_{\text{ring}}$  of black spruce was more than twice as strong as that estimated for  $\text{iWUE}_{\text{ring}}$  of jack pine, suggesting some species-specific adjustments of leaf gas-exchange variables to rising  $\text{C}_a$ . For jack pine, the  $\text{C}_i/\text{C}_a$  ratio was relatively constant over the study period (Annexe C, Figure S3.11), as it was observed for many species and regions (Bonal *et al.*, 2011 ; Franks *et al.*, 2013 ; Saurer *et al.*, 2004 ; Ward *et al.*, 2005). This suggests that, for jack pine,  $\text{C}_i$  could have increased proportionally with  $\text{C}_a$ , leading to an increase in  $\text{iWUE}_{\text{ring}}$  of approximately

20 % since 1900. For black spruce, all three leaf gas-exchange variables were non-stationary over the study period, as previously highlighted by a meta-analysis encompassing numerous woody species (Voelker *et al.*, 2016). For this species,  $iWUE_{ring}$  increased on average by 55 % since 1900. Previous findings already reported steeper  $iWUE$  trends in spruce compared to pine in the boreal Siberia (Saurer *et al.*, 2004). During the last two decades (1980-2004),  $C_a - C_i$  of black spruce stabilized at ~120 ppm (Figure 3.4b), suggesting that  $C_i$  increased in parallel with  $C_a$  over this recent period. This could be the result of a less intense regulation of leaf gas-exchange variables compared to the pre-1980s period, even if the  $iWUE_{ring}$  of black spruce remains higher than that of jack pine. This may potentially lead to a lowering in the capacity of black spruce trees to resist and recover from droughts in the future, especially in old and dense stands located on dry substrates (Sohn *et al.*, 2012, 2014, 2016). This lowering in the historical increase in black spruce  $iWUE_{ring}$ , which has been reported elsewhere in other tree species (Gagen *et al.*, 2008 ; Linares et Camarero, 2012 ; Waterhouse *et al.*, 2004), may contribute to reinforce the hypothesis of nutrient-limited, saturated photosynthesis. This decrease in black spruce  $iWUE$  trends could also be the result of a limitation of photosynthetic activity by photooxidative damages as it was previously observed in *Picea abies* (Yang *et al.*, 2020). This, in complement with the observation of similar post-1980  $iWUE_{ring}$  levels in poor and fertile stands despite huge differences in pre-1980 levels (Annexe C, Figure S3.8), suggests that black spruce could have already reached its maximum photosynthesis capacity, and may be physiologically not able to further improve it.

We also observed lower  $iWUE_{ring}$  for jack pine than for black spruce, regardless of fertility level and time-period (Annexe C, Figure S3.5; S3.8 and S3.11). Previous studies based on model simulations within the same study area and in-situ gas-exchange measurements in Saskatchewan have found higher water use efficiency for jack pine compared to black spruce (Girardin *et al.*, 2012 ; Sullivan *et al.*, 1997). Even if our results appear to contradict these previous findings, these are very different

variables which are not readily comparable. Indeed, while Girardin *et al.* (2012) and Sullivan *et al.* (1997) reported results from instantaneous water-use efficiency, i.e. the ratio between assimilation and transpiration at the leaf level, tree-ring  $\delta^{13}\text{C}$ -derived  $i\text{WUE}_{\text{ring}}$  are estimates of the leaf-level ratio between assimilation and stomatal conductance integrated across the whole canopy and the entire growing season (Medrano *et al.*, 2015). These contradictory results could also arise from high environmental and inter-individual variability (Lavergne *et al.*, 2019). Such species-specific variability in physiological processes could be linked with diverging adaptive strategies. Jack pine has a lower specific conductivity, a lower leaf area, and a deeper rooting system than black spruce (Blake et Li, 2003), that might be the result of an adaptation of the former to drier, better-drained environments. As a consequence, jack pine is less vulnerable to cavitation (Blake et Li, 2003), more drought tolerant and better able to cope with moisture limitations as it is less parsimonious at using water resources than is black spruce.

### 3.4.5 Methodological limitations

In this study, we used a specific sampling strategy to target growth rings of interest, i.e. one life-period of cambial ages 11-30 years and one time-period of calendar years 1985-1993, allowing to disentangle the effects of CO<sub>2</sub>, nitrogen deposition and climate from those induced by developmental processes. More specifically, the 11-30 years life-period allowed to compare trees at a similar developmental stage. However, one drawback of this strategy is a low sample replication over a large part of the study period (Figures 3.1c and 3.4d). While this could potentially lead to results not representative of the whole tree population, running ‘Control’ GAMMs on a subset of the data including only years represented by at least ten trees showed that the patterns of the variables’ partial effects were very similar to those obtained using the full dataset (Annexe C, Figure S3.12).

Another uncertainty may originate from the use of  $i\text{WUE}_{\text{ring}}$  to investigate the  $\text{CO}_2$  effect on tree physiology. Indeed,  $i\text{WUE}_{\text{ring}}$  is not statistically independent of  $C_a$  since it is calculated using  $C_a$  and  $\Delta^{13}\text{C}_{\text{ring}}$ , and testing for the effect of  $C_a$  on  $i\text{WUE}_{\text{ring}}$  could be considered as circular in reasoning. We reported results based both on  $i\text{WUE}_{\text{ring}}$  (main document) and  $\Delta^{13}\text{C}_{\text{ring}}$  (Annexe C) as a sensitivity analysis. Our conclusions on partial effects of tree size, stand age, climate, nitrogen deposition and site fertility were found to be similar using either  $i\text{WUE}_{\text{ring}}$  or carbon discrimination (Annexe C, Figure S3.13). However, in jack pine we observed that the effect of  $\text{PCO}_2$  switched to non-significant when considering  $\text{RES}\Delta^{13}\text{C}_{\text{ring}}$  instead of  $\text{RES}i\text{WUE}_{\text{ring}}$  (Annexe C, Table S3.3), which is in line with the relatively constant  $C_i/C_a$  ratio we observed for this species over the study period (Figure 3.4c and Annexe C, Figure S3.11). This comparison suggests that the long-term variability in  $i\text{WUE}_{\text{ring}}$  should be studied in parallel with temporal variability in each of the three leaf gas-exchange variables in order to avoid any logical fallacy (circular reasoning) or misinterpretation. Despite these apparent shortcomings,  $i\text{WUE}$  is still largely reported in ecophysiological studies based on tree-ring isotopes (e.g. Giguère-Croteau *et al.*, 2019 ; Savard *et al.*, 2020), as it is easier to interpret than the atmosphere-to-tree-ring carbon discrimination ( $\Delta^{13}\text{C}$ ) and is a useful metric for parameterization and benchmarking of predictive models of forest growth (Charney *et al.*, 2016 ; Frank *et al.*, 2015 ; Girardin *et al.*, 2016b).

Finally, numerous other environmental variables could have induced changes in  $i\text{WUE}_{\text{ring}}$ . For example, higher summer air temperature increases  $i\text{WUE}_{\text{ring}}$  as a result of increased photosynthesis rates and a stronger stomatal control (Reich *et al.*, 2018). However, temperature and VPD are highly collinear since the former is used to compute the latter. Sensitivity analyses showed that inclusion of maximum summer temperature did not increase the r-squared of our GAMMs, but instead increased concurvity between variables, and consequently, the uncertainty related to estimated partial effects (Annexe C, Figure S3.9, Table S3.2). Moreover, soil moisture availability would have been a more representative variable of changes in trees water

availability through time. However, proxies of soil moisture are available only since 1901, which means that their use is at the expense of sample size and statistical power. Alternative models that include soil moisture index (SMI; Hogg *et al.*, 2013), nonetheless, corroborated our conclusion by indicating significantly decreased  $iWUE_{ring}$  of both black spruce and jack pine (Annexe C, Figure S3.9). Additionally, atmospheric pollution, e.g. industrial pollutants such as  $SO_2$  and  $NO_x$ , could contribute to increase  $iWUE$  (Savard *et al.*, 2020). However, these pollutants may have had a low impact on our sampled trees because of the relatively remote location of the study plots, far from any major city. We considered nitrogen depositions in our analyses, which had a limited effect on  $iWUE_{ring}$ , as already observed in the northeastern US (Lévesque *et al.*, 2017). Finally, information at the plot level is lacking about changes that have occurred in the structure and composition of the stands. More specifically, variations in competition pressure through time could have contributed to modify  $iWUE_{ring}$  (Sohn *et al.*, 2016). The inclusion of TSF is expected to have helped counteract this drawback commonly encountered in dendroecological studies by partly accounting for these temporal changes in stand demography.

### 3.4.6 Conclusions

In this study, we observed a high contribution of tree size and stand age to  $iWUE$  trends, which highlights the need to sample various developmental stages to obtain results that are representative of the response of the whole tree community to climate change. This also points to an urgent need of a standard statistical procedure to remove these developmental trends prior to evaluating the effect of rising  $C_a$  on tree-ring  $iWUE$ ; the one we propose here can serve as a starting point. Secondly, the high spatial heterogeneity we observed in the magnitude of the  $CO_2$  effect underscores the need to make optimum use of currently available forest inventory datasets and sample collections. Considering our results, tree-ring based isotope analyses should be systematically included in national forest inventory protocols as a means of monitoring

the physiological response of trees to climate change under diverse environmental conditions. Last, our findings show that black spruce trees are continuously and dynamically adjusting their leaf gas-exchange variables to maximise the ratio between carbon gain and water loss. This temporal instability, combined with any undetected adaptive variation at the species level (Depardieu *et al.*, 2020), will add to the difficulty to accurately estimating future physiological response of trees under a warmer climate. Ultimately, overestimated iWUE<sub>ring</sub> responses to C<sub>a</sub> could lead to biased inferences about the future net carbon balance of the boreal forest.

### 3.5 Acknowledgements

This study was made possible thanks to the financial support that was provided by the Strategic and Discovery Grant programs of NSERC (Natural Sciences and Engineering Research Council of Canada), doctoral and travel scholarships funded by FRQNT (B2X and international internship programs), and a MITACS scholarship cofunded by Ouranos. Additional financial support was provided by the Centre for Forest Research (Centre d'Étude de la Forêt, CEF), the Canadian Forest Service, the UQAM Foundation (De Sève Foundation fellowship and TEMBEC forest ecology fellowship) and the Quebec Ministère de l'économie, de la Science et de l'innovation (programme PSR-SIIRI). We want to thank the two anonymous reviewers for their highly constructive and positive comments that helped to greatly improve the manuscript. We thank Dan McKenney and Pia Papadopol (Canadian Forest Service) for providing the ANUSPLIN climate data. We are very grateful to Marie Moulin, David Gervais and Christine Simard for the huge help with the processing of wood samples. Many thanks to XiaoJing Guo (Canadian Forest Service) for helpful advice during statistical analyses, to Savoyane Lambert, Heike Geilmann and Iris Kuhlmann (Max Planck Institute for Biogeochemistry) for isotope measurements, and to Martine Savard, Joëlle Marion, Lauriane Dinis, Joëlle Berthier, Claude Durocher, Marie-Claude Gros-Louis, Philippe Labrie, Alexis Achim and Mathilde Pau for help and advice with the processing of wood samples, and to W.F.J. Parsons for language editing.

## CHAPITRE IV

### CONCLUSION GÉNÉRALE

#### 4.1 Faits saillants et contributions à l'avancée des connaissances

Tout au long de cette thèse, nous avons étudié tour à tour l'effet de la variabilité climatique inter-annuelle sur les taux de croissance radiale de l'épinette noire et du pin gris (chapitre 1), l'effet d'un épisode de sécheresse sévère sur la croissance et la physiologie des deux espèces (chapitre 2) et l'effet de l'augmentation de la concentration en CO<sub>2</sub> atmosphérique sur leur efficience d'utilisation de l'eau (chapitre 3).

Plus précisément, le premier chapitre a permis d'établir un état des lieux de la sensibilité au climat pour chacune des deux espèces et de déterminer quels facteurs environnementaux étaient impliqués dans la relation croissance-climat, au sein de la zone boréale québécoise. L'étude est basée sur des données d'inventaire forestier et inclut un nombre relativement conséquent d'arbres et de sites, ce qui reste rare actuellement (mais voir Girardin *et al.*, 2016a pour le Canada ; Ols *et al.*, 2020 pour l'Europe). Les résultats saillants de ce premier chapitre sont des taux de croissance à la baisse chez l'épinette pour la période 1970-2005, associés à une sensibilité élevée aux fortes chaleurs de l'été précédant la formation du cerne sur la quasi-totalité de la zone

d'étude. La croissance du pin ne présentait, au contraire, pas de tendances marquées et était peu impactée par les étés chauds et secs. Un point intriguant de ce premier chapitre est l'effet négatif de printemps plus chauds sur la croissance des épinettes localisées dans la portion centrale de notre zone d'étude. Les individus situés le plus en élévation, c'est-à-dire généralement en haut de pente, sont apparus particulièrement affectés. Dans ce chapitre, nous avons fait l'hypothèse que cet effet négatif provenait de l'impact des épisodes de gel tardif sur le feuillage nouvellement formé. Le facteur éolien, plus intense en haut de pente où les arbres sont plus isolés et donc plus exposés au vent, pourrait être un élément d'explication supplémentaire à cette relation contraintuitive (Marquis *et al.*, 2020b). Enfin, les chronologies médianes d'indices de croissance ont montré, chez les deux espèces, une baisse prononcée de la croissance survenue dès 1988-1989 et qui s'est maintenue jusqu'en 1992 dans le cas de l'épinette. Les possibles causes physiologiques de ce creux de croissance ont été investiguées dans le second chapitre.

L'année 1989, outre la chute brutale des taux de croissance chez les deux espèces étudiées, était caractérisée par une superficie brûlée exceptionnelle (Soja *et al.*, 2007), ce qui suggérait des conditions exceptionnellement sèches. Cela nous a conduit à sélectionner l'année 1989 comme année focale pour étudier l'effet d'un épisode de sécheresse extrême sur la variabilité inter-annuelle de la physiologie et de la croissance des arbres, dans le cadre du second chapitre. Nous avons pu observer que la chute de croissance relevée précédemment intervenait de façon synchrone à des variations significatives des ratios en isotopes stables du carbone et de l'oxygène. Cette observation tend à indiquer des modifications des paramètres physiologiques des arbres, à savoir une efficience d'utilisation de l'eau plus élevée et une conductance stomatique plus faible en 1988-1989 comparativement aux valeurs moyennes. Cette variabilité dans les ratios isotopiques a pu être reliée aux variations inter-annuelles du climat, et notamment à une balance en eau plus faible et à une atmosphère déficitaire en eau. Cela suggère que des stress climatiques sont bien à l'origine de la chute de croissance

observée. Un autre résultat intéressant de ce second chapitre est un impact de l'épisode de sécheresse de 1988-1989 qui perdure plus longtemps chez l'épinette que chez le pin, potentiellement en raison de traits d'histoire de vie différents comme un réseau racinaire essentiellement superficiel et adventif couplé à une moins bonne gestion des ressources en carbone chez l'épinette comparativement au pin (Burns et Honkala, 1990 ; Way et Sage, 2008b, 2008a).

Enfin, le troisième chapitre relate les changements intervenus dans le statut hydrique des arbres entre la période pré-industrielle (avant 1850) et le début du 21<sup>ème</sup> siècle, en réponse à l'augmentation de la concentration en CO<sub>2</sub> atmosphérique. L'intérêt majeur et le caractère novateur de ce chapitre résident avant tout dans l'aspect méthodologique qui y est développé. Il a notamment été testé trois modèles statistiques différentes pour évaluer l'effet CO<sub>2</sub> à partir d'un jeu de données isotopiques relativement conséquent et couvrant un important gradient géographique. Un fait saillant est la mise en évidence, au sein des données d'efficience d'utilisation de l'eau, de tendances liées à l'augmentation en taille des arbres et aux changements de structure et de composition intervenant au cours de la maturation du peuplement. Ces effets développementaux sont de plus forte intensité que les effets du climat. S'ils ne sont pas retirés ou contrôlés de façon adéquate, ils peuvent induire une estimation biaisée de l'effet CO<sub>2</sub>. Si certaines études incluent un ou plusieurs de ces facteurs développementaux dans leurs modèles statistiques (Dietrich *et al.*, 2016 ; Sullivan *et al.*, 2017), cela reste encore peu usité et les méthodes employées diffèrent. Nous avons montré dans ce chapitre que l'intensité de l'effet CO<sub>2</sub> variait selon le modèle statistique employé. Cela suggère que la comparaison des résultats entre différentes études doit être effectuée avec prudence. La méthodologie statistique proposée ici pour retirer les tendances induites par le développement des arbres et des peuplements, si elle peut servir de base à une méthode statistique commune, gagnerait sûrement à être approfondie et améliorée.

Cette thèse était également l'occasion de valoriser sous forme de publications scientifiques les données et échantillons accumulés dans le cadre de l'inventaire écoforestier nordique du Ministère des Forêts, de la Faune et des Parcs du Québec. Ces données sont précieuses en termes de quantité d'échantillons, du nombre et de la diversité des variables écoforestières mesurées et de la couverture géographique des placettes inventoriées. Les coûts, tant en termes de temps que d'argent investis dans l'échantillonnage de terrain, la préparation et la mesure des échantillons, sont très élevés. Malgré ces investissements, les données, notamment les analyses de tiges, sont relativement peu exploitées pour analyser les effets du climat sur la croissance forestière (mais voir D'Orangeville *et al.*, 2018 ; Girardin *et al.*, 2016a). De même, les échantillons physiques résultant des analyses de tiges, outre les mesures de largeur de cernes, n'avaient pas fait l'objet, jusqu'à récemment, d'autres analyses, par exemple des analyses des propriétés physico-chimiques des cernes. Ces données et échantillons, propriété de la province du Québec, et plus généralement les résultats d'inventaires appartenant à diverses structures gouvernementales sont des sources de données exceptionnelles qui gagneraient à être utilisées plus largement par la communauté scientifique. Un portail internet, offrant une meilleure visibilité et une meilleure accessibilité aux données disponibles, pourrait être une piste à suivre. Celui-ci répertorierait, par exemple, les localisations pour lesquelles des données sont disponibles, la nature de celles-ci, et la procédure à suivre pour y accéder (voir Girardin *et al.*, 2021 pour un tel projet à l'échelle du Canada).

#### 4.2 Forte variabilité spatiale et temporelle des effets des changements climatiques sur la croissance et la physiologie des conifères boréaux

Dans le premier chapitre, nous avons observé que les tendances de croissance sur la période 1970-2005, de même que la sensibilité au climat, variaient fortement au sein de la zone d'étude. Nous avons pu identifier certains facteurs de l'environnement de croissance des arbres qui contribuaient, partiellement, à cette variabilité spatiale. Parmi

ces facteurs, la position de l'arbre le long du gradient d'élévation agit en amplifiant la sensibilité des épinettes aux fortes chaleurs printanières et estivales. Dans le troisième chapitre, nous avons également identifié la fertilité du site comme étant inversement corrélée à l'efficience d'utilisation de l'eau des épinettes, et comme un facteur accentuant l'effet CO<sub>2</sub>. Les sites en élévation sont parmi les moins fertiles au sein de notre aire d'étude (voir Figure S3.10) et sont caractérisés par un substrat rocheux et donc relativement sec. Cela laisse à penser que ces environnements pauvres restreignent la capacité d'assimilation photosynthétique de l'épinette, une espèce par ailleurs relativement peu adaptée aux milieux secs. Sur ces milieux, la croissance des arbres pourrait être encore moins bonne si l'environnement venait à se réchauffer trop vite et trop intensément et si ces arbres étaient soumis de plus en plus fréquemment à des sécheresses et à des vagues de chaleur exceptionnelles. Des conditions plus chaudes au printemps leur seraient défavorables car elles pourraient engendrer un débourrement trop hâtif. La phénologie de ces populations est, en effet, adaptée à un climat plus rude, ce qui permet aux arbres de limiter le risque associé aux gelées tardives (Bigler et Bugmann, 2018). Au contraire, les épinettes localisées dans la zone la plus à l'ouest de l'aire étudiée semblent réagir positivement aux fortes températures printanières. Elles apparaissent également être moins sensibles aux températures estivales de la saison précédant la formation du cerne. Ces observations pourraient indiquer que ces populations d'épinettes sont soumises à un degré moindre aux stress climatiques récents, ce qui pourrait expliquer qu'elles aient maintenu de meilleures performances de croissance. La zone ouest, outre un climat plus chaud, est caractérisée par un sol bien développé, à forte composante organique et au paysage dépourvu de reliefs. Ces résultats tendent donc à indiquer, comme discuté brièvement dans le deuxième chapitre de cette thèse ainsi que dans plusieurs articles de synthèse récents (McLaughlin *et al.*, 2017 ; Stralberg *et al.*, 2020), que certaines zones caractérisées par un environnement physique adéquat, par exemple une capacité de drainage modérée à faible, agiraient comme facteur d'atténuation des effets des changements climatiques sur les espèces ligneuses boréales. Les populations d'épinettes dans la zone ouest ont également pu,

au fil des différentes générations, sélectionner des traits morphologiques et physiologiques leur permettant de se maintenir et de profiter du climat plus chaud et sec, comme par exemple des canaux conducteurs plus résistants à la cavitation.

Outre cette forte hétérogénéité spatiale, nous avons pu observer une importante variabilité temporelle dans l'évolution de l'efficience d'utilisation de l'eau, notamment chez l'épinette. Nous avons noté qu'après une période de fort accroissement, l'efficience d'utilisation de l'eau de cette espèce se stabilisait à partir du début des années 1980s. Ceci, comme discuté au troisième chapitre, pourrait marquer l'atteinte d'un seuil physiologique au-delà duquel l'épinette n'est plus capable d'augmenter ses taux d'assimilation photosynthétique, même sous une atmosphère plus riche en CO<sub>2</sub>. Ce seuil pourrait être modulé par la disponibilité en nutriments, imposant une plus forte contrainte à la croissance des arbres localisés sur les sols les plus pauvres. Les sites les plus fertiles, sur lesquels les arbres avaient maintenu une efficience d'utilisation de l'eau relativement faible jusqu'à la seconde moitié du 20<sup>ème</sup> siècle, semblent avoir été soumis, récemment, à des changements ayant affecté leur physiologie de façon importante. Cela se traduit, chez les épinettes, par une augmentation de l'efficience d'utilisation de l'eau beaucoup plus marquée sur ces sites fertiles que sur les sites pauvres (chapitre 3). Cela pourrait indiquer que les changements environnementaux, et surtout climatiques, deviennent de plus en plus contraignants, surtout au sein de ces populations les plus productives. Contrairement aux arbres sur sites pauvres et secs, ces populations étaient jusqu'à récemment épargnées par les stress chroniques affectant les individus sur le long terme. Elles pourraient donc être peu adaptées à une atmosphère plus chaude et sèche qui viendrait se superposer à des stress climatiques ponctuels de plus en plus fréquents. Ces populations pourraient donc voir leurs taux de croissance chuter drastiquement et leurs taux de mortalité augmenter de façon plus importante que ceux des populations implantées sur les sites qui restent actuellement les moins productifs (McNulty *et al.*, 2014 ; Ols *et al.*, 2020). Pour être en mesure de vérifier cette hypothèse, des analyses plus approfondies sont nécessaires, par exemple

en groupant les sites en fonction de leurs similarités. Une analyse par clusters de l'effet CO<sub>2</sub> (Chapitre 3) est présentée à la Figure S4.1, où les sites ont été groupés selon leur fertilité (IQS), l'âge du peuplement, et sa productivité, approximée par la moyenne des BAI des arbres sur les 20 dernières années. Les conclusions sont sensiblement les mêmes que celles présentées au chapitre 3. En regardant la relation entre le BAI et la concentration en CO<sub>2</sub> atmosphérique uniquement sur les sites les plus productifs, on observe des valeurs de BAI significativement plus élevées aux plus fortes concentrations de CO<sub>2</sub>, pour les épinettes (Figure S4.2). Néanmoins, cette relation reste faible et marginalement significative.

#### 4.3 Un effet des variations interannuelles et des tendances climatiques dépendant de l'espèce

Tout au long de cette thèse, nous avons mis en évidence un effet des variations climatiques inter-annuelles sur la physiologie des arbres et des impacts sur leur croissance qui différaient pour chacune des deux espèces étudiées. Le pin, bien qu'affecté physiologiquement par l'épisode de sécheresse extrême de 1989 (chapitre 2), a conservé un ratio C<sub>i</sub>/C<sub>a</sub> relativement stable sur le long terme. Cela indique un ajustement modéré des paramètres physiologiques chez cette espèce au cours du temps. Cette observation suggère également un degré moindre de stress face aux conditions de croissance plus chaudes (chapitre 3). La croissance du pin gris a, en conséquence, été peu impactée par les changements climatiques des trois dernières décennies. Pour certaines localisations, le pin apparaît même bénéficié de ces modifications de son environnement. Au contraire, l'épinette est apparue négativement affectée par les changements environnementaux intervenus depuis l'industrialisation. Chez cette espèce, l'augmentation de l'efficience d'utilisation de l'eau depuis 1850, loin de bénéficier à la croissance des arbres, semble au contraire marquer un stress de plus en plus prononcé (chapitres 1 et 3). Ces stress climatiques se traduisent à leur tour par une baisse générale de la croissance au cours des trois dernières décennies (chapitre 1).

Ces effets propres à l'espèce pourraient provenir d'une sélection de traits divergente, en relation avec les niches écologiques occupées par chacune des deux espèces. Le pin, retrouvé habituellement sur les milieux sableux, relativement secs et bien drainés, peut avoir sélectionné un ensemble de traits morpho-physiologiques lui permettant de maintenir plus efficacement sa croissance lors d'une sécheresse, et de retrouver plus rapidement des taux de croissance comparables à ceux d'avant la sécheresse (chapitre 2). Ces adaptations, incluant un réseau racinaire permettant l'accès à des ressources en eau localisées dans les couches profondes du sol, peuvent également avoir rendu l'espèce plus apte à maintenir sa croissance sous le climat des dernières décennies (chapitre 1). Au contraire, l'épinette est beaucoup plus généraliste quant aux conditions édaphiques des sites qu'elle occupe. Elle présente, en particulier les populations nordiques installées sur les sites les plus entourbés, des adaptations morpho-physiologiques à des sols gorgés d'eau, froids et à forte composante argileuse et organique, tel qu'un réseau racinaire essentiellement superficiel et adventif (Burns et Honkala, 1990). Cette espèce peut, en conséquent, être peu ou mal adaptée à un environnement devenant plus chaud et plus sec. Les différences visibles à la figure 2.4, notamment une remontée plus rapide des taux de croissance et des valeurs de  $\Delta^{13}\text{C}$  chez le pin comparativement à l'épinette, seraient possiblement le fruit de différences au niveau physiologique plutôt que liées à la profondeur à laquelle chacune des deux espèces peut capter l'eau ou à des différences au niveau de l'environnement physique. En effet, l'utilisation du z-score plutôt que des valeurs brutes rend les valeurs indépendantes de toute variabilité liée au site ou à l'individu. Les résultats observés dans le chapitre 3, c'est-à-dire une forte instabilité temporelle du statut hydrique des arbres et une forte augmentation de l'efficience d'utilisation de l'eau sur les sites les plus fertiles, suggèrent néanmoins une certaine capacité de l'épinette à s'adapter aux changements intervenant dans son environnement. Cette capacité d'adaptation pourrait provenir d'une forte plasticité physiologique, notamment sur les sites choisis pour les analyses isotopiques, caractérisés par un drainage modéré à rapide (pas de sites paludifiés ou gorgés d'eau). Schoonmaker et al. (2010) arrivent à une hypothèse

semblable en étudiant les traits hydrauliques de semis de conifères boréaux, incluant l'épinette noire, dans des conditions d'ombrage contrastées. Cependant, les tendances de croissance généralement à la baisse que nous avons relevées pour l'épinette dans le premier chapitre tendent à indiquer que cette forte plasticité n'est pas suffisante pour permettre à l'espèce de maintenir ses performances de croissance face à des changements environnementaux trop rapides et intenses. Dans ce premier chapitre, l'ensemble des sites disponibles dans la base de données avait été inclus dans les analyses. Le signal observé dans les tendances de croissance pourrait donc être, au moins en partie, associé à des sites moins bien drainés.

#### 4.4 Préconisations et enjeux de recherche futurs

Nous avons vu, notamment avec le troisième chapitre, que certaines interrogations subsistent quant aux résultats des études antérieures. Certaines de ces incertitudes ont pour origine les méthodes statistiques employées pour détecter les tendances dans les séries temporelles de croissance et de signatures isotopiques (Marchand *et al.*, 2018). Une évaluation des méthodes de standardisation employées pour retirer les tendances biologiques dans les séries de largeurs de cernes et leur mise à jour ou remplacement éventuel par d'autres méthodes plus performantes devraient être effectués (Dietrich et Anand, 2019). Une remise en question de certaines suppositions qui étaient jusqu'à récemment considérées comme une norme, notamment la supposition de l'absence de tendances biologiques au sein des séries de ratios isotopiques du carbone à l'exception d'un « effet juvénile » perdurant seulement dans les 50 premiers cernes formés par l'arbre (Gagen *et al.*, 2008 ; Loader *et al.*, 2007), devrait également être réalisée. Enfin, un consensus devrait être trouvé afin d'employer des méthodes d'analyses permettant une comparaison rapide et non biaisée des résultats entre les différentes études. Par exemple, une méthode de standardisation unique pourrait être choisie et utilisée dans l'ensemble des nouvelles études dendrochronologiques, ce qui permettrait de comparer plus efficacement les tendances de croissance. De plus, la méthode de régression

partielle (chapitre 3) gagnerait à être généralisée afin de mieux séparer les effets de certaines variables présentant une forte colinéarité (par exemple l'effet de l'augmentation de la concentration en CO<sub>2</sub> atmosphérique et celui de l'augmentation de la taille de l'arbre, ou encore l'effet de l'augmentation des températures de surface).

De plus, mis à part les différences au niveau des méthodes d'analyses, la forte variabilité spatiale et temporelle à la fois dans les processus physiologiques (chapitre 3) et dans la sensibilité au climat (chapitre 1), complique la comparaison des résultats entre les études. Cette variabilité se traduit par des tendances de croissance pouvant différer, pour une même espèce, selon le site d'étude mais également en fonction de la fenêtre temporelle analysée. En effet, l'environnement a un effet marqué tant sur la physiologie que sur la croissance et la sensibilité des arbres au climat, et les résultats sont hautement spécifiques au site étudié. Il est également à noter que les tendances de croissance peuvent différer selon la période couverte par les analyses. Ici, les tendances sont assez similaires qu'elles soient calculées à partir de 1970 ou de 1950 (chapitre 1). Cependant, des études s'intéressant à une fenêtre temporelle plus large (e.g. Dietrich *et al.*, 2016 ; Lloyd et Bunn, 2007), ou au contraire plus réduite (e.g. Bond-Lamberty *et al.*, 2014), peuvent observer des résultats divergents, qui ne sont pas forcément basés sur les mêmes objectifs. Une fenêtre temporelle réduite aux décennies les plus récentes pourrait notamment fournir des résultats plus représentatifs de la situation actuelle des forêts et donc des taux de croissance dans un avenir proche. Cependant, ces résultats seraient aussi potentiellement plus influencés par l'effet des épisodes climatiques extrêmes, et n'incorporent pas forcément la variabilité climatique à long terme. Les épisodes de sécheresses récents pourraient notamment tirer les tendances de croissance vers le bas si ces dernières sont calculées sur des séries temporelles courtes. Au contraire, une fenêtre temporelle large, c'est-à-dire de l'ordre du siècle, serait représentative de l'effet à long terme des changements climatiques sur la croissance des arbres. Or, des tendances de croissances calculées sur une fenêtre temporelle aussi large ne permettraient pas de visualiser l'évolution temporelle récente des taux de

croissance des arbres. Là encore, ces spécificités spatiales et temporelles sont à considérer lors de la comparaison des résultats entre des études dont les objectifs et hypothèses diffèrent. En outre, cette forte variabilité spatio-temporelle complique l'estimation des paramètres physiologiques des arbres dans un environnement plus chaud, et donc les prédictions des possibilités forestières futures.

Les modèles servant à estimer la productivité végétale à l'échelle globale (Dynamic Global Vegetation Models, DGVM) considèrent actuellement, pour modéliser la dynamique de la physiologie des arbres, des paramètres qui évoluent de façon semblable quels que soient la qualité du site ou le stade de développement considérés. Or, nos résultats montrent, au moins en ce qui concerne le statut hydrique des arbres lorsque dérivé de la composition chimique des cernes de croissance, une forte tendance induite par les facteurs développementaux et un effet CO<sub>2</sub> qui diffère selon la fertilité du site. Il est donc probable que les prédictions actuelles de l'effet CO<sub>2</sub> induisent une vision trop optimiste du statut hydrique des arbres sous un climat plus chaud et plus sec. Ce biais est, peut-être, accentué par le fait que les arbres habituellement échantillonnés lors des campagnes d'inventaires forestiers sont ceux implantés dans les forêts productives et dans les zones où le climat est le plus contraignant pour leur croissance (Kresse *et al.*, 2018). Les coefficients obtenus au chapitre 3 relatant l'effet CO<sub>2</sub> exempt des tendances liées au développement de l'arbre et du peuplement pourraient permettre d'améliorer la fiabilité des prédictions issues de ces modèles, notamment si la fertilité de la zone était considérée comme paramètre d'entrée. Cependant, la forte instabilité temporelle, et notamment la phase de plateau que semble avoir atteint l'efficience d'utilisation de l'eau de l'épinette depuis les années 1980s, induit une nouvelle part d'incertitude quant au futur statut hydrique des arbres. Cette non-linéarité dans l'évolution temporelle des processus physiologiques des arbres en réponse aux changements environnementaux est retranscrite dans les relations croissance-climat. Par exemple, dans le cas des forêts nordiques, la température avait, jusque dans les années 1950, un effet positif et hautement significatif sur la croissance

des arbres. Or, cet effet s'est peu à peu affaibli, puis inversé dans les décennies récentes (« divergence problem »; D'Arrigo *et al.*, 2008). Ainsi, les arbres répondront fort probablement d'une manière différente au climat futur comparativement à la réponse passée, inférée à partir des cernes de croissance (Klesse *et al.*, 2020). Cela représente un frein supplémentaire à la projection des performances de croissance des arbres dans le futur.

Pour conclure sur l'aspect méthodologique, une grande part des incertitudes provient de l'approximation qui est faite des taux de croissance et des paramètres physiologiques des arbres par l'utilisation de paramètres dérivés des cernes de croissance. Pour y remédier, un réseau de mesures directes, en continu, des échanges gazeux des arbres (flux de CO<sub>2</sub> et de vapeur d'eau) et des flux d'isotopes stables du carbone et de l'oxygène devrait être mis en place à grande échelle et en milieu naturel. Le réseau de tours à flux qui était en activité entre 1993 et 2014 (Fluxnet Canada Team, 2016 ; Lee *et al.*, 2020 ; Sturm *et al.*, 2012), dont les mesures corrèlent fortement aux prédictions de modèles bioclimatiques et aux mesures de largeurs de cernes de certaines études (Girardin *et al.*, 2014, 2016b), devrait être remis en fonction et pourrait être bonifié. De plus, les données de largeur de cernes issues des inventaires forestiers sont, en général, très répliquées temporellement et spatialement, mais très peu répliquées à l'échelle du site d'étude (Babst *et al.*, 2018 ; Ols *et al.*, 2020). Notamment, les conditions micro-environnementales peuvent influencer la réponse des arbres au climat. La variabilité qui y est associée est difficilement estimable ou contrôlable à partir de données d'inventaires forestiers, issues de peuplements en conditions naturelles. En outre, les arbres sélectionnés à l'intérieur de chaque placette peuvent ne pas être représentatifs de la réponse du peuplement dans sa globalité (Babst *et al.*, 2018). Les résultats de cette thèse ne sont, en effet, basés que sur des données issues d'arbres dominants et co-dominants, et de peuplements relativement accessibles. Les conclusions auraient pu être différentes si des individus opprimés, plus jeunes, et issus des peuplements les moins accessibles (par exemple dans les milieux les plus riches en

matière organique, sur les zones les plus au nord, ou sur les sols les plus argileux) avaient été considérés. Notamment, des arbres plus jeunes (s'étant régénérés au cours de la dernière décennie) pourraient être moins sensibles aux conditions chaudes et sèches, et même profiter des températures plus chaudes. Les résultats du chapitre 1, et notamment les relations entre la sensibilité des arbres aux températures estivales de la saison précédente et l'âge du peuplement, tendent à montrer que les arbres jeunes réagissent positivement, contrairement aux arbres de plus de 150 ans (Figure 1.7). Certaines études, notamment celles étudiant la croissance en hauteur des arbres, vont également dans ce sens (e.g. Marchand et DesRochers, 2016). Ces arbres récemment régénérés, ayant débuté leur croissance sous un climat proche du climat actuel, pourraient être d'ores et déjà acclimatés à ces conditions plus chaudes, au travers d'une adaptation de leurs paramètres physiologiques. Cependant, chez des arbres jeunes, le réseau racinaire peu développé pourrait également agir comme facteur amplificateur des stress hydriques ponctuels. Un problème récurrent lié à l'utilisation de données d'inventaires forestiers est l'absence de données issues d'arbres morts ou fossiles. Plus un individu a des taux de croissance importants et plus il est à risque de mourir des conséquences d'un stress biotique (insecte, maladie, infection fongique) ou abiotique (stress climatique, chablis). Ainsi, les vieux arbres encore en vie au moment de l'échantillonnage sont probablement ceux ayant eu la croissance la plus lente. Au contraire, les arbres les plus jeunes et les plus gros au moment de l'échantillonnage sont ceux qui présentent les taux de croissance les plus élevés (Piovesan et Biondi, 2021). Ainsi, les études basées sur les données d'inventaire forestier, incluant cette thèse, ne sont pas représentatives de l'ensemble du peuplement ciblé, mais uniquement d'un sous-échantillon des arbres les plus gros (dominants et co-dominants) à l'instant de l'échantillonnage. Si l'ensemble des arbres avait été considéré (incluant des arbres morts ou fossiles), les tendances de croissance auraient, potentiellement, pu être revues à la hausse dans les peuplements les plus anciennement régénérés, et à la baisse dans les peuplements les plus récents.

Une intégration d'autres types de données, par l'intermédiaire de modèles prédictifs par exemple, pourrait aider à obtenir une estimation plus précise de la réponse de la forêt aux changements climatiques à une échelle plus large du peuplement ou du biome forestier. Par exemple, les données Lidar (Thomas *et al.*, 2008), et celles issues de drones (Wong *et al.*, 2020), semblent particulièrement prometteuses pour obtenir une estimation du statut physiologique des arbres à l'échelle du peuplement forestier et ainsi améliorer les estimations des flux de carbone (Babst *et al.*, 2018). Une analyse du contenu en glucides et amidon des cernes de croissance pourrait également améliorer notre compréhension des processus en jeu. En particulier, la comparaison des concentrations en carbohydrates des cernes formés avant et après une sécheresse ou une vague de chaleur permettrait de préciser si ces conditions extrêmes impactent la capacité des arbres à accumuler des réserves (hypothèse invoquée au chapitre 1), ou si les arbres modifient leur stratégie d'allocation du carbone en priorisant l'accumulation de réserves au détriment de la croissance radiale (hypothèse invoquée au chapitre 2). Au cours de cette thèse, une tentative a été effectuée pour mesurer les concentrations en glucides et amidons des cernes formés entre 1985 et 1993 en suivant le protocole développé par Landhäusser *et al.* (2018). Ces tests ont montré une absence de glucides et d'amidon sur l'ensemble des échantillons. Cela pourrait être dû soit au fait que les sections radiales utilisées avaient été récoltées plus de 10 ans avant leur utilisation, soit au fait que les cernes analysés étaient déjà trop anciens (i.e. trop internes), situés dans le bois de cœur (duramen), et que les arbres auraient déjà remobilisé l'ensemble des carbohydrates qui auraient pu y être présents. Si cette dernière hypothèse est la plus probable, il pourrait être intéressant d'effectuer d'autres tests sur les cernes les plus récemment formés (i.e. entre 2005 et 2009), et sur des échantillons de bois fraîchement récoltés.

Des travaux récents montrent que les populations de pin tordu (*Pinus contorta*) situées le plus au nord du gradient latitudinal dans l'Ouest canadien sont moins tolérantes aux sécheresses comparativement aux populations méridionales (Isaac-Renton *et al.*, 2018).

L'hypothèse invoquée par les auteurs, i.e. un manque d'adaptation physiologiques à des conditions plus sèches, pourrait également s'appliquer à nos résultats. Cette mauvaise adaptation pourrait, en partie, expliquer la baisse de croissance observée entre 1970 et 2005 chez l'épinette, ainsi que la plus forte variabilité temporelle dans les paramètres physiologiques dérivés des ratios isotopiques observée chez cette espèce. Plus au sud, certains traits anatomiques, notamment des canaux conducteurs plus résistants à la cavitation et un bois plus dense (Hacke *et al.*, 2001), pourraient avoir été sélectionnés et donneraient potentiellement à ces populations de meilleures facultés d'adaptation face aux conditions climatiques futures. La localisation de nos placettes échantillon au nord du 49<sup>ème</sup> parallèle ainsi que l'absence de tout génotypage des arbres nous ont néanmoins empêché de vérifier si différentes populations présentaient une sensibilité différente au climat.

Ces résultats suggèrent que des stratégies de plantation pour pallier à une régénération naturelle insuffisante des peuplements nordiques seraient inadaptées si elles sont réalisées à partir de semences locales. L'utilisation de semences issues de populations méridionales au travers de programmes de migration assistée pourrait cependant être envisagée. En effet, le climat futur au nord se rapprochera probablement du climat sous lequel les populations plus au sud se développent actuellement, et auquel elles sont donc, potentiellement, déjà adaptées d'un point de vue physiologique et anatomique (Marris, 2009). Cependant, la performance de ces arbres, sortis de leur région d'origine, n'est pas garantie. En effet, l'impact négatif des printemps plus chauds sur la croissance des épinettes suggère que les arbres provenant de populations du sud dont la phénologie apparaît adaptée à un climat plus doux pourraient être fortement impactés par les épisodes de gels tardifs (Zohner *et al.*, 2020). Une étude récente fait d'ailleurs état de tels effets négatifs des gels tardifs chez trois espèces d'épinettes, et particulièrement chez des populations d'épinettes blanches plantées plus au nord de leur région d'origine (Marquis *et al.*, 2020b). La forte variabilité inter-individuelle, notamment dans les signatures isotopiques des cernes de croissance (chapitre 2), tend cependant à indiquer

que certains génotypes présents dans les populations nordiques seraient d'ores et déjà mieux adaptés que d'autres à des conditions plus chaudes et sèches. Les divers programmes de sélection génomiques pourraient ainsi permettre de cibler les populations qui seraient les plus à même de maintenir une bonne performance dans le futur. L'accent devrait par ailleurs être mis non seulement sur les traits de résistance aux vagues de chaleur et aux sécheresses, mais aussi sur les traits permettant aux arbres de se prémunir contre les effets des gels tardifs, par exemple un contrôle hormonal induisant une phénologie synchrone avec le risque de gels tardifs propre à la région ciblée.

En outre, les résultats présentés ici montrent que le pin gris est moins affecté que l'épinette noire par les changements environnementaux et en particulier les stress climatiques. En faisant l'hypothèse d'un maintien de cette tendance dans le futur, les aménagiste forestiers devraient logiquement favoriser le pin gris lorsque l'environnement physique lui est favorable, c'est-à-dire sur les milieux sableux bien drainés. Or, les deux espèces étudiées sont tributaires, pour leur régénération, du cycle des perturbations naturelles. Un raccourcissement du cycle de feux est attendu dans le futur. Cela pourrait réduire la capacité de régénération des peuplements forestiers (Boucher *et al.*, 2020), surtout chez l'épinette noire (Splawinski *et al.*, 2018). L'effet d'un cycle de feux plus court sur les espèces n'a pas été étudié dans cette thèse, amenuisant ainsi les possibilités d'extrapolation des résultats aux décennies futures.

Dans le cadre de la limite nordique des forêts commerciales, ces résultats suggèrent que certains peuplements, classés comme faiblement sensibles à l'aménagement écosystémique et donc exploitables, pourraient être à risque, dans le futur, de se régénérer en des peuplements dont la capacité de production serait inadéquate. Les tendances de croissance généralement à la baisse qui ont été relevées pour l'épinette dans le premier chapitre, ainsi que la forte sensibilité de l'espèce aux étés chauds, vont dans le sens d'une diminution de la capacité de production des peuplements d'épinette.

Les peuplements présents dans les zones actuellement les plus fertiles sont ceux pour lesquels l'augmentation de l'efficience d'utilisation de l'eau depuis 1850 a été la plus forte (chapitre 3), en réponse à un ou plusieurs facteurs de stress. Par conséquent, ces peuplements pourraient voir leur productivité diminuer de façon drastique au cours des prochaines décennies. Les taux de mortalité de ces peuplements productifs seraient notamment à surveiller, en vue de réévaluer leur sensibilité à un aménagement forestier durable, dont leur capacité à se régénérer en des peuplements denses, exploitables et économiquement intéressants. Dans le cas des peuplements peu productifs, le niveau de stress physiologique des épinettes apparaît élevé mais relativement constant. Ces peuplements sont ceux pour lesquels il a été identifié un effet négatif des printemps plus chauds que la moyenne. Cela suggère qu'en raison d'une phénologie inadaptée, la capacité de production de ces peuplements restera, au moins à court terme, faible. Cependant, les taux de mortalité de ces peuplements s'ils venaient à être soumis à des conditions plus chaudes et plus sèches pourraient ne pas augmenter significativement comparativement à ceux des peuplements très productifs. En ce qui concerne le pin gris, même si les résultats de cette thèse suggèrent que l'espèce serait moins sensible au réchauffement global, il est difficile de conclure que les peuplements de pin maintiendront leur capacité de production dans le futur. En effet, les changements dans le cycle de feux induits par le réchauffement global ne sont pas encore connus avec certitude, même si une tendance au raccourcissement des cycles de feux est prédictive. De même, la manière dont le pin répondra à ces changements dans le régime des feux est encore incertaine et devrait, elle aussi, faire l'objet d'études complémentaires.

## **ANNEXE A**

### **MATÉRIEL SUPPLÉMENTAIRE DU CHAPITRE I**

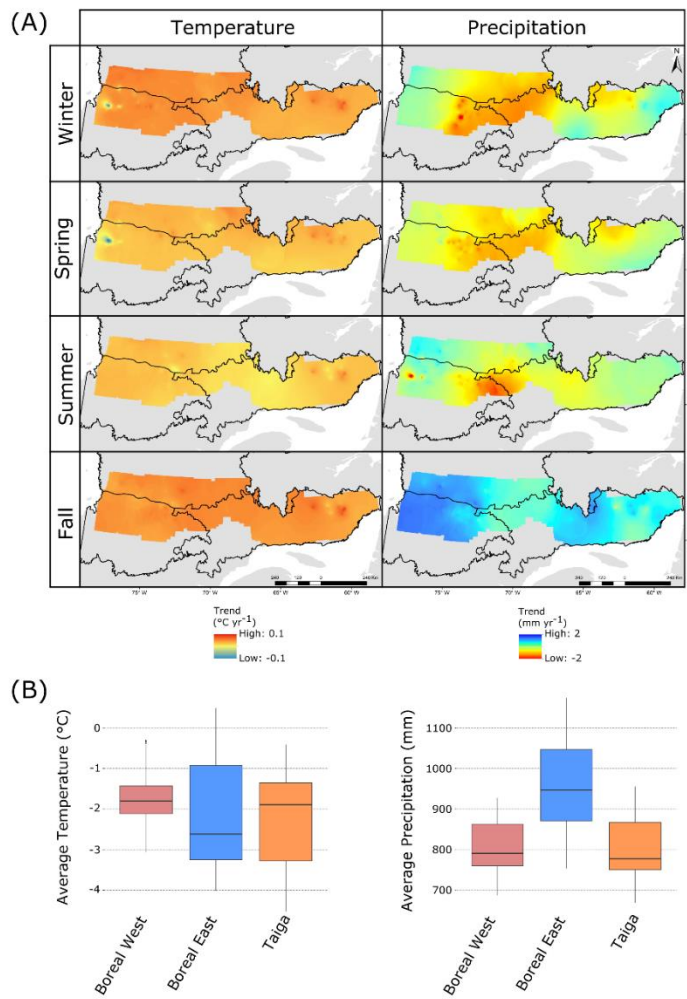


Figure S1.1. West-to-East climate gradient. (A) Kriging-interpolated trends in seasonal mean temperature (left) and total precipitation (right) over the 1970-2005 period. Trends were computed at the plot level as the slope of the linear regression between the climate variable and the calendar year and were interpolated over the whole study area using the “empirical Bayesian kriging” function in ArcMap 10.4.1 (search radius =  $1^{\circ}$ , resolution =  $0.05^{\circ}$ ). (B) Average mean annual temperature and total precipitation over the 1970-2005 period, by bioclimatic domain.

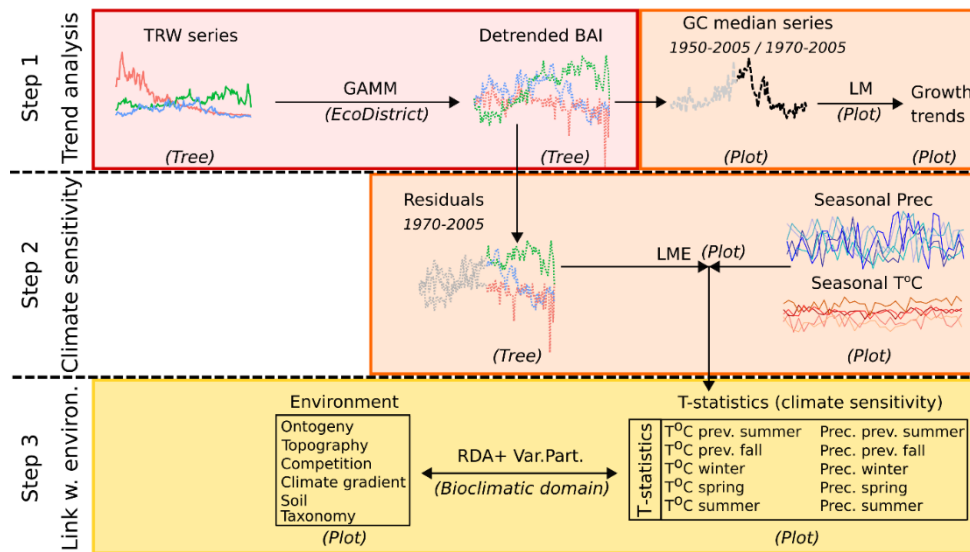


Figure S1.2. Workflow diagram of the statistical procedure. The sequential design of the analysis is in 3 steps. (1) The detrending model globally removes the effects of size, age and some spatial effects represented by OLT. (2) The climate model tries to discover the relationship between the detrended series and each climate variable (temporal effect) for each plot. The relationship (direction and magnitude) is represented by the t-statistics of the coefficients of each predictors. (3) The above t-statistics (time-independence) was involved in RDA analysis to quantify the effects of several ecological drivers. Spatial scales are indicated in parenthesis at each step. Different shadings represent different time-intervals and spatial scales for analyses: red shading highlights analyses by ecological district and species involving the whole tree-ring series; orange shadings are for 1970-2005 and 1950-2005 time-window and analyses by plot and species; and yellow shading is for time-independent analyses (those analyses involving no temporal replications of the response variable) by bioclimatic domain.

### S1.3. Raw tree-ring width series statistics.

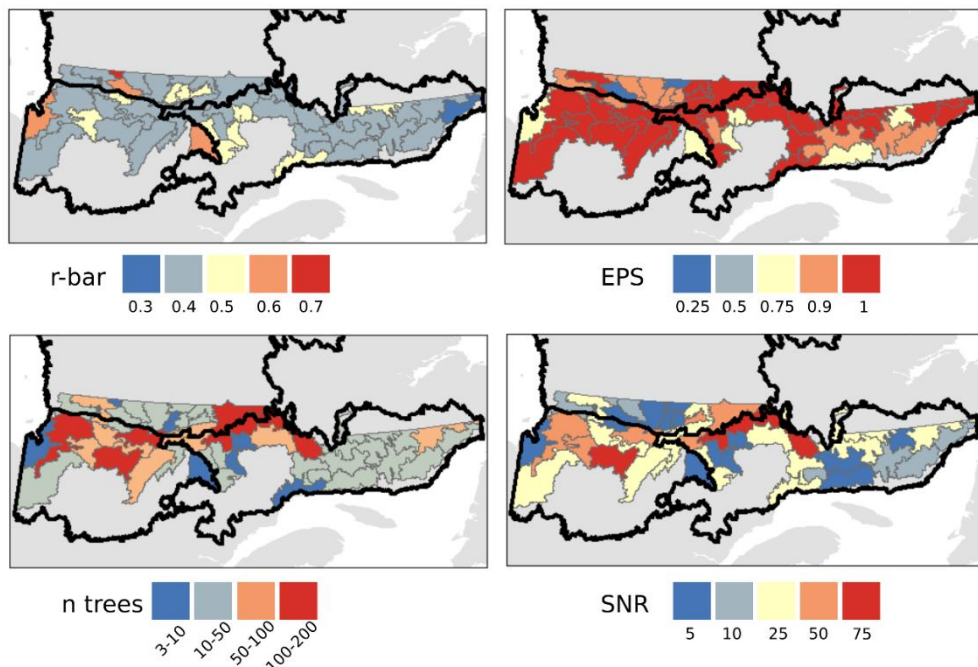


Figure S1.3.1. Mean intertree correlation (r-bar), expressed population signal (EPS), number of trees and signal to noise ratio (SNR) by landscape unit. The r-bar is an estimation of the common variance shared between tree-ring series, i.e. the strength of the shared signal (Speer, 2010). Here, r-bar values were computed as cross-correlations between detrended and whitened measurement series, and a reference chronology (defined by the average of all series within a landscape unit). For information, the mean of the correlations  $r$  computed between individual series and their associated landscape unit master chronology generated by the program COFECHA was 0.39. EPS is a measure of the ability of the studied chronology, built from a sub-population, to represent the entire (theoretically infinite) population (Buras, 2017). SNR is a measure of the strength of this shared signal (mostly the high-frequency signal), i.e. the proportion of signal originating from factors of interest versus background noise (random variations, and unwanted signals; Speer (2010)). EPS and SNR were computed using the R-package *dplR*.

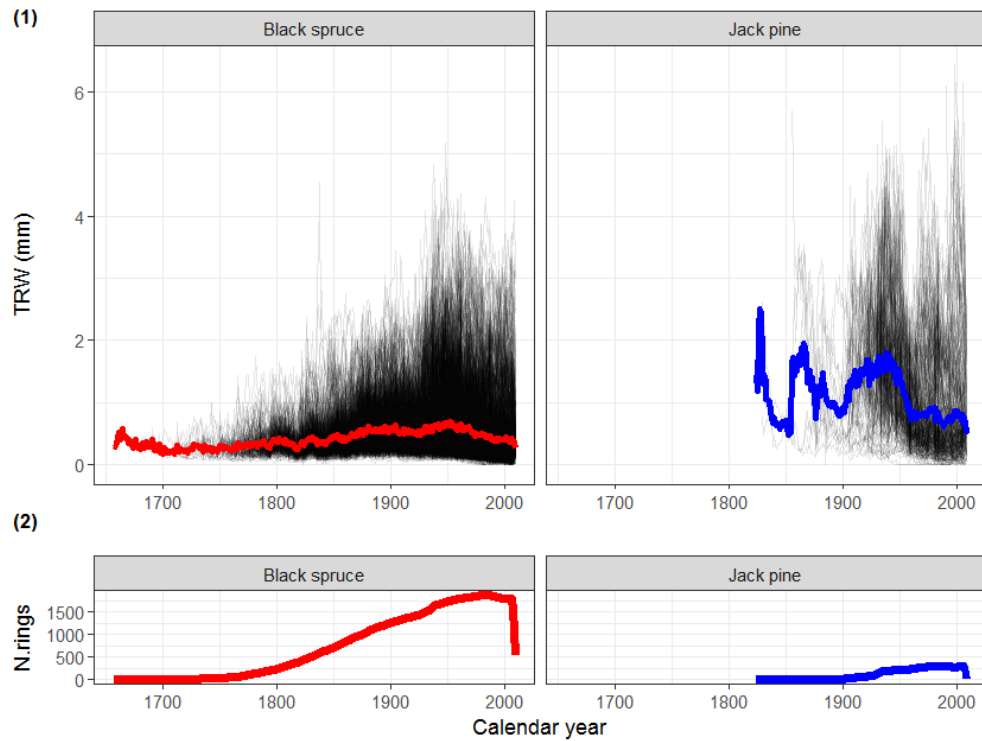


Figure S1.3.2. Raw tree-ring width series. (1) Black lines: raw tree-ring width series (average of the four radii, before removing the first 10 years); blue and red thick lines: average (arithmetic mean) chronology by species. (2) Sample depth, i.e. the number of rings by calendar year and species.

Table S1.3.1. Additional tree-ring width series statistics, by landscape unit. N trees is the total number of trees sampled by landscape unit, N BS and N JP are the number of spruce and pine trees by landscape unit, respectively, mean N rings is the average number of rings per year, N rings is the total number of rings by landscape unit, mean (and sd) RW BS and mean (and sd) RW JP are the average (and standard deviation) ring widths of black spruce and jack pine series respectively, start BS and start JP are the average start dates (i.e. first year recorded) for spruce and pine respectively, end BS and end JP are the average end dates (i.e. last year recorded) for spruce and pine respectively, N years BS and N years JP are average series length for black spruce and jack pine, respectively.

Landscape Unit	N trees	N BS	N JP	mean N rings	N rings	mean RW BS	s.d. RW BS	start BS	end BS	N years BS	mean RW JP	s.d. RW JP	start JP	end JP	N years JP
172	101	67	34	37.479	6828 <sub>8</sub>	0.752	0.380	1886	2005	486.866	1.437	0.664	1948	2004	226.941
136	87	47	40	30.844	5448 <sub>0</sub>	0.714	0.351	1870	2005	544.681	1.173	0.655	1939	2005	268.100
135	170	100	70	71.757	2028 <sub>00</sub>	0.908	0.464	1905	2006	406.250	1.286	0.849	1941	2006	265.600
171	71	34	37	23.745	3581 <sub>2</sub>	0.911	0.468	1915	2006	368.941	1.049	0.526	1941	2004	254.054
174	95	95	0	49.19	7187 <sub>8</sub>	0.483	0.197	1847	2007	642.821	NA	NA	NA	NA	NA
137	12	12	0	9.105	1128	0.451	0.229	1828	2007	719.333	NA	NA	NA	NA	NA
184	12	12	0	6.248	946	0.888	0.275	1898	2006	437.333	NA	NA	NA	NA	NA
170	58	26	32	22.521	1951 <sub>2</sub>	0.952	0.482	1941	2005	257.538	1.224	0.781	1934	2000	270.094
187	43	34	9	19.46	1020 <sub>4</sub>	0.580	0.280	1875	2003	515.882	1.355	0.508	1974	2003	120.000
186	9	6	3	7.556	630	0.437	0.244	1861	2004	576.000	0.447	0.255	1846	2006	642.667
185	18	15	3	10.391	2016	0.435	0.185	1863	2007	580.800	0.990	0.306	1954	2006	213.333
175	170	170	0	88.776	2227 <sub>74</sub>	0.481	0.219	1835	2007	691.765	NA	NA	NA	NA	NA
173	91	88	3	45.196	6304 <sub>2</sub>	0.604	0.252	1868	2007	559.545	1.603	0.567	1968	2007	158.667
145	24	24	0	13.72	4560	0.719	0.325	1871	2007	570.333	NA	NA	NA	NA	NA
151	21	19	2	8.931	3146	0.733	0.348	1901	2004	416.211	0.627	0.521	1881	1993	452.000
180	103	98	5	49.558	7230 <sub>0</sub>	0.556	0.248	1866	2005	560.898	0.658	0.539	1921	2001	325.600
182	23	23	0	14.737	4186	0.420	0.181	1852	2007	622.783	NA	NA	NA	NA	NA
183	45	45	0	28.704	1611 <sub>0</sub>	0.419	0.230	1855	2007	612.889	NA	NA	NA	NA	NA
139	3	3	0	2.83	66	1.286	0.371	1958	2007	200.000	NA	NA	NA	NA	NA
188	19	16	3	12.551	2850	0.517	0.247	1868	2007	558.250	0.943	0.825	1932	2007	304.000
189	13	10	3	4.581	507	1.033	0.400	1927	2005	309.500	3.157	0.864	1976	1999	94.667
192	17	11	6	8.861	1975	0.652	0.231	1882	2006	500.364	1.080	0.763	1933	1990	224.833
191	57	41	16	24.574	1882 <sub>7</sub>	0.724	0.399	1905	2003	398.634	1.482	0.836	1946	2001	213.250
190	8	0	8	7.31	496	NA	NA	NA	NA	NA	1.527	0.524	1970	2007	153.500
133	80	56	24	31.509	4478 <sub>2</sub>	0.945	0.515	1917	2008	366.786	1.056	0.754	1940	2006	269.833

178	129	126	3	63.179	1263 32	0.618	0.289	1861	2007	586.984	1,073	0.853	1933	2009	306.667
125	146	114	32	55.227	1365 22	0.634	0.312	1873	2008	542.807	1.382	0.760	1950	2007	228.625
119	28	28	0	15.502	6216	0.661	0.397	1881	2007	509.143	NA	NA	NA	NA	NA
177	70	64	6	29.474	3850 8	0.671	0.300	1884	2008	498.625	0.793	0.669	1918	2009	366.667
176	3	3	0	2.584	66	0.511	0.225	1820	2008	754.667	NA	NA	NA	NA	NA
155	42	42	0	22.594	1400 0	0.896	0.373	1880	2008	514.571	NA	NA	NA	NA	NA
156	39	39	0	27.472	1209 0	0.590	0.222	1860	2008	597.333	NA	NA	NA	NA	NA
157	42	42	0	15.915	1402 8	0.800	0.326	1898	2009	445.714	NA	NA	NA	NA	NA
124	3	3	0	2.818	66	0.557	0.238	1875	2008	537.333	NA	NA	NA	NA	NA
150	6	6	0	5.105	276	1.118	0.489	1928	2008	323.333	NA	NA	NA	NA	NA
168	50	50	0	26.477	1911 0	0.503	0.236	1861	2008	583.440	NA	NA	NA	NA	NA
162	12	12	0	7.778	1128	0.358	0.167	1835	2009	701.000	NA	NA	NA	NA	NA
165	91	91	0	46.207	6117 6	0.710	0.259	1869	2009	560.659	NA	NA	NA	NA	NA
179	44	44	0	23.039	1451 8	0.629	0.316	1873	2007	542.545	NA	NA	NA	NA	NA
166	30	30	0	19.251	7032	0.480	0.174	1847	2004	634.133	NA	NA	NA	NA	NA
158	23	23	0	11.79	4178	0.931	0.351	1902	2009	430.957	NA	NA	NA	NA	NA
167	50	50	0	19.419	1757 8	0.671	0.324	1872	2009	549.040	NA	NA	NA	NA	NA
163	42	42	0	29.02	1402 8	0.419	0.159	1834	2009	702.190	NA	NA	NA	NA	NA
164	33	33	0	22.545	8646	0.343	0.140	1837	2009	691.394	NA	NA	NA	NA	NA
193	33	20	13	13.457	6555	0.699	0.310	1878	2006	516.800	1.485	1.031	1939	2003	257.077

### S1.4. Diagnostics for the GAMM models

Table S1.4.1. Statistics of the BAI series processed into the GAMM models. We fitted one GAMM model by ecological district and species. Note that the number of individual BAI series (i.e. number of trees) used for detrending is lower than the initial number of black spruce and jack pine series because we previously eliminated incomplete series (missing values) and series spanning less than 20 years. We then eliminated the first 10 years of growth (the 10 innermost rings of each series, *i.e.* cambial ages 1 to 10) before fitting the GAMM models. Note that trees were sampled early during the growing season, leading to incompletely-formed outermost rings (*i.e.*, latewood was not formed at the time of sampling). For trees sampled in 2006, the 2005 growth-ring was the last whole growth ring (*i.e.*, with both earlywood and latewood), so, both for the main analysis and the sensitivity analysis, we decided to exclude the years 2006-2009 to avoid potential biases due to incomplete rings and to ensure consistency between chronologies.

	Black spruce	Jack pine
Number of ecodistricts (Number of GAMM models)	254	59
Number of trees	1800	280
Median (min max) number of trees by ecodistrict	6 (1 25)	3 (1 17)
Median (min max) number of plots by ecodistrict	2 (1 11)	2 (1 7)
Median (min max) starting date of BAI series	1825 (1682 1992)	1936 (1834 1997)
Median (min max) ending date of BAI series	2008 (1981 2009)	2007 (1981 2009)
Median (min max) length of BAI series	127.5 (10 321)	64 (10 168)

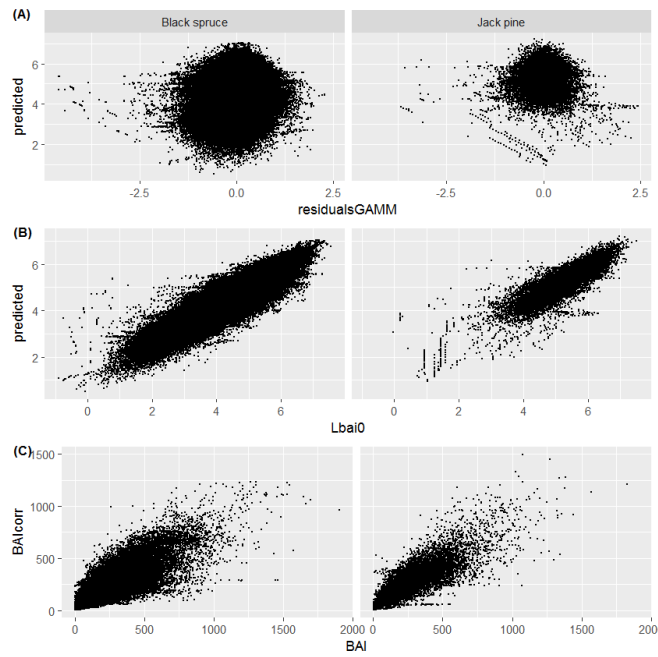


Figure S1.4.1. Diagnostic plots of the GAMM models, by species. (A) Residuals vs fitted values. (B) Observed BAI (log scale) vs fitted values. (C) Observed BAI (in mm<sup>2</sup>) vs corrected BAI (in mm<sup>2</sup>).

### S1.5. Sensitivity analysis for trends computation (period 1970-2005).

In the main document, we presented plot-level growth trends computed from BAI chronologies detrended using a GAMM modelling approach. However, as stated by Sullivan et al. (2016), the magnitude and direction of trends could be strongly dependent of the statistical procedure used for detrending the data. To assess the amount of confidence to be placed in the GAMM detrending-based trends, we detrended the BAI series using two additional detrending strategies more widely used in dendrochronological studies. First, we fitted a modified negative exponential model ( $f(t) = a \exp(b t) + k$ ) to the individual BAI series (one model by tree). Secondly, we applied the regional curve standardization (RCS) approach to the set of BAI series, by species. This approach aligned the BAI series by cambial age, computed the arithmetic mean of BAI for each ring age, and created a regional curve by fitting a smoothing spline to the average series (one curve by species was built here). Whatever the method, detrended BAI values were computed as the ratio of observed BAI values to predicted values. Trends were computed similarly to those from GAMM models, i.e. as the slope of the linear regression of the detrended BAIs with calendar years, over the period 1970-2005. Detrending was done using the functions *detrend* and *rcs* of R package *dplR*. Comparison with the map of the Figure 1.2 was done by performing Spearman's rank correlation tests (function *cor.test* in the base statistics R-package) on values extracted from the raster maps using a regular  $0.5^\circ$ -point grid. Note that the Empirical Bayesian Kriging used to display trends as surface raster maps is sensitive to extreme values, i.e. the spatial patterns could be affected by a single, or a few highly positive or negative values only representative of a small geographical area.

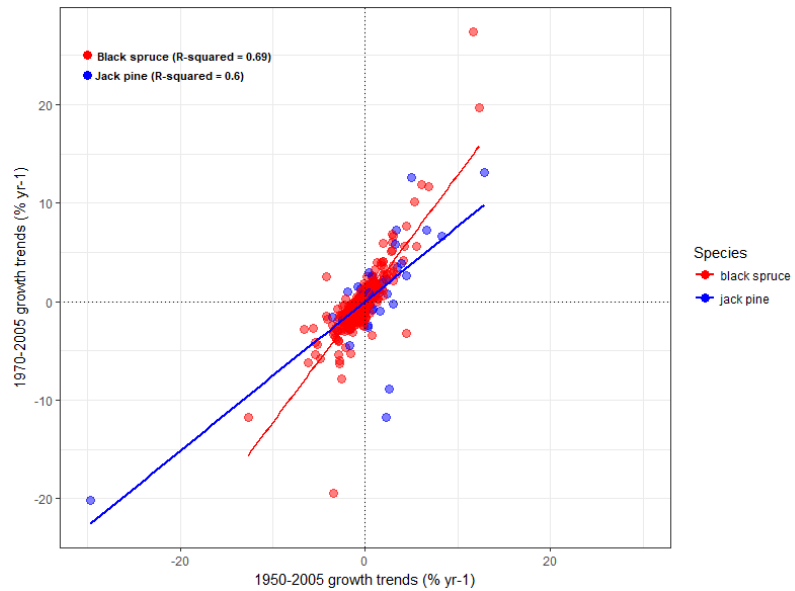


Figure S1.5.1. Comparison of GAMM-based plot-level trends within the two studied periods, *i.e.* 1950-2005 and 1970-2005 (maps in Figure 1.2 (A) in the main document), by species. Red and blue lines are linear regressions for black spruce and jack pine respectively. Dots are plot-level observed values. R-squared values were computed as the square of the Pearson's correlation coefficients.

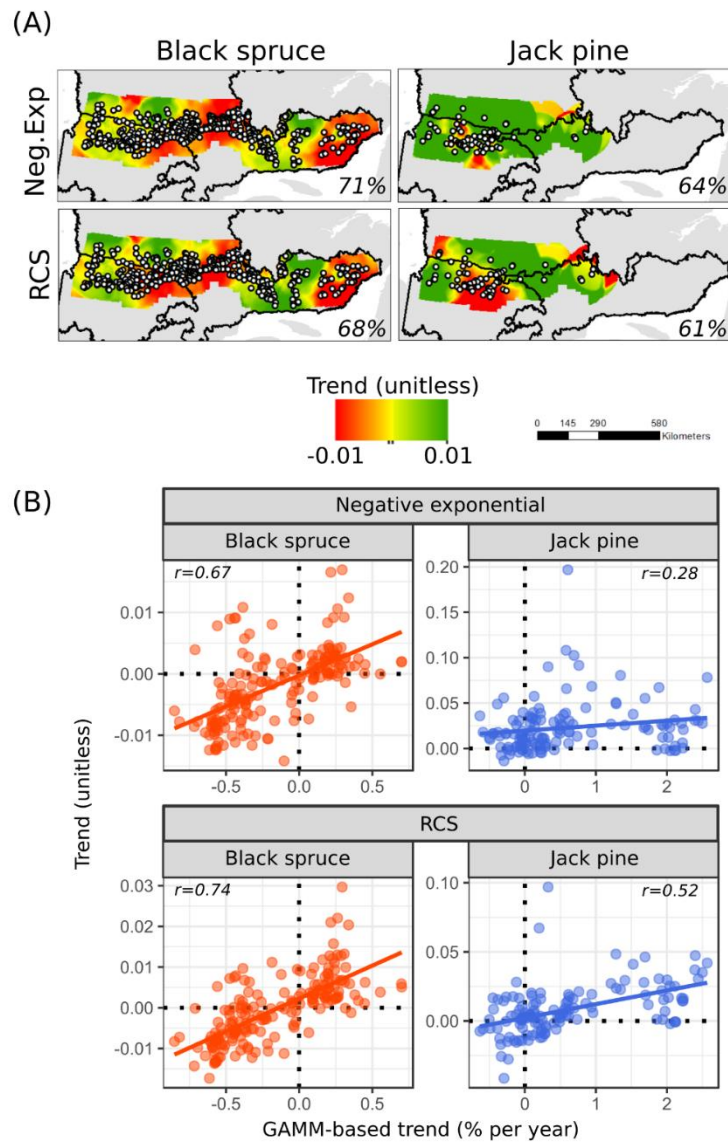


Figure S1.5.2. 1970-2005 trends based on Negative Exponential and RCS detrending approaches. (A) Kriging-interpolated maps of the 1970-2005 growth trends, according to the detrending procedure and species. The percentage of plots for which trends are of the same sign than the GAMM-based trends is shown below maps. (B) Comparisons with maps of 1970-2005 GAMM-based trends shown in Figure 1.2 of the main document. Dots are interpolated values extracted from each raster map using a regular  $0.5^\circ$ -point grid. Spearman's rho coefficients were computed between a given map and the GAMM-based map.

S1.6. Diagnostics of the linear mixed models used to assess plot-level growth-climate relationships (Step 2 in statistical procedure SI2).

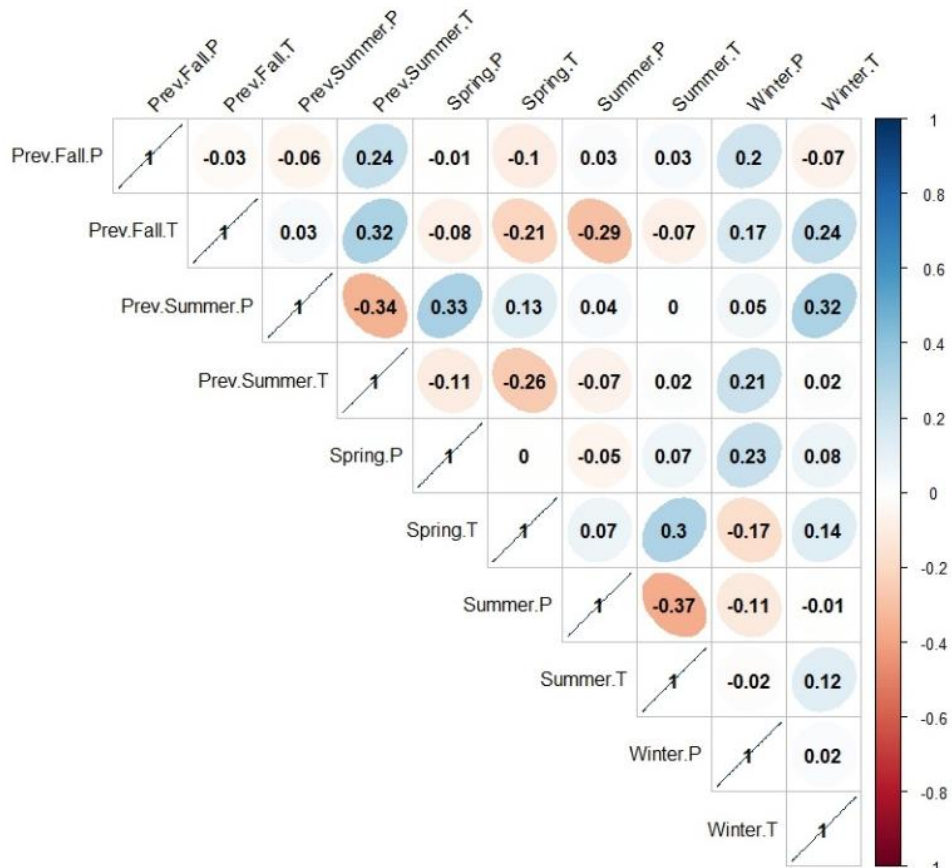


Figure S1.6.1. Correlation matrix (Pearson's correlations) between seasonal climate variables used in plot-level growth-climate analyses. Prev.Fall.P = previous fall precipitation, Prev.Fall.T = previous fall temperature, Prev.Summer.P = previous summer precipitation, Prev.Summer.T = previous summer temperature, Spring.P = spring precipitation, Spring.T = spring temperature, Summer.P = summer precipitation, Summer.T = summer temperature, Winter.P = winter precipitation, Winter.T = winter temperature.

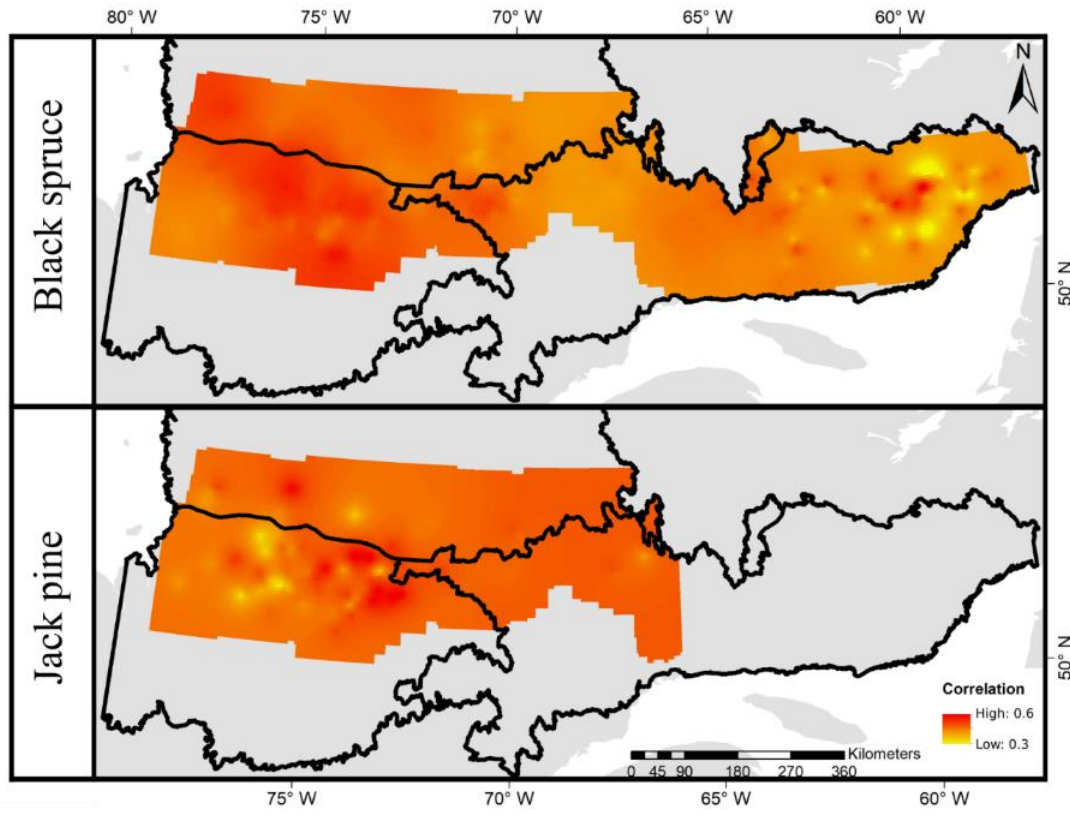


Figure S1.6.2. Kriging-interpolated Pearson's correlation coefficients between residuals from the GAMM model and predicted residuals from the climate models for the 1970-2005 period by species.

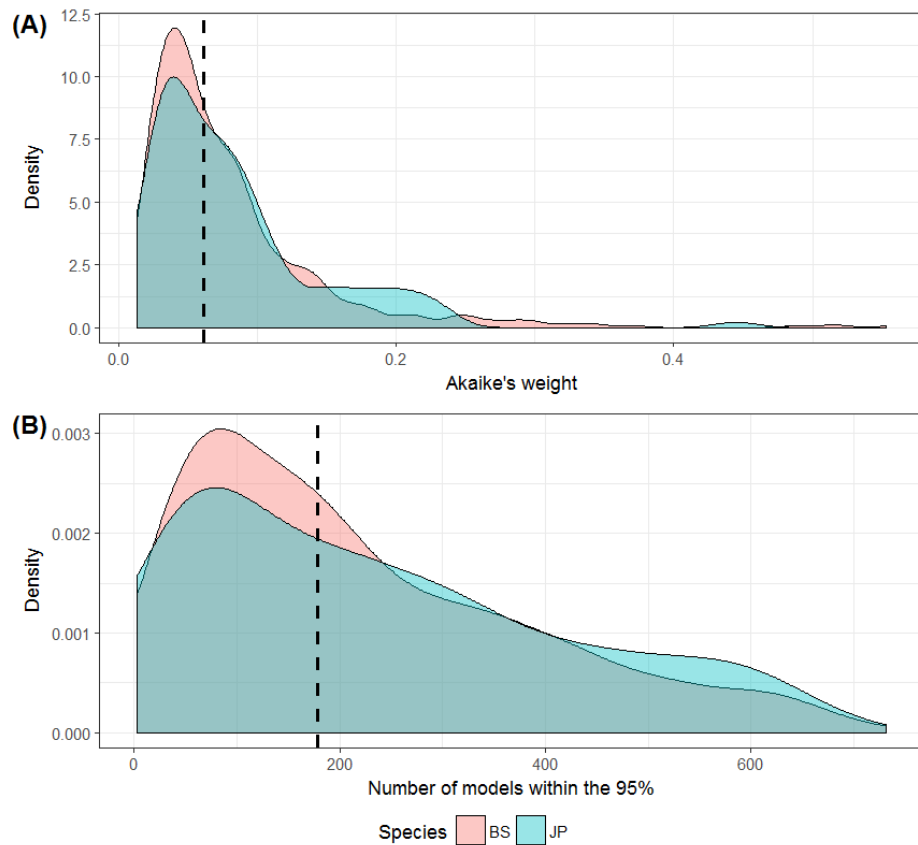


Figure S1.6.3. Density plots of (A) the Akaike's weights of the best model (i.e. model with the lowest AICc value) and (B) the number of models whose Akaike's weight fall within the 95% range (i.e. the set of best approximating models), by plot and species. Black dashed lines are median values.

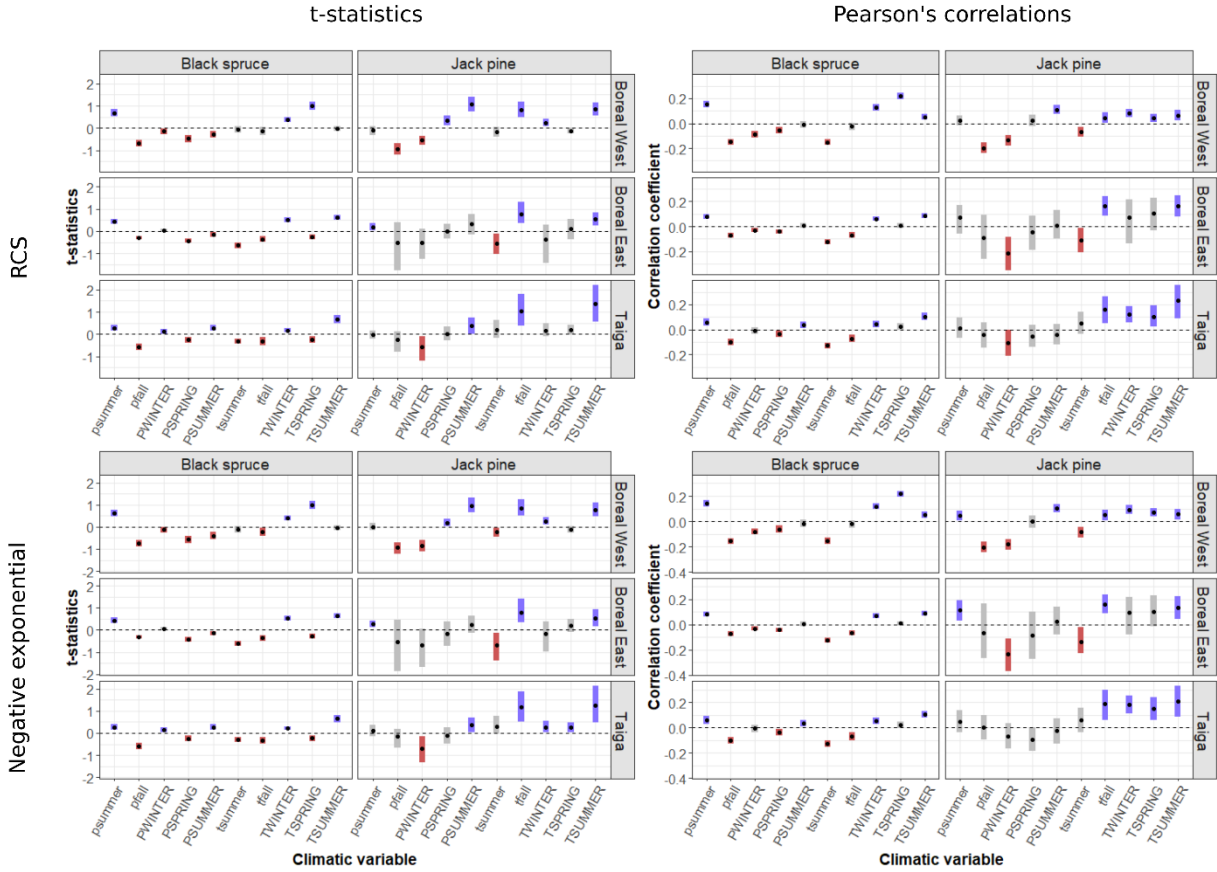


Figure S1.7. Sensitivity analysis for the growth-climate relationships. To assess the reliability of growth-climate analyses, we conducted additional analyses using prewitheened residuals from the two other detrending procedures described in S5 (RCS and Negative Exponential). We reported both mean t-statistics and bootstrapped 95% CI from linear mixed models (same statistical procedure as used for Figure 1.4 in the main text) and mean Pearson's correlation coefficients and bootstrapped 95% CI computed between each of the climatic variable and the median residual chronology by plot.

S1.8. Assessing the relationship between trees' sensitivity to climate and ecological factors

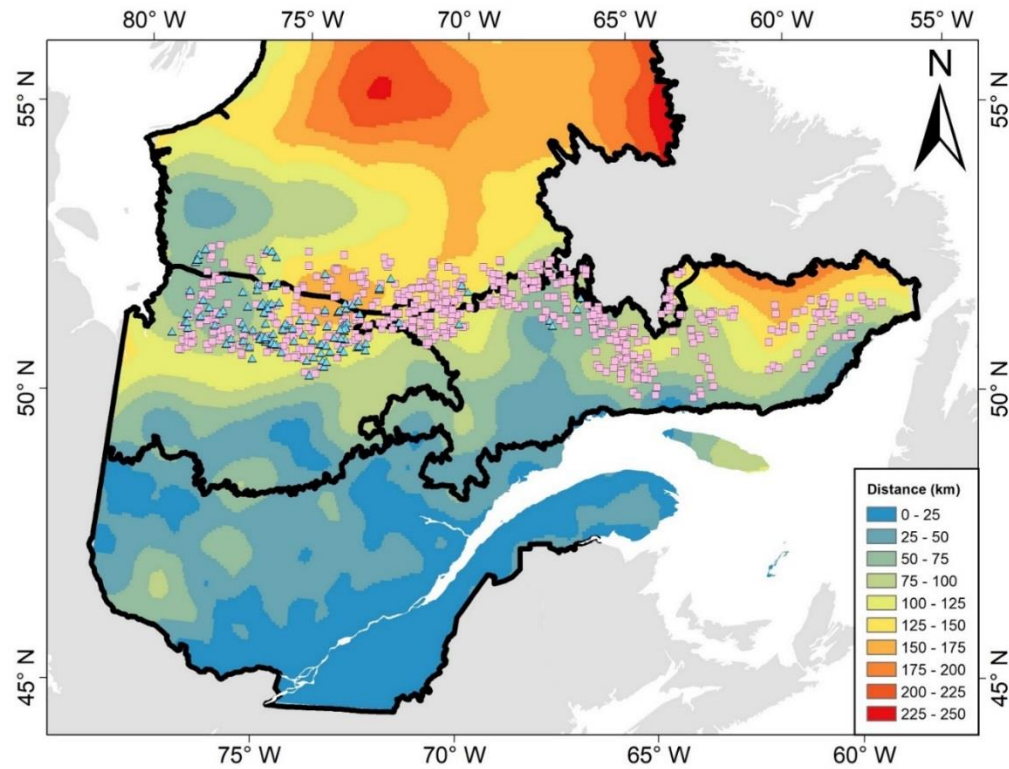


Figure S1.8.1. Kriging interpolated (universal Bayesian kriging) average distance to the four nearest weather stations.

Distances, in kilometers, were computed using the “Near” tool in AcMap 10.4.1. Weather stations taken into account are those from the network implemented in the BioSIM software version 10. More stations were implemented in the newest version (v.11). Sample plots (blue triangles: jack pine plots, pink squares: black spruce plots) are also shown. The network of weather stations is quite scarce within our sampling area, with a maximum average value of 153 km between inventory plots and the four nearest weather stations (see also Ols (2016)). Furthermore, weather stations are

usually located in open lowland areas, and temperature or precipitation data is potentially missing over an extended period. Therefore, the accuracy of available climate data to match the climate conditions of our sample plots is questionable, particularly for precipitation data, which present high spatial variability (Ols *et al.*, 2017 ; Pederson *et al.*, 2013). Poorly accurate weather data could introduce bias in our capacity to detect growth-climate relationships (Wilson *et al.*, 2007). However, it appeared there was no impact of the distance to the nearest weather station, nor of the elevation gradient, on the predictive capacity of climate models (correlation between Pearson coefficients (displayed in 5.2) and elevation = -0.06 and 0.18 for black spruce and jack pine plots, respectively; correlation between Pearson coefficients and average distance to the four nearest stations = 0.05 and 0.173 for black spruce and jack pine plots, respectively).

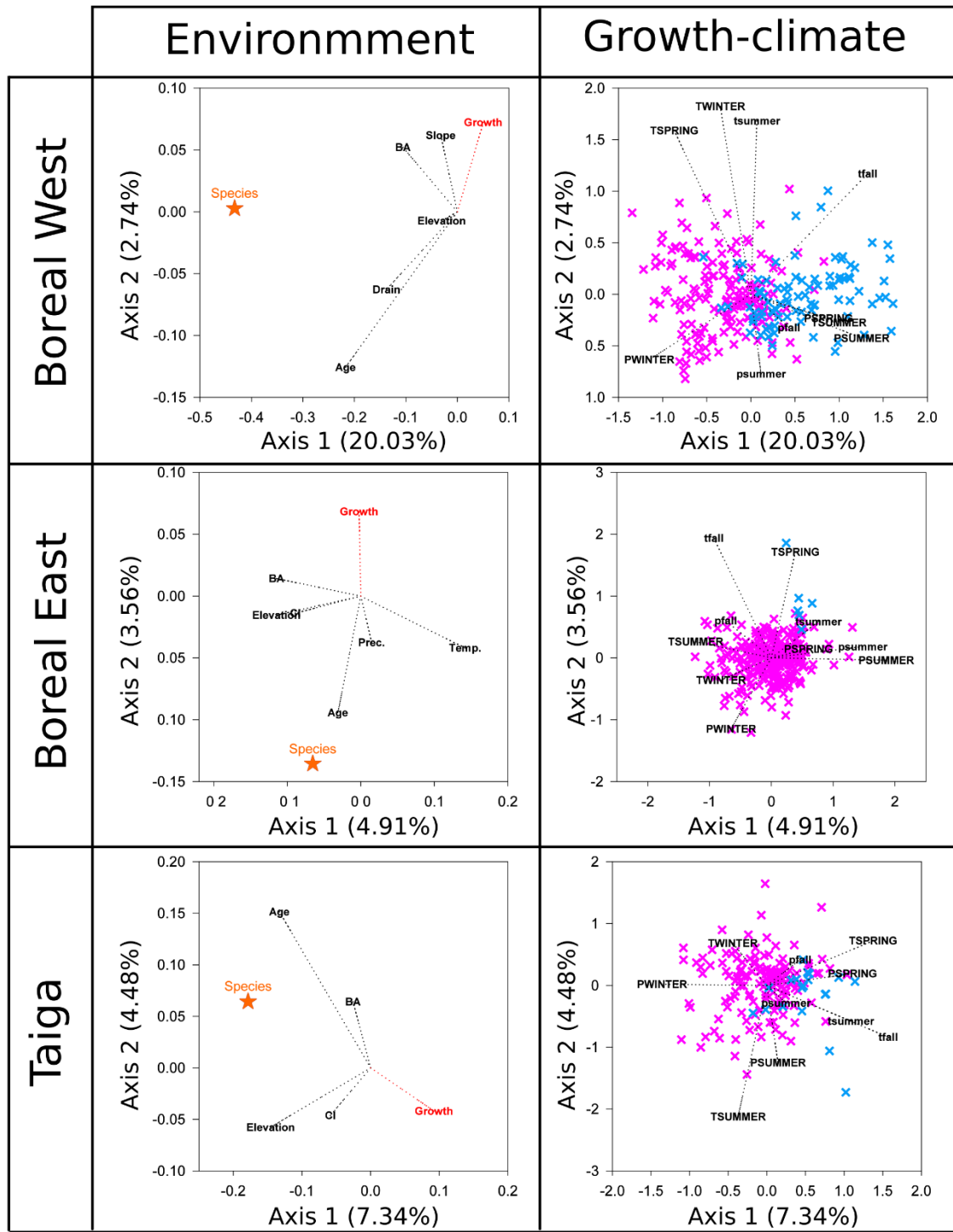


Figure S1.8.2. Ordination plots by bioclimatic domain, based on a RDA method. “Growth-Climate” plots are biplots of species (i.e., t-statistics for each of the 10 studied climatic variables) and samples (i.e., sampled stands) projected onto the ordination axes, summarizing the differences in trees’ response to climate, after removing the effects of the distance to the nearest weather station and accounting for spatial correlation (effect of latitude and longitude). Because both tree sensitivity to climate and ecological conditions are highly variable from east to west (see Figure 1.4 and Table 1.1 in the main text), factors might affect growth-climate relationships depending on the location of the plot (Wu *et al.*, 2018). If averaged over the whole gradient, the effect of these ecological factors could cancel each other out, so one RDA was conducted per bioclimatic domain as a tradeoff between data aggregation and ecological relevance, as recommended by Ols *et al.* (2018b). Lowercase letters are for climatic variables of the previous growing season, capital letters are for climatic variables of the current growing season. Pink and blue crosses represent black spruce and jack pine stands, respectively. “Environment” plots summarize the effect of environmental gradients on growth-climate relationships. “Growth” represents the projection of long-term growth trends onto the ordination axes. Also shown are the scores (percentage of variance explained) for each canonical axis. Note that numeric environmental variables were transformed using the *TransformTukey* function of the R-package *RCompanion* and standardized prior to analyses. “Species” is a dummy variable showing the difference between jack pine (the reference level) and black spruce samples.

Table S1.8.1. Sets of predictor variables used for variation partitioning. In each bioclimatic domain, only variables selected by the RDA (i.e. accounting for a significant proportion of the variability in the species matrix at alpha = 0.05) were kept for the variance partition analysis. See Figure 1.6 in the main text for the list of selected variables by bioclimatic domain.

<b>Group</b>	<b>Predictor variables</b>
<b>Stand maturity</b>	Stand age
<b>Competition</b>	Competition index (CI), Basal area (BA)
<b>Altitudinal gradient</b>	Elevation
<b>Soil</b>	% Clay, % Sand, % Silt, OLT, Slope, Drainage
<b>Regional climate</b>	1970-2005 temperature and precipitation normals
<b>Species identity</b>	Species (Jack pine = reference level « 0 », Black spruce = « 1 »)

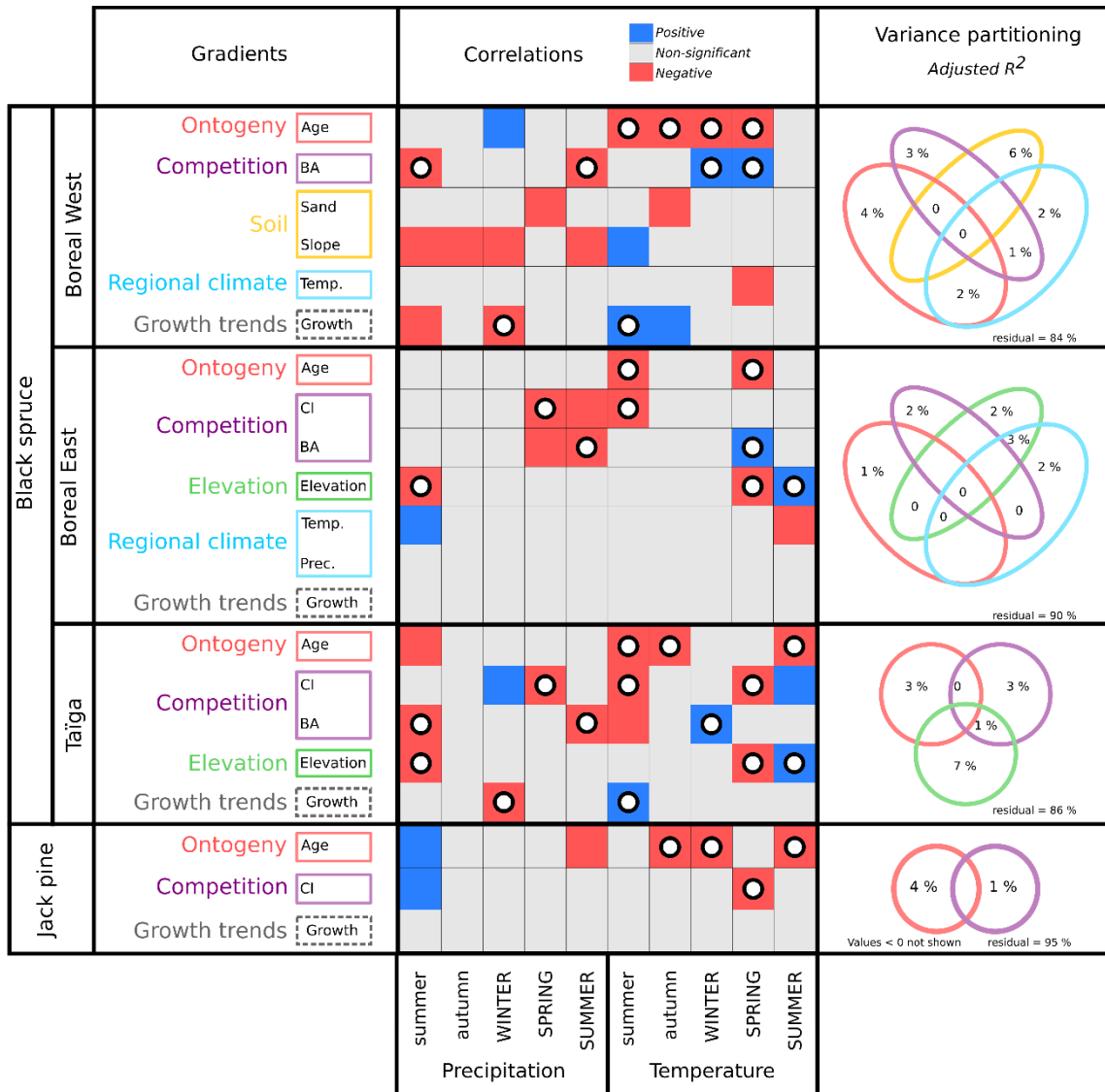


Figure S1.8.3. Same as Figure 1.6 in the main text, but with a separate analysis conducted for jack pine sample plots. One variance partitioning was conducted for all jack pine sample plots without separating them by bioclimatic domain because of the very low number of jack pine plots in the Boreal East and Taiga. For black spruce plots, one analysis was conducted by bioclimatic domain. For the statistical procedure and figure legend, please refer to the method section and caption of Figure 1.6 in the main document.

Table S1.9. Average, median, minimum, maximum and standard deviation values of black spruce and jack pine growth trends by bioclimatic domain, for the 1950-2005 and 1970-2005 periods

		1950-2005					1970-2005				
		Mean	Median	Min	Max	Sd	Mean	Median	Min	Max	Sd
Boreal West	<b>Black spruce</b>	-0.20	-0.22	-5.64	5.35	1.30	0.02	-0.24	-4.62	10.18	1.76
	<b>Jack pine</b>	0.07	0.01	-29.63	12.86	3.62	0.14	0.10	-20.14	13.15	3.32
Boreal East	<b>Black spruce</b>	-0.54	-0.44	-6.63	11.66	1.46	-0.27	-0.20	-19.48	27.38	2.50
	<b>Jack pine</b>	0.08	0.04	-0.64	0.73	0.53	0.49	0.52	-0.95	2.49	1.17
Taiga	<b>Black spruce</b>	-0.16	-0.27	-12.66	12.36	2.07	-0.04	-0.19	-11.71	19.68	2.92
	<b>Jack pine</b>	0.99	0.19	-2.50	8.24	2.41	0.50	0.38	-11.74	7.22	3.78
All	<b>Black spruce</b>	-0.35	-0.3	-12.66	12.36	1.61	-0.14	-0.2	-19.48	27.38	2.44
	<b>Jack pine</b>	0.21	0.04	-29.63	12.86	3.37	0.21	0.11	-20.14	13.15	3.31

### S1.10. Sensitivity analysis for the relationships between trees' sensitivity to climate and ecological factors.

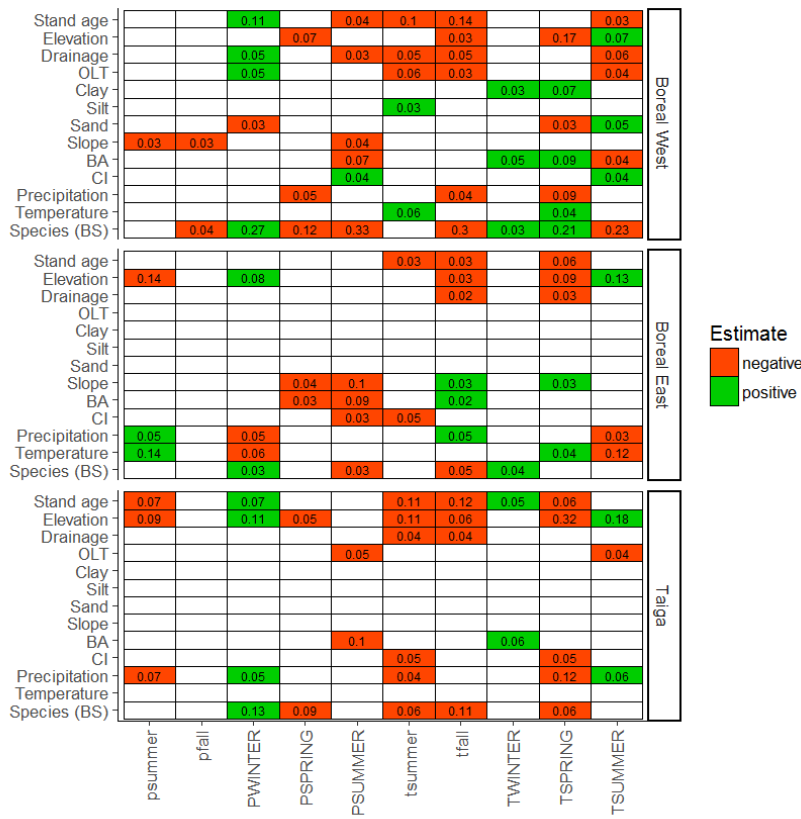


Figure S1.10.1. Regression slopes between ecological factors and t-statistics obtained from the LMM using GAMM-detrended chronologies. Red and green shadings highlight significant (significance based on p-value,  $\alpha = 0.01$ ) negative and positive regression slopes (i.e. sign of the estimated effect of the ecological factor on the trees response to climate), respectively. Numbers inside pixels are r-squared coefficients. One linear model was fitted by bioclimatic domain, ecological factor and climatic variable (390 separate regressions were conducted). Note that, unlike for RDA analyses, each of the r-squared values reports the percentage of variance explained by a single ecological factor. Additionally, the spatial correlation was not accounted for in the regression models (the simplest r-function *lm* was used, no correlation term allowed).

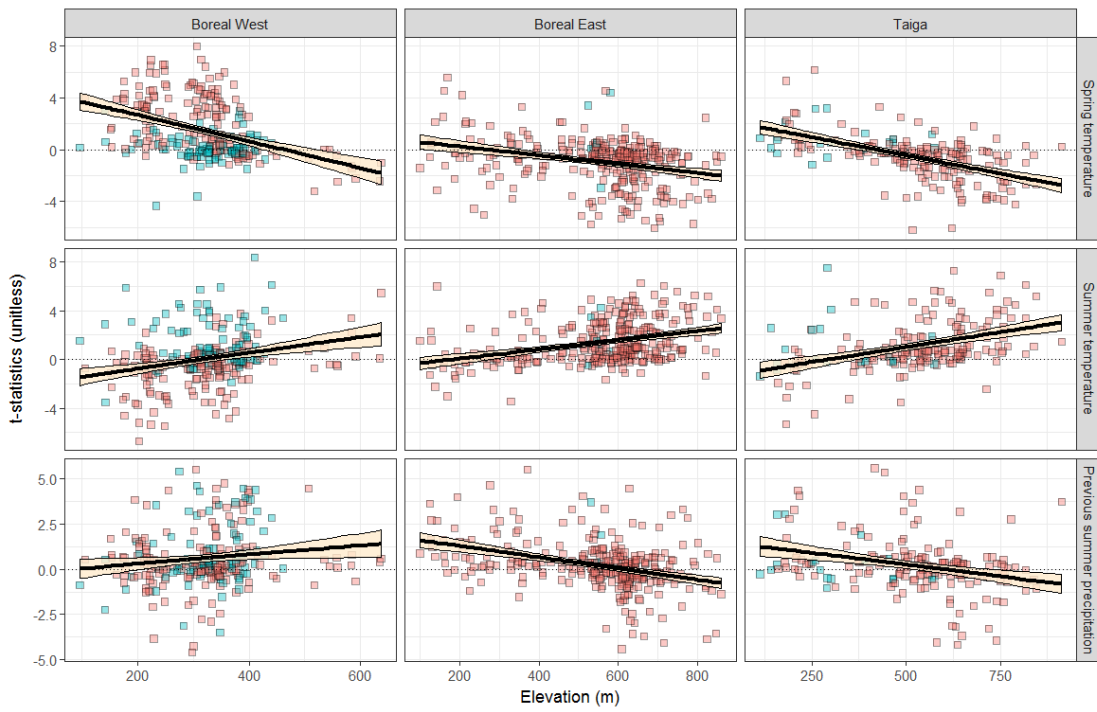


Figure S1.10.2. Sensitivity to spring and summer temperature, and to previous summer precipitation within the elevation gradient. Black lines and cream shadings are predicted values and 95% confidence intervals from linear regressions described in S12.1. Red and Blue dots are “observed” values for back spruce and jack pine, respectively.

### S1.11. Assessing the relationship between long-term (1970-2005) growth trends and ecological gradients

The impact of environmental and demographic gradients on long-term growth trajectories was determined using linear mixed models, using the 1970-2005 growth trend values as response variables. Environmental and demographic parameters as well as species type (black spruce vs jack pine) were added as explanatory variables, and ecological district identity was included as random effect. All continuous variables were scaled and centered. Outliers were removed (function *romr.fnc*, package *LMERConvenienceFunctions* (Tremblay et Ransijn, 2015), percentage of removed values below 5%) to improve the normality of the residuals. From a global model including all ecological variables, we built a set of models trying to best represent the different combinations of variables without exaggeratedly increasing the number of models. We tested the linear relationships between trends and environmental variables, excepted for slope, for which we also tested the significance of a quadratic term (squared values). If there was a high (i.e.,  $r \geq |0.40|$ ) correlation between two explanatory variables, they were added into separate models. First-order interactions were tested between all variables and were retained when they were significant (backward selection procedure;  $\alpha = 0.05$ ). If any interaction was significant for a model, an additional model without interaction terms was built. A multi-model selection based on AICc scores was conducted (function *aictab*, package *AICcmodavg* (Mazerolle, 2017)). The “best” candidate models among the entire set of models were those with delta AICc  $\leq 4$ . To quantify the effect of each ecological variable, estimates, unconditional 95% confidence intervals and standard errors were computed from a subset of models that contained the focal variable without interaction terms (function *modavg*, package *AICcmodavg* (Mazerolle, 2017)). A variable was considered to explain a significant part of the variance in growth trends when the 95% confidence intervals excluded zero. For variables with a significant contribution, a multi-model inference was conducted (function *modavgPred*, package *AICcmodavg* (Mazerolle, 2017)) to compute predicted growth trends values. Since our plot network is located

within a broad geographical area, a huge diversity of environmental conditions is represented, which could introduce excessive noise. We decided to conduct one analysis per bioclimatic zone ( $n = 3$  analyses) to increase our capacity to detect smaller-scale relationships. For the Boreal East bioclimatic domain, only black spruce data was considered, because of the very low number of jack pine stands ( $n = 6$  plots).

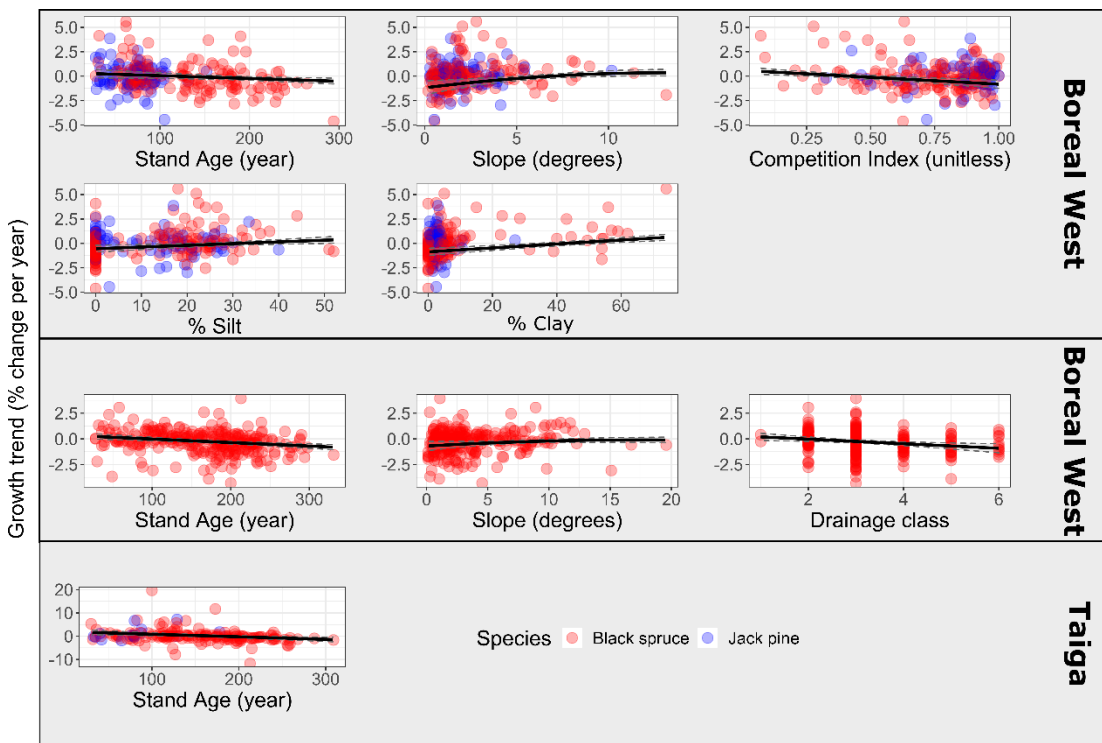


Figure S1.11.1. Predicted values of growth trends depending on significant contributing factors, by bioclimatic domain. Pink dots represent observed values for black spruce, and blue dots represent observed values for jack pine. Note that only significant relationships were displayed.

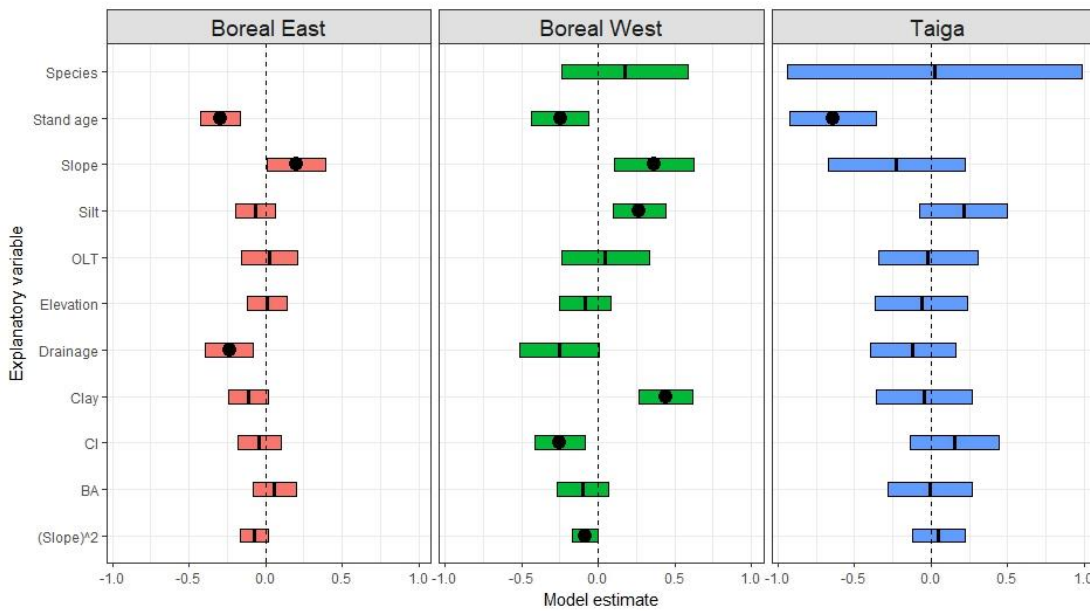


Figure S1.11.2. Model-averaged estimates of explanatory variables. Model averaging was done among all models containing the variable of interest (function *modavg*). Black dots denote a significant effect of the variable on growth trends (95% confidence intervals exclude zero).

Table S1.11.1. Set of models for each bioclimatic domain. Also reported are the AICc score, delta AICc, AICc weight and cumulative weight. Best candidate models are those with AICc values below 4.

Models	AICc	Delta_AICc	AICcWt	Cum.Wt
Boreal West				
Global Interactions	807.41	0	0.999663	0.999663
Global	824.29	16.88	0.000216	0.99988
BA + CI + Species + % Clay Interactions	825.47	18.06	0.00012	0.999999
BA + CI + Species + % Clay	837.01	29.60	3.73E-07	1
Age + BA + CI + Species Interactions	839.52	32.11	1.07E-07	1
Drainage + % Clay + OLT	840.50	33.09	6.51E-08	1
BA + CI + % Silt + Drainage Interactions	843.09	35.68	1.79E-08	1
Age + Elevation + Slope + (Slope) <sup>2</sup>	844.68	37.26	8.09E-09	1
Elevation + Drainage + % Silt + Species Interactions	848.65	41.24	1.11E-09	1
Age + BA + CI + Species	848.73	41.32	1.07E-09	1
Elevation + OLT + Slope + (Slope) <sup>2</sup>	850.66	43.25	4.06E-10	1
OLT + Silt + Species Interactions	850.84	43.43	3.71E-10	1
Slope + (Slope) <sup>2</sup> + % Silt + Drainage	853.31	45.90	1.08E-10	1
BA + CI + % Silt + Drainage	854.26	46.85	6.72E-11	1
Elevation + Drainage + % Silt + Species	856.42	49.01	2.28E-11	1

OLT + Silt + Species	857.10	49.69	1.62E-11	1
Boreal East				
Age + BA + CI Interactions	828.64	0	0.450513	0.450513
Age + Elevation + Slope + (Slope) <sup>2</sup>	830.09	1.45	0.217695	0.668208
Global Interactions	830.67	2.04	0.162834	0.831042
Age + BA + CI	831.58	2.94	0.10334	0.934382
Global	833.36	4.72	0.042559	0.976941
Slope + (Slope) <sup>2</sup> + % Silt + Drainage Interactions	836.10	7.46	0.010796	0.987738
Drainage + % Clay + OLT	837.41	8.77	0.005605	0.993343
Slope + (Slope) <sup>2</sup> + % Silt + Drainage	838.41	9.78	0.003396	0.996739
Elevation + Drainage + % Silt	839.21	10.57	0.00228	0.999019
BA + CI + % Silt + Drainage	841.26	12.63	0.000816	0.999835
Elevation + OLT + Slope + (Slope) <sup>2</sup>	845.85	17.21	8.25E-05	0.999917
OLT + % Silt	846.11	17.48	7.23E-05	0.999989
BA + CI + % Clay	849.94	21.31	1.06E-05	1
Taiga				
Global Interactions	598.96	0	0.964811	0.964811
Age + Elevation + Slope + (Slope) <sup>2</sup> Interactions	606.12	7.16	0.026899	0.99171
Age + Elevation + Slope + (Slope) <sup>2</sup>	609.74	10.78	0.004399	0.996109

Age + BA + CI + Species	610.06	11.10	0.003755	0.999863
Global	617.14	18.18	0.000109	0.999972
BA + CI + % Silt + Drainage Interactions	621.10	22.14	1.50E-05	0.999987
Elevation + OLT + Slope + (Slope) <sup>2</sup> Interactions	623.66	24.71	4.16E-06	0.999991
Elevation + Drainage + % Silt + Species	624.24	25.28	3.13E-06	0.999994
OLT + % Silt + Species	625.31	26.35	1.83E-06	0.999996
BA + CI + Species + % Clay Interactions	625.40	26.44	1.75E-06	0.999998
Elevation + OLT + Slope + (Slope) <sup>2</sup>	627.18	28.22	7.18E-07	0.999999
BA + CI + Species + % Clay	627.59	28.63	5.85E-07	0.999999
BA + CI + % Silt + Drainage	627.87	28.91	5.09E-07	1
Drainage + % Clay + OLT	629.55	30.60	2.19E-07	1
Slope + (Slope) <sup>2</sup> + % Silt + Drainage	630.13	31.17	1.64E-07	1

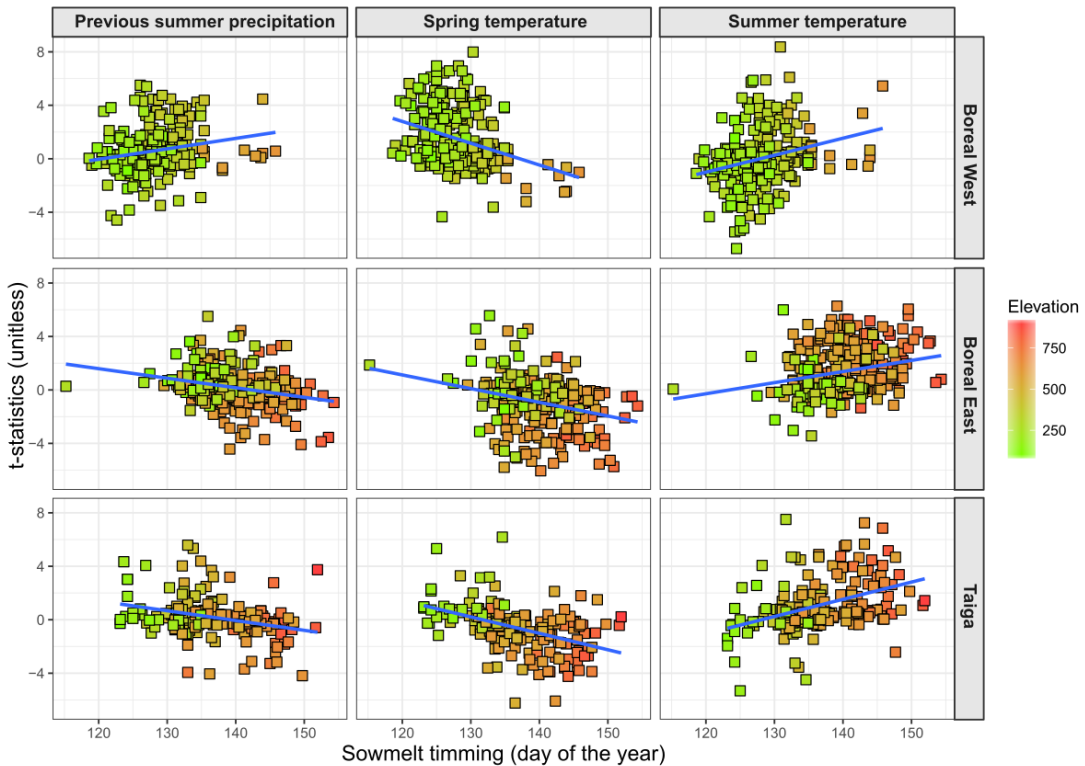


Figure S1.12 Relationship between the day of snowmelt (averaged over the 2001–2015 period, O’Leary et al. (2017)) and the trees’ sensitivity to previous summer precipitation (first column), spring temperature (second column) and summer temperature (third column), by bioclimatic domain. The elevation gradient is shown as a color gradient. Blue lines denote the linear regression between the two variables.

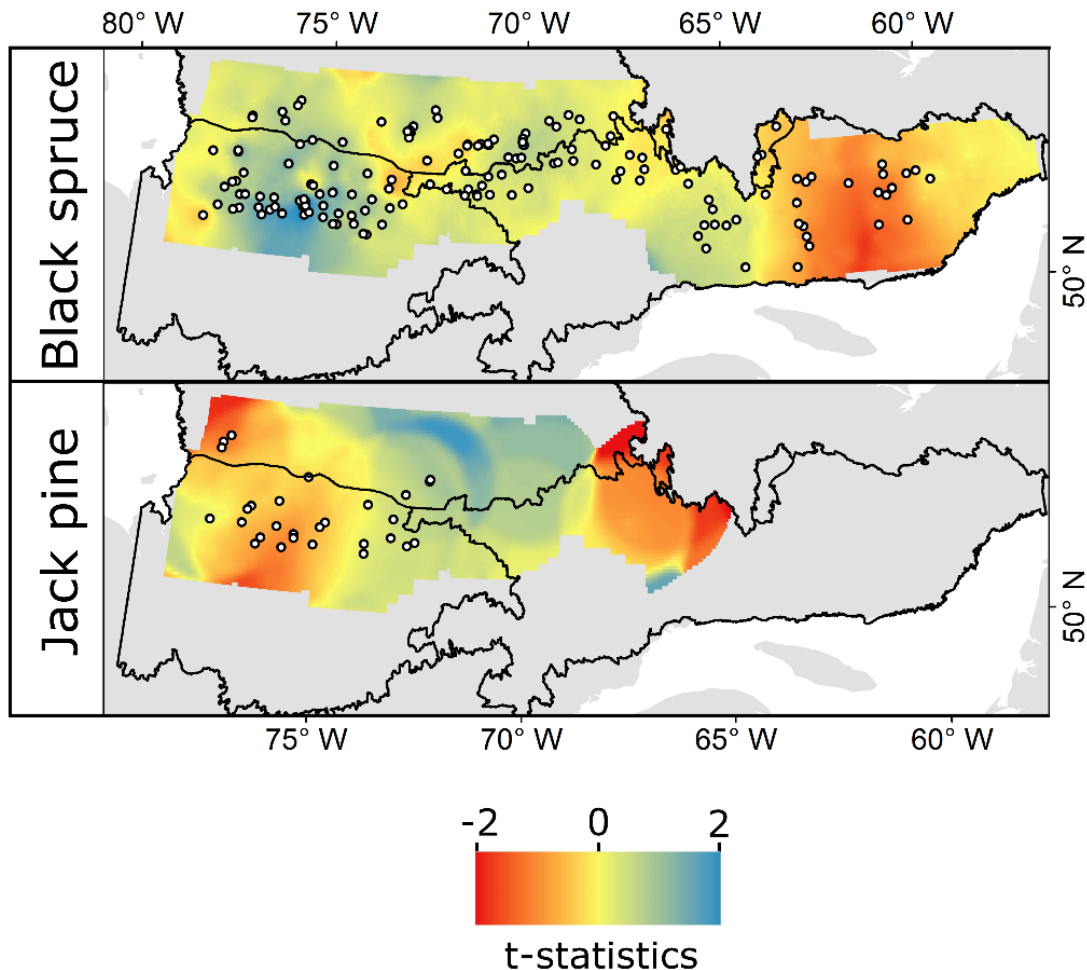


Figure S1.13. Kriging-interpolated response (t-statistics) of black spruce and jack pine to the annual area burned (summed over the whole area), as a proxy for drought. We used fire data from the SOPFEU fire database. The statistical method used to compute t-statistics was the same as for the determination of the trees' sensitivity to climate, except that the burned area was the only response variable of the plot-scaled mixed-models and, consequently, no model selection was applied. For details about the statistical methods, please refer to the main text.

## ANNEXE B

### MATÉRIEL SUPPLÉMENTAIRE DU CHAPITRE II

#### Supplement S2.1. Supplementary method for the detrending of raw BAIs

The following text was originally published in Marchand et al. (2019) as part of the materials and methods section. It is provided here as a means to ease readers' understanding of the way raw BAIs were detrended.

Ring-width measurements of the four radii were averaged (arithmetic mean statistics, see Supporting Information S3 for descriptive statistics of the raw series), and the mean ring-width series were converted into basal area increments ( $BAI_t = \pi R_t^2 - \pi R_{t-1}^2$ ) using the function *bai.out* in the R-package *dplr* (Bunn, 2008). We assumed the cross-sections were perfectly circular in shape, and used these as a proxy for secondary growth so to provide an accurate quantification of wood production with ever-increasing tree diameter (Biondi & Qeadan, 2008). Rings that were formed during the first 10 years were then eliminated, given that they usually exhibit an atypical response to environmental drivers compared with more mature rings (Loader, McCarroll, Gagen, Robertson, & Jalkanen, 2007) (See Supporting Information S2.4 for information about the BAI chronologies and diagnostic plots of the GAMM models). Next, BAI were

detrended using Generalised Additive Mixed Models (GAMM) to remove the remaining ontogeny-induced (i.e., tree age and size) trends. One model was constructed for each species and ecological district (See Supporting Information S4 for information about the BAI chronologies and diagnostic plots of the GAMM models). Organic layer thickness (OLT) was added as a fixed term to account for the spatially-heterogeneous and mostly time-independent effect of site quality on tree growth (Lavoie, Harper, Paré, & Bergeron, 2007). BAI values were log-transformed to improve the normality of their distributions. The structure of the GAMM model is as follows:

$$\log(BAI_{ijklt}) = \log(BA_{ijklt}) + OLT_{kl} + s(AgeC_{ijkt}) + (TreeID_{ijkl}) + corAR1_{ijkl}$$

where i represents the individual tree, j represents the species, k represents the plot, l represents the ecological district, and t represents the year. BAI is the basal area increment of tree i in specific year t, BA is the basal area of tree i at specific year t (computed as the sum of BAI of previous years), OLT is the organic layer thickness of plot k, and AgeC is the cambial age (1-m height ring count) of tree i at year t. An autoregressive term, AR1 (autoregressive order p = 1, moving average order q = 0), was added to account for temporal autocorrelation. We tested the significance of a nested random effect (tree nested in plot) by conducting ANOVAs and likelihood ratio tests. Because it did not improve the model's fit and led to the same results (data not shown), we discarded the random term of the plot from the final model and kept only the random effect of the tree (TreeID).

The original, published article from which this text was extracted can be found here:

Marchand, W, Girardin, MP, Hartmann, H, Gauthier, S, Bergeron, Y. Taxonomy, together with ontogeny and growing conditions, drives needleleaf species' sensitivity to climate in boreal North America. *Glob Change Biol.* 2019; 25: 2793– 2809. <https://doi.org/10.1111/gcb.14665>

Supplement S2.2. Computation of the site index

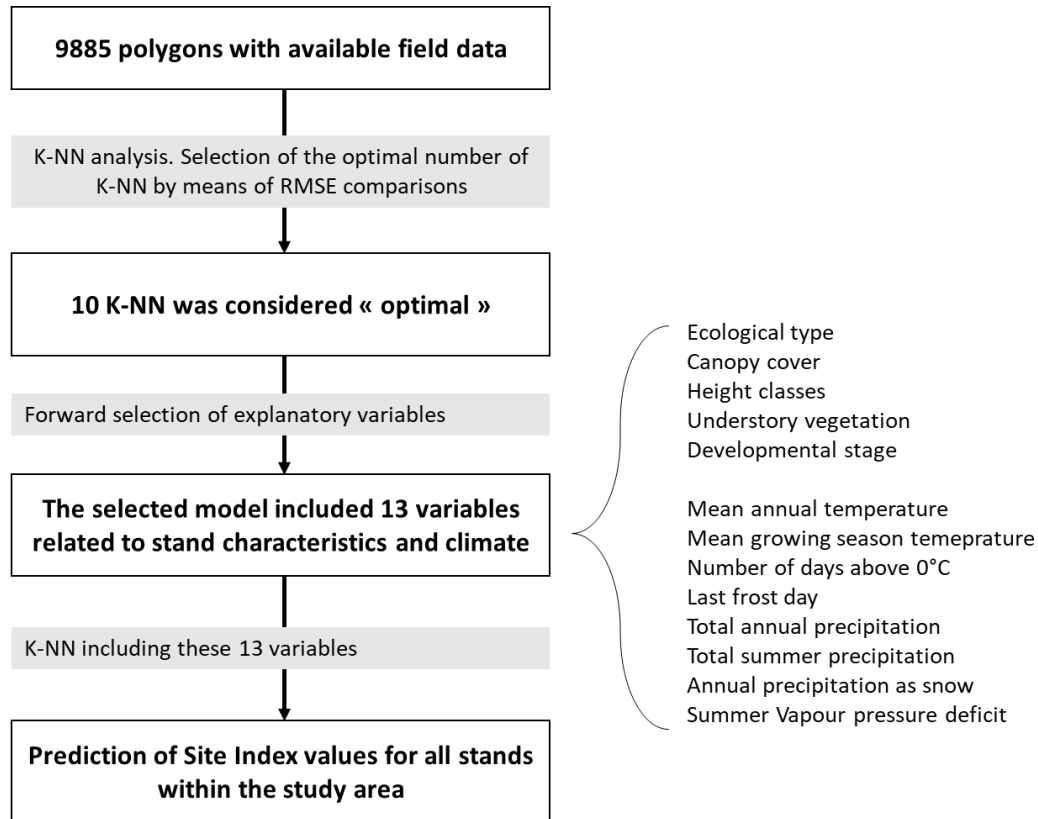


Figure S2.2.1. diagram explaining the extrapolation of SI values to the whole area. Readers are referred to Gauthier et al. (2015) for the full methods.

### Supplement S2.3. results based on iWUE instead of $\Delta^{13}\text{C}$

iWUE was inferred from  $\Delta^{13}\text{C}$  as in Marchand et al. (2020). To ensure readers understanding, the part of the text that refers to the computation of iWUE, including equations, is reported here:

According to Farquhar *et al.* (1982b), the relationship between atmosphere-to-plant isotope discrimination and the ratio of intercellular-to-atmospheric CO<sub>2</sub> concentration (C<sub>i</sub>/C<sub>a</sub>) is as follows:

$$\underline{\text{Eq.4}} \quad \Delta^{13}\text{C}_{ring} = a + (b - a) \times \frac{C_i}{C_a} - f \frac{\Gamma^*}{C_a}$$

where a is the fractionation rate of <sup>13</sup>CO<sub>2</sub> relative to <sup>12</sup>CO<sub>2</sub> during stomatal diffusion ( $\approx 4.4\text{‰}$ ), and b the fractionation rate during assimilation ( $\approx 27\text{‰}$ ). f is the fractionation associated with photorespiration ( $\approx 12\text{‰}$ ) and  $\Gamma^*$  is the CO<sub>2</sub> compensation point in the absence of mitochondrial respiration (Bernacchi *et al.*, 2001).  $\Gamma^*$  was computed using the *rpmmodel* R package (Stocker *et al.*, 2019) using the average summer maximum temperature, which is representative of the temperature of the photosynthetically-active period. Since no climate data were available before 1866 in our study area, 1783-1865  $\Gamma^*$  values were estimated using the average summer maximum temperature of the 1866-1900 period. The fractionation term for photorespiration ( $-f \frac{\Gamma^*}{C_a}$ ) was added as recommended by several previous studies (Keeling *et al.*, 2017 ; Lavergne *et al.*, 2019, 2020 ; Schubert et Jahren, 2018).

Intrinsic water use efficiency (iWUE<sub>ring</sub>) is defined as the ratio of assimilation rate (A) to stomatal conductance (g<sub>s</sub>). A can be calculated from C<sub>i</sub> / C<sub>a</sub> using Fick's law:

$$\underline{\text{Eq.5}} \quad A = \frac{g_s \times (C_a - C_i)}{1.6}$$

where 1.6 is the ratio of diffusivity of water vapor and CO<sub>2</sub> in the atmosphere.

Using Eq.4-5, iWUE<sub>ring</sub> can be derived as:

$$\text{Eq.6} \quad iWUE_{ring} = \frac{A}{g_s} = \frac{(C_a - C_i)}{1.6} = \frac{c_a \left( b - \left[ \frac{(\delta^{13}C_a - \delta^{13}C_{ring})}{1 + \frac{\delta^{13}C_{ring}}{1000}} \right] - f \frac{r^*}{c_a} \right)}{1.6 \times (b - a)}$$

with C<sub>a</sub> the atmospheric CO<sub>2</sub> concentration, obtained from Frank *et al.* (2010).

The original, published article from which this text was extracted can be found here:

Marchand, W, Girardin, MP, Hartmann, H, et al. Strong overestimation of water-use efficiency responses to rising CO<sub>2</sub> in tree-ring studies. *Glob Change Biol.* 2020; 26: 4538– 4558. <https://doi.org/10.1111/gcb.15166>

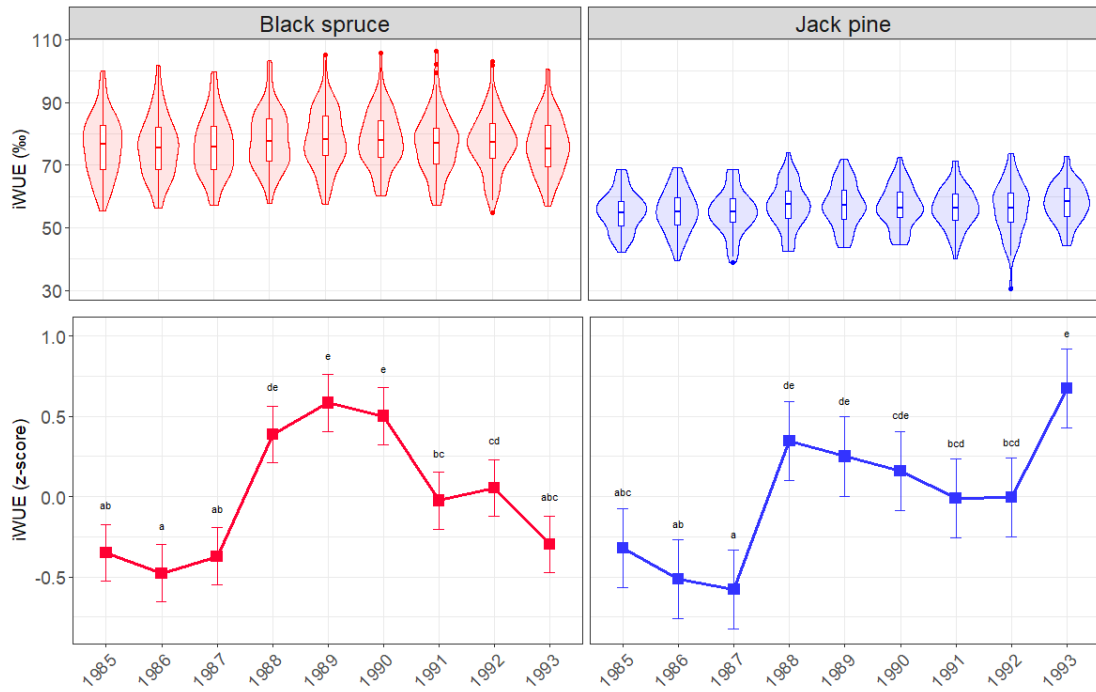


Figure S2.3.1. raw values and least-square means based on z-scored values of iWUE data, by species and year. Readers are referred to the main document for methods and full figure captions.

Table S2.3.2. results from linear mixed models linking iWUE to climate. One model was fitted by species. Significant effects are highlighted with gray shadings, with significance levels as follows: “ \*\*\* ” p-value  $\leq 0.001$ ; “ \*\* ” p-values  $\leq 0.01$ ; “ \* ” p-value  $\leq 0.05$  and “ NS ” indicates non-significant variables. Also shown the marginal and conditional r-squared, i.e. the percentage of variance explained by the fixed part and the fixed plus random part of the model, respectively. Since each value of explanatory variables was mean centered and divided by the corresponding standard-deviation prior to analyses, estimate regression coefficients are on the same scale (and thus directly comparable), except for the intercept.

		Variables	Estimate	Std.Error	t-value	Signif.
Black spruce	Fixed effects	Intercept	77.382	1.244	62.200	***
		CMI	-0.124	0.111	-1.113	NS
		CMI <sub>prev</sub>	0.014	0.119	0.121	NS
		Snow	0.439	0.101	4.358	***
		VPD	0.752	0.247	3.042	**
		VPD <sub>prev</sub>	1.451	0.281	5.163	***
		BA	0.573	1.096	0.523	NS
		TSF	0.403	1.102	0.366	NS
		SI	-0.050	1.160	-0.043	NS
	Random effects (SD)	Plot	5.685			
		Tree in Plot	6.941			
R <sup>2</sup> (Marginal/Conditional)			0.060/0.857			
Jack pine	Fixed effects	Intercept	56.117	1.361	41.221	***
		CMI	0.113	0.147	0.764	NS
		CMI <sub>prev</sub>	0.234	0.187	1.254	NS
		Snow	0.273	0.175	1.561	NS
		VPD	1.047	0.305	3.435	***
		VPD <sub>prev</sub>	0.583	0.344	1.698	NS
		BA	0.410	0.912	0.449	NS
		TSF	1.376	1.766	0.779	NS
		SI	1.572	1.253	1.254	NS
	Random effects (SD)	Plot	2.883			
		Tree in Plot	5.709			
R <sup>2</sup> (Marginal/Conditional)			0.099/0.856			

Supplement S2.4: results based on  $\delta^{18}\text{O}$  data non-corrected for precipitation  $\delta^{18}\text{O}$ 

To approximate the inter-annual variability in precipitation  $\delta^{18}\text{O}$ , we used a published, global equation. However, this procedure could induce additional noise in the data, and does not fully correct for the  $\delta^{18}\text{O}$  of source water, as the later also depends on fractionation occurring as a result of evaporation within the soil layers. Here we present additional analyses based on uncorrected  $\delta^{18}\text{O}$  values. Methods are the same as those indicated in the main document.

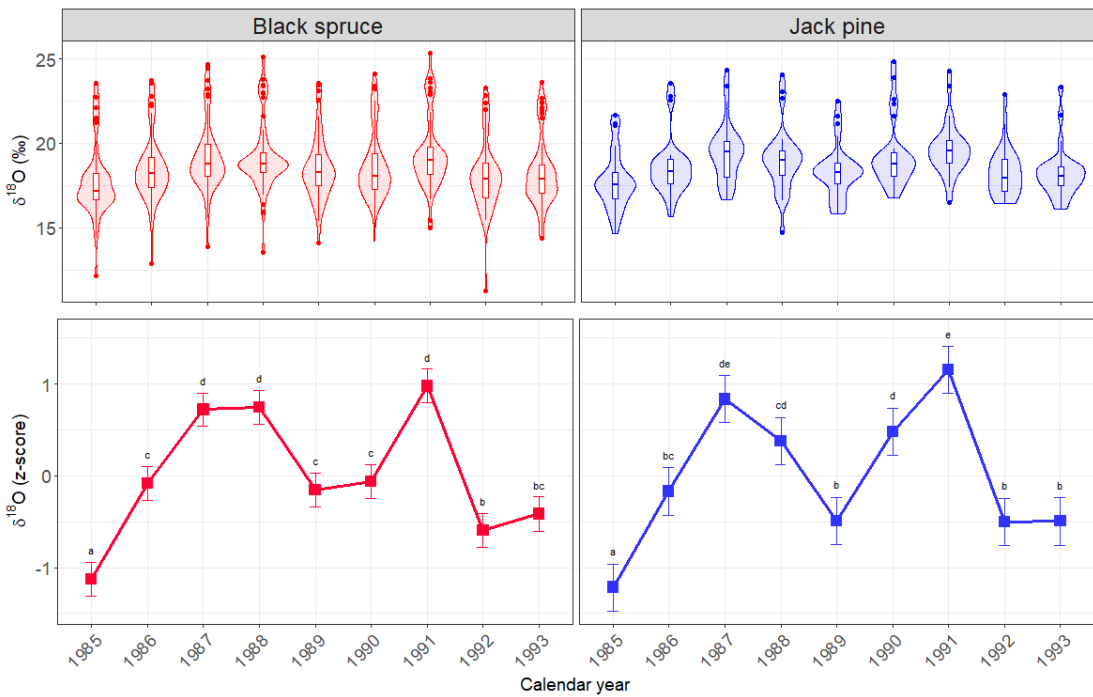


Figure S2.4.1: raw values and least-square means based on z-scored values of  $\delta^{18}\text{O}$ , by species and year. Readers are referred to the main document for methods and full figure captions.

Table S2.4.2: results from linear mixed models linking tree-ring  $\delta^{18}\text{O}$  to climate. One model was fitted by species. Significant effects are highlighted with gray shadings, with significance levels as follows: “ \*\*\* ” p-value  $\leq 0.001$ ; “ \*\* ” p-values  $\leq 0.01$ ; “ \* ” p-value  $\leq 0.05$  and “ NS ” indicates non-significant variables. Also shown the marginal and conditional r-squared, i.e. the percentage of variance explained by the fixed part and the fixed plus random part of the model, respectively. Since each value of explanatory variables was mean centered and divided by the corresponding standard-deviation prior to analyses, estimate regression coefficients are on the same scale (and thus directly comparable), except for the intercept.

		Variables	Estimate	Std.Error	t-value	Signif.
Black spruce	Fixed effects	Intercept	18.849	0.364	51.754	***
		CMI	-0.111	0.041	-2.731	**
		$\text{CMI}_{\text{prev}}$	0.150	0.045	3.360	***
		Snow	-0.020	0.042	-0.472	NS
		VPD	0.352	0.087	4.023	***
		$\text{VPD}_{\text{prev}}$	0.259	0.096	2.688	**
		BA	-0.285	0.279	-1.019	NS
		TSF	-0.499	0.302	-1.651	NS
		SI	0.014	0.351	0.039	NS
	Random effects (SD)		Plot	1.728		
			Tree in Plot	0.993		
$R^2$ (Marginal/Conditional)				0.117/0.855		
Jack pine	Fixed effects	Intercept	18.459	0.405	45.567	***
		CMI	0.102	0.066	1.540	NS
		$\text{CMI}_{\text{prev}}$	0.099	0.081	1.218	NS
		Snow	-0.161	0.077	-2.077	*
		VPD	0.292	0.143	2.048	*
		$\text{VPD}_{\text{prev}}$	0.347	0.169	2.061	*
		BA	-0.451	0.301	-1.498	NS
		TSF	-0.042	0.505	-0.084	NS
		SI	-0.295	0.417	-0.709	NS
	Random effects (SD)	Plot	< 0.001			
		Tree in Plot	1.547			
$R^2$ (Marginal/Conditional)				0.099/0.713		

### Supplement S2.5. PCA on t-values from LMEs

A principal component analysis (PCA) was conducted to ease interpretation of the results from LMMs linking growth,  $\Delta^{13}\text{C}_{\text{ring}}$  and  $\Delta^{18}\text{O}_{\text{ring}}$  to environmental variables (see Table 2.1 in the main document). Here, we considered t-values obtained from these models as input variables (6 variables: GI,  $\Delta^{13}\text{C}_{\text{ring}}$  and  $\Delta^{18}\text{O}_{\text{ring}}$  for each of the two studied tree species). We considered as “samples” (rows of the data matrix) each of the explanatory variables used in LMMs (8 “samples”: VPD, VPD of the previous year, CMI, CMI of the previous year, total annual snowfall, TSF, SI, BA). PCA was fitted using the R function *prcomp*, based on the covariance matrix, since t-values are all unitless (i.e. on a same scale). The biplot demonstrates the covariance between the variables and the principal components. As well, the plot approximates the covariance among the descriptors themselves. Variables (vectors) pointing in the same direction are positively correlated. By contrast, an obtuse angle between variables indicates a negative correlation. Here, the plot shows that environmental variables have an opposite effect on  $\Delta^{18}\text{O}_{\text{ring}}$  compared to  $\Delta^{13}\text{C}_{\text{ring}}$ . The strength of the relationships between environmental variables and isotope discriminations varies between the two species, but the direction (i.e. signs) of these relationships remains the same. We can see that isotope discriminations are mainly driven by climate conditions of the year of ring formation. Drier conditions as well as a higher snowfall the year of ring formation decrease carbon discrimination but increase oxygen discrimination. In the case of jack pine, the effect of these environmental variables on growth is similar to their effect on  $\Delta^{13}\text{C}_{\text{ring}}$ . However, for black spruce, the effect of environment on growth is decoupled from the effect on isotope discrimination, and depends mainly on climate conditions of the year prior to ring formation (VPD<sub>prev</sub>, CMI<sub>prev</sub>: drier the conditions of the previous year, lower than expected the growth rates) and on the size of the tree (BA: bigger the tree, lower than expected the growth rates).

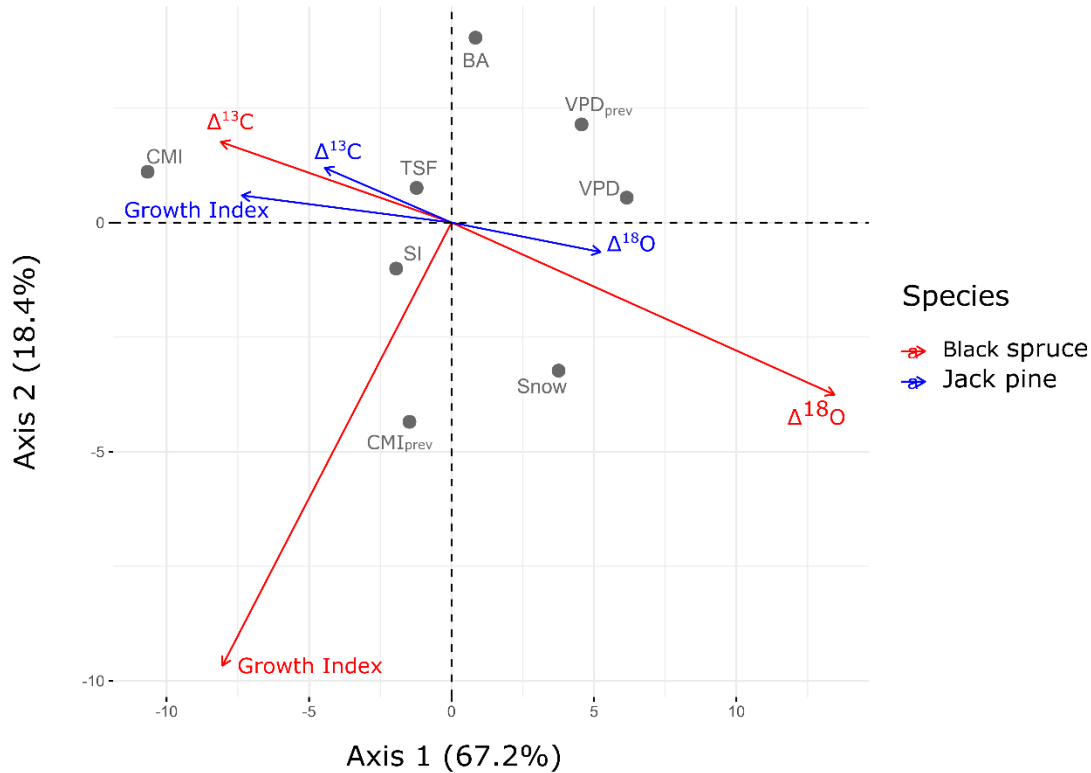


Figure S2.5.2. Biplot from a principal component analysis (PCA). The effects of environmental variables (gray dots in the biplot, estimated with t-statistics from linear mixed models, see Methods in the main text) on growth, carbon discrimination and oxygen enrichment displayed against these response variables (arrows in the biplot), for both species (red for black spruce, blue for jack pine)

## ANNEXE C

### MATÉRIEL SUPPLÉMENTAIRE DU CHAPITRE III

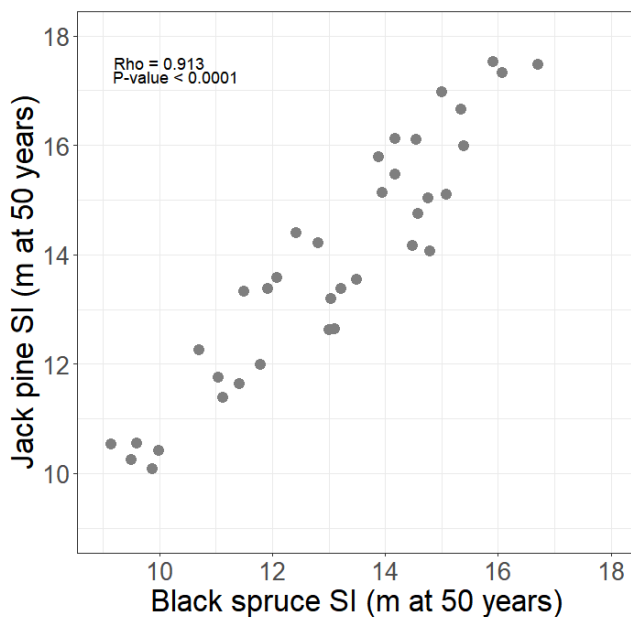


Figure S3.1. Comparison between potential site indices of black spruce and jack pine. Comparison was made between pairs of data points ( $N = 36$  pairs) from the same ecological region and ecological type. The figure displays a strong, positive correlation between the SI of the two species, meaning that, when a site is suitable for black spruce growth, it also provides good growing conditions for jack pine. Data are taken from (Laflèche *et al.*, 2013, Table 9). Data are average SI values by ecological type and species for stands south of our sampling plots, but a similar relationship is expected within our area. Also shown are the Spearman rho coefficient and p-value.

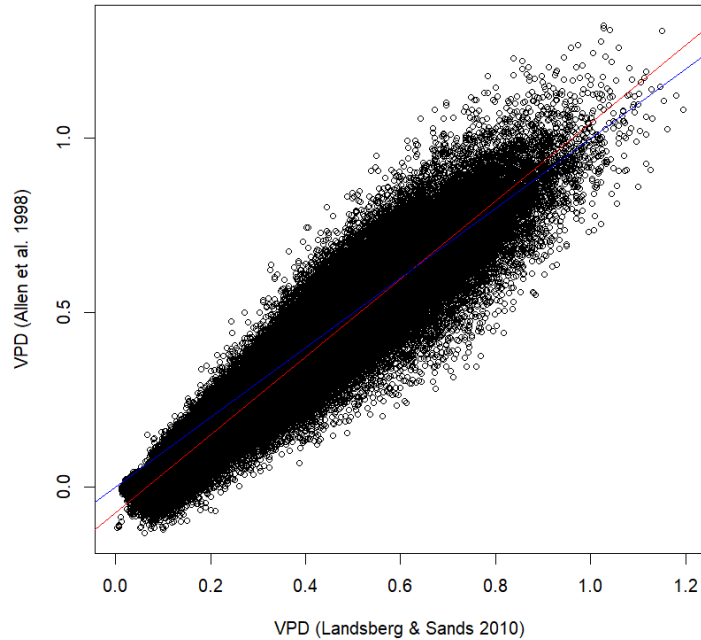


Figure S3.2. Comparison between monthly mean VPD computed from climate data obtained from BioSIM 11 for 500 random locations for the period 1970-2005 using the formula of Landsberg and Sands (as used in the main text) and the VPD formula of Allen et al. (1998), which includes actual vapor pressure (VAP):

$$\text{VPD} = (\varepsilon T_{max} + \varepsilon T_{min})/2 - \text{VAP}$$

The later formula was not used in our study because of the lack of dewpoint temperature or relative humidity data (necessary to derive VAP) in our sampling area for a time-period extending back to 1866. Correlation between the estimated VPD values was very high (Pearson R=0.97, N=216 000 monthly values; red line is the regression line between the two datasets, and blue line is the 1:1 line)

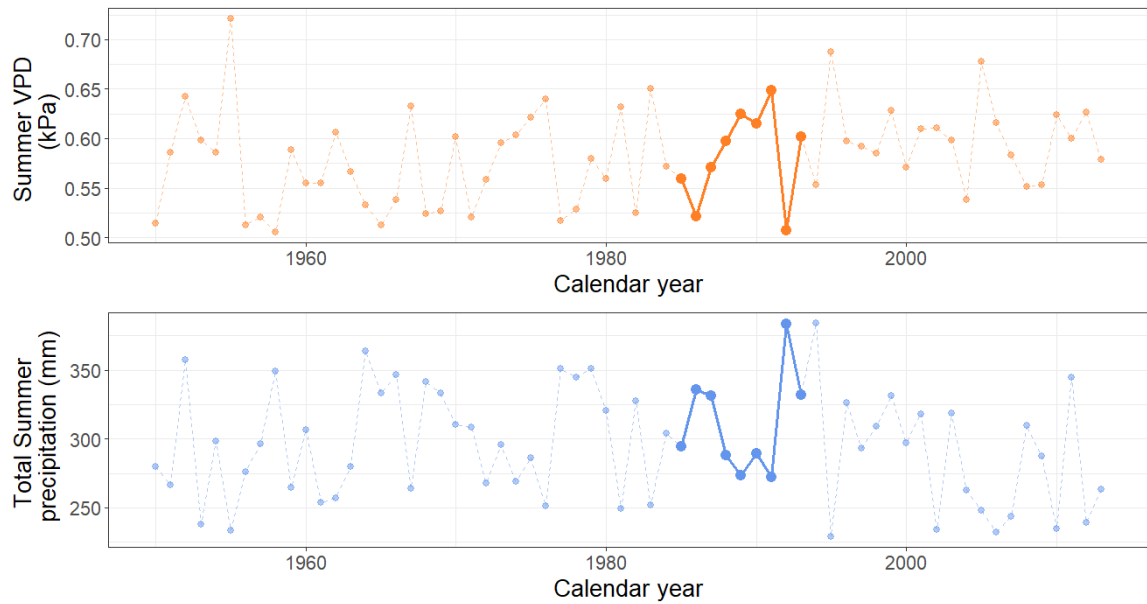


Figure S3.3. Median 1950-2013 chronologies of summer vapor pressure deficit (top panel) and summer total precipitation (bottom panel), for our study plots. The 1985-1993 period is highlighted with plain thick lines.

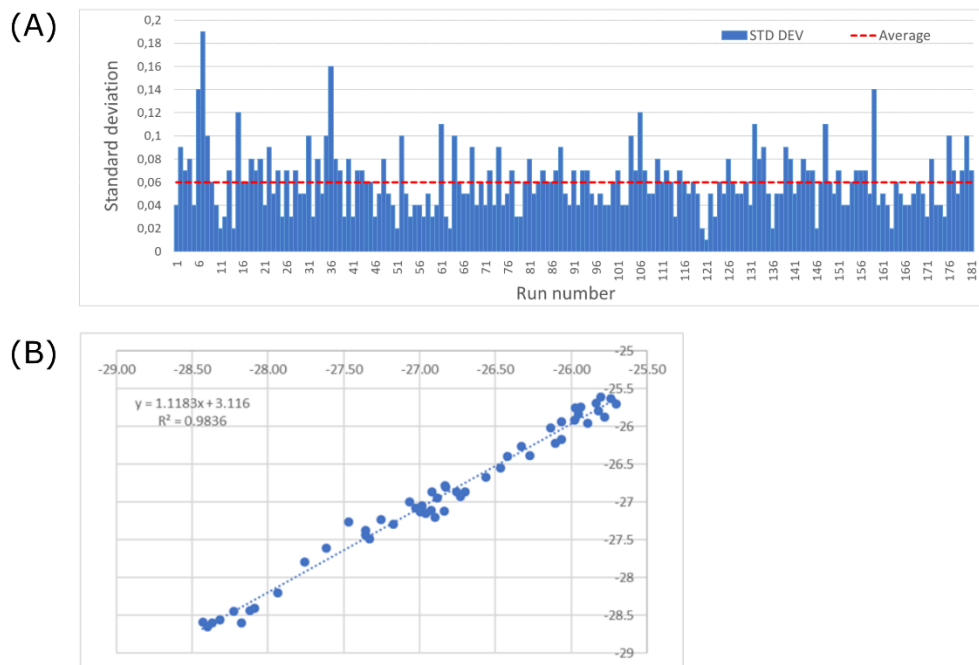


Figure S3.4. (A) Standard deviations for quality control measurements of all Isotope-Ratio Mass Spectrometry (IRMS) runs (181 runs), as a quantification of measurement uncertainty. Quality control standard used in the Isolab is caffeine (Caf-j3), with a  $\delta^{13}\text{C}$  of  $-40.46 \pm 0.1\text{‰}$ . The average standard deviation of the 181 runs is  $0.06\text{‰}$  (red dashed line). (B) Replicated  $\delta^{13}\text{C}$  measurements of study samples. Correlation between replicates is quite high. The average standard deviation of the 53 duplicates is  $\pm 0.07\text{‰}$ , which denotes a good homogenization of the wood powder.

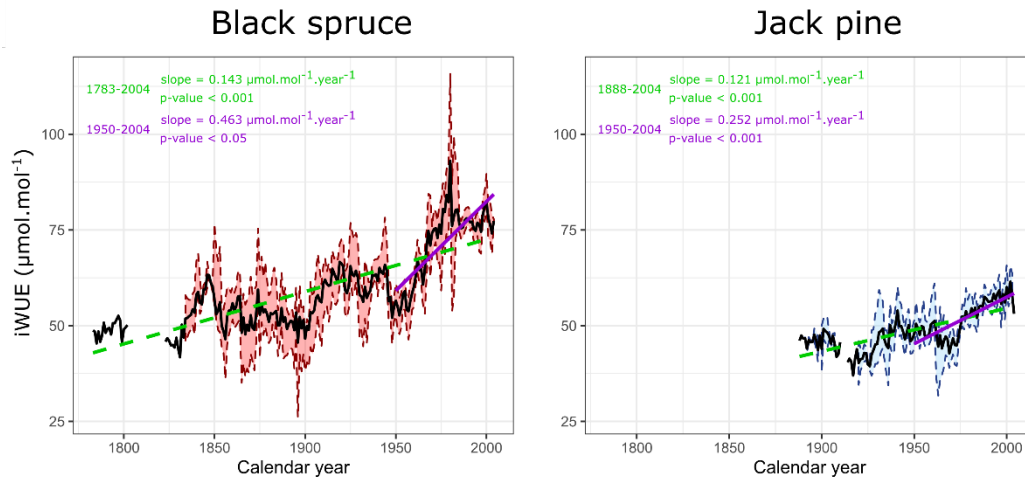


Figure S3.5. Median  $i\text{WUE}_{\text{ring}}$  chronologies. Black lines are median values of  $i\text{WUE}_{\text{ring}}$  by year and species, shading displays 95 % confidence intervals. Green dashed lines and violet solid lines represent linear regressions over the entire period and over the period 1950-2004, respectively. Also shown are the Theil-Sen slopes (slope of the linear trend according to the Sen test) and adjusted p-values from the Mann-Kendall trend test. Slopes and p-values were computed using the *mkTrend* function of R-package *fume* (Yue et Wang, 2004).

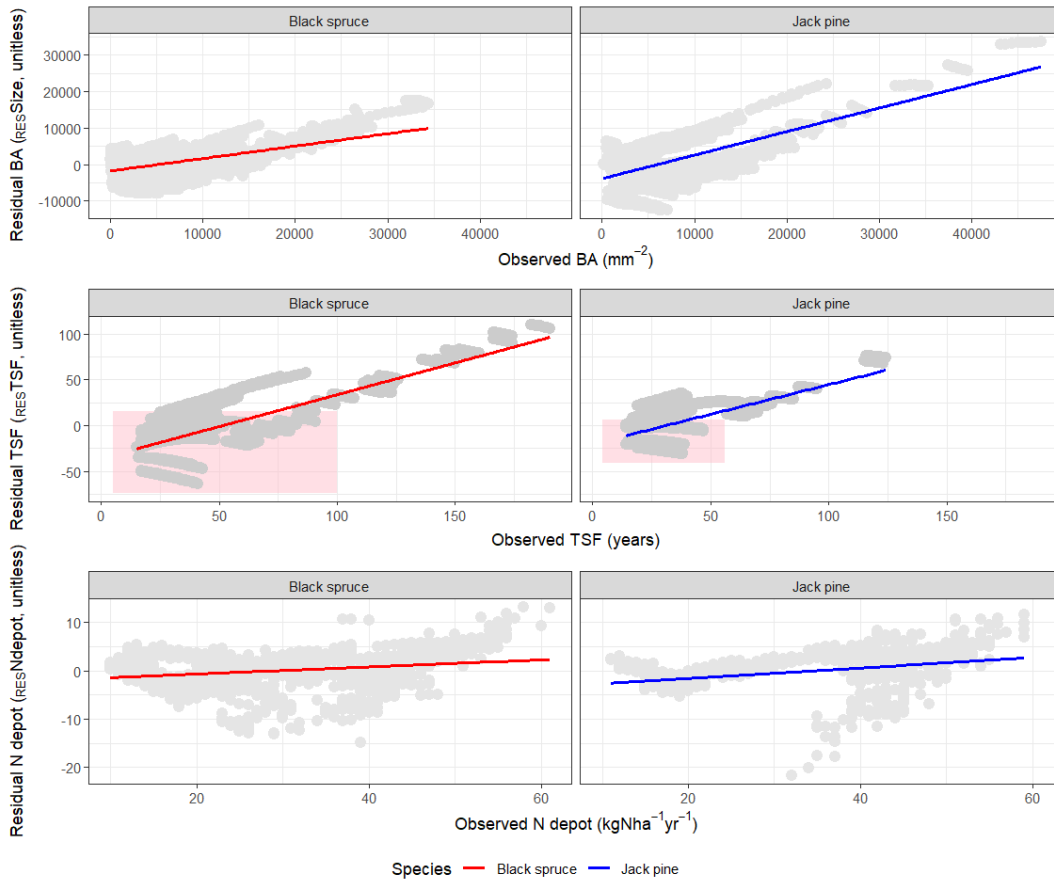


Figure S3.6. Relationship between observed values of tree basal area, time-since-fire (TSF) and total annual nitrogen deposition (Ndepot) and variables that were transformed to remove the variability shared with  $C_a$ , i.e.  $\text{RES}_{\text{Size}}$ ,  $\text{RES}_{\text{TSF}}$  and  $\text{RES}_{\text{Ndepot}}$ . Lines are linear regressions between the two variables. For the middle panel, pink rectangles emphasize values of  $\text{RES}_{\text{TSF}}$  within the phase of initial decrease in Figure 3.6 in the main text. For black spruce, this corresponds approximately to a minimum time-since-fire between 15 and 66 years. For jack pine, this corresponds to a minimum time-since-fire between 14 and 46 years.

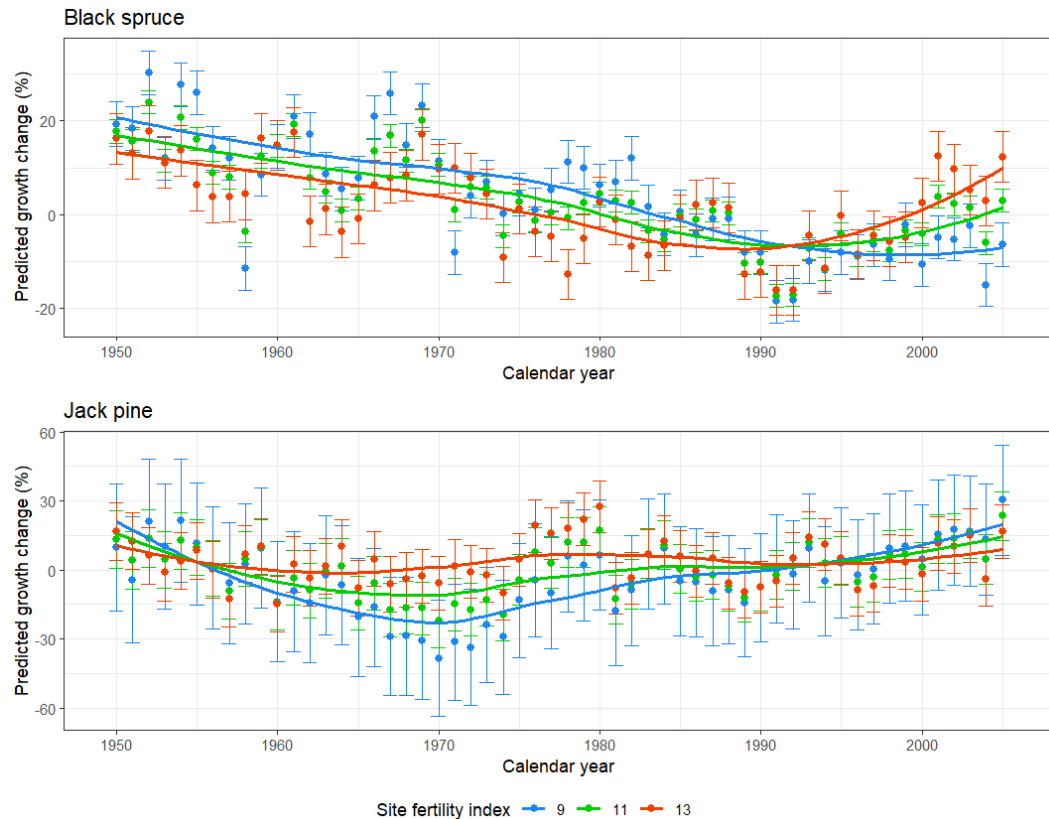


Figure S3.7. Growth analysis on the entire tree-ring dataset. 1m-height Basal area increments (BAI) of 1,914 black spruce and 352 jack pine trees were detrended using a generalized additive mixed modelling procedure, by ecological district and species. Then, a growth change index (GC) was computed as the percent difference between the observed and predicted BAI. Reader should refer to Marchand et al. (2019) for the complete statistical procedure. Here, we considered this detrended data over the period 1950-2005. We fitted a species-specific linear mixed effect model that included GC as response variable, site fertility level, calendar year (as a factorial variable) and their interaction as explanatory variables, and the effect of the tree nested within the plot as random term together with an order 1 autocorrelation structure, using the function *lme* from the R-package *nlme*. The figure displays predicted values of GC by year and species (filled dots), for three fertility levels, obtained using the function *predictSE* from the R-package *AICcmodavg*. Error bars are 1.96 standard error. Loess smoothings (lines) were added to ease interpretation. One can see that black spruce growth globally decreased over 1950-2005 but, for the more fertile stands, this decrease reversed in the last decade while, for the poorer stands black spruce growth declined continuously. On the opposite growth of jack pine was mostly unchanged.

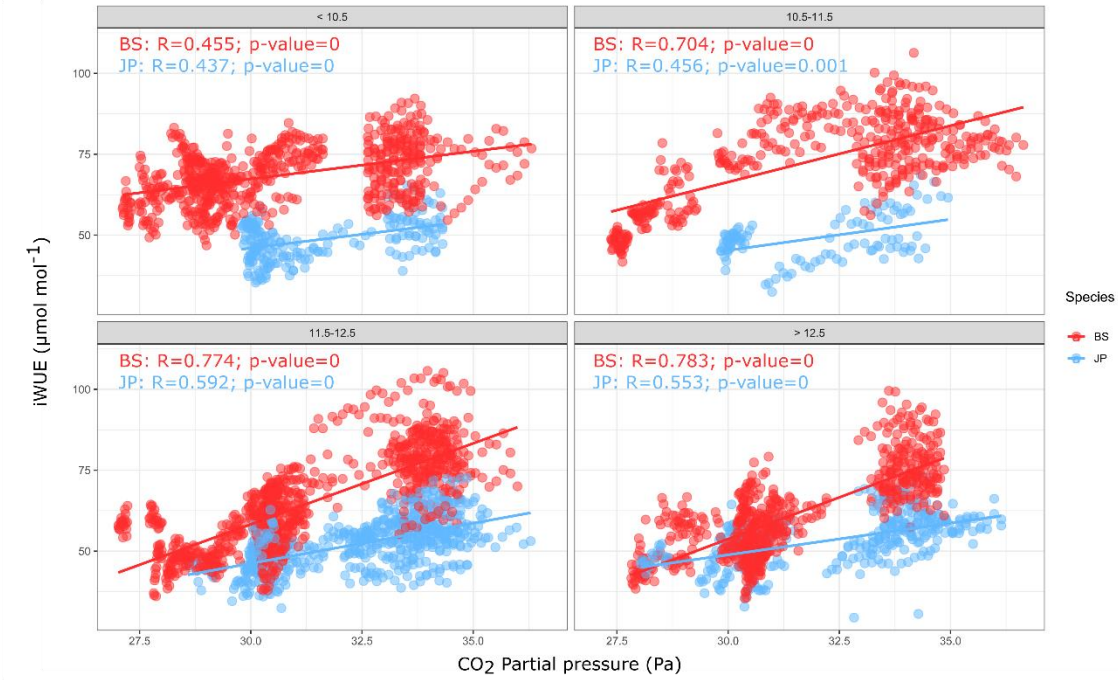


Figure S3.8. Similar to displays presented in Figure 3.3b, but by classes of site fertility indices. Raw  $i\text{WUE}_{\text{ring}}$  values are displayed by species, with the linear regression line, from least productive stands (“<10.5”) to more productive stands (“>12.5”).

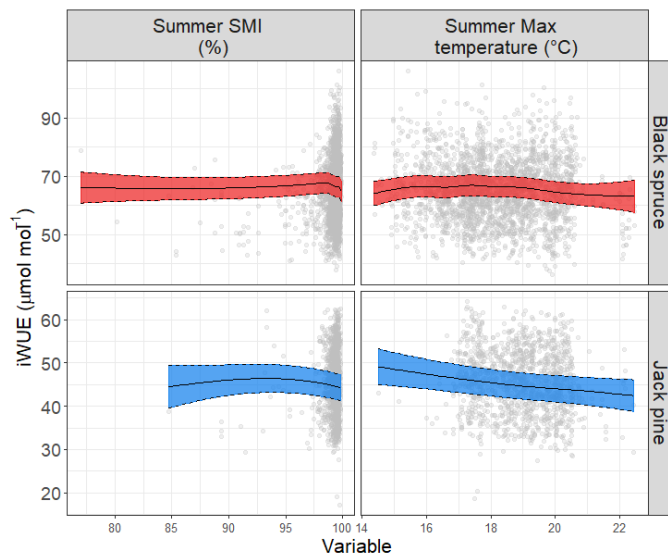


Figure S3.9. Partial effects of summer maximum temperature (extracted from ANUSPLIN dataset; and computed as the average maximum temperature of June-august) and summer soil moisture index (Summer SMI; obtained from BioSIM 11 software for the period 1901-2004; as the average SMI of june-august) on  $i\text{WUE}_{\text{ring}}$ , by species. Gray dots represent partial residuals from the GAMMs, i.e. the estimates for the variable plus the residuals. Black lines and red and blue shadings are respectively for the predicted values and 95% confidence intervals from the “Control” GAMMs, i.e. models using residual size, residual TSF and residual N deposit as covariates (equation 10 in Figure 3.2 and in the Materials and Methods section in the main text). Compared to models used in the main analyses, these models considered the two variables (Summer SMI and Summer Temperature) as additional covariates (no variables dropped). Since SMI was available only for the period 1901-2004, the number of samples dropped to 2322 and 1244 for black spruce and jack pine models, respectively. Adding these variables into models increased concrury. ‘Estimate’ concrury coefficients associated with the variables Summer VPD and Summer maximum temperature increased above 0.4 for black spruce and jack pine models, because of the high collinearity between the two variables (VPD is derived from maximum Temperature, Pearson R=0.91, p-value < 0.001).

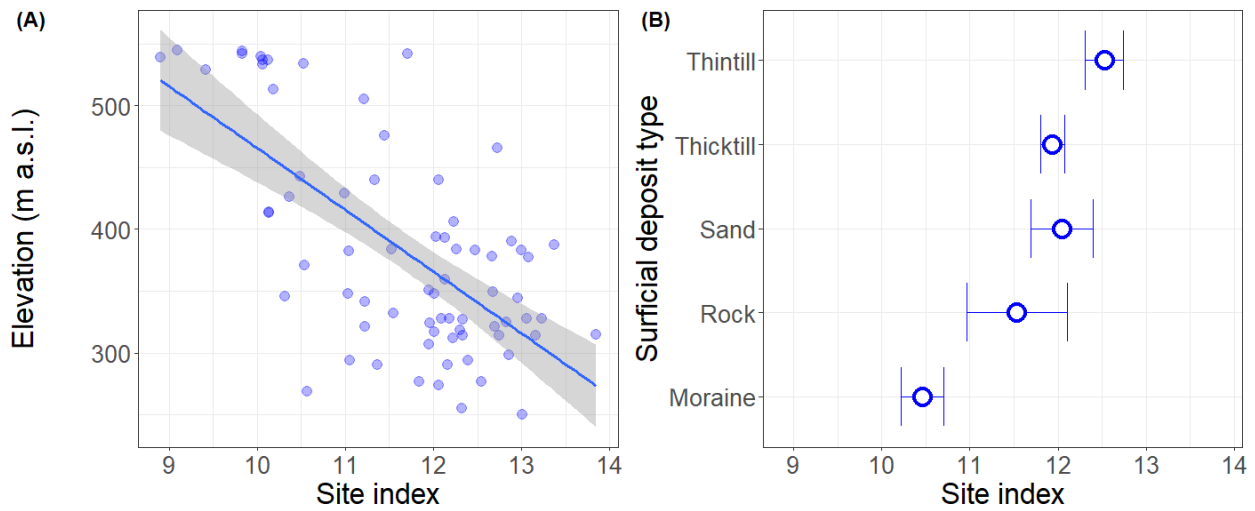


Figure S3.10. (A) Relationship between site fertility index and elevation. Dots represent observed values for our study plots, the line and shading display the linear regression and 95 % confidence intervals, respectively. (B) Median values of site index by surficial deposit class. Error bars in (B) are standard errors.

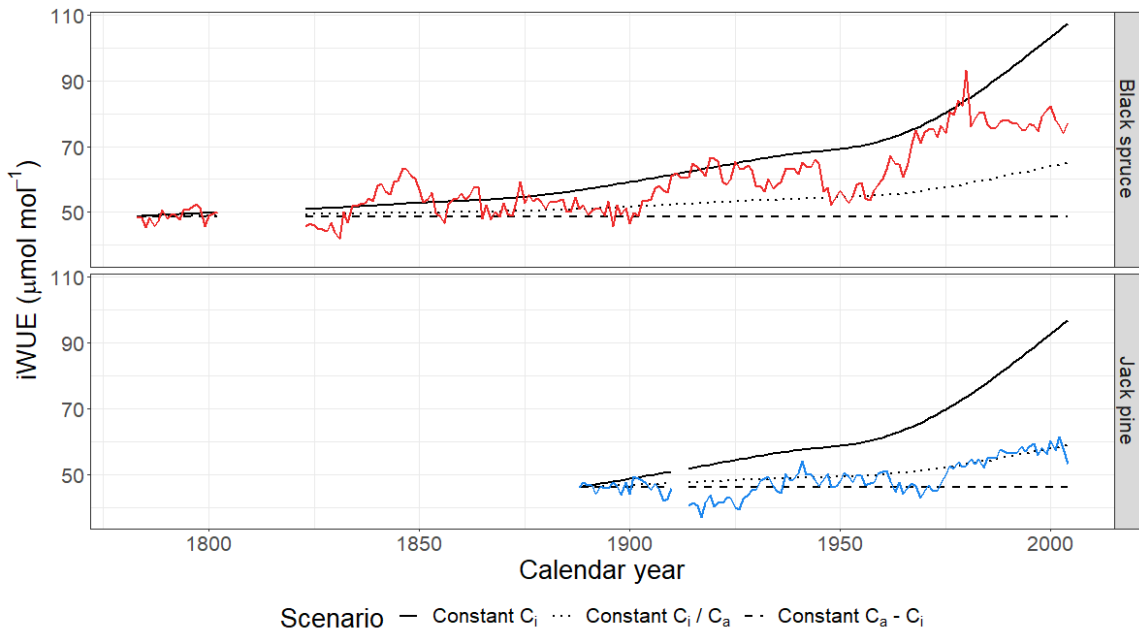


Figure S3.11.  $i\text{WUE}_{ring}$  according to the three theoretical scenarios describing the response of leaf internal  $\text{CO}_2$  concentrations ( $C_i$ ) to atmospheric  $\text{CO}_2$  concentrations ( $C_a$ ), i.e. a constant  $C_i$  (Scenario 1, solid lines), a constant  $C_i/C_a$  (Scenario 2, dotted lines) and a constant  $C_a-C_i$  (Scenario 3, dashed lines; (Saurer *et al.*, 2004)). Starting values that were considered for  $C_a$  and  $C_i$  are those that were derived from  $\delta^{13}\text{C}$  values of the samples corresponding to the first calendar year recorded for each species. The red and blue lines are median values of the observed raw  $i\text{WUE}$  (Not corrected for the effect of development, climate, and site) for black spruce and jack pine, respectively.

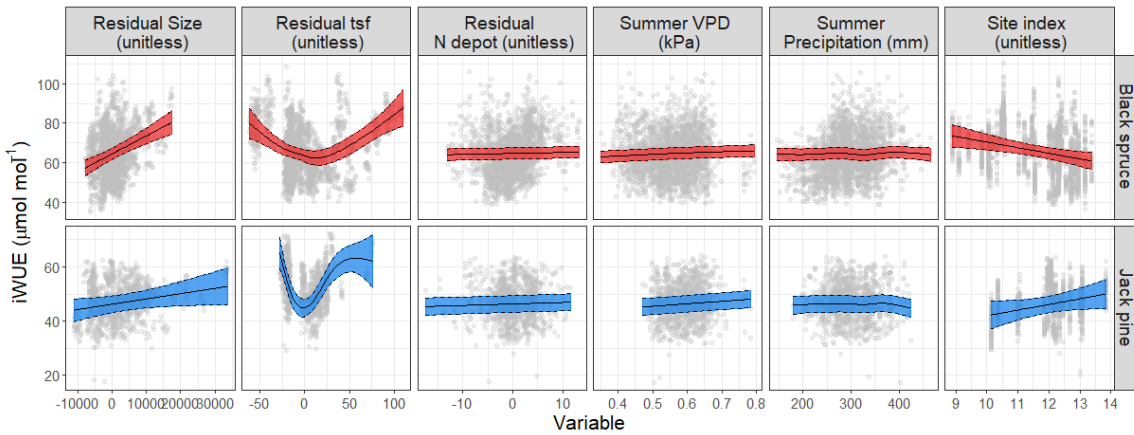


Figure S3.12. Sensitivity analysis to test for the effect of sample replication on GAMMs results. Here we selected only years with at least 10 samples by species (i.e. years represented by at least 10 trees). This dropped the number of years analyzed to 93 years for black spruce and 46 years for jack pine, and the number of samples to 2277 and 1027 for black spruce and jack pine respectively. We re-run ‘Control’ GAMMs on this dataset, to test if patterns observed when including all years (including those years with low sample replication) were representative of the whole tree population. As one can see by comparing this figure with the figure in the main document (Figure 3.6), results are similar. No changes in conclusions, except for the effect of tree size on jack pine iWUE, which is non-significant when considering only years with more than 10 trees (but one should note that this effect was only barely significant when considering the full dataset).

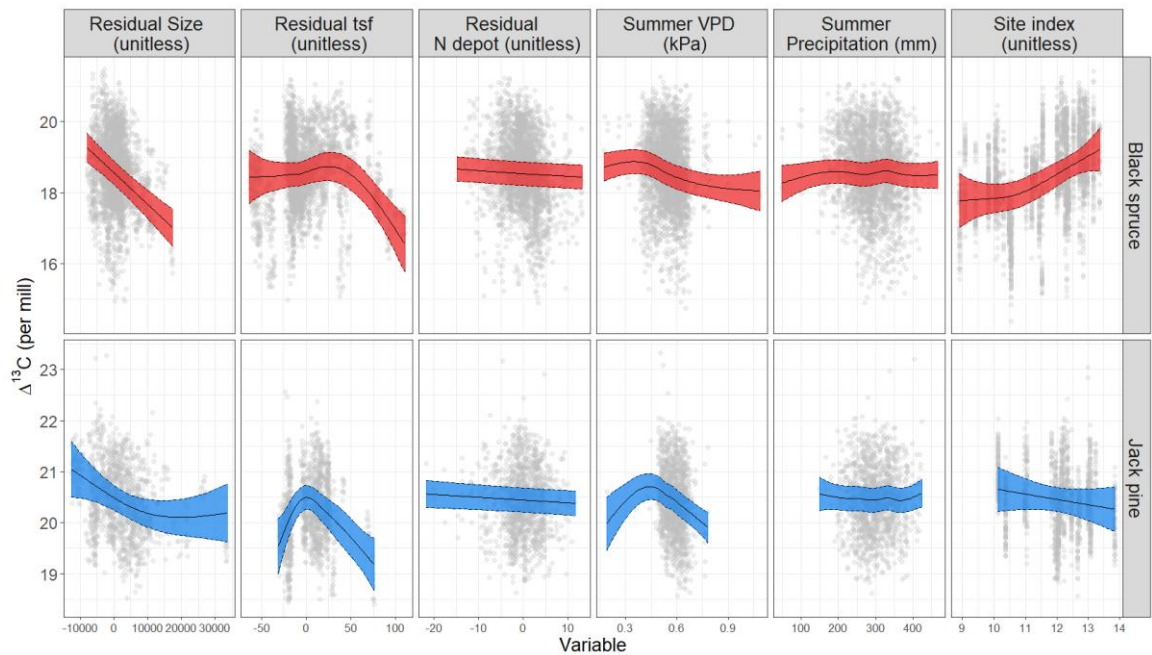


Figure S3.13. Partial residuals from GAMMs including  $\Delta^{13}\text{C}_{\text{ring}}$  instead of  $i\text{WUE}_{\text{ring}}$  as response variable.

Table S3.1. Sensitivity analysis to test for the effects of summer maximum temperature and summer soil moisture index (SMI) on iWUE. The table displays estimated degrees of freedom (EDF), F-values and p-values by species, obtained when fitting a GAMM considering the same variables as the ‘control’ GAMMs in the main text with addition to these two new variables. Because summer SMI was available only for the period 1901-2004, the analysis was restrained to this shorter time-period. Please refer to Figure S3.9.1 for partial residuals for these two variables.

	Black spruce			Jack pine		
Variable	EDF	F-value	p-value	Df	F-value	p-value
Summer Max Temperature	7.226	5.457	< 0.001	2.161	6.145	<0.01
Summer SMI	6.590	12.236	< 0.001	2.030	5.701	< 0.01

Table S3.2. ANOVA tables from the LMMs linking growth rates (as GC values) with year, site index, and their interaction. Please refer to Figure S3.7.1 caption for details about the dataset and statistical analysis. numDF specifies the numerator degree of freedom, denDF means denominator degree of freedom.

			Black spruce				Jack pine	
	numDF	denDF	F-value	p-value	numDF	denDF	F-value	p-value
Site Index	1	646	0.012	0.915	1	119	0.077	0.782
Year	55	91725	213.161	< 0.001	55	11972	37.149	< 0.001
Site Index x Year	55	91725	27.347	< 0.001	55	11972	1.808	< 0.001

Table S3.3. Sensitivity analysis to test for the effect of the non-independence between iWUE and C<sub>a</sub>. Results from LMMs including RESΔ<sup>13</sup>C<sub>ring</sub> instead of iWUE<sub>ring</sub> as response variable.

		Black spruce RESΔ <sup>13</sup> C <sub>ring</sub>				Jack pine RESΔ <sup>13</sup> C <sub>ring</sub>			
		β	Std. error	t-value	p-value	β	Std. error	t-value	p-value
Null	PCO <sub>2</sub>	<b>-0.153</b>	<b>0.016</b>	<b>-9.73</b>	<b>0</b>	<b>-0.085</b>	<b>0.014</b>	<b>-6.198</b>	<b>0</b>
	SI	<b>0.272</b>	<b>0.089</b>	<b>3.06</b>	<b>0.0039</b>	-0.134	0.099	-1.353	0.187
	PCO <sub>2</sub> x SI	<b>-0.167</b>	<b>0.013</b>	<b>-12.72</b>	<b>0</b>	-0.016	0.014	-1.150	0.250
Full	PCO <sub>2</sub>	0.011	0.014	0.753	0.452	0.010	0.012	0.770	0.442
	SI	-0.012	0.092	-0.134	0.894	-0.007	0.098	-0.079	0.938
	PCO <sub>2</sub> x SI	<b>-0.129</b>	<b>0.012</b>	<b>-10.711</b>	<b>0</b>	-0.017	0.012	-1.36	0.017
Control	PCO <sub>2</sub>	<b>-0.077</b>	<b>0.015</b>	<b>-5.090</b>	<b>0</b>	-0.015	0.013	-1.080	0.280
	SI	0.002	0.096	0.025	0.980	-0.002	0.099	-0.022	0.982
	PCO <sub>2</sub> x SI	<b>-0.128</b>	<b>0.013</b>	<b>-10.176</b>	<b>0</b>	-0.010	0.013	-0.740	0.460

ANNEXE D

MATÉRIEL SUPPLÉMENTAIRE DU CHAPITRE VI

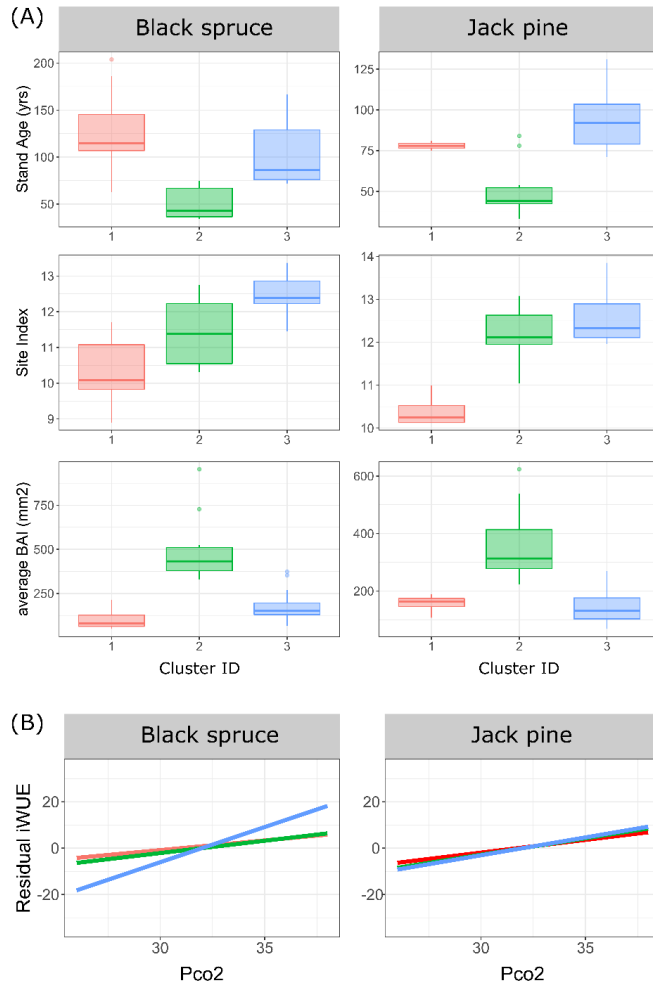


Figure S4.1. Analyses par cluster de l'effet  $\text{CO}_2$ . Les clusters ont été identifiés en réalisant une analyse K-moyennes; au moyen de la fonction kmeans dans R. Les variables qui ont été considérées pour déterminer les clusters sont l'âge du peuplement, l'IQS et le BAI moyen des arbres sur la période 1985-2005. Le nombre optimal de clusters, identifié au moyen de la fonction fviz\_nbclust, était de 3. Par la suite, les modèles du troisième chapitre ont été relancés, cette fois-ci en séparant les sites selon le cluster qui leur avait été attribué. En (A), boxplots des variables incluses dans l'identification des clusters, par espèce. En (B), résultats des modèles identifiant l'effet  $\text{CO}_2$ , par espèce. L'indice de fertilité (IQS) n'a pas été inclus dans les modèles car il était déjà utilisé pour identifier les clusters, et donc pour séparer les sites. Les patrons d'effet  $\text{CO}_2$  sont assez similaires à ceux observés dans les analyses présentées au chapitre 3, à savoir un effet plus important pour les épinettes présentes sur les sites les plus fertiles (courbe bleue, cluster #3). Il est intéressant de noter que, pour ces sites les plus fertiles, les arbres sont assez peu productifs (BAI moyen assez faible, voir (A)).

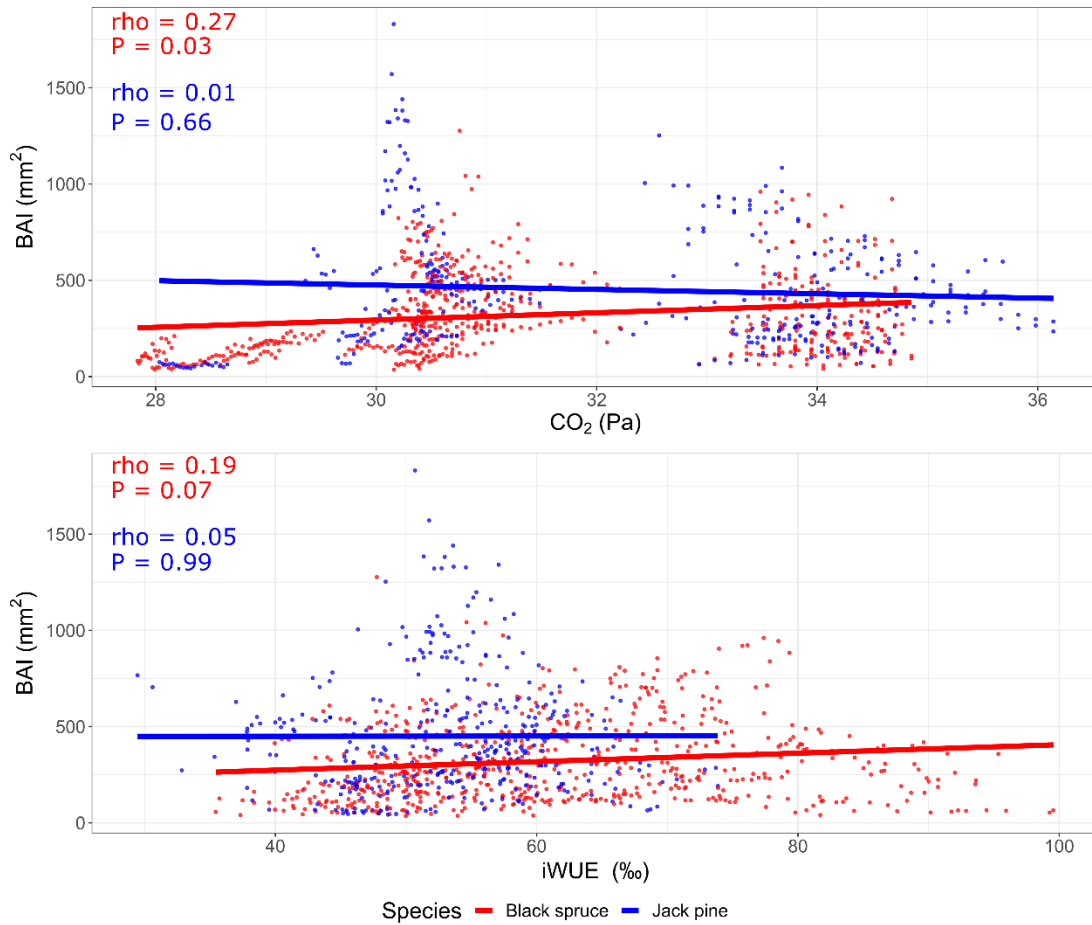


Figure S4.2. Relations entre le BAI et la pression partielle de  $\text{CO}_2$  (panneau du haut), et l'efficience d'utilisation de l'eau (panneau du bas), pour les épinettes noires et les pins gris localisés sur les sites les plus fertiles ( $\text{IQS} > 12.5$ ). Les p-values présentées ont été corrigées pour l'autocorrélation spatiale au moyen d'un test t modifié. Pour la méthode, le lecteur est invité à se référer au chapitre 3 du présent document.

## RÉFÉRENCES

- Adams, H. D., Macalady, A. K., Breshears, D. D., Allen, C. D., Stephenson, N. L., Saleska, S. R., ... McDowell, N. G. (2010). Climate-induced tree mortality: earth system consequences. *Eos, Transactions American Geophysical Union*, 91(17), 153-154. doi: 10.1029/2010EO170003
- Adams, H. D., Zeppel, M. J. B., Anderegg, W. R. L., Hartmann, H., Landhäuser, S. M., Tissue, D. T., ... McDowell, N. G. (2017). A multi-species synthesis of physiological mechanisms in drought-induced tree mortality. *Nature Ecology & Evolution*, 1(9), 1285-1291. doi: 10.1038/s41559-017-0248-x
- Allen, Barros, V., Broome, J., Cramer, W., Christ, R., Church, J., ... Urge-Vorsatz, D. (2014). *Climate Change 2014: Synthesis Report*. (s. l. : n. é.).
- Allen, C. D., Macalady, A. K., Chenchouni, H., Bachelet, D., McDowell, N., Vennetier, M., ... Cobb, N. (2010). A global overview of drought and heat-induced tree mortality reveals emerging climate change risks for forests. *Forest Ecology and Management*, 259(4), 660-684. doi: 10.1016/j.foreco.2009.09.001
- Allen, R. G., Pereira, L. S., Raes, D. et Smith, M. (1998). *Crop evapotranspiration - Guidelines for computing crop water requirements - FAO Irrigation and drainage paper 56* (FAO-Food and Agriculture Organization of the United Nations). (s. l. : n. é.).
- Altman, J., Fibich, P., Santruckova, H., Dolezal, J., Stepanek, P., Kopacek, J., ... Cienciala, E. (2017). Environmental factors exert strong control over the climate-growth relationships of *Picea abies* in Central Europe. *Science of the Total Environment*, 609, 506-516. doi: 10.1016/j.scitotenv.2017.07.134
- Anderegg, W. R. L. et Anderegg, L. D. L. (2013). Hydraulic and carbohydrate changes in experimental drought-induced mortality of saplings in two conifer species. *Tree Physiology*, 33(3), 252-260. doi: 10.1093/treephys/tpt016
- Anderegg, W. R. L., Flint, A., Huang, C., Flint, L., Berry, J. A., Davis, F. W., ... Field, C. B. (2015a). Tree mortality predicted from drought-induced vascular damage. *Nature Geoscience*, 8(5), 367-371. doi: 10.1038/ngeo2400
- Anderegg, W. R. L., Schwalm, C., Biondi, F., Camarero, J. J., Koch, G., Litvak, M., ... Pacala, S. (2015b). Pervasive drought legacies in forest ecosystems and their implications for carbon cycle models. *Science*, 349(6247), 528-532. doi: 10.1126/science.aab1833
- Andrieux, B., Beguin, J., Bergeron, Y., Grondin, P. et Paré, D. (2018). Drivers of postfire soil organic carbon accumulation in the boreal forest. *Global Change Biology*, 24(10), 4797-4815. doi: 10.1111/gcb.14365

- Ansseau, C., Bélanger, L., Bergeron, J. F., Bouchard, A., Brisson, J., De Grandpré, L., ... Vasseur, L. (1997). Écologie forestière. Dans *Manuel de foresterie* (1st Edition, p. 134-279). Sainte-Foy, Québec : Presses de l'Université Laval.
- Arco Molina, J. G., Helle, G., Hadad, M. A. et Roig, F. A. (2019). Variations in the intrinsic water-use efficiency of north Patagonian forests under a present climate change scenario: tree age, site conditions and long-term environmental effects. *Tree Physiology*, 39(4), 661-678. doi: 10.1093/treephys/tpy144
- Aussenac, R., Bergeron, Y., Mekontchou, C. G., Gravel, D., Pilch, K. et Drobyshev, I. (2017). Intraspecific variability in growth response to environmental fluctuations modulates the stabilizing effect of species diversity on forest growth. *Journal of Ecology*, 105(4), 1010-1020. doi: 10.1111/1365-2745.12728
- Austin, M. P. et Niel, K. P. V. (2011). Improving species distribution models for climate change studies: variable selection and scale. *Journal of Biogeography*, 38(1), 1-8. doi: 10.1111/j.1365-2699.2010.02416.x
- Avanzi, C., Piermattei, A., Piotti, A., Büntgen, U., Heer, K., Opgenoorth, L., ... Leonardi, S. (2019). Disentangling the effects of spatial proximity and genetic similarity on individual growth performances in Norway spruce natural populations. *Science of the Total Environment*, 650, 493-504. doi: 10.1016/j.scitotenv.2018.08.348
- Babst, F., Alexander, M. R., Szejner, P., Bouriaud, O., Klesse, S., Roden, J., ... Trouet, V. (2014). A tree-ring perspective on the terrestrial carbon cycle. *Oecologia*, 176(2), 307-322. doi: 10.1007/s00442-014-3031-6
- Babst, F., Bodesheim, P., Charney, N., Friend, A. D., Girardin, M. P., Klesse, S., ... Evans, M. E. K. (2018). When tree rings go global: Challenges and opportunities for retro- and prospective insight. *Quaternary Science Reviews*, 197, 1-20. doi: 10.1016/j.quascirev.2018.07.009
- Babst, F., Carrer, M., Poulter, B., Urbinati, C., Neuwirth, B. et Frank, D. C. (2012a). 500 years of regional forest growth variability and links to climatic extreme events in Europe. *Environmental Research Letters*, 7(4), 045705.
- Babst, F., Poulter, B., Trouet, V., Tan, K., Neuwirth, B., Wilson, R., ... Frank, D. C. (2012b). Site- and species-specific responses of forest growth to climate across the European continent. *Global Ecology and Biogeography*, 22(6), 706-717. doi: 10.1111/geb.12023
- Balducci, L., Deslauriers, A., Giovannelli, A., Rossi, S. et Rathgeber, C. B. K. (2013). Effects of temperature and water deficit on cambial activity and woody ring features in *Picea mariana* saplings. *Tree Physiology*, 33(10), 1006-1017. doi: 10.1093/treephys/tpt073
- Balland, V., Bhatti, J., Errington, R., Castonguay, M. et Arp, P. A. (2006). Modeling snowpack and soil temperature and moisture conditions in a jack pine, black spruce and aspen forest stand in central Saskatchewan (BOREAS SSA). *Canadian Journal of Soil Science*, 86(Special Issue), 203-217. doi: 10.4141/S05-088
- Barber, V. A., Juday, G. P. et Finney, B. P. (2000). Reduced growth of Alaskan white spruce in the twentieth century from temperature-induced drought stress. *Nature*, 405(6787), 668-673. doi: 10.1038/35015049
- Bartoń, K. (2018). *MuMIn: Multi-Model Inference* (version 1.40.4). Récupéré de <https://CRAN.R-project.org/package=MuMIn>

- Battipaglia, G., Saurer, M., Cherubini, P., Calfapietra, C., McCarthy, H. R., Norby, R. J. et Cotrufo, M. F. (2013). Elevated CO<sub>2</sub> increases tree-level intrinsic water use efficiency: insights from carbon and oxygen isotope analyses in tree rings across three forest FACE sites. *New Phytologist*, 197(2), 544-554. doi: 10.1111/nph.12044
- Beck, P. S. A., Juday, G. P., Alix, C., Barber, V. A., Winslow, S. E., Sousa, E. E., ... Goetz, S. J. (2011). Changes in forest productivity across Alaska consistent with biome shift. *Ecology Letters*, 14(4), 373-379. doi: 10.1111/j.1461-0248.2011.01598.x
- Bégin, C., Gingras, M., Savard, M. M., Marion, J., Nicault, A. et Bégin, Y. (2015). Assessing tree-ring carbon and oxygen stable isotopes for climate reconstruction in the Canadian northeastern boreal forest. *Palaeogeography, Palaeoclimatology, Palaeoecology*, 423, 91-101. doi: 10.1016/j.palaeo.2015.01.021
- Bélisle, A. C., Gauthier, S., Cyr, D., Bergeron, Y. et Morin, H. (2011). Fire regime and old-growth boreal forests in central Quebec, Canada: an ecosystem management perspective. *Silva Fennica*, 45(5), id 77. doi: https://doi.org/10.14214/sf.77
- Belleau, A., Bergeron, Y., Leduc, A., Gauthier, S. et Fall, A. (2007). Using spatially explicit simulations to explore size distribution and spacing of regenerating areas produced by wildfires: recommendations for designing harvest agglomerations for the Canadian boreal forest. *The Forestry Chronicle*, 83(1), 72-83. doi: 10.5558/tfc83072-1
- Benomar, L., Lamhamedi, M. S., Pepin, S., Rainville, A., Lambert, M.-C., Margolis, H. A., ... Beaulieu, J. (2018). Thermal acclimation of photosynthesis and respiration of southern and northern white spruce seed sources tested along a regional climatic gradient indicates limited potential to cope with temperature warming. *Annals of Botany*, 121(3), 443-457. doi: 10.1093/aob/mcx174
- Bergeron, Y., Cyr, D., Drever, C. R., Flannigan, M., Gauthier, S., Kneeshaw, D., ... Logan, K. (2006). Past, current, and future fire frequencies in Quebec's commercial forests: implications for the cumulative effects of harvesting and fire on age-class structure and natural disturbance-based management. *Canadian Journal of Forest Research*, 36(11), 2737-2744. doi: 10.1139/x06-177
- Bergeron, Y., Leduc, A., Harvey, B. D. et Gauthier, S. (2002). Natural fire regime: A guide for sustainable management of the Canadian boreal forest. *Silva Fennica*, 36(1), 81-95.
- Bernacchi, C. J., Singsaas, E. L., Pimentel, C., Portis Jr, A. R. et Long, S. P. (2001). Improved temperature response functions for models of Rubisco-limited photosynthesis. *Plant, Cell & Environment*, 24(2), 253-259. doi: 10.1111/j.1365-3040.2001.00668.x
- Bert, D., Leavitt, S. W. et Dupouey, J.-L. (1997). Variations of wood δ<sup>13</sup>C and water-use efficiency of *Abies alba* during the last century. *Ecology*, 78(5), 1588-1596. doi: 10.1890/0012-9658(1997)078[1588:VOWCAW]2.0.CO;2
- Bhaskar, R., Valiente-Banuet, A. et Ackerly, D. D. (2007). Evolution of hydraulic traits in closely related species pairs from mediterranean and nonmediterranean environments of North America. *New Phytologist*, 176(3), 718-726. doi: 10.1111/j.1469-8137.2007.02208.x
- Bigler, C. et Bugmann, H. (2018). Climate-induced shifts in leaf unfolding and frost risk of European trees and shrubs. *Scientific Reports*, 8(1), 9865. doi: 10.1038/s41598-018-27893-1

- Biondi, F. et Qeadan, F. (2008). A theory-driven approach to tree-ring standardization: defining the biological trend from expected basal area increment. *Tree-Ring Research*, 64(2), 81-96. doi: 10.3959/2008-6.1
- Black, R. A. et Bliss, L. C. (1980). Reproductive ecology of *Picea mariana* (Mill.) BSP., at tree line near Inuvik, Northwest Territories, Canada. *Ecological Monographs*, 50(3), 331-354. doi: 10.2307/2937255
- Blake, T. J. et Li, J. (2003). Hydraulic adjustment in jack pine and black spruce seedlings under controlled cycles of dehydration and rehydration. *Physiologia Plantarum*, 117(4), 532-539.
- Boisvenue, C., Smiley, B. P., White, J. C., Kurz, W. A. et Wulder, M. A. (2016). *Integration of Landsat time series and field plots for forest productivity estimates in decision support models.*, 376, 284-297. doi: 10.1016/j.foreco.2016.06.022
- Bonal, D., Ponton, S., Thiec, D. L., Richard, B., Ningre, N., Hérault, B., ... Guehl, J.-M. (2011). Leaf functional response to increasing atmospheric CO<sub>2</sub> concentrations over the last century in two northern Amazonian tree species: a historical δ<sup>13</sup>C and δ<sup>18</sup>O approach using herbarium samples. *Plant, Cell & Environment*, 34(8), 1332-1344. doi: 10.1111/j.1365-3040.2011.02333.x
- Bonan, G. B. (2008). Forests and climate change: forcings, feedbacks, and the climate benefits of forests. *Science*, 320(5882), 1444-1449. doi: 10.1126/science.1155121
- Bonan, G. B. et Cleve, K. V. (1992). Soil temperature, nitrogen mineralization, and carbon source–sink relationships in boreal forests. *Canadian Journal of Forest Research*, 22(5), 629-639. doi: 10.1139/x92-084
- Bond-Lamberty, B., Rocha, A. V., Calvin, K., Holmes, B., Wang, C. et Goulden, M. L. (2014). Disturbance legacies and climate jointly drive tree growth and mortality in an intensively studied boreal forest. *Global Change Biology*, 20(1), 216-227. doi: 10.1111/gcb.12404
- Boucher, D., Gauthier, S., Thiffault, N., Marchand, W., Girardin, M. et Urli, M. (2020). How climate change might affect tree regeneration following fire at northern latitudes: a review. *New Forests*, 51(4), 543-571. doi: 10.1007/s11056-019-09745-6
- Brandt, J. P. (2009). The extent of the North American boreal zone. *Environmental Reviews*, 17, 101-161. doi: 10.1139/A09-004
- Brandt, J. P., Flannigan, M. D., Maynard, D. G., Thompson, I. D. et Volney, W. J. A. (2013). An introduction to Canada's boreal zone: ecosystem processes, health, sustainability, and environmental issues. *Environmental Reviews*, 21(4), 207-226. doi: 10.1139/er-2013-0040
- Bréda, N., Huc, R., Granier, A. et Dreyer, E. (2006). Temperate forest trees and stands under severe drought: a review of ecophysiological responses, adaptation processes and long-term consequences. *Annals of Forest Science*, 63(6), 625-644. doi: 10.1051/forest:2006042
- Brienen, R. J. W., Gloor, E., Clerici, S., Newton, R., Arppe, L., Boom, A., ... Timonen, M. (2017). Tree height strongly affects estimates of water-use efficiency responses to climate and CO<sub>2</sub> using isotopes. *Nature Communications*, 8(1), 288. doi: 10.1038/s41467-017-00225-z

- Brienen, R. J. W., Helle, G., Pons, T. L., Guyot, J.-L. et Gloor, M. (2012). Oxygen isotopes in tree rings are a good proxy for Amazon precipitation and El Niño-Southern Oscillation variability. *Proceedings of the National Academy of Sciences U.S.A.*, 109(42), 16957-16962. doi: 10.1073/pnas.1205977109
- Brodbeck, L., Adamson, K., Julio Camarero, J., Castaño, C., Drenkhan, R., Lehtijärvi, A., ... Oliva, J. (2019). Diplodia tip blight on its way to the north: drivers of disease emergence in northern Europe. *Frontiers in Plant Science*, 9, 1818. doi: 10.3389/fpls.2018.01818
- Brodrribb, T. J., McAdam, S. A. M., Jordan, G. J. et Martins, S. C. V. (2014). Conifer species adapt to low-rainfall climates by following one of two divergent pathways. *Proceedings of the National Academy of Sciences U.S.A.*, 111(40), 14489-14493. doi: 10.1073/pnas.1407930111
- Buechling, A., Martin, P. H. et Canham, C. D. (2017). Climate and competition effects on tree growth in Rocky Mountain forests. *Journal of Ecology*, 105(6), 1636-1647. doi: 10.1111/1365-2745.12782
- Bunn, A. G. (2008). A dendrochronology program library in R (dpLR). *Dendrochronologia*, 26(2), 115-124. doi: 10.1016/j.dendro.2008.01.002
- Buras, A. (2017). A comment on the expressed population signal. *Dendrochronologia*, 44, 130-132. doi: 10.1016/j.dendro.2017.03.005
- Burnham, K. P. et Anderson, D. R. (2002). *Model Selection and Multimodel Inference: A Practical Information-Theoretic Approach* (2<sup>e</sup> éd.). New York : Springer-Verlag.  
Récupéré de <https://www.springer.com/us/book/9780387953649>
- Burns, R. M. et Honkala, B. H. (1990). Silvics of North America: Volume 1. Conifers. *United States Department of Agriculture (USDA), Forest Service, Agriculture Handbook 654*.  
Récupéré de <https://www.fs.usda.gov/treesearch/pubs/1547>
- Cahoon, S. M. P., Sullivan, P. F., Brownlee, A. H., Pattison, R. R., Andersen, H.-E., Legner, K. et Hollingsworth, T. N. (2018). Contrasting drivers and trends of coniferous and deciduous tree growth in interior Alaska. *Ecology*, 99(6), 1284-1295. doi: 10.1002/ecy.2223
- Canadian Forest Service. (2010). *National Fire Database - Agency Fire Data*. Edmonton, AB. : Natural Resources Canada, Canadian Forest Service, Northern Forestry Centre.
- Carrer, M. et Urbinati, C. (2004). Age-dependent tree-ring growth responses to climate in *Larix decidua* and *Pinus cembra*. *Ecology*, 85(3), 730-740. doi: 10.1890/02-0478
- Castagneri, D., Petit, G. et Carrer, M. (2015). Divergent climate response on hydraulic-related xylem anatomical traits of *Picea abies* along a 900-m altitudinal gradient. *Tree Physiology*, 35(12), 1378-1387. doi: 10.1093/treephys/tpv085
- Cavard, X., Bergeron, Y., Paré, D., Nilsson, M.-C. et Wardle, D. A. (2018). Disentangling effects of time since fire, overstory composition and organic layer thickness on nutrient availability in Canadian boreal forest. *Ecosystems*, 1-16. doi: 10.1007/s10021-018-0251-3
- Cernusak, L. A., Ubierna, N., Winter, K., Holtum, J. A. M., Marshall, J. D. et Farquhar, G. D. (2013). Environmental and physiological determinants of carbon isotope discrimination in terrestrial plants. *New Phytologist*, 200(4), 950-965. doi: 10.1111/nph.12423

- Charney, N. D., Babst, F., Poulter, B., Record, S., Trouet, V. M., Frank, D. C., ... Evans, M. E. K. (2016). Observed forest sensitivity to climate implies large changes in 21st century North American forest growth. *Ecology Letters*, 19(9), 1119-1128. doi: 10.1111/ele.12650
- Charru, M., Seynave, I., Hervé, J.-C. et Bontemps, J.-D. (2014). Spatial patterns of historical growth changes in Norway spruce across western European mountains and the key effect of climate warming. *Trees*, 28(1), 205-221. doi: 10.1007/s00468-013-0943-4
- Chen, H. Y. H., Luo, Y., Reich, P. B., Searle, E. B. et Biswas, S. R. (2016). Climate change-associated trends in net biomass change are age dependent in western boreal forests of Canada. *Ecology Letters*, 19(9), 1150-1158. doi: 10.1111/ele.12653
- Choat, B., Jansen, S., Brodribb, T. J., Cochard, H., Delzon, S., Bhaskar, R., ... Zanne, A. E. (2012). Global convergence in the vulnerability of forests to drought. *Nature*, 491(7426), 752-755. doi: 10.1038/nature11688
- Christidis, N., Jones, G. S. et Stott, P. A. (2015). Dramatically increasing chance of extremely hot summers since the 2003 European heatwave. *Nature Climate Change*, 5(1), 46-50. doi: 10.1038/nclimate2468
- Cochard, H., Barigah, S. T., Kleinhentz, M. et Eshel, A. (2008). Is xylem cavitation resistance a relevant criterion for screening drought resistance among *Prunus* species? *Journal of Plant Physiology*, 165(9), 976-982. doi: 10.1016/j.jplph.2007.07.020
- Cortini, F. et Comeau, P. G. (2020). Pests, climate and competition effects on survival and growth of trembling aspen in western Canada. *New Forests*, 51(1), 175-190. doi: 10.1007/s11056-019-09726-9
- Cortini, F., Comeau, P. G. et Bokalo, M. (2012). Trembling aspen competition and climate effects on white spruce growth in boreal mixtures of Western Canada. *Forest Ecology and Management*, 277, 67-73. doi: 10.1016/j.foreco.2012.04.022
- Dai, A. (2013). Increasing drought under global warming in observations and models. *Nature Climate Change*, 3(1), 52-58. doi: 10.1038/nclimate1633
- D'Arrigo, R. D., Kaufmann, R. K., Davi, N., Jacoby, G. C., Laskowski, C., Myneni, R. B. et Cherubini, P. (2004). Thresholds for warming-induced growth decline at elevational tree line in the Yukon Territory, Canada. *Global Biogeochemical Cycles*, 18(3). doi: 10.1029/2004GB002249
- D'Arrigo, R., Wilson, R., Liepert, B. et Cherubini, P. (2008). On the 'Divergence Problem' in Northern Forests: A review of the tree-ring evidence and possible causes. *Global and Planetary Change*, 60(3), 289-305. doi: 10.1016/j.gloplacha.2007.03.004
- Daux, V., Michelot-Antalik, A., Lavergne, A., Pierre, M., Stievenard, M., Bréda, N. et Damesin, C. (2018). Comparisons of the performance of  $\delta^{13}\text{C}$  and  $\delta^{18}\text{O}$  of *Fagus sylvatica*, *Pinus sylvestris*, and *Quercus petraea* in the record of past climate variations. *Journal of Geophysical Research: Biogeosciences*, 123(4), 1145-1160. doi: 10.1002/2017JG004203
- De Grandpré, L., Kneeshaw, D. D., Perigon, S., Boucher, D., Marchand, M., Pureswaran, D. et Girardin, M. P. (2019). Adverse climatic periods precede and amplify defoliator-induced tree mortality in eastern boreal North America. *Journal of Ecology*, 107(1), 452-467. doi: 10.1111/1365-2745.13012

- de Oliveira, E. A. D., Approbato, A. U., Legracie, J. R. et Martinez, C. A. (2012). Soil-nutrient availability modifies the response of young pioneer and late successional trees to elevated carbon dioxide in a Brazilian tropical environment. *Environmental and Experimental Botany*, 77, 53-62. doi: 10.1016/j.envexpbot.2011.11.003
- Depardieu, C., Girardin, M. P., Nadeau, S., Lenz, P., Bousquet, J. et Isabel, N. (2020). Adaptive genetic variation to drought in a widely distributed conifer suggests a potential for increasing forest resilience in a drying climate. *New Phytologist*, 227(2), 427-439. doi: 10.1111/nph.16551
- DesRochers, A. et Gagnon, R. (1997). Is ring count at ground level a good estimation of black spruce age? *Canadian Journal of Forest Research*, 27(8), 1263-1267. doi: 10.1139/x97-086
- Dietrich, R. et Anand, M. (2019). Trees do not always act their age: size-deterministic tree ring standardization for long-term trend estimation in shade-tolerant trees. *Biogeosciences*, 16(24), 4815-4827. doi: <https://doi.org/10.5194/bg-16-4815-2019>
- Dietrich, R., Bell, F. W., Silva, L. C. R., Cecile, A., Horwath, W. R. et Anand, M. (2016). Climatic sensitivity, water-use efficiency, and growth decline in boreal jack pine (*Pinus banksiana*) forests in Northern Ontario. *Journal of Geophysical Research: Biogeosciences*, 121(10), 2016JG003440. doi: 10.1002/2016JG003440
- Dittmar, C., Zech, W. et Elling, W. (2003). Growth variations of Common beech (*Fagus sylvatica* L.) under different climatic and environmental conditions in Europe—a dendroecological study. *Forest Ecology and Management*, 173(1), 63-78. doi: 10.1016/S0378-1127(01)00816-7
- D'Orangeville, L., Houle, D., Duchesne, L., Phillips, R. P., Bergeron, Y. et Kneeshaw, D. (2018). Beneficial effects of climate warming on boreal tree growth may be transitory. *Nature Communications*, 9(1), 3213. doi: 10.1038/s41467-018-05705-4
- Dormann, C. F., Elith, J., Bacher, S., Buchmann, C., Carl, G., Carré, G., ... Lautenbach, S. (2013). Collinearity: a review of methods to deal with it and a simulation study evaluating their performance. *Ecography*, 36(1), 27-46. doi: 10.1111/j.1600-0587.2012.07348.x
- Drobyshev, I., Simard, M., Bergeron, Y. et Hofgaard, A. (2010). Does soil organic layer thickness affect climate-growth relationships in the black spruce boreal ecosystem? *Ecosystems*, 13(4), 556-574. doi: 10.1007/s10021-010-9340-7
- Dulamsuren, C., Hauck, M., Kopp, G., Ruff, M. et Leuschner, C. (2017). European beech responds to climate change with growth decline at lower, and growth increase at higher elevations in the center of its distribution range (SW Germany). *Trees*, 31(2), 673-686. doi: 10.1007/s00468-016-1499-x
- Dusenge, M. E., Madhavji, S. et Way, D. A. (2020). Contrasting acclimation responses to elevated CO<sub>2</sub> and warming between an evergreen and a deciduous boreal conifer. *Global Change Biology*, 26(6), 3639-3657. doi: 10.1111/gcb.15084
- Eisenach, C. et Meinzer, F. C. (2020). Hydraulics of woody plants. *Plant, Cell & Environment*, 43(3), 529-531. doi: 10.1111/pce.13715
- Esper, J., Frank, D. C., Battipaglia, G., Büntgen, U., Holert, C., Treydte, K., ... Saurer, M. (2010). Low-frequency noise in δ<sup>13</sup>C and δ<sup>18</sup>O tree ring data: A case study of *Pinus*

- uncinata in the Spanish Pyrenees. *Global Biogeochemical Cycles*, 24(4). doi: 10.1029/2010GB003772
- Evans, J. R. (1989). Photosynthesis and nitrogen relationships in leaves of C3 plants. *Oecologia*, 78(1), 9-19. doi: 10.1007/BF00377192
- Farquhar, G. D., Ball, M. C., von Caemmerer, S. et Roksandic, Z. (1982a). Effect of salinity and humidity on  $\delta^{13}\text{C}$  value of halophytes—Evidence for diffusional isotope fractionation determined by the ratio of intercellular/atmospheric partial pressure of CO<sub>2</sub> under different environmental conditions. *Oecologia*, 52(1), 121-124. doi: 10.1007/BF00349020
- Farquhar, G. D., Hubick, K. T., Condon, A. G. et Richards, R. A. (1989). Carbon Isotope Fractionation and Plant Water-Use Efficiency. Dans P. W. Rundel, J. R. Ehleringer et K. A. Nagy (dir.), *Stable Isotopes in Ecological Research* (p. 21-40). New York, NY : Springer. doi: 10.1007/978-1-4612-3498-2\_2
- Farquhar, G. D., O'Leary, M. H. et Berry, J. A. (1982b). On the relationship between carbon isotope discrimination and the intercellular carbon dioxide concentration in leaves. *Functional Plant Biology*, 9(2), 121-137. doi: 10.1071/pp9820121
- Farquhar, G. D. et Richards, R. (1984). Isotopic composition of plant carbon correlates with water-use efficiency of wheat genotypes. *Functional Plant Biology*, 11(6), 539-552.
- Feng, X., Ackerly, D. D., Dawson, T. E., Manzoni, S., McLaughlin, B., Skelton, R. P., ... Thompson, S. E. (2019). Beyond isohydricity: The role of environmental variability in determining plant drought responses. *Plant, Cell & Environment*, 42(4), 1104-1111. doi: 10.1111/pce.13486
- Fernández-de-Uña, L., McDowell, N. G., Cañellas, I. et Gea-Izquierdo, G. (2016). Disentangling the effect of competition, CO<sub>2</sub> and climate on intrinsic water-use efficiency and tree growth. *Journal of Ecology*, 104(3), 678-690. doi: 10.1111/1365-2745.12544
- Ficklin, D. L. et Novick, K. A. (2017). Historic and projected changes in vapor pressure deficit suggest a continental-scale drying of the United States atmosphere. *Journal of Geophysical Research: Atmospheres*, 122(4), 2061-2079. doi: 10.1002/2016JD025855
- Fluxnet Canada Team. (2016). FLUXNET Canada Research Network - Canadian Carbon Program Data Collection, 1993-2014. ORNL DAAC. doi: <https://doi.org/10.3334/ORNLDaac/1335>
- Ford, K. R., Breckheimer, I. K., Franklin, J. F., Freund, J. A., Kroiss, S. J., Larson, A. J., ... HilleRisLambers, J. (2016). Competition alters tree growth responses to climate at individual and stand scales. *Canadian Journal of Forest Research*, 47(1), 53-62. doi: 10.1139/cjfr-2016-0188
- Fortin, M., Bernier, S., Saucier, J.-P. et Labbé, F. (2009, 1<sup>er</sup> janvier). *Une relation hauteur-diamètre tenant compte de l'influence de la station et du climat pour 20 espèces commerciales du Québec* (153). Québec (Province) : Direction de la Recherche Forestière. Récupéré de ResearchGate :
- Fox, J. et Weisberg, S. (2019). *An {R} Companion to Applied Regression* (Third). Thousand Oaks CA : Sage. Récupéré de <https://socialsciences.mcmaster.ca/jfox/Books/Companion/>

- Francey, R. J., Allison, C. E., Etheridge, D. M., Trudinger, C. M., Enting, I. G., Leuenberger, M., ... Steele, L. P. (1999). A 1000-year high precision record of  $\delta^{13}\text{C}$  in atmospheric CO<sub>2</sub>. *Tellus B*, 51(2), 170-193. doi: 10.1034/j.1600-0889.1999.t01-1-00005.x
- Frank, D. C., Esper, J., Raible, C. C., Büntgen, U., Trouet, V., Stocker, B. et Joos, F. (2010). Ensemble reconstruction constraints on the global carbon cycle sensitivity to climate. *Nature*, 463, 527.
- Frank, D. C., Poulter, B., Saurer, M., Esper, J., Huntingford, C., Helle, G., ... Weigl, M. (2015). Water-use efficiency and transpiration across European forests during the Anthropocene. *Nature Climate Change*, 5(6), 579-583. doi: 10.1038/nclimate2614
- Franks, P. J., Adams, M. A., Amthor, J. S., Barbour, M. M., Berry, J. A., Ellsworth, D. S., ... von Caemmerer, S. (2013). Sensitivity of plants to changing atmospheric CO<sub>2</sub> concentration: from the geological past to the next century. *New Phytologist*, 197(4), 1077-1094. doi: 10.1111/nph.12104
- Frey, W. (1983). The influence of snow on growth and survival of planted trees. *Arctic, Antarctic, and Alpine Research*, 15(2), 241-251. doi: 10.1080/00040851.1983.12004347
- Fritts, H. C. (1971). Dendroclimatology and Dendroecology. *Quaternary Research*, 1(4), 419-449. doi: 10.1016/0033-5894(71)90057-3
- Fu, L., Xu, Y., Xu, Z., Wu, B. et Zhao, D. (2020). Tree water-use efficiency and growth dynamics in response to climatic and environmental changes in a temperate forest in Beijing, China. *Environment International*, 134, 105209. doi: 10.1016/j.envint.2019.105209
- Gaboriau, D., Asselin, H., Ali, A. A., Héli, C. et Girardin, M. P. (s. d.). *Main drivers of recent extreme wildfire years and identification of climatic thresholds on the territory of the Tlicho First Nation, northwestern Canada* [Paper submitted for publication to International Journal of Wildland Fire].
- Gagen, M., McCarroll, D., Robertson, I., Loader, N. J. et Jalkanen, R. (2008). Do tree ring  $\delta^{13}\text{C}$  series from *Pinus sylvestris* in northern Fennoscandia contain long-term non-climatic trends? *Chemical Geology*, 252(1), 42-51. doi: 10.1016/j.chemgeo.2008.01.013
- Gaige, E., Dail, D. B., Hollinger, D. Y., Davidson, E. A., Fernandez, I. J., Sievering, H., ... Halteman, W. (2007). Changes in canopy processes following whole-forest canopy nitrogen fertilization of a mature spruce-hemlock forest. *Ecosystems*, 10(7), 1133-1147. doi: 10.1007/s10021-007-9081-4
- Gauthier, S., Bernier, P., Kuuvainen, T., Shvidenko, A. Z. et Schepaschenko, D. G. (2015a). Boreal forest health and global change. *Science*, 349(6250), 819-822. doi: 10.1126/science.aaa9092
- Gauthier, S., Raulier, F., Ouzennou, H. et Saucier, J.-P. (2015b). Strategic analysis of forest vulnerability to risk related to fire: an example from the coniferous boreal forest of Quebec. *Canadian Journal of Forest Research*, 45(5), 553-565. doi: 10.1139/cjfr-2014-0125
- Gauthier, S. et Vaillancourt, M.-A. (2008). *Aménagement écosystémique en forêt boréale*. Québec (Province) : PUQ.
- Gennaretti, F., Arseneault, D., Nicault, A., Perreault, L. et Bégin, Y. (2014). Volcano-induced regime shifts in millennial tree-ring chronologies from northeastern North America.

- Proceedings of the National Academy of Sciences U.S.A.*, 111(28), 10077-10082. doi: 10.1073/pnas.1324220111
- Gessler, A., Ferrio, J. P., Hommel, R., Treydte, K., Werner, R. A. et Monson, R. K. (2014). Stable isotopes in tree rings: towards a mechanistic understanding of isotope fractionation and mixing processes from the leaves to the wood. *Tree Physiology*, 34(8), 796-818. doi: 10.1093/treephys/tpu040
- Gewehr, S., Drobyshev, I., Berninger, F. et Bergeron, Y. (2014). Soil characteristics mediate the distribution and response of boreal trees to climatic variability. *Canadian Journal of Forest Research*, 44, 487-498. doi: 10.1139/cjfr-2013-0481
- Giguère-Croteau, C., Boucher, É., Bergeron, Y., Girardin, M. P., Drobyshev, I., Silva, L. C. R., ... Garneau, M. (2019). North America's oldest boreal trees are more efficient water users due to increased [CO<sub>2</sub>], but do not grow faster. *Proceedings of the National Academy of Sciences U.S.A.*, 116(7), 2749-2754. doi: 10.1073/pnas.1816686116
- Gill, R. A., Polley, H. W., Johnson, H. B., Anderson, L. J., Maherli, H. et Jackson, R. B. (2002). Nonlinear grassland responses to past and future atmospheric CO<sub>2</sub>. *Nature*, 417(6886), 279-282. doi: 10.1038/417279a
- Girardin, M. P., Bernier, P. Y., Raulier, F., Tardif, J. C., Conciatori, F. et Guo, X. J. (2011). Testing for a CO<sub>2</sub> fertilization effect on growth of Canadian boreal forests. *Journal of Geophysical Research: Biogeosciences*, 116(G1), G01012. doi: 10.1029/2010JG001287
- Girardin, M. P., Bouriaud, O., Hogg, E. H., Kurz, W., Zimmermann, N. E., Metsaranta, J. M., ... Bhatti, J. (2016a). No growth stimulation of Canada's boreal forest under half-century of combined warming and CO<sub>2</sub> fertilization. *Proceedings of the National Academy of Sciences U.S.A.*, 113(52), E8406-E8414. doi: 10.1073/pnas.1610156113
- Girardin, M. P., Guo, X. J., Bernier, P. Y., Raulier, F. et Gauthier, S. (2012). Changes in growth of pristine boreal North American forests from 1950 to 2005 driven by landscape demographics and species traits. *Biogeosciences*, 9, 2523-2536. doi: 10.5194/bg-9-2523-2012
- Girardin, M. P., Guo, X. J., De Jong, R., Kinnard, C., Bernier, P. et Raulier, F. (2014). Unusual forest growth decline in boreal North America covaries with the retreat of Arctic sea ice. *Global Change Biology*, 20(3), 851-866. doi: 10.1111/gcb.12400
- Girardin, M. P., Guo, X. J., Metsaranta, J., Gervais, D., Campbell, E., Arsenault, A., ... Hogg, E. H. (2021). A national tree-ring data repository for Canadian forests (CFS-TRenD): structure, synthesis, and applications. *Environmental Reviews*. doi: 10.1139/er-2020-0099
- Girardin, M. P., Hogg, E. H., Bernier, P. Y., Kurz, W. A., Guo, X. J. et Cyr, G. (2016b). Negative impacts of high temperatures on growth of black spruce forests intensify with the anticipated climate warming. *Global Change Biology*, 22(2), 627-643. doi: 10.1111/gcb.13072
- Girardin, M. P., Raulier, F., Bernier, P. Y. et Tardif, J. C. (2008). Response of tree growth to a changing climate in boreal central Canada: A comparison of empirical, process-based, and hybrid modelling approaches. *Ecological Modelling*, 213(2), 209-228. doi: 10.1016/j.ecolmodel.2007.12.010

- Gleason, K. E., Bradford, J. B., Bottero, A., D'Amato, A. W., Fraver, S., Palik, B. J., ... Kern, C. C. (2017). Competition amplifies drought stress in forests across broad climatic and compositional gradients. *Ecosphere*, 8(7), e01849. doi: 10.1002/ecs2.1849
- Gouvernement du Québec. (2003). *Vegetation zones and bioclimatic domains in Québec*. Québec (Province).
- Granda, E. et Camarero, J. J. (2017). Drought reduces growth and stimulates sugar accumulation: new evidence of environmentally driven non-structural carbohydrate use. *Tree Physiology*, 37(8), 997-1000. doi: 10.1093/treephys/tpx097
- Graven, H., Allison, C. E., Etheridge, D. M., Hammer, S., Keeling, R. F., Levin, I., ... White, J. W. C. (2017). Compiled records of carbon isotopes in atmospheric CO<sub>2</sub> for historical simulations in CMIP6. *Geoscientific Model Development*, 10(12), 4405-4417. doi: <https://doi.org/10.5194/gmd-10-4405-2017>
- Grossiord, C., Buckley, T. N., Cernusak, L. A., Novick, K. A., Poulter, B., Siegwolf, R. T. W., ... McDowell, N. G. (2020). Plant responses to rising vapor pressure deficit. *New Phytologist*, 226(6), 1550-1566. doi: <https://doi.org/10.1111/nph.16485>
- Gu, L., Hanson, P. J., Post, W. M., Kaiser, D. P., Yang, B., Nemani, R., ... Meyers, T. (2008). The 2007 Eastern US spring freeze: Increased cold damage in a warming world. *BioScience*, 58(3), 253-262. doi: 10.1641/B580311
- Guerrieri, R., Belmecheri, S., Ollinger, S. V., Asbjornsen, H., Jennings, K., Xiao, J., ... Richardson, A. D. (2019). Disentangling the role of photosynthesis and stomatal conductance on rising forest water-use efficiency. *Proceedings of the National Academy of Sciences U.S.A.*, 201905912. doi: 10.1073/pnas.1905912116
- Gunderson, C. A., O'hara, K. H., Campion, C. M., Walker, A. V. et Edwards, N. T. (2010). Thermal plasticity of photosynthesis: the role of acclimation in forest responses to a warming climate. *Global Change Biology*, 16(8), 2272-2286. doi: 10.1111/j.1365-2486.2009.02090.x
- Guntiñas, M. E., Leirós, M. C., Trasar-Cepeda, C. et Gil-Sotres, F. (2012). Effects of moisture and temperature on net soil nitrogen mineralization: A laboratory study. *European Journal of Soil Biology*, 48, 73-80. doi: 10.1016/j.ejsobi.2011.07.015
- Hacke, U. G., Sperry, J. S., Pockman, W. T., Davis, S. D. et McCulloch, K. A. (2001). Trends in wood density and structure are linked to prevention of xylem implosion by negative pressure. *Oecologia*, 126(4), 457-461. doi: 10.1007/s004420100628
- Hanes, C. C., Wang, X., Jain, P., Parisien, M.-A., Little, J. M. et Flannigan, M. D. (2018). Fire-regime changes in Canada over the last half century. *Canadian Journal of Forest Research*, 49(3), 256-269. doi: 10.1139/cjfr-2018-0293
- Harlow, B. A., Marshall, J. D. et Robinson, A. P. (2006). A multi-species comparison of δ<sup>13</sup>C from whole wood, extractive-free wood and holocellulose. *Tree Physiology*, 26(6), 767-774. doi: 10.1093/treephys/26.6.767
- Hartmann, H. (2011). Will a 385 million year-struggle for light become a struggle for water and for carbon? – How trees may cope with more frequent climate change-type drought events. *Global Change Biology*, 17(1), 642-655. doi: 10.1111/j.1365-2486.2010.02248.x

- Hartmann, H., Link, R. M. et Schuldt, B. (2021). A whole-plant perspective of isohydry: stem-level support for leaf-level plant water regulation. *Tree Physiology*, (tpab011). doi: 10.1093/treephys/tpab011
- Hartmann, H., McDowell, N. G. et Trumbore, S. (2015). Allocation to carbon storage pools in Norway spruce saplings under drought and low CO<sub>2</sub>. *Tree Physiology*, 35(3), 243-252. doi: 10.1093/treephys/tpv019
- Harvey, B. D., Leduc, A., Gauthier, S. et Bergeron, Y. (2002). Stand-landscape integration in natural disturbance-based management of the southern boreal forest. *Forest Ecology and Management*, 155(1), 369-385. doi: 10.1016/S0378-1127(01)00573-4
- Hasler, A., Geertsema, M., Foord, V., Gruber, S. et Noetzli, J. (2015). The influence of surface characteristics, topography and continentality on mountain permafrost in British Columbia. *The Cryosphere*, 9(3), 1025-1038. doi: 10.5194/tc-9-1025-2015
- Helama, S., Arppe, L., Timonen, M., Mielikäinen, K. et Oinonen, M. (2015). Age-related trends in subfossil tree-ring δ<sup>13</sup>C data. *Chemical Geology*, 416, 28-35. doi: 10.1016/j.chemgeo.2015.10.019
- Hember, R. A. (2018). Spatially and temporally continuous estimates of annual total nitrogen deposition over North America, 1860–2013. *Data in Brief*, 17, 134-140. doi: 10.1016/j.dib.2017.12.052
- Hember, R. A., Kurz, W. A. et Coops, N. C. (2016). Relationships between individual-tree mortality and water-balance variables indicate positive trends in water stress-induced tree mortality across North America. *Global Change Biology*, 23(4), 1691-1710. doi: 10.1111/gcb.13428
- Hember, R. A., Kurz, W. A. et Coops, N. C. (2017). Increasing net ecosystem biomass production of Canada's boreal and temperate forests despite decline in dry climates. *Global Biogeochemical Cycles*, 31(1), 2016GB005459. doi: 10.1002/2016GB005459
- Hetherington, A. M. et Woodward, F. I. (2003). The role of stomata in sensing and driving environmental change. *Nature*, 424(6951), 901. doi: 10.1038/nature01843
- Hietz, P., Wanek, W. et Dünisch, O. (2005). Long-term trends in cellulose δ<sup>13</sup>C and water-use efficiency of tropical *Cedrela* and *Swietenia* from Brazil. *Tree Physiology*, 25(6), 745-752. doi: 10.1093/treephys/25.6.745
- Hobbie, S. E., Schimel, J. P., Trumbore, S. E. et Randerson, J. R. (2000). Controls over carbon storage and turnover in high-latitude soils. *Global Change Biology*, 6(S1), 196-210. doi: 10.1046/j.1365-2486.2000.06021.x
- Hochberg, U., Rockwell, F. E., Holbrook, N. M. et Cochard, H. (2018). Iso/anisohydry: a plant–environment interaction rather than a simple hydraulic trait. *Trends in Plant Science*, 23(2), 112-120. doi: 10.1016/j.tplants.2017.11.002
- Hogg, E. H., Barr, A. G. et Black, T. A. (2013). A simple soil moisture index for representing multi-year drought impacts on aspen productivity in the western Canadian interior. *Agricultural and Forest Meteorology*, 178-179, 173-182. doi: 10.1016/j.agrformet.2013.04.025
- Holmes, R. L. (1983). *Computer assisted quality control in tree-ring dating and measurement*. Récupéré de

- <https://www.scienceopen.com/document?vid=a110a27a-36fa-41dd-8536-434bb4d62436>
- Housset, J. M., Carcailliet, C., Girardin, M. P., Xu, H., Tremblay, F. et Bergeron, Y. (2016). In situ comparison of tree-ring responses to climate and population genetics: The need to control for local climate and site variables. *Frontiers in Ecology and Evolution*, 4. doi: 10.3389/fevo.2016.00123
- Huang, M., Wang, X., Keenan, T. F. et Piao, S. (2018). Drought timing influences the legacy of tree growth recovery. *Global Change Biology*, 24(8), 3546-3559. doi: 10.1111/gcb.14294
- Huber, P., J. (2005). Generalities. Dans *Robust Statistics* (2ème édition, p. 1-19). Hoboken, New Jersey : John Wiley & Sons, Ltd. doi: 10.1002/0471725250.ch1
- IPCC. (2013). *Climate Change 2013 : The physical science basis. Contribution of Working Group I to the Fifth Assessment Report of the Intergovernmental Panel on Climate Change.*
- Isaac-Renton, M., Montwé, D., Hamann, A., Spiecker, H., Cherubini, P. et Treydte, K. (2018). Northern forest tree populations are physiologically maladapted to drought. *Nature Communications*, 9(1), 1-9. doi: 10.1038/s41467-018-07701-0
- Isaac-Renton, M., Schneider, L. et Treydte, K. (2016). Contamination risk of stable isotope samples during milling. *Rapid Communications in Mass Spectrometry*, 30(13), 1513-1522. doi: 10.1002/rcm.7585
- Jamieson, M. A., Trowbridge, A. M., Raffa, K. F. et Lindroth, R. L. (2012). Consequences of climate warming and altered precipitation patterns for plant-insect and multitrophic interactions. *Plant Physiology*, 160(4), 1719-1727. doi: 10.1104/pp.112.206524
- Jarvis, A., Reuter, H., Nelson, A. et Guevara, E. (2008, 1<sup>er</sup> janvier). *Hole-filled seamless SRTM data v4*. International Centre for Tropical Agriculture (CIAT). Récupéré de <http://srtm.csi.cgiar.org>
- Jarvis, P. et Linder, S. (2000). Constraints to growth of boreal forests. *Nature*, 405(6789), 904-905. doi: 10.1038/35016154
- Jiang, X., Huang, J.-G., Cheng, J., Dawson, A., Stadt, K. J., Comeau, P. G. et Chen, H. Y. H. (2018). Interspecific variation in growth responses to tree size, competition and climate of western Canadian boreal mixed forests. *Science of The Total Environment*, 631-632, 1070-1078. doi: 10.1016/j.scitotenv.2018.03.099
- Jobidon, R., Bergeron, Y., Robitaille, A., Raulier, F., Gauthier, S., Imbeau, L., ... Boudreault, C. (2015). A biophysical approach to delineate a northern limit to commercial forestry: the case of Quebec's boreal forest. *Canadian Journal of Forest Research*, 45(5), 515-528. doi: 10.1139/cjfr-2014-0260
- Johns, T. C., Gregory, J. M., Ingram, W. J., Johnson, C. E., Jones, A., Lowe, J. A., ... Woodage, M. J. (2003). Anthropogenic climate change for 1860 to 2100 simulated with the HadCM3 model under updated emissions scenarios. *Clim. Dynam.*, 20(6), 583-612. doi: 10.1007/s00382-002-0296-y
- Johnstone, J. F., McIntire, E. J. B., Pedersen, E. J., King, G. et Pisaric, M. J. F. (2010). A sensitive slope: estimating landscape patterns of forest resilience in a changing climate. *Ecosphere*, 1(6), art14. doi: 10.1890/ES10-00102.1

- Ju, J. et Masek, J. G. (2016). The vegetation greenness trend in Canada and US Alaska from 1984–2012 Landsat data. *Remote Sensing of Environment*, 176, 1-16. doi: 10.1016/j.rse.2016.01.001
- Juday, G. P. et Alix, C. (2012). Consistent negative temperature sensitivity and positive influence of precipitation on growth of floodplain *Picea glauca* in Interior Alaska. *Canadian Journal of Forest Research*, 42(3), 561-573. doi: 10.1139/x2012-008
- Kaufman, D. S., McKay, N., Routson, C., Erb, M., Dätwyler, C., Sommer, P. S., ... Davis, B. (2020). Holocene global mean surface temperature, a multi-method reconstruction approach. *Scientific Data*, 7(1), 201. doi: 10.1038/s41597-020-0530-7
- Kaufman, D. S., Schneider, D. P., McKay, N. P., Ammann, C. M., Bradley, R. S., Briffa, K. R., ... Members, A. L. 2k P. (2009). Recent warming reverses long-term Arctic cooling. *Science*, 325(5945), 1236-1239. doi: 10.1126/science.1173983
- Kauppi, P. E., Posch, M. et Pirinen, P. (2014). Large impacts of climatic warming on growth of boreal forests since 1960. *PLOS ONE*, 9(11), e111340. doi: 10.1371/journal.pone.0111340
- Keeling, C. D. (1979). The Suess effect:  $^{13}\text{C}$ - $^{14}\text{C}$  interrelations. *Environment International*, 2(4), 229-300. doi: 10.1016/0160-4120(79)90005-9
- Keeling, R. F., Graven, H. D., Welp, L. R., Resplandy, L., Bi, J., Piper, S. C., ... Meijer, H. A. J. (2017). Atmospheric evidence for a global secular increase in carbon isotopic discrimination of land photosynthesis. *Proceedings of the National Academy of Sciences U.S.A.*, 114(39), 10361. doi: 10.1073/pnas.1619240114
- Keeling, R. F., Walker, S. J., Piper, S. C. et Bollenbacher, A. F. (2015). *Monthly atmospheric CO<sub>2</sub> concentration data (1958 to present) derived from in-situ air measurements at Mauna Loa Observatory, Hawaii*. Récupéré de <http://www.scrippsco2.ucsd.edu/>
- Kidd, K. R., Copenheaver, C. A. et Zink-Sharp, A. (2014). Frequency and factors of earlywood frost ring formation in jack pine (*Pinus banksiana*) across northern lower Michigan. *Écoscience*, 21(2), 157-167. doi: 10.2980/21-2-3708
- Klein, T. (2014). The variability of stomatal sensitivity to leaf water potential across tree species indicates a continuum between isohydric and anisohydric behaviours. *Functional Ecology*, 28(6), 1313-1320. doi: 10.1111/1365-2435.12289
- Klein, T. et Ramon, U. (2019). Stomatal sensitivity to CO<sub>2</sub> diverges between angiosperm and gymnosperm tree species. *Functional Ecology*, 33(8), 1411-1424. doi: 10.1111/1365-2435.13379
- Klesse, S., DeRose, R. J., Babst, F., Black, B. A., Anderegg, L. D. L., Axelson, J., ... Evans, M. E. K. (2020). Continental-scale tree-ring-based projection of Douglas-fir growth: Testing the limits of space-for-time substitution. *Global Change Biology*, 00, 1-18. doi: 10.1111/gcb.15170
- Klesse, S., DeRose, R. J., Guiterman, C. H., Lynch, A. M., O'Connor, C. D., Shaw, J. D. et Evans, M. E. K. (2018). Sampling bias overestimates climate change impacts on forest growth in the southwestern United States. *Nature Communications*, 9(1), 5336. doi: 10.1038/s41467-018-07800-y
- Koch, G. W., Sillett, S. C., Jennings, G. M. et Davis, S. D. (2004). The limits to tree height. *Nature*, 428(6985), 851-854. doi: 10.1038/nature02417

- Konter, O., Holzkämper, S., Helle, G., Büntgen, U., Saurer, M. et Esper, J. (2014). Climate sensitivity and parameter coherency in annually resolved  $\delta^{13}\text{C}$  and  $\delta^{18}\text{O}$  from *Pinus uncinata* tree-ring data in the Spanish Pyrenees. *Chemical Geology*, 377, 12-19. doi: 10.1016/j.chemgeo.2014.03.021
- Körner, C. (2015). Paradigm shift in plant growth control. *Current Opinion in Plant Biology*, 25, 107-114. doi: 10.1016/j.pbi.2015.05.003
- Kumarathunge, D. P., Drake, J. E., Tjoelker, M. G., López, R., Pfautsch, S., Vårhammar, A. et Medlyn, B. E. (2020). The temperature optima for tree seedling photosynthesis and growth depend on water inputs. *Global Change Biology*, 26, 2544-2560. doi: 10.1111/gcb.14975
- Kurz, W. A., Shaw, C. H., Boisvenue, C., Stinson, G., Metsaranta, J., Leckie, D., ... Neilson, E. T. (2013). Carbon in Canada's boreal forest — A synthesis. *Environmental Reviews*, 21(4), 260-292. doi: 10.1139/er-2013-0041
- Laflèche, V., Bernier, S., Saucier, J.-P. et Gagné, C. (2013). *Indices de qualité de station des principales essences commerciales en fonction des types écologiques du Québec méridional* [Technical Report]. Québec : Ministère des ressources naturelles, Direction des inventaires forestiers. Récupéré de [https://www.researchgate.net/publication/269094817\\_Indices\\_de\\_qualite\\_de\\_stati on\\_des\\_principales\\_essences\\_commerciales\\_en\\_fonction\\_des\\_types\\_ecologiques\\_ du\\_Quebec\\_meridional](https://www.researchgate.net/publication/269094817_Indices_de_qualite_de_stati on_des_principales_essences_commerciales_en_fonction_des_types_ecologiques_ du_Quebec_meridional)
- Landhäusser, S. M., Chow, P. S., Dickman, L. T., Furze, M. E., Kuhlman, I., Schmid, S., ... Adams, H. D. (2018). Standardized protocols and procedures can precisely and accurately quantify non-structural carbohydrates. *Tree Physiology*, 38(12), 1764-1778. doi: 10.1093/treephys/tpy118
- Landsberg, J. J. et Sands, P. (2010). *Physiological ecology of forest production: Principles, processes and models*. Cambridge, Massachusetts, États-Unis : Academic Press.
- Larsen, J. A. (2013). *The Boreal Ecosystem*. Cambridge, Massachusetts, États-Unis : Academic Press.
- Larter, M., Brodribb, T. J., Pfautsch, S., Burlett, R., Cochard, H. et Delzon, S. (2015). Extreme aridity pushes trees to their physical limits. *Plant Physiology*, 168(3), 804-807. doi: 10.1104/pp.15.00223
- Lavergne, A., Graven, H., Kauwe, M. G. D., Keenan, T. F., Medlyn, B. E. et Prentice, I. C. (2019). Observed and modelled historical trends in the water-use efficiency of plants and ecosystems. *Global Change Biology*, 25(7), 2242-2257. doi: 10.1111/gcb.14634
- Lavergne, A., Voelker, S. L., Csank, A., Graven, H., de Boer, H. J., Daux, V., ... Prentice, I. C. (2020). Historical changes in the stomatal limitation of photosynthesis: empirical support for an optimality principle. *New Phytologist*, 225(6), 2484-2497. doi: 10.1111/nph.16314
- Lavigne, M. B. et Ryan, M. G. (1997). Growth and maintenance respiration rates of aspen, black spruce and jack pine stems at northern and southern BOREAS sites. *Tree Physiology*, 17(8-9), 543-551. doi: 10.1093/treephys/17.8-9.543
- Lavoie, M., Harper, K., Paré, D. et Bergeron, Y. (2007). Spatial pattern in the organic layer and tree growth: A case study from regenerating *Picea mariana* stands prone to

- paludification. *Journal of Vegetation Science*, 18(2), 213-222. doi: 10.1111/j.1654-1103.2007.tb02532.x
- Le Goff, H. et Sirois, L. (2004). Black spruce and jack pine dynamics simulated under varying fire cycles in the northern boreal forest of Quebec, Canada. *Canadian Journal of Forest Research*, 34(12), 2399-2409. doi: 10.1139/x04-121
- Lee, S.-C., Christen, A., Black, T. A., Jassal, R. S., Ketler, R. et Nesic, Z. (2020). Partitioning of net ecosystem exchange into photosynthesis and respiration using continuous stable isotope measurements in a Pacific Northwest Douglas-fir forest ecosystem. *Agricultural and Forest Meteorology*, 292-293, 108109. doi: 10.1016/j.agrformet.2020.108109
- Legendre, P., Dale, M. R. T., Fortin, M.-J., Gurevitch, J., Hohn, M. et Myers, D. (2002). The consequences of spatial structure for the design and analysis of ecological field surveys. *Ecography*, 25(5), 601-615. doi: 10.1034/j.1600-0587.2002.250508.x
- Lens, F., Sperry, J. S., Christman, M. A., Choat, B., Rabaey, D. et Jansen, S. (2011). Testing hypotheses that link wood anatomy to cavitation resistance and hydraulic conductivity in the genus *Acer*. *New Phytologist*, 190(3), 709-723. doi: 10.1111/j.1469-8137.2010.03518.x
- Leonardi, S., Gentilesca, T., Guerrieri, R., Ripullone, F., Magnani, F., Mencuccini, M., ... Borghetti, M. (2012). Assessing the effects of nitrogen deposition and climate on carbon isotope discrimination and intrinsic water-use efficiency of angiosperm and conifer trees under rising CO<sub>2</sub> conditions. *Global Change Biology*, 18(9), 2925-2944. doi: 10.1111/j.1365-2486.2012.02757.x
- Létourneau, J. P., Matejek, S., Morneau, C., Robitaille, A., Roméo, T., Brunelle, J. et Leboeuf, A. (2008). *Norme de cartographie écoforestière du Programme d'inventaire écoforestier nordique*. Québec : Ministère des Ressources naturelles et de la Faune du Québec.
- Levanič, T., Čater, M. et McDowell, N. G. (2011). Associations between growth, wood anatomy, carbon isotope discrimination and mortality in a *Quercus robur* forest. *Tree Physiology*, 31(3), 298-308. doi: 10.1093/treephys/tpq111
- Lévesque, M., Andreu-Hayles, L. et Pederson, N. (2017). Water availability drives gas exchange and growth of trees in northeastern US, not elevated CO<sub>2</sub> and reduced acid deposition. *Scientific Reports*, 7(1), 46158. doi: 10.1038/srep46158
- Li, X., Blackman, C. J., Choat, B., Duursma, R. A., Rymer, P. D., Medlyn, B. E. et Tissue, D. T. (2018). Tree hydraulic traits are coordinated and strongly linked to climate-of-origin across a rainfall gradient. *Plant, Cell & Environment*, 41(3), 646-660. doi: 10.1111/pce.13129
- Li, X., Piao, S., Wang, K., Wang, X., Wang, T., Ciais, P., ... Peñuelas, J. (2020). Temporal trade-off between gymnosperm resistance and resilience increases forest sensitivity to extreme drought. *Nature Ecology & Evolution*, 1-9. doi: 10.1038/s41559-020-1217-3
- Linares, J. C. et Camarero, J. J. (2012). From pattern to process: linking intrinsic water-use efficiency to drought-induced forest decline. *Global Change Biology*, 18(3), 1000-1015. doi: 10.1111/j.1365-2486.2011.02566.x
- Liu, X., Shao, X., Liang, E., Zhao, L., Chen, T., Qin, D. et Ren, J. (2007). Species-dependent responses of juniper and spruce to increasing CO<sub>2</sub> concentration and to climate in

- semi-arid and arid areas of northwestern China. *Plant Ecology*, 193(2), 195. doi: 10.1007/s11258-006-9258-5
- Lloyd, A. H. et Bunn, A. G. (2007). Responses of the circumpolar boreal forest to 20th century climate variability. *Environmental Research Letters*, 2(4). Récupéré de [https://works.bepress.com/andrew\\_bunn/1/](https://works.bepress.com/andrew_bunn/1/)
- Lloyd, A. H., Bunn, A. G. et Berner, L. (2011). A latitudinal gradient in tree growth response to climate warming in the Siberian taiga. *Global Change Biology*, 17(5), 1935-1945. doi: 10.1111/j.1365-2486.2010.02360.x
- Loader, N. J., McCarroll, D., Gagen, M., Robertson, I. et Jalkanen, R. (2007). Extracting climatic information from stable isotopes in tree rings. Dans *Terrestrial Ecology* (vol. 1, p. 25-48). Elsevier. doi: 10.1016/S1936-7961(07)01003-2
- Logan, J. A., Régnière, J. et Powell, J. A. (2003). Assessing the impacts of global warming on forest pest dynamics. *Frontiers in Ecology and the Environment*, 1(3), 130-137. doi: 10.1890/1540-9295(2003)001[0130:ATIOGW]2.0.CO;2
- Lükewille, A. et Wright, R. (1997). Experimentally increased soil temperature causes release of nitrogen at a boreal forest catchment in southern Norway. *Global Change Biology*, 3(1), 13-21. doi: 10.1046/j.1365-2486.1997.00088.x
- Magnani, F., Mencuccini, M. et Grace, J. (2000). Age-related decline in stand productivity: the role of structural acclimation under hydraulic constraints. *Plant, Cell & Environment*, 23(3), 251-263. doi: 10.1046/j.1365-3040.2000.00537.x
- Maherali, H., Pockman, W. T. et Jackson, R. B. (2004). Adaptive variation in the vulnerability of woody plants to xylem cavitation. *Ecology*, 85(8), 2184-2199. doi: 10.1890/02-0538
- Mangiafico, S. (2017). *rcompanion: functions to support extension education program evaluation* (version 1.11.1). Récupéré de <https://cran.r-project.org/web/packages/rcompanion/index.html>
- Manrique-Alba, À., Ruiz-Yanetti, S., Moutahir, H., Novak, K., De Luis, M. et Bellot, J. (2017). Soil moisture and its role in growth-climate relationships across an aridity gradient in semiarid *Pinus halepensis* forests. *Science of The Total Environment*, 574, 982-990. doi: 10.1016/j.scitotenv.2016.09.123
- Mantgem, P. J. van, Stephenson, N. L., Byrne, J. C., Daniels, L. D., Franklin, J. F., Fulé, P. Z., ... Veblen, T. T. (2009). Widespread increase of tree mortality rates in the western United States. *Science*, 323(5913), 521-524. doi: 10.1126/science.1165000
- Manzoni, S., Vico, G., Katul, G., Palmroth, S., Jackson, R. B. et Porporato, A. (2013). Hydraulic limits on maximum plant transpiration and the emergence of the safety–efficiency trade-off. *New Phytologist*, 198(1), 169-178. doi: 10.1111/nph.12126
- Marchand, W. et DesRochers, A. (2016). Temporal variability of aging error and its potential effects on black spruce site productivity estimations. *Forest Ecology and Management*, 369, 47-58. doi: 10.1016/j.foreco.2016.02.034
- Marchand, W., Girardin, M. P., Gauthier, S., Hartmann, H., Bouriaud, O., Babst, F. et Bergeron, Y. (2018). Untangling methodological and scale considerations in growth and productivity trend estimates of Canada's forests. *Environmental Research Letters*, 13(9), 093001. doi: 10.1088/1748-9326/aad82a

- Marchand, W., Girardin, M. P., Hartmann, H., Gauthier, S. et Bergeron, Y. (2019). Taxonomy, together with ontogeny and growing conditions, drives needleleaf species' sensitivity to climate in boreal North America. *Global Change Biology*, 25(8), 2793-2809. doi: 10.1111/gcb.14665
- Marquis, B., Bergeron, Y., Simard, M. et Tremblay, F. (2020a). Growing-season frost is a better predictor of tree growth than mean annual temperature in boreal mixedwood forest plantations. *Global Change Biology*, n/a(n/a). doi: 10.1111/gcb.15327
- Marquis, B., Bergeron, Y., Tremblay, F. et Simard, M. (2020b). Probability of spring frosts, not growing degree-days, drives onset of spruce bud burst in plantations at the boreal-temperate forest ecotone. *Frontiers in Plant Science*, 11. doi: 10.3389/fpls.2020.01031
- Marquis, B., Duval, P., Bergeron, Y., Simard, M., Thiffault, N. et Tremblay, F. (2021). Height growth stagnation of planted spruce in boreal mixedwoods: Importance of landscape, microsite, and growing-season frosts. *Forest Ecology and Management*, 479, 118533. doi: 10.1016/j.foreco.2020.118533
- Marris, E. (2009). Forestry: Planting the forest of the future. *Nature*, 459(7249), 906-908. doi: 10.1038/459906a
- Marshall, J. D. et Monserud, R. A. (1996). Homeostatic gas-exchange parameters inferred from  $^{13}\text{C}/^{12}\text{C}$  in tree rings of conifers. *Oecologia*, 105(1), 13-21. doi: 10.1007/BF00328786
- Martínez-Vilalta, J., Poyatos, R., Aguadé, D., Retana, J. et Mencuccini, M. (2014). A new look at water transport regulation in plants. *New Phytologist*, 204(1), 105-115. doi: 10.1111/nph.12912
- Masri, B. E., Schwalm, C., Huntzinger, D. N., Mao, J., Shi, X., Peng, C., ... Michalak, A. M. (2019). Carbon and water use efficiencies: A comparative analysis of ten terrestrial ecosystem models under changing climate. *Scientific Reports*, 9(1), 1-9. doi: 10.1038/s41598-019-50808-7
- Matías, L., Linares, J. C., Sánchez-Miranda, Á. et Jump, A. S. (2017). Contrasting growth forecasts across the geographical range of Scots pine due to altitudinal and latitudinal differences in climatic sensitivity. *Global Change Biology*, 23(10), 4106-4116. doi: 10.1111/gcb.13627
- Maxwell, T. M., Silva, L. C. R. et Horwath, W. R. (2018). Integrating effects of species composition and soil properties to predict shifts in montane forest carbon–water relations. *Proceedings of the National Academy of Sciences U.S.A.*, 115(18), E4219. doi: 10.1073/pnas.1718864115
- Mazerolle, M. J. (2017). *AICmodavg: Model Selection and Multimodel Inference Based on (Q)AIC(c)* (version 2.1-1). Récupéré de <https://cran.r-project.org/web/packages/AICmodavg/index.html>
- McCarroll, D. et Loader, N. J. (2004). Stable isotopes in tree rings. *Quaternary Science Reviews*, 23(7), 771-801. doi: 10.1016/j.quascirev.2003.06.017
- McCarthy, J. (2001). Gap dynamics of forest trees: A review with particular attention to boreal forests. *Environmental Reviews*, 9(1), 1-59. doi: 10.1139/a00-012

- McDowell, N. G., Bond, B. J., Dickman, L. T., Ryan, M. G. et Whitehead, D. (2011). Relationships between tree height and carbon isotope discrimination. In: *Meinzer, F. C.; Dawson, T. E.; Lachenbruch, B., editors. Size- and Age-Related Changes in Tree Structure and Function. New York: Springer.*, 255-286.
- McDowell, N. G., Grossiord, C., Adams, H. D., Pinzón-Navarro, S., Mackay, D. S., Breshears, D. D., ... Xu, C. (2019). Mechanisms of a coniferous woodland persistence under drought and heat. *Environmental Research Letters*, 14(4), 045014. doi: 10.1088/1748-9326/ab0921
- McDowell, N. G. et Sevanto, S. (2010). The mechanisms of carbon starvation: how, when, or does it even occur at all? *New Phytologist*, 186(2), 264-266. doi: 10.1111/j.1469-8137.2010.03232.x
- McDowell, N., Pockman, W. T., Allen, C. D., Breshears, D. D., Cobb, N., Kolb, T., ... Yepez, E. A. (2008). Mechanisms of plant survival and mortality during drought: why do some plants survive while others succumb to drought? *New Phytologist*, 178(4), 719-739. doi: 10.1111/j.1469-8137.2008.02436.x
- McKenney, D. W., Pedlar, J. H., Papadopol, P. et Hutchinson, M. F. (2006). The development of 1901–2000 historical monthly climate models for Canada and the United States. *Agricultural and Forest Meteorology*, 138(1), 69-81. doi: 10.1016/j.agrformet.2006.03.012
- McKown, A. D., Guy, R. D., Klápník, J., Geraldès, A., Friedmann, M., Cronk, Q. C. B., ... Douglas, C. J. (2014). Geographical and environmental gradients shape phenotypic trait variation and genetic structure in *Populus trichocarpa*. *New Phytologist*, 201(4), 1263-1276. doi: 10.1111/nph.12601
- McLaughlin, B. C., Ackerly, D. D., Klos, P. Z., Natali, J., Dawson, T. E. et Thompson, S. E. (2017). Hydrologic refugia, plants, and climate change. *Global Change Biology*, 23(8), 2941-2961. doi: 10.1111/gcb.13629
- McLaughlin, S. B., Downing, D. J., Blasing, T. J., Cook, E. R. et Adams, H. S. (1987). An analysis of climate and competition as contributors to decline of red spruce in high elevation Appalachian forests of the Eastern United states. *Oecologia*, 72(4), 487-501. doi: 10.1007/BF00378973
- McNulty, S. G., Boggs, J. L. et Sun, G. (2014). The rise of the mediocre forest: why chronically stressed trees may better survive extreme episodic climate variability. *New Forests*, 45(3), 403-415. doi: 10.1007/s11056-014-9410-3
- Medrano, H., Tomás, M., Martorell, S., Flexas, J., Hernández, E., Rosselló, J., ... Bota, J. (2015). From leaf to whole-plant water use efficiency (WUE) in complex canopies: Limitations of leaf WUE as a selection target. *The Crop Journal*, 3(3), 220-228. doi: 10.1016/j.cj.2015.04.002
- Melillo, J. M., Butler, S., Johnson, J., Mohan, J., Steudler, P., Lux, H., ... Tang, J. (2011). Soil warming, carbon–nitrogen interactions, and forest carbon budgets. *Proceedings of the National Academy of Sciences U.S.A.*, 108(23), 9508-9512. doi: 10.1073/pnas.1018189108
- Michaelian, M., Hogg, E. H., Hall, R. J. et Arsenault, E. (2011). Massive mortality of aspen following severe drought along the southern edge of the Canadian boreal forest. *Global Change Biology*, 17(6), 2084-2094. doi: 10.1111/j.1365-2486.2010.02357.x

- Minasny, B. et McBratney, A. B. (2017). Limited effect of organic matter on soil available water capacity. *European Journal of Soil Science*, 69(1), 39-47. doi: 10.1111/ejss.12475
- Ministère des Ressources Naturelles du Québec. (2008). *Norme d'inventaire écodynamique nordique*. Québec (Province) : Direction des inventaires forestiers.
- Ministère des Ressources Naturelles du Québec. (2013). *Rapport du Comité scientifique chargé d'examiner la limite nordique des forêts attribuables*. Québec (Province) : Secteur des forêts.
- Molinari, C., Lehsten, V., Blarquez, O., Carcaillet, C., Davis, B. A. S., Kaplan, J. O., ... Bradshaw, R. H. W. (2018). The climate, the fuel and the land use: Long-term regional variability of biomass burning in boreal forests. *Global Change Biology*, 24, 4929-4945. doi: 10.1111/gcb.14380
- Monserud, R. A. et Marshall, J. D. (2001). Time-series analysis of  $\delta^{13}\text{C}$  from tree rings. I. Time trends and autocorrelation. *Tree Physiology*, 21(15), 1087-1102. doi: 10.1093/treephys/21.15.1087
- Muller, B., Pantin, F., Genard, M., Turc, O., Freixes, S., Piques, M. et Gibon, Y. (2011). Water deficits uncouple growth from photosynthesis, increase C content, and modify the relationships between C and growth in sink organs. *Journal of Experimental Botany*, 62(6), 1715-1729.
- Nicklen, E. F., Roland, C. A., Csank, A. Z., Wilmking, M., Ruess, R. W. et Muldoon, L. A. (2018). Stand basal area and solar radiation amplify white spruce climate sensitivity in interior Alaska: Evidence from carbon isotopes and tree rings. *Global Change Biology*, 0(0), 1-16. doi: 10.1111/gcb.14511
- Nicklen, E. F., Roland, C. A., Ruess, R. W., Schmidt, J. H. et Lloyd, A. H. (2016). Local site conditions drive climate-growth responses of *Picea mariana* and *Picea glauca* in interior Alaska. *Ecosphere*, 7(10), e01507. doi: 10.1002/ecs2.1507
- Norby, R. J., Hartz-Rubin, J. S. et Verbrugge, M. J. (2003). Phenological responses in maple to experimental atmospheric warming and CO<sub>2</sub> enrichment. *Global Change Biology*, 9(12), 1792-1801. doi: 10.1111/j.1365-2486.2003.00714.x
- Norby, R. J. et Luo, Y. (2004). Evaluating ecosystem responses to rising atmospheric CO<sub>2</sub> and global warming in a multi-factor world. *New Phytologist*, 162(2), 281-293. doi: 10.1111/j.1469-8137.2004.01047.x
- Oksanen, J., Blanchet, F. G., Friendly, M., Kindt, R., Legendre, P., McGlinn, D., ... Wagner, H. (2018). *vegan: Community Ecology Package* (version 2.5-2). Récupéré de <https://CRAN.R-project.org/package=vegan>
- O'Leary, D., Hall, D. K., Medler, M., Mattews, R. et Flower, A. (2017). *Snowmelt timing maps derived from MODIS for North America, 2001-2015*. ORNL Distributed Active Archive Center. doi: 10.3334/ORNLDAA/1504
- Ols, C. (2016). *Northeastern North America as a potential refugium for boreal forests in a warming climate: the unfortunate reality of Canada's weather stations network*.
- Ols, C., Girardin, M. P., Hofgaard, A., Bergeron, Y. et Drobyshev, I. (2017). Monitoring climate sensitivity shifts in tree-rings of eastern boreal North America using model-data comparison. *Ecosystems*, 1-16. doi: 10.1007/s10021-017-0203-3

- Ols, C., Girardin, M. P., Hofgaard, A., Bergeron, Y. et Drobyshev, I. (2018a). Monitoring Climate Sensitivity Shifts in Tree-Rings of Eastern Boreal North America Using Model-Data Comparison. *Ecosystems*, 21(5), 1042-1057. doi: 10.1007/s10021-017-0203-3
- Ols, C., Hervé, J.-C. et Bontemps, J.-D. (2020). Recent growth trends of conifers across Western Europe are controlled by thermal and water constraints and favored by forest heterogeneity. *Science of The Total Environment*, 742, 140453. doi: 10.1016/j.scitotenv.2020.140453
- Ols, C., Trouet, V., Girardin, M. P., Hofgaard, A., Bergeron, Y. et Drobyshev, I. (2018b). Post-1980 shifts in the sensitivity of boreal tree growth to North Atlantic Ocean dynamics and seasonal climate. *Global and Planetary Change*, 165, 1-12. doi: 10.1016/j.gloplacha.2018.03.006
- Osorio, F., Vallejos, R., Cuevas, F. et Mancilla, D. (2018). *SpatialPack: Tools for assessment of the association between two spatial processes* (version 0.3). Récupéré de <https://CRAN.R-project.org/package=SpatialPack>
- Pan, Y., Birdsey, R. A., Fang, J., Houghton, R., Kauppi, P. E., Kurz, W. A., ... Hayes, D. (2011). A large and persistent carbon sink in the world's forests. *Science*, 333(6045), 988-993. doi: 10.1126/science.1201609
- Parmesan, C. et Yohe, G. (2003). A globally coherent fingerprint of climate change impacts across natural systems. *Nature*, 421(6918), 37-42. doi: 10.1038/nature01286
- Payette, S. (1992). Fire as a controlling process in the North American boreal forest . Cambridge Core. Dans G. B. Bonan, H. H. Shugart et R. Leemans (dir.), *A Systems Analysis of the Global Boreal Forest* (p. 144-169). Cambridge : Cambridge University Press. doi: 10.1017/CBO9780511565489.006
- Pederson, G. T., Betancourt, J. L. et McCabe, G. J. (2013). Regional patterns and proximal causes of the recent snowpack decline in the Rocky Mountains, U.S. *Geophysical Research Letters*, 40(9), 1811-1816. doi: 10.1002/grl.50424
- Peel, A. J. (2013). *Transport of nutrients in plants*. Oxford, UK : Elsevier, Butterworth-Heinemann.
- Peng, C., Ma, Z., Lei, X., Zhu, Q., Chen, H., Wang, W., ... Zhou, X. (2011). A drought-induced pervasive increase in tree mortality across Canada's boreal forests. *Nature Climate Change*, 1(9), 467-471. doi: 10.1038/nclimate1293
- Peñuelas, J., Canadell, J. G. et Ogaya, R. (2011). Increased water-use efficiency during the 20th century did not translate into enhanced tree growth. *Global Ecology and Biogeography*. doi: 10.1111/j.1466-8238.2010.00608.x
- Pepin, N., Bradley, R. S., Diaz, H. F., Caceres, E. B., Forsythe, N., Fowler, H., ... Yang, D. Q. (2015). Elevation-dependent warming in mountain regions of the world. *Nature Climate Change*, 5, 424-430.
- Peres-Neto, P. R., Legendre, P., Dray, S. et Borcard, D. (2006). Variation partitioning of species data matrices: estimation and comparison of fractions. *Ecology*, 87(10), 2614-2625. doi: 10.1890/0012-9658(2006)87[2614:VPOSDM]2.0.CO;2
- Pinheiro, J., Bates, D., DebRoy, S., Sarkar, D., Heisterkamp, S., Van Willigen, B. et R Core Team. (2019). *nlme: Linear and Nonlinear Mixed Effects Models*. Récupéré de <https://CRAN.R-project.org/package=nlme>

- Piovesan, G. et Biondi, F. (2021). On tree longevity. *New Phytologist*, n/a(n/a). doi: <https://doi.org/10.1111/nph.17148>
- Piovesan, G., Biondi, F., Filippo, A. D., Alessandrini, A. et Maugeri, M. (2008). Drought-driven growth reduction in old beech (*Fagus sylvatica* L.) forests of the central Apennines, Italy. *Global Change Biology*, 14(6), 1265-1281. doi: 10.1111/j.1365-2486.2008.01570.x
- Ponton, S., Dupouey, J.-L., Bréda, N., Feuillat, F., Bodénès, C. et Dreyer, E. (2001). Carbon isotope discrimination and wood anatomy variations in mixed stands of *Quercus robur* and *Quercus petraea*. *Plant, Cell & Environment*, 24(8), 861-868. doi: 10.1046/j.0016-8025.2001.00733.x
- Powell, J. A. et Bentz, B. J. (2009). Connecting phenological predictions with population growth rates for mountain pine beetle, an outbreak insect. *Landscape Ecology*, 24(5), 657-672. doi: 10.1007/s10980-009-9340-1
- Price, D. T., Alfaro, R. I., Brown, K. J., Flannigan, M. D., Fleming, R. A., Hogg, E. H., ... Venier, L. A. (2013). Anticipating the consequences of climate change for Canada's boreal forest ecosystems. *Environmental Reviews*, 21(4), 322-365. doi: 10.1139/er-2013-0042
- Price, D. T., McKenney, D. W., Joyce, L. A., Siltanen, R. M., Papadopol, P. et Lawrence, K. (2011). *High-resolution interpolation of climate scenarios for Canada derived from general circulation model simulations* (Information Report NOR-X-421.). Edmonton, AB : Natural Resources Canada, Canadian Forest Service, Northern Forestry Centre. Récupéré de [www.fs.usda.gov](http://www.fs.usda.gov) : <https://www.fs.usda.gov/treesearch/pubs/39890>
- Pureswaran, D. S., Grandpré, L. D., Paré, D., Taylor, A., Barrette, M., Morin, H., ... Kneeshaw, D. D. (2015). Climate-induced changes in host tree-insect phenology may drive ecological state-shift in boreal forests. *Ecology*, 96(6), 1480-1491. doi: 10.1890/13-2366.1
- Raney, P. A., Leopold, D. J., Dovciak, M. et Beier, C. M. (2016). Hydrologic position mediates sensitivity of tree growth to climate: Groundwater subsidies provide a thermal buffer effect in wetlands. *Forest Ecology and Management*, 379, 70-80. doi: 10.1016/j.foreco.2016.08.004
- Régnière, J. et Bolstad, P. (1994). Statistical simulation of daily air temperature patterns eastern North America to forecast seasonal events in insect pest management. *Environmental Entomology*, 23(6), 1368-1380. doi: 10.1093/ee/23.6.1368
- Reich, P. B., Sendall, K. M., Stefanski, A., Rich, R. L., Hobbie, S. E. et Montgomery, R. A. (2018). Effects of climate warming on photosynthesis in boreal tree species depend on soil moisture. *Nature*, 562(7726), 263-267. doi: 10.1038/s41586-018-0582-4
- Ressources Naturelles Canada. (2018). *The state of Canada's forests. Annual report 2018*. Natural Resources Canada, Canadian Forest Service. Récupéré de Zotero :
- Restaino, C. M., Peterson, D. L. et Littell, J. (2016). Increased water deficit decreases Douglas fir growth throughout western US forests. *Proceedings of the National Academy of Sciences U.S.A.*, 113(34), 9557-9562. doi: 10.1073/pnas.1602384113
- Rezaie, N., D'Andrea, E., Bräuning, A., Matteucci, G., Bombi, P. et Lauteri, M. (2018). Do atmospheric CO<sub>2</sub> concentration increase, climate and forest management affect

- iWUE of common beech? Evidences from carbon isotope analyses in tree rings. *Tree Physiology*, 38(8), 1110-1126. doi: 10.1093/treephys/tpy025
- Richardson, A. D., Hufkens, K., Milliman, T., Aubrecht, D. M., Furze, M. E., Seyednasrollah, B., ... Hanson, P. J. (2018). Ecosystem warming extends vegetation activity but heightens vulnerability to cold temperatures. *Nature*, 560(7718), 368-371. doi: 10.1038/s41586-018-0399-1
- Robitaille, A., Saucier, J.-P., Chabot, M., Côté, D. et Boudreault, C. (2015). An approach for assessing suitability for forest management based on constraints of the physical environment at a regional scale. *Canadian Journal of Forest Research*, 45(5), 529-539. doi: 10.1139/cjfr-2014-0338
- Rossi, S., Simard, S., Rathgeber, C. B. K., Deslauriers, A. et De Zan, C. (2009). Effects of a 20-day-long dry period on cambial and apical meristem growth in *Abies balsamea* seedlings. *Trees*, 23(1), 85-93. doi: 10.1007/s00468-008-0257-0
- Ryan, M. G., Lavigne, M. B. et Gower, S. T. (1997). Annual carbon cost of autotrophic respiration in boreal forest ecosystems in relation to species and climate. *Journal of Geophysical Research: Atmospheres*, 102(D24), 28871-28883. doi: 10.1029/97JD01236
- Ryan, M. G., Phillips, N. et Bond, B. J. (2006). The hydraulic limitation hypothesis revisited. *Plant, Cell & Environment*, 29(3), 367-381. doi: 10.1111/j.1365-3040.2005.01478.x
- Ryan, M. G. et Yoder, B. J. (1997). Hydraulic limits to tree height and tree growth. *BioScience*, 47(4), 235-242. doi: 10.2307/1313077
- Sakai, A. (1983). Comparative study on freezing resistance of conifers with special reference to cold adaptation and its evolutive aspects. *Canadian Journal of Botany*, 61(9), 2323-2332. doi: 10.1139/b83-255
- Sala, A., Piper, F. et Hoch, G. (2010). Physiological mechanisms of drought-induced tree mortality are far from being resolved. *New Phytologist*, 186(2), 274-281. doi: 10.1111/j.1469-8137.2009.03167.x
- Sala, A., Woodruff, D. R. et Meinzer, F. C. (2012). Carbon dynamics in trees: feast or famine? *Tree Physiology*, 32(6), 764-775. doi: 10.1093/treephys/tpr143
- Santander Meteorology Group. (2012). *fume: FUME package* (version R package version 1.0). Récupéré de <https://CRAN.R-project.org/package=fume>
- Saurer, M., Siegwolf, R. T. W. et Schweingruber, F. H. (2004). Carbon isotope discrimination indicates improving water-use efficiency of trees in northern Eurasia over the last 100 years. *Global Change Biology*, 10(12), 2109-2120. doi: 10.1111/j.1365-2486.2004.00869.x
- Saurer, M., Spahni, R., Frank, D. C., Joos, F., Leuenberger, M., Loader, N. J., ... Young, G. H. F. (2014). Spatial variability and temporal trends in water-use efficiency of European forests. *Global Change Biology*, 20(12), 3700-3712. doi: 10.1111/gcb.12717
- Savard, M. M., Bégin, C. et Marion, J. (2020). Response strategies of boreal spruce trees to anthropogenic changes in air quality and rising pCO<sub>2</sub>. *Environmental Pollution*, 114209. doi: 10.1016/j.envpol.2020.114209
- Scheidegger, Y., Saurer, M., Bahn, M. et Siegwolf, R. (2000). Linking stable oxygen and carbon isotopes with stomatal conductance and photosynthetic capacity: a conceptual model. *Oecologia*, 125(3), 350-357. doi: 10.1007/s004420000466

- Schoonmaker, A. L., Hacke, U. G., Landhäuser, S. M., Lieffers, V. J. et Tyree, M. T. (2010). Hydraulic acclimation to shading in boreal conifers of varying shade tolerance. *Plant, Cell & Environment*, 33(3), 382-393. doi: 10.1111/j.1365-3040.2009.02088.x
- Schubert, B. A. et Jahren, A. H. (2018). Incorporating the effects of photorespiration into terrestrial paleoclimate reconstruction. *Earth-Science Reviews*, 177, 637-642. doi: 10.1016/j.earscirev.2017.12.008
- Schuster, R. et Oberhuber, W. (2013). Age-dependent climate-growth relationships and regeneration of *Picea abies* in a drought-prone mixed-coniferous forest in the Alps. *Canadian Journal of Forest Research*, 43, 609-618. doi: 10.1139/cjfr-2012-0426
- Shestakova, T. A., Voltas, J., Saurer, M., Berninger, F., Esper, J., Andreu-Hayles, L., ... Gutiérrez, E. (2019). Spatio-temporal patterns of tree growth as related to carbon isotope fractionation in European forests under changing climate. *Global Ecology and Biogeography*, 0(0), 1-15. doi: 10.1111/geb.12933
- Silva, L. C. R., Gómez-Guerrero, A., Doane, T. A. et Horwath, W. R. (2015). Isotopic and nutritional evidence for species- and site-specific responses to N deposition and elevated CO<sub>2</sub> in temperate forests. *Journal of Geophysical Research: Biogeosciences*, 120(6), 1110-1123. doi: 10.1002/2014JG002865
- Silva, L. C. R. et Madhur, A. (2013). Probing for the influence of atmospheric CO<sub>2</sub> and climate change on forest ecosystems across biomes. *Global Ecology and Biogeography*, 22(1), 83-92. doi: 10.1111/j.1466-8238.2012.00783.x
- Singer, J. D. et Willett, J. B. (2003). *Applied longitudinal data analysis: Modeling change and event occurrence*. New York, NY, US : Oxford University Press. doi: 10.1093/acprof:oso/9780195152968.001.0001
- Sohn, J. A., Brooks, J. R., Bauhus, J., Kohler, M., Kolb, T. E. et McDowell, N. G. (2014). Unthinned slow-growing ponderosa pine (*Pinus ponderosa*) trees contain muted isotopic signals in tree rings as compared to thinned trees. *Trees*, 28(4), 1035-1051. doi: 10.1007/s00468-014-1016-z
- Sohn, J. A., Kohler, M., Gessler, A. et Bauhus, J. (2012). Interactions of thinning and stem height on the drought response of radial stem growth and isotopic composition of Norway spruce (*Picea abies*). *Tree Physiology*, 32(10), 1199-1213. doi: 10.1093/treephys/tps077
- Sohn, J. A., Saha, S. et Bauhus, J. (2016). Potential of forest thinning to mitigate drought stress: A meta-analysis. *Forest Ecology and Management*, 380, 261-273. doi: 10.1016/j.foreco.2016.07.046
- Soja, A. J., Tchebakova, N. M., French, N. H. F., Flannigan, M. D., Shugart, H. H., Stocks, B. J., ... Stackhouse, P. W. (2007). Climate-induced boreal forest change: Predictions versus current observations. *Global and Planetary Change*, 56(3), 274-296. doi: 10.1016/j.gloplacha.2006.07.028
- Speer, J. H. (2010). *Fundamentals of Tree-ring Research*. (s. l.) : University of Arizona Press.
- Splawinski, T. B., Cyr, D., Gauthier, S., Jetté, J.-P. et Bergeron, Y. (2018). Analyzing risk of regeneration failure in the managed boreal forest of northwestern Quebec. *Canadian Journal of Forest Research*, 49(6), 680-691. doi: 10.1139/cjfr-2018-0278

- Sternberg, L. D. S. L., Deniro, M. J. et Savidge, R. A. (1986). Oxygen isotope exchange between metabolites and water during biochemical reactions leading to cellulose synthesis. *Plant Physiology*, 82(2), 423-427. doi: 10.1104/pp.82.2.423
- Sternberg, L. da S. L. O. (2009). Oxygen stable isotope ratios of tree-ring cellulose: the next phase of understanding. *New Phytologist*, 181(3), 553-562. doi: 10.1111/j.1469-8137.2008.02661.x
- Stocker, B. D., Wang, H., Smith, N. G., Harrison, S. P., Keenan, T. F., Sandoval, D., ... Prentice, I. C. (2019). P-model v1.0: An optimality-based light use efficiency model for simulating ecosystem gross primary production. *Geoscientific Model Development Discussions*, 1-59. doi: <https://doi.org/10.5194/gmd-2019-200>
- Stocks, B. J., Mason, J. A., Todd, J. B., Bosch, E. M., Wotton, B. M., Amiro, B. D., ... Skinner, W. R. (2002). Large forest fires in Canada, 1959–1997. *Journal of Geophysical Research: Atmospheres*, 107(D1), FFR 5-1-FFR 5-12. doi: 10.1029/2001JD000484
- Stralberg, D., Arseneault, D., Baltzer, J. L., Barber, Q. E., Bayne, E. M., Boulanger, Y., ... Whitman, E. (2020). Climate-change refugia in boreal North America: what, where, and for how long? *Frontiers in Ecology and the Environment*, 18(5), 261-270. doi: 10.1002/fee.2188
- Strömgren, M. et Linder, S. (2002). Effects of nutrition and soil warming on stemwood production in a boreal Norway spruce stand. *Global Change Biology*, 8(12), 1194-1204. doi: 10.1046/j.1365-2486.2002.00546.x
- Strong, W. L. et La Roi, G. H. (1983). Root-system morphology of common boreal forest trees in Alberta, Canada. *Canadian Journal of Forest Research*, 13(6), 1164-1173. doi: 10.1139/x83-155
- Sturm, P., Eugster, W. et Knohl, A. (2012). Eddy covariance measurements of CO<sub>2</sub> isotopologues with a quantum cascade laser absorption spectrometer. *Agricultural and Forest Meteorology*, 152, 73-82. doi: 10.1016/j.agrformet.2011.09.007
- Sullivan, J. H., Bovard, B. D. et Middleton, E. M. (1997). Variability in leaf-level CO<sub>2</sub> and water fluxes in *Pinus banksiana* and *Picea mariana* in Saskatchewan. *Tree Physiology*, 17(8-9), 553-561. doi: 10.1093/treephys/17.8-9.553
- Sullivan, P. F., Pattison, R. R., Brownlee, A. H., Cahoon, S. M. P. et Hollingsworth, T. N. (2017). Limited evidence of declining growth among moisture-limited black and white spruce in interior Alaska. *Scientific Reports*, 7(1), 15344. doi: 10.1038/s41598-017-15644-7
- Sun, S., He, C., Qiu, L., Li, C., Zhang, J. et Meng, P. (2018). Stable isotope analysis reveals prolonged drought stress in poplar plantation mortality of the Three-North Shelter Forest in Northern China. *Agricultural and Forest Meteorology*, 252, 39-48. doi: 10.1016/j.agrformet.2017.12.264
- Tang, K. et Feng, X. (2001). The effect of soil hydrology on the oxygen and hydrogen isotopic compositions of plants' source water. *Earth and Planetary Science Letters*, 185(3), 355-367. doi: 10.1016/S0012-821X(00)00385-X
- Tans, P. P., De Jong, A. F. M. et Mook, W. G. (1979). Natural atmospheric <sup>14</sup>C variation and the Suess effect. *Nature*, 280(5725), 826-828. doi: 10.1038/280826a0
- Tardieu, F. et Simonneau, T. (1998). Variability among species of stomatal control under fluctuating soil water status and evaporative demand: modelling isohydric and

- anisohydric behaviours. *Journal of Experimental Botany*, 49(Special\_Issue), 419-432. doi: 10.1093/jxb/49.Special\_Issue.419
- Tarnocai, C., Canadell, J. G., Schuur, E. a. G., Kuhry, P., Mazhitova, G. et Zimov, S. (2009). Soil organic carbon pools in the northern circumpolar permafrost region. *Global Biogeochemical Cycles*, 23(2), GB2023. doi: 10.1029/2008GB003327
- ter Braak, C. et Smilauer, P. (2009). *Canoco for Windows Version 4.56*. (s. l.) : Biometris - Plant Research International.
- Terrier, A., Girardin, M. P., Cantin, A., Groot, W. J. de, Anyomi, K. A., Gauthier, S. et Bergeron, Y. (2015). Disturbance legacies and paludification mediate the ecological impact of an intensifying wildfire regime in the Clay Belt boreal forest of eastern North America. *Journal of Vegetation Science*, 26(3), 588-602. doi: 10.1111/jvs.12250
- Thomas, V., Treitz, P., McCaughey, J. H., Noland, T. et Rich, L. (2008). Canopy chlorophyll concentration estimation using hyperspectral and lidar data for a boreal mixedwood forest in northern Ontario, Canada. *International Journal of Remote Sensing*, 29(4), 1029-1052. doi: 10.1080/01431160701281023
- Tissier, J., Lambs, L., Peltier, J.-P. et Marigo, G. (2004). Relationships between hydraulic traits and habitat preference for six *Acer* species occurring in the French Alps. *Annals of Forest Science*, 61(1), 81-86. doi: 10.1051/forest:2003087
- Tremblay, A. et Ransijn, J. (2015). *LMERConvenienceFunctions: Model Selection and Post-hoc Analysis for (G)LMER Models* (version 2.10). Récupéré de <https://cran.r-project.org/web/packages/LMERConvenienceFunctions/index.html>
- Trenberth, K. E. (1983). What are the Seasons? *Bulletin of the American Meteorological Society*, 64(11), 1276-1282. doi: 10.1175/1520-0477(1983)064<1276:WATS>2.0.CO;2
- Trugman, A. T., Medvigy, D., Anderegg, W. R. L. et Pacala, S. W. (2018). Differential declines in Alaskan boreal forest vitality related to climate and competition. *Global Change Biology*, 24(3), 1097-1107. doi: 10.1111/gcb.13952
- Tukey, J. W. (1977). *Exploratory data analysis*. Reading, MA : Pearson.
- Urban, J., Ingwers, M. W., McGuire, M. A. et Teskey, R. O. (2017). Increase in leaf temperature opens stomata and decouples net photosynthesis from stomatal conductance in *Pinus taeda* and *Populus deltoides x nigra*. *Journal of Experimental Botany*, 68(7), 1757-1767. doi: 10.1093/jxb/erx052
- USDA Forest Service. (2002). *USDA Forest Service RWU NE-4153: Little's ranges and FIA importance value distribution maps*. Récupéré de [https://www.fs.fed.us/nrs/atlas/littlefia/species\\_table.html#](https://www.fs.fed.us/nrs/atlas/littlefia/species_table.html#)
- Vaganov, E. A., Hughes, M. K., Kirdyanov, A. V., Schweingruber, F. H. et Silkin, P. P. (1999). Influence of snowfall and melt timing on tree growth in subarctic Eurasia. *Nature*, 400(6740), 149-151. doi: 10.1038/22087
- Verbyla, D. (2015). Remote sensing of interannual boreal forest NDVI in relation to climatic conditions in interior Alaska. *Environmental Research Letters*, 10(12), 125016. doi: 10.1088/1748-9326/10/12/125016
- Vicente-Serrano, S. M., Lopez-Moreno, J.-I., Beguería, S., Lorenzo-Lacruz, J., Sanchez-Lorenzo, A., García-Ruiz, J. M., ... Espejo, F. (2014). Evidence of increasing drought

- severity caused by temperature rise in southern Europe. *Environmental Research Letters*, 9(4), 044001. doi: 10.1088/1748-9326/9/4/044001
- Vitasse, Y., Signarbieux, C. et Fu, Y. H. (2017). Global warming leads to more uniform spring phenology across elevations. *Proceedings of the National Academy of Sciences U.S.A.*, 201717342. doi: 10.1073/pnas.1717342115
- Voelker, S. L., Brooks, J. R., Meinzer, F. C., Anderson, R., Bader, M. K.-F., Battipaglia, G., ... Wingate, L. (2016). A dynamic leaf gas-exchange strategy is conserved in woody plants under changing ambient CO<sub>2</sub>: evidence from carbon isotope discrimination in paleo and CO<sub>2</sub> enrichment studies. *Global Change Biology*, 22(2), 889-902. doi: 10.1111/gcb.13102
- Voelker, S. L., Muzika, R. M., Guyette, R. P. et Stambaugh, M. C. (2006). Historical CO<sub>2</sub> growth enhancement declines with age in *Quercus* and *Pinus*. *Ecological monographs*. Récupéré de <http://agris.fao.org/agris-search/search.do?recordID=US201300769433>
- Voortman, B. R., Bartholomeus, R. P., Bodegom, P. M. van, Gooren, H., Zee, S. E. A. T. M. van der et Witte, J.-P. M. (2013). Unsaturated hydraulic properties of xerophilous mosses: towards implementation of moss covered soils in hydrological models. *Hydrological Processes*, 28(26), 6251-6264. doi: 10.1002/hyp.10111
- Walker, X. J. et Johnstone, J. F. (2014). Widespread negative correlations between black spruce growth and temperature across topographic moisture gradients in the boreal forest. *Environmental Research Letters*, 9(6), 064016. doi: 10.1088/1748-9326/9/6/064016
- Walker, X. J., Mack, M. C. et Johnstone, J. F. (2015). Stable carbon isotope analysis reveals widespread drought stress in boreal black spruce forests. *Global Change Biology*, 21(8), 3102-3113. doi: 10.1111/gcb.12893
- Ward, J. K., Harris, J. M., Cerling, T. E., Wiedenhoeft, A., Lott, M. J., Dearing, M.-D., ... Ehleringer, J. R. (2005). Carbon starvation in glacial trees recovered from the La Brea tar pits, southern California. *Proceedings of the National Academy of Sciences U.S.A.*, 102(3), 690-694. doi: 10.1073/pnas.0408315102
- Waterhouse, J. S., Switsur, V. R., Barker, A. C., Carter, A. H. C., Hemming, D. L., Loader, N. J. et Robertson, I. (2004). Northern European trees show a progressively diminishing response to increasing atmospheric carbon dioxide concentrations. *Quaternary Science Reviews*, 23(7), 803-810. doi: 10.1016/j.quascirev.2003.06.011
- Way, D. A. et Sage, R. F. (2008a). Elevated growth temperatures reduce the carbon gain of black spruce [*Picea mariana* (Mill.) B.S.P.]. *Global Change Biology*, 14(3), 624-636. doi: 10.1111/j.1365-2486.2007.01513.x
- Way, D. A. et Sage, R. F. (2008b). Thermal acclimation of photosynthesis in black spruce [*Picea mariana* (Mill.) B.S.P.]. *Plant, Cell & Environment*, 31(9), 1250-1262. doi: 10.1111/j.1365-3040.2008.01842.x
- Weber, P., Bugmann, H., Fonti, P. et Rigling, A. (2008). Using a retrospective dynamic competition index to reconstruct forest succession. *Forest Ecology and Management*, 254(1), 96-106. doi: 10.1016/j.foreco.2007.07.031

- Whitman, E., Parisien, M.-A., Thompson, D. K., Hall, R. J., Skakun, R. S. et Flannigan, M. D. (2018). Variability and drivers of burn severity in the northwestern Canadian boreal forest. *Ecosphere*, 9(2), e02128. doi: 10.1002/ecs2.2128
- Willeit, M., Ganopolski, A., Calov, R. et Brovkin, V. (2019). Mid-Pleistocene transition in glacial cycles explained by declining CO<sub>2</sub> and regolith removal. *Science Advances*, 5(4), eaav7337. doi: 10.1126/sciadv.aav7337
- Williams, A. P., Allen, C. D., Macalady, A. K., Griffin, D., Woodhouse, C. A., Meko, D. M., ... McDowell, N. G. (2013). Temperature as a potent driver of regional forest drought stress and tree mortality. *Nature Climate Change*, 3(3), 292-297. doi: 10.1038/nclimate1693
- Wilmking, M. et Myers-Smith, I. (2008). Changing climate sensitivity of black spruce (*Picea mariana* Mill.) in a peatland–forest landscape in Interior Alaska. *Dendrochronologia*, 25(3), 167-175. doi: 10.1016/j.dendro.2007.04.003
- Wilson, R., D'Arrigo, R., Buckley, B., Büntgen, U., Esper, J., Frank, D. C., ... Youngblut, D. (2007). A matter of divergence: Tracking recent warming at hemispheric scales using tree ring data. *Journal of Geophysical Research: Atmospheres*, 112(D17), D17103. doi: 10.1029/2006JD008318
- Wong, C. Y. S., D'Odorico, P., Arain, M. A. et Ensminger, I. (2020). Tracking the phenology of photosynthesis using carotenoid-sensitive and near-infrared reflectance vegetation indices in a temperate evergreen and mixed deciduous forest. *New Phytologist*, 226(6), 1682-1695. doi: 10.1111/nph.16479
- Wood, S. N. (2017). *Generalized additive models. An introduction with R* (2nd Edition). New York : Chapman and Hall/CRC. Récupéré de <https://doi.org/10.1201/9781315370279>
- Wu, G., Guan, K., Li, Y., Novick, K. A., Feng, X., McDowell, N. G., ... Jiang, C. (2020). Assessing and interpreting the interannual variability of plant iso/anisohydry at species and ecosystem levels [Article submitted for publication].
- Wu, G., Liu, X., Chen, T., Xu, G., Wang, W., Zeng, X. et Zhang, X. (2015). Elevation-dependent variations of tree growth and intrinsic water-use efficiency in Schrenk spruce (*Picea schrenkiana*) in the western Tianshan Mountains, China. *Frontiers in Plant Science*, 6. doi: 10.3389/fpls.2015.00309
- Wu, X., Li, X., Liu, H., Ciais, P., Li, Y., Xu, C., ... Zhang, C. (2018). Uneven winter snow influence on tree growth across temperate China. *Global Change Biology*. doi: 10.1111/gcb.14464
- Xu, G., Liu, X., Sun, W., Szejner, P., Zeng, X., Yoshimura, K. et Trouet, V. (2020). Seasonal divergence between soil water availability and atmospheric moisture recorded in intra-annual tree-ring δ<sup>18</sup>O extremes. *Environmental Research Letters*. doi: 10.1088/1748-9326/ab9792
- Yang, Q., Blanco, N. E., Hermida-Carrera, C., Lehotai, N., Hurry, V. et Strand, Å. (2020). Two dominant boreal conifers use contrasting mechanisms to reactivate photosynthesis in the spring. *Nature Communications*, 11(1), 1-12. doi: 10.1038/s41467-019-13954-0

- Yuan, W., Zheng, Y., Piao, S., Ciais, P., Lombardozzi, D., Wang, Y., ... Yang, S. (2019). Increased atmospheric vapor pressure deficit reduces global vegetation growth. *Science Advances*, 5(8), eaax1396. doi: 10.1126/sciadv.aax1396
- Yue, S. et Wang, C. (2004). The Mann-Kendall test modified by effective sample size to detect trend in serially correlated hydrological series. *Water Resources Management*, 18(3), 201-218. doi: 10.1023/B:WARM.0000043140.61082.60
- Zhang, K., Kimball, J. S., Hogg, E. H., Zhao, M., Oechel, W. C., Cassano, J. J. et Running, S. W. (2008). Satellite-based model detection of recent climate-driven changes in northern high-latitude vegetation productivity. *Journal of Geophysical Research: Biogeosciences*, 113(G3), G03033. doi: 10.1029/2007JG000621
- Zhang, Q., Ficklin, D. L., Manzoni, S., Wang, L., Way, D., Phillips, R. P. et Novick, K. A. (2019). Response of ecosystem intrinsic water use efficiency and gross primary productivity to rising vapor pressure deficit. *Environmental Research Letters*, 14(7), 074023. doi: 10.1088/1748-9326/ab2603
- Zhou, Z., Ollinger, S. V. et Lepine, L. (2018). Landscape variation in canopy nitrogen and carbon assimilation in a temperate mixed forest. *Oecologia*, 188(2), 595-606. doi: 10.1007/s00442-018-4223-2
- Zhu, Z., Piao, S., Myneni, R. B., Huang, M., Zeng, Z., Canadell, J. G., ... Zeng, N. (2016). Greening of the Earth and its drivers. *Nature Climate Change*, 6(8), 791-795. doi: 10.1038/nclimate3004
- Zobel, M. (1990). Soil oxygen conditions in paludifying boreal forest sites. *Suo*, 41(4-5), 81-89.
- Zohner, C. M., Mo, L., Renner, S. S., Svenning, J.-C., Vitasse, Y., Benito, B. M., ... Crowther, T. W. (2020). Late-spring frost risk between 1959 and 2017 decreased in North America but increased in Europe and Asia. *Proceedings of the National Academy of Sciences U.S.A.*, 117(22), 12192-12200. doi: 10.1073/pnas.1920816117